

https://dspace.org/

Stratigraphy and basin modelling of the Gemsbok Sub-Basin (Karoo Supergroup) of Botswana and Namibia

Nxumalo, Valerie

2011-06-22
http://hdl.handle.net/10539/10167

Downloaded from a DSpace repository. https://dspace.org/

STRATIGRAPHY AND BASIN MODELLING OF THE GEMSBOK SUB-BASIN (KAROO SUPERGROUP) OF BOTSWANA AND NAMIBIA

Valerie Nxumalo

A dissertation submitted to the Faculty of Science, University of the Witwatersrand, Johannesburg, in fulfilment of requirements for the degree of Master of Science

Johannesburg, 2011

DECLARATION

I declare that this dissertation is my own, unaided work. It is being submitted for the Degree of Master of Science at the University of the Witwatersrand, Johannesburg. It has not been submitted before for any degree or examination in any other University. The information presented in this dissertation was obtained by me while employed by the Council for Geoscience, Pretoria.

_____

(V. Nxumalo)

_____day of _____201____

ABSTRACT

The Gemsbok Sub-basin is situated in the south-western corner of the Kalahari Karoo Basin and extends south from the Kgalagadi District of Botswana into the Northern Cape (South Africa); and west into the Aranos Basin (southeast Namibia). The Sub-basin preserves a heterogeneous succession of Upper Palaeozoic to Lower Mesozoic sedimentary and volcanic rocks of the Karoo Supergroup. Because the succession is largely covered by the Cenozoic Kalahari Group, the stratigraphy of the succession is not as well understood as the Main Karoo Basin in South Africa. Most research in the Gemsbok Sub-basin is based on borehole data. This study focuses on the intrabasinal correlation, depositional environments and provenance of the Karoo Supergroup in the Gemsbok Sub-basin in Botswana and Namibia.

Based on detailed sedimentological analyses of 11 borehole cores of the Karoo Supergroup in the Gemsbok Sub-basin of Botswana and Namibia, 8 facies associations (FAs) comprising 14 lithofacies and 2 trace fossil assemblages (*Cruziana* and *Skolithos* ichnofacies) were identified. The facies associations (FA1 to FA8) correspond to the lithostratigraphic subdivisions (the Dwyka Group, Ecca Group, Beaufort equivalent Group, Lebung Group [Mosolotsane and Ntane formations] and Neu Loore Formation) of the Karoo Supergroup. Sedimentological characteristics of the identified facies associations indicate the following depositional environments: glaciomarine or glaciolacustrine (FA1, Dwyka Group), deep-water (lake or sea) (FA2, Ecca Group), prodelta (FA3, Ecca Group), delta front (FA4, Ecca Group), delta plain (FA5, Ecca Group), floodplain (probably shallow lakes) (FA6, Beaufort Group equivalent), fluvial (FA7, Mosolotsane and Neu Loore formations) and aeolian (FA8, Ntane Sandstone Formation).

The Dwyka Group (FA1) forms the base of the Karoo Supergroup in the Gemsbok Sub-basin and overlain by the Ecca Group deposits. Three types of deltas exist within the Ecca Group: fluvial-dominated; fluvial-wave interaction and wave-dominated deltas. The Gemsbok Sub-basin was characterised by rapid uplift and subsidence and high sediment

influx during the deposition of the Ecca Group. Petrographic and geochemical analyses of the Ecca Group sandstones revealed immature arkose and subarkose type sandstones dominated by angular to subangular detrital grains, sourced from transitional continental and basement uplifted source areas. The sandstones of Ntane Sandstone Formation are classified as subarkoses and sourced from the craton interior provenances.

Key words: Gemsbok Sub-basin, Kalahari Karoo Basin, Karoo Supergroup, facies associations, provenance.

ACKNOWLEDGEMENTS

This project forms part of a larger project titled 'Tri-Nations Karoo Basin Correlation Project' (Project No. CO-2007-562) that was initiated by the Council for Geoscience. Financial support was provided by the Department of Science and Technology (DST), South Africa. I would like to thank the geological surveys of Botswana and Namibia for giving access to borehole cores for this study. Dr. J. Neveling, Prof. B.S. Rubidge and Prof. G. Drennan are thanked for their wonderful supervision, patience and understanding. I would also like to thank my colleagues at the Council for Geoscience for their support on the project. Particular gratitude is extended to Prof. J.A. MacEarchern (Simon Fraser University, Canada) and Associate Prof. L. Buatois (University of Saskatchewan, Canada) for assisting me in identifying trace fossils in the borehole cores in this study.

TABLE OF CONTENTS

DECLARATION i
ABSTRACT ii
ACKNOWLEDGEMENTS iv
TABLE OF CONTENTS v
LIST OF FIGURES vii
LIST OF TABLES xiv
LIST OF APPENDIX FIGURES xv

CHAPTER ONE: INTRODUCTION 1
1.1 General Introduction 1
1.2 Tectonic framework of the Karoo-age basins across southern Africa 2
1.3 Stratigraphic review of southern African Karoo-aged basins 5
1.4 Provenance of the rocks in the Kalahari Karoo Basin 22
1.5 Structural framework of the Kalahari Karoo Basin 25
1.6 Correlation of the Karoo Supergroup in the Kalahari Karoo Basin of Namibia and Botswana 26

CHAPTER TWO: AIMS AND METHODS 28
2.1 Introduction 28
2.2 Location of the study area 28
2.3 Methodology 31

CHAPTER THREE: SEDIMENTOLOGY 35
3.1 Introduction 35
3.2 Facies analysis 35
3.3 Lithofacies description 37
3.4 Invertebrate Palaeontology 45
3.5 Facies associations 52

CHAPTER FOUR: SANDSTONE PETROLOGY, GEOCHEMISTRY AND PROVENANCE 72
4.1 Introduction 72
4.2 Sandstone petrography 72
4.3 Detrital framework grains 77
4.4 Detrital modes 82
4.5 Geochemistry of sandstones 86
4.6 Sandstone classification using geochemistry 92
4.7 Sandstone provenance and tectonic settings 92

CHAPTER FIVE: DISCUSSION 97
5.1 Stratigraphy 97
5.2 Depositional Environments 108
5.3 Geographic distribution of facies associations 126
5.4 Geological history of the Gemsbok Sub-basin 129

CHAPTER SIX: CONCLUSIONS 135

CHAPTER SEVEN: REFERENCES 138
7.1 List of References 138

APPENDICES 151

LIST OF FIGURES

Figure 1.1 The distribution of Karoo-aged basins in southern Africa 1
Figure 1.2 Pan-Gondwanian foreland system generated through compression, collision and terrain accretion along the southern margin of Gondwana and the associated foreland basins..... 4
Figure 1.3 Generalised model of the Main Karoo Foreland Basin in relation to the Cape Fold Belt, and the inferred position of the magmatic arc and subduction zone in the south 4
Figure 1.4 Continental configuration of the Southern Hemisphere during the late Palaeozoic times, showing the position of the Kalahari Karoo Basin and the Main Karoo Basin in relation to the Windhoek Highlands, Cargonian Highlands, Southern Highlands and South America and the Antarctica 7
Figure 1.5 Karoo sub-divisions in Botswana 9
Figure 1.6 Correlation panel of the Karoo Supergroup lithostratigraphic units from the Main Karoo Basin (western foredeep) through the Aranos , Kalahari Karoo basins 13
Figure 1.7 Generalised stratigraphic columns of the Karoo Supergroup in the Aranos Basin (I) and the southwest Botswana (II)..... 14
Figure 1.8 Lithostratigraphy of the Karoo Supergroup in the Kalahari Karoo Basin of Botswana 16
Figure 1.9 Palaeocurrent directions for the Dwyka Group, Ecca Group, Beaufort Group and the Lebung Group in the Kalahari Karoo Basin of Botswana 24
Figure 1.10 Palaeocurrent and palaeo-ice flow directions of the Ecca Group and the Dwyka Group in the Aranos Basin 24
Figure 1.11 Geophysical map of southern Africa with major structural elements and cratons 25
Figure 2.1 Geological map of the study area and the location of the boreholes used in this study..... 29
Figure 3.1 Clast-supported, massive conglomerate (lithofacies Gcm), borehole W1 39
Figure 3.2 Matrix-supported, massive diamictite (lithofacies Dmm), borehole W3 39
Figure 3.3 Clast-supported, massive diamictite (lithofacies Dcm), borehole W3 39

Figure 3.4 Clast-supported breccia (lithofacies Bc), borehole CKP8A 39
Figure 3.5 Massive or faint laminated sandstone (lithofacies Sm), borehole W1 40
Figure 3.6 Trough cross-bedded sandstone (lithofacies St), borehole CKP8A 40
Figure 3.7 Horizontally laminated sandstone (lithofacies Sh), borehole CKP8C 41
Figure 3.8 Ripple cross-laminated sandstone (lithofacies Sr), borehole ACP24..... 41
Figure 3.9 Bioturbated sandstone (lithofacies Sb), borehole ACP24 41
Figure 3.10 Fine laminated sandstone, siltstone and mudrock (lithofacies Fl), borehole ACP13..... 43
Figure 3.11 Bioturbated massive mudrock and siltstone (lithofacies Fr), borehole ACP19 43
Figure 3.12 Massive mudrock (lithofacies Fsm), borehole ACP13..... 43
Figure 3.13 Carbonaceous mudrocks (lithofacies Fc), borehole CKP8C 44
Figure 3.14 Coal (lithofacies C), borehole W1 44
Figure 3.15 Horizontal laminated sandstone with fugichnia (Fu) and trace fossils *Siphonichnus* (*Si*) and *Conichnus* (*Co*), borehole ACP24 47
Figure 3.16 Horizontal laminated (Sh) sandstone with *Diplocraterion* (*Di*) trace fossil, borehole ACP24 47
Figure 3.17 Massive sandstone (Sm) and horizontal laminated (Sh) sandstone with *Rosselia* (*Ro*) trace fossil and fugichnia (Fu), borehole W3..... 47
Figure 3.18 Massive sandstone (Sm) with *Planolites* (*Pl*), *Thalassinoides* (*Th*) and *Pheobichnus* (*Ph*) trace fossils, borehole ACP24..... 48
Figure 3.19 Laminated sandstone, siltstone and mudrock (Fl) with *Planolites* (*Pl*), *Thalassinoides* (*Th*) and *Teichichnus* (T*e*) trace fossils, borehole ACP4..... 49
Figure 3.20 Laminated sandstone, siltstone and mudrock (Fl) with *Teichichnus* (T*e*) trace fossil, borehole ACP24..... 49
Figure 3.21 Massive carbonaceous mudrock (Fc) with *Asterosoma* (*As*) and *Thalassinoides* (*Th*) trace fossils, borehole W3..... 50
Figure 3.22 Bioturbated mudrock (Fr) with Zoophycos (*Zo*) and *Asterosoma* (*As*) trace fossils, borehole W3..... 50

Figure 3.23 Laminated sandstone, silststone and mudrock (Fl) with *Palaeophycus tubularis* (*Pa*), *Schaubcylindrichnus* (*Sc*), *Conichnus* (*Co*), *Teichichnus* (*Te*) and *Siphonichnus* (*Si*) trace fossils, borehole ACP3 50
Figure 3.24 Matrix-supported, massive diamictite (Dmm), borehole ACP3..... 54
Figure 3.25 Soft-sediment deformation structures (micro-folds), borehole W3..... 55
Figure 3.26 Clast-supported diamictite (Dcm) and alternating layers of sandstones and mudrocks displaying upward-fining cycles, borehole W3 55
Figure 3.27 Upward-fining cycles within sandstones of facies association 2 in borehole ACP4..... 57
Figure 3.28 Facies association 2 in borehole W3 57
Figure 3.29 Upward-fining cycles (red triangles) within the sandstone-dominated facies association 2 in borehole W3. Red dotted lines show break between two upward-fining cycles and **?** indicates unidentified sedimentary structures 58
Figure 3.30 Facies association 3 in borehole ACP4 59
Figure 3.31 Facies association3 in borehole W3 59
Figure 3.32 Upward-coarsening succession of facies association 4 in borehole ACP4 .. 60
Figure 3.33 Upward-coarsening succession of facies association 4 in borehole W3 61
Figure 3.34 Upward-coarsening succession of facies association 4 in borehole CKP8C-1 62
Figure 3.35 Upward-fining successions of facies association 5 65
Figure 3.36 Upward-fining succession from sandstones (Sh, St, Sb) at the base grading upwards into bioturbated siltstone and mudrock (Fr) and carbonaceous mudrocks (Fc) interbedded with thin coals (C). Borehole CKP8C..... 65
Figure 3.37 Poorly sorted, pebbly massive sandstones (Sm) with carbonaceous mudrock clast sharply overlain by laminated sandstone, siltstone and mudrock lithofacies (Fl). Borehole CKP8C 66
Figure 3.38 Upward-coarsening successions of facies association 5..... 66
Figure 3.39 Carbonaceous mudrocks (Fc) with *Planolites* trace fossil grading upwards into ripple cross-laminated sandstones (Sr) of facies association 4, borehole ACP24..... 67
Figure 3.40 Bioturbated siltstones (Fr) of facies association 6 in borehole CKP8A 69

Figure 3.41 Siltstones (Fsm) with pale red nodules (probably heamatite), borehole CKP8A 69
Figure 3.42 Reddish mudrocks (Fsm) of facies association 7 in borehole ACP13. Core tray caring 6.02 m of core 70
Figure 3.43 Basal clast-supported conglomerate (Gcm) overlain by sandstones (Sm, Sr) of facies association 7 in borehole W1 71
Figure 3.44 Reddish mudrocks of facies association 7 sharply overlain (erosive contact) by well sorted, fine-grained sandstones (Sm) of facies association 8 in borehole W1..... 71
Figure 3.45 Facies association 8 massive(Sm), mica-free sandstones in borehole W1... 71
Figure 4.1 Photomicrograph of sample N8, Facies association 4, western part of the study area 74
Figure 4.2 Photomicrograph of sample N11. Facies association 5, western part of the study area 74
Figure 4.3 Photomicrograph of sample B7, Facies association 4 northern part of the study area 76
Figure 4.4 Photomicrograph of sample B20, Facies association 4 eastern part of the study area 76
Figure 4.5 Photomicrograph of sample B17, Facies association 5 eastern part of the study area 77
Figure 4.6 Photomicrograph of sample B1, Facies association 8 northern part of the study area 77
Figure 4.7 Photomicrograph of sample BB, facies association 5, borehole CKP8C, depth 298.93 m – 299.00 m. Polycrystalline quartz (Qp) with more than five non-sutured quartz crystals (Cross Polarised Light) 78
Figure 4.8 Photomicrograph of sample B15, facies association 5, borehole CKP8C-1, depth 411.25 m – 411.31 m. Polycrystalline quartz (Qp) with more than five sutured quartz crystals (Cross Polarised Light) 78
Figure 4.9 Photomicrograph of sample N13, facies association 5, borehole ACP13, depth 226.56 m – 226.61 m. Angular to subangular quartz-feldspar rock fragment (FR), microcline (Mi) grains and matrix (M) (Cross Polarised Light)..... 79

Figure 4.10 Photomicrograph of sample N6, facies association 5, borehole ACP3, depth 265.06 – 265.11 m. Quartz-feldspar rock fragment (RF), quartz grain (Qm) showing undulatory extinction and fine-grained matrix (Cross Polarised Light) 79
Figure 4.11 Photomicrograph of sample B5, facies association 4, borehole W2, depth 170.20 m – 170.24 m. Micaceous sandstone with bent mica minerals (Cross Polarised Light)..... 80
Figure 4.12 Photomicrograph of sample B17, facies association 5, borehole CKP8C-1, depth 278.19 – 278.35 m. Calcite (Ca) cement (Cross Polarised Light) 80
Figure 4.13 Photomicrograph of sample B17, facies association 5, borehole CKP8C-1, depth 278.19 m – 278.35 m. Euhedral zircon (Zr) grain (Cross Polarised Light)..... 81
Figure 4.14 Photomicrograph of sample N1, facies association 5, borehole ACP4, depth 234.17 m – 234.24 m. Angular garnet (Ga) grain and rounded zircon (Zr) grain (Plane Polarised Light)..... 81
Figure 4.15 Photomicrograph of sample B6, facies association 4, borehole W2, depth 230.69 m – 230.77 m. Sandstone with subrounded quartz (Qm) grains and partially euhedral green tourmaline (To) grain (Plane Polarised Light) 81
Figure 4.16 Photomicrograph of sample B6, facies association 4, borehole W2, depth 230.69 m – 230.77 m. Tourmaline grain showing zonation (Cross Polarised Light)..... 81
Figure 4.17 Photomicrograph of sample B6, facies association 4, borehole W2, depth 230.69 m – 230.77 m. Rutile grain (Ru) with irregular cleavage fractures (Cross Polarised Light)..... 81
Figure 4.18 Photomicrograph of sample N13, facies association 5, borehole ACP13, depth 226.56 m – 226.61 m. Rutile (Ru) grain (Plane Polarised Light)..... 81
Figure 4.19 Photomicrograph of sample B15, facies association 5, borehole CKP8C-1, depth 411.25 m – 411.31 m. Garnet (Ga) grain with irregular fractures (Plane Polarised Light)..... 82
Figure 4.20 Photomicrograph of sample B12, facies association 5, borehole CKP8A, depth 283.74 m – 283.89 m. Garnet (Ga) grains and subrounded brown tourmaline (To) grain (Plane Polarised Light) 82
Figure 4.21 Photomicrograph of sample N8, facies association 4, borehole ACP19, depth 324.92 m – 325.00 m. Sandstone with angular to subangular detrital grains, apatite (Ap)

minerals occur as inclusions within the monocrystalline quartz grain (Cross Polarised Light)..... 82
Figure 4.22 Photomicrograph of sample B17, facies association 5, borehole CKP8C-1, depth 278.19 – 278.35 m. Pyrite (Py) grains (Plane Polarised Light) 82
Figure 4.23 QFL triangular classification plot of facies associations 4 and 5 sandstones in the western part of the study area 83
Figure 4.24 QmFLt diagram with tectonic fields of Dickinson and Suczek (1979) for facies associations 4 and 5 sandstones in the western part of the study area 83
Figure 4.25 QFL triangular classification plot of facies associations 4, 5 and 8 sandstones in the northern and eastern parts of the study area (after Folk, 1980) 84
Figure 4.26 QmFLt diagram with tectonic fields of Dickinson and Suczek (1979) for facies associations 4, 5 and 8 sandstones in the northern and eastern parts of the study area 84
Figure 4.27 Chemical classification scheme of sandstones from facies associations 4, 5 and 8 in the northern and eastern parts of the study area based on log (SiO_2/Al_2O_3) *vs.* log (Fe_2O_3/K_2O) diagram of Herron (1988) 93
Figure 4.28 Characterisation of source rock composition based on Ni *vs.* TiO_2 diagram for the facies association 4, 5 and 8 sandstones in the northern and eastern parts of the study area 93
Figure 4.29 Facies associations 4, 5 and 8 sandstones in the northern and eastern parts of the study area, based on the discrimination function diagram of Roser and Korsch (1988) 94
Figure 4.30 Facies associations 4, 5 and 8 sandstones in the northern and eastern parts of the study area, based on Th-Sc-Zr/10 tectonic discrimination diagram of Bhatia and Crook (1986) 95
Figure 5.1 Vertical distribution and preliminary interpretation of the eight different facies associations of the Karoo Supergroup in the Gemsbok Sub-basin 98
Figure 5.2 Cross-section line W3 – CKP8C-1/CKP8C in the northern and eastern part of the Gemsbok Sub-basin 100
Figure 5.3 Cross-section W3- CKP8C-1/CKP8C showing thickness variations of different facies associations 100

Figure 5.4 Cross-section line across the Gemsbok Sub-basin (from west to east direction) 101
Figure 5.5 Cross-section from the west to the east direction showing thickness variations of different facies associations across the Gemsbok Sub-basin 101
Figure 5.6 Cross-section line W3 – ACP19 – ACP4 – ACP3 from the northern part to the western part of the Gemsbok Sub-basin 102
Figure 5.7 Cross-section W3 – ACP19 – ACP4 – ACP3 showing thickness variations of different facies associations 102
Figure 5.8 Classification of deltas based on grain size and on sediment supply mechanism 116
Figure 5.9 3D diagram of the Karoo Supergroup boreholes in the Gemsbok Sub-basin showing different facies associations..... 127
Figure 5.10 3D stratigraphic model of the Karoo Supergroup facies associations in the Gemsbok Sub-basin 128

LIST OF TABLES

Table 1 Preliminary correlations of the Karoo Supergroup rocks in the Kalahari Karoo Basin, Aranos Basin and the Main Karoo Basin 27

Table 2 Classification and Symbols of Grain Types 33

Table 3 Sedimentary lithofacies identified in the Karoo Supergroup boreholes in the Gemsbok Sub-basin (study area) 36

Table 4 Facies associations identified in the boreholes of the Karoo Supergroup in the Gemsbok Sub-basin of Botswana and Namibia..... 53

Table 5 Detrital modes of the Ecca Group facies association 4 and 5 sandstones in the western part of the Gemsbok Sub-basin 73

Table 6 Detrital modes of the Ecca Group facies association 4 and 5 and Ntane Sandstone Formation facies association 8 in the northern and eastern parts of the Gemsbok Sub-basin 73

Table 7 Chemical composition (major element concentrations) in weight percent (Wt%) of the Ntane Sandstone Formation (facies association 8) and the Ecca Group (facies association s 4 and 5) sandstones in the northern and eastern parts of the study area..... 87

Table 8 Chemical composition (trace element concentrations) in parts per million (ppm) of the sandstones of the Ntane Sandstone Formation (facies association 8) and the Ecca Group (facies association 4 and 5) in the northern and eastern parts of the study area.... 88

Table 9 Summary table for provenances of the Ntane Sandstone Formation and the Ecca Group sandstones in the Gemsbok Sub-basin 96

LIST OF APPENDIX FIGURES

Appendix Figure. 1 ACP3 borehole log..... 170

Appendix Figure. 2 ACP4 borehole log 171

Appendix Figure. 3 ACP13 borehole log 172

Appendix Figure. 4 ACP19 borehole log 173

Appendix Figure. 5 ACP24 borehole log 174

Appendix Figure. 6 W1 borehole log 175

Appendix Figure. 7 W2 borehole log..... 176

Appendix Figure. 8 W3 borehole 177

Appendix Figure. 9 CKP8A borehole log 178

Appendix Figure. 10 CKP8C borehole log..... 179

Appendix Figure. 11 CKP8C-1 borehole log 180

Appendix Figure. 12 MP1 borehole log 181

Appendix Figure. 13 VREDA 281 borehole log..... 182

CHAPTER ONE: INTRODUCTION

1.1 General Introduction

Carboniferous to Jurassic Karoo-aged basins occur in most southern African countries such as Namibia, Botswana, South Africa, Malawi, Zambia, Zimbabwe, Swaziland, Tanzania, Congo and Angola (Fig. 1.1) with exposures crossing international boundaries (Johnson et al., 1996; Cairncross, 2001). These basins have a cumulative aerial extent of 4.5 million km^2 and a maximum thickness of about 12 km in the southern part of the Main Karoo Basin (Johnson et al., 1997; Bumby and Guiraud, 2005; Johnson et al., 2006). The Main Karoo Basin of South Africa is the largest Phanerozoic depositional basin in southern Africa, followed by the Kalahari Karoo Basin, which stretches from Namibia (Aranos Basin) through Botswana (Kalahari Karoo Basin) into Zimbabwe (Mid-Zambezi Basin) (Bordy et al., 2010).

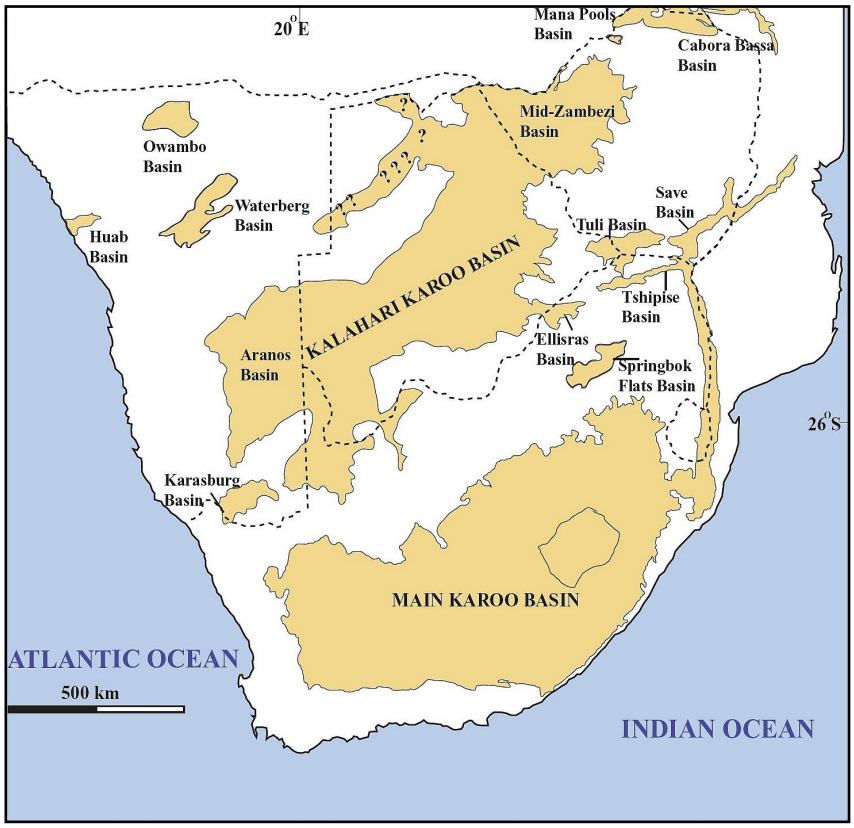


Figure 1.1 The distribution of Karoo-aged basins in southern Africa (after Johnson et al., 1996).

The Karoo-aged rocks of South Africa have been relatively well studied; largely because of the abundant terrestrial vertebrate fossils found in these rocks, extensive exposure, fairly complete stratigraphic succession, extensive flood basalts and coal resources (Smith, 1990; Smith et al., 1993; Hancox and Rubidge, 2001; Neveling, 2002; Catuneanu et al., 2005; Rubidge, 2005; Johnson et al., 2006; Bordy et al., 2010). The Main Karoo Basin has therefore been considered the reference basin with which all other Karoo-aged sequences are compared (Smith et al., 1993; Johnson et al., 1996). In contrast little is known about Karoo-aged sedimentary basins in the Southern African Development Community (SADC) region, mainly due to extensive cover by Kalahari Group sands during the latest Mesozoic and Cenozoic times (Catuneanu et al., 2005; Haddon and McCarthy, 2005). Large parts of the Kalahari Karoo Basin (Botswana) are covered by the Kalahari Group sediments and knowledge of their nature and extent is limited to borehole studies (Haddon and McCarthy, 2005). This dearth of knowledge impeded inter-basinal and cross-border correlation as well as the understanding of tectonic framework controlling the deposition of these rocks in southern Africa. As a result, the Council for Geoscience (CGS), Botswana Department of Geological Survey (BDGS) and the Namibian Geological Survey Department (NGSD) developed a joint cross-border Karoo correlation project entitled: 'The Tri-Nations Karoo Basin Correlation Project'. The main purpose of this collaborative project is to establish a broad improved correlative framework for Karoo-aged sequences in South Africa, Botswana and Namibia, with the primary research focus on rocks of the Kalahari Karoo Basin. The current study forms part of the Tri-Nations Karoo Basin Project and is specifically intended to address questions of intrabasinal correlation, depositional environments and sediment source areas in the Kalahari Karoo Basin.

1.2 Tectonic framework of the Karoo-age basins across southern Africa

The Karoo-aged basins formed during a first order cycle of supercontinent assembly and subsequent breakup when Pangaea was under the influence of two different tectonic regimes sourced from the convergent (southern) and divergent (northern) margins of Gondwana (Rust, 1975; Bumby and Guiraud, 2005; Catuneanu et al., 2005). These two tectonic regimes resulted in the formation of different basin types across Africa, with accommodation generated by tectonic and dynamic loads in the south and rifting to the

north (Catuneanu et al., 2005). The tectonic regimes in the convergent margin of Gondwana were characterised by shallow-angle subduction of the palaeo-Pacific plate beneath the supercontinent resulting in the formation of a retroarc foreland system in South Africa and related foreland basins in South America, Antarctica and Australia (Catuneanu and Elango, 2001; Fig. 1.2, 1.3). North of the Main Karoo Basin structural control changed, giving away to extensional regimes along the eastern side of the African part of Gondwana and to syneclisic type sag basins on the western part (Rust, 1975; Catuneanu et al., 2005). Therefore, the dividing line between the two regimes is followed roughly by the present watershed of the Congo River (Catuneanu et al., 2005).

The eastern basin region developed a complex rift system, which extended from the Zambesi River (Cabora Bassa Basin) to the Horn of Africa and the southern margin of the Arabian Peninsula (Catuneanu et al., 2005). From south to north, the rift system comprises the Luangwa and Lukasashi basins in Zambia, some remnant basins (the Metangula basin) in northern Malawi, straddling Mozambique and Tanzania, the Ruhuhu, Illima, Galula and Selous basins in Tanzania and the Tanga or Duruma Basin, which overlaps the border between Tanzania and Kenya (Wopfner, 2002; Catuneanu et al., 2005). The tectonic history of these rift basins is reflected in their lithofacies successions, which show close resemblance to one another, indicating that their evolution was controlled by similar forces (Catuneanu et al., 2005).

The Karoo basins in the western region are not as well studied as their counterparts in the east, largely because of extensive cover of younger sediments. Thus information on the deeper parts of the basin is restricted to a few boreholes (Rust, 1975; Catuneanu et al., 2005). The western region basins are interpreted as sag basins that developed in depressions between the dividing ridge and hypothetical rift shoulder thermal swells associated with the pre-opening history of the Atlantic Ocean (Catuneanu et al., 2005), with the Congo Basin as the best developed example (Johnson et al., 1996). They represent tectonically much quieter environments compared to the eastern rift basins, and exhibited slower subsidence rates (Catuneanu et al., 2005).

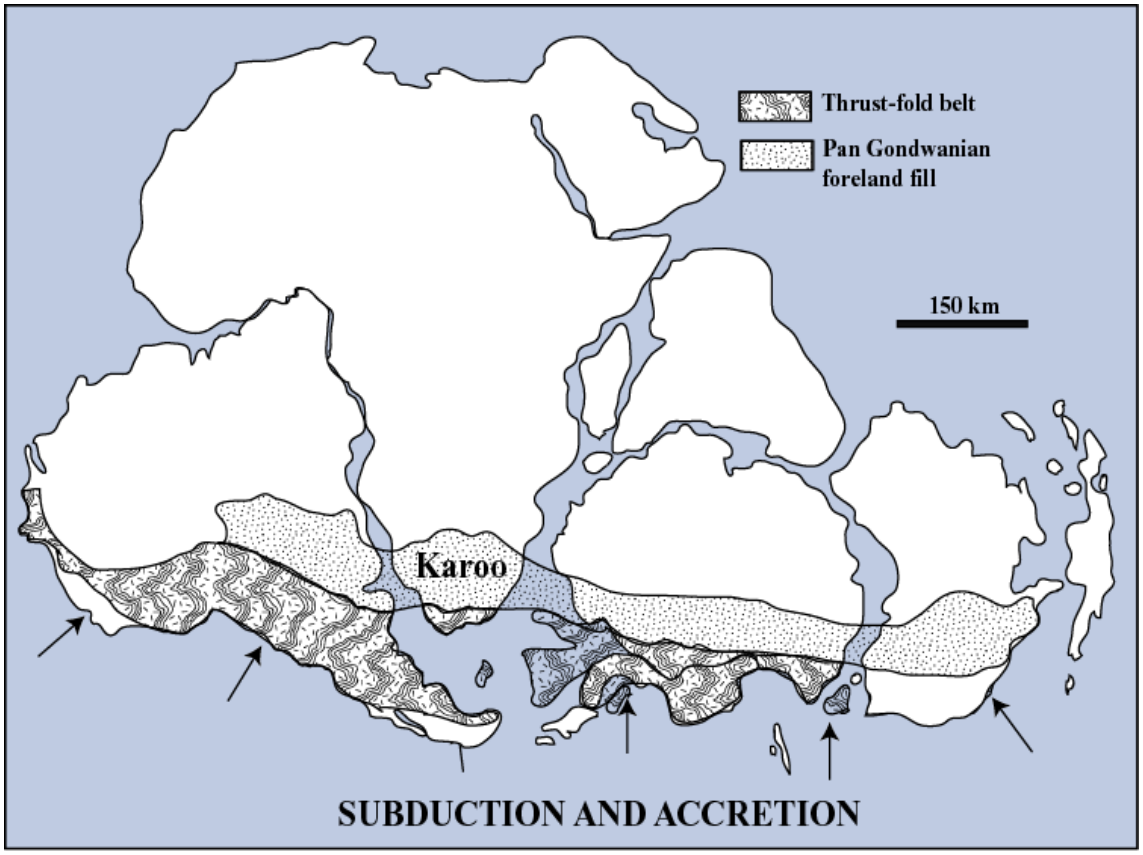


Figure 1.2 Pan-Gondwanian foreland system generated through compression, collision and terrain accretion along the southern margin of Gondwana and the associated foreland basins (modified after Catuneanu and Elango, 2001).

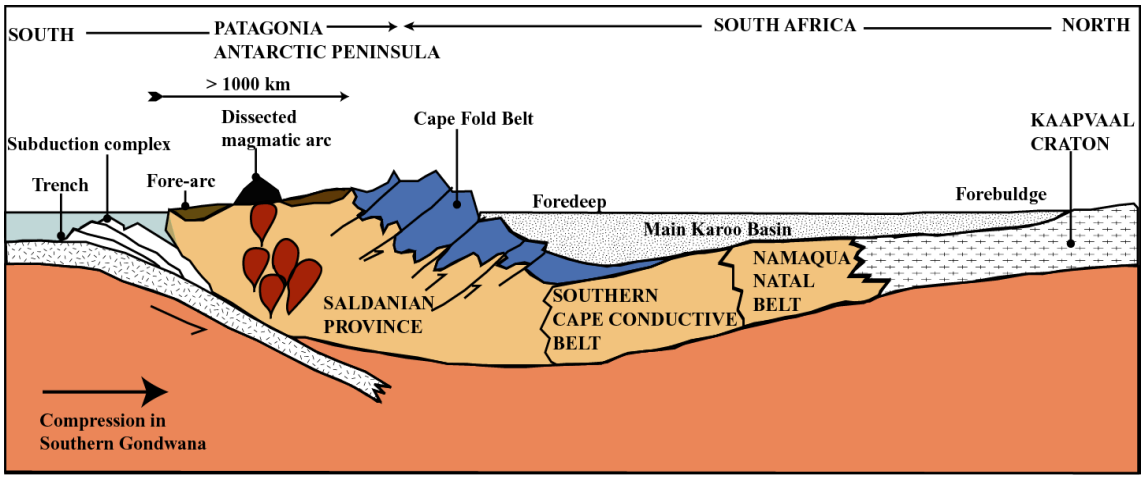


Figure 1.3 Generalised model of the Main Karoo Foreland Basin in relation to the Cape Fold Belt, and the inferred position of the magmatic arc and subduction zone in the south (modified after Turner, 1999).

1.3 Stratigraphic review of southern African Karoo-aged basins

The Karoo Supergroup in southern Africa comprises rocks which were deposited successively in glacial, deep marine (including turbidite), shallow marine, deltaic, fluvial, lacustrine and aeolian environments (Johnson et al., 1996). In southern Africa, the Karoo Supergroup comprises five groups: the basal Dwyka followed by the Ecca and Beaufort groups, Molteno, Elliot and Clarens formations and the Drakensberg Group (Smith et al., 1993; Johnson et al., 2006).

Smith et al. (1993) reviewed the stratigraphy and sedimentary environments of all the Karoo-aged basins in southern Africa and recorded changes in the tectono-climatic framework of the Karoo basins of the south-western Gondwana from the late Carboniferous through to the early Jurassic. Johnson et al. (1996) provided an overview of the stratigraphic correlations of the Karoo Supergroup in basins throughout southern Africa, pointing out that the Main Karoo Basin of South Africa developed as a retro-arc foreland basin and that the rest of the basins are intracratonic sag basins or rift basins (Catuneanu et al., 2005).

1.3.1 The Main Karoo Basin of South Africa

The Main Karoo retroarc foreland basin is underlain by a stable basement comprising the Kaapvaal Craton in the north and the Namaqua-Natal Metamorphic Belt in the south, and bounded in the south by a fold thrust belt (Cape Fold Belt; Johnson et al., 2006). It contains volcanic and sedimentary rocks of the Karoo Supergroup which range in age from Late Carboniferous to Middle Jurassic (Johnson et al., 1997). The Karoo Supergroup preserves a maximum thickness of 12 km in the southeastern portion of the Main Karoo Basin (Johnson et al., 1996, 1997; Catuneanu et al., 2005, Johnson et al., 2006). At present, the basin is about 700000 km^2 in areal extent, but was much more extensive during the Permian (Johnson et al., 2006).

The Karoo Supergroup overlies the Ordovician to Early Carboniferous Cape Supergroup sedimentary rocks in the southwest and unconformably or paraconformably overlies the Natal Group and Msikaba Formation in the east. It unconformably onlaps onto

Precambrian rocks in an inland and northeastward direction (Exploration Consultants Limited, 1998; Johnson et al., 2006).

1.3.1.1 Stratigraphy and depositional environments of the Main Karoo Basin

Deposition in the Main Karoo Basin began with the Late Carboniferous to Early Permian glacial deposits of the Dwyka Group, followed by the Permian Ecca Group which contains significant coal deposits associated with deltaic, continental slope and lacustrine deposits. The Ecca Group is overlain by the Middle Permian – Middle Triassic Beaufort Group consisting of fluvio-lacustrine rocks (Bumby and Guiraud, 2005; Johnson et al., 2006).

Rocks of the Beaufort Group are in turn overlain by the Late Triassic Molteno Formation which was deposited under seasonally warm to humid climatic conditions, in a broad, perennial braided system associated with braidplain areas of limited extent (Hancox, 2000; Bordy et al., 2005; Bumby and Guiraud, 2005). In contrast, the overlying argillaceous Elliot Formation was deposited by high and low sinuosity fluvial systems under semi-arid climatic conditions (Hancox, 2000; Bordy et al., 2005). Progressive aridification led to the deposition of aeolian dune complexes of the Clarens Formation (Smith et al., 1993; Johnson et al., 2006). Continental flood basalts of the Drakensberg Group are dated at 180 Ma and mark the initiation of Gondwana breakup and the end of the Karoo sedimentation (Smith et al., 1993; Pinetown et al., 2007).

1.3.2 The Kalahari Karoo Basin

The northeast-southwest trending Kalahari Karoo Basin occurs principally in Botswana and extends from southeast Namibia (Aranos Basin), into the Northern Cape Province of South Africa, through Botswana (the main part of the Kalahari Karoo Basin) into the western part of the Limpopo Province of South Africa (forming the Ellisras Basin), and is continuous with the Mid-Zambezi Basin in Zimbabwe (Cairncross, 1995; Key et al., 1998; Cairncross, 2001; Advanced Resources International, 2003; Fig. 1.1). This basin is considered to be an intracratonic basin that formed between the Windhoek Highlands (in the north) and the Cargonian Highlands (Fig. 1.4) in the south during Late Palaeozoic

times (Visser, 1995). It occurs along the southern extension of a structural zone that can be traced from the northeast Africa down to Namibia (Visser, 1995).

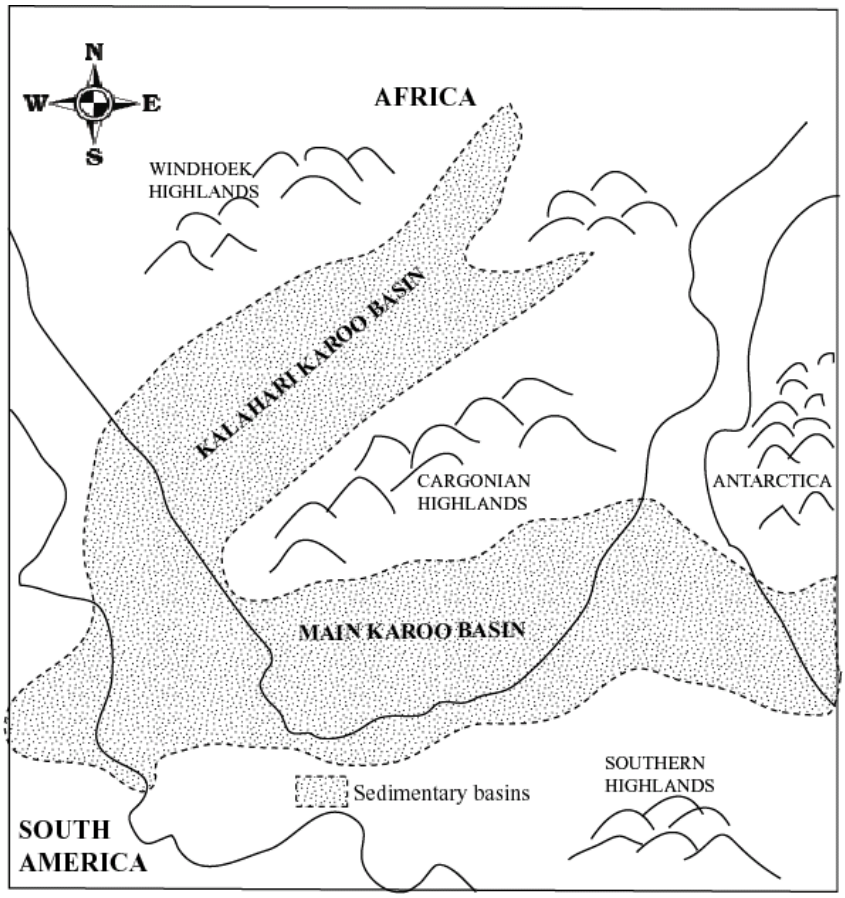


Figure 1.4 Continental configuration of the Southern Hemisphere during the late Palaeozoic times, showing the position of the Kalahari Karoo Basin and the Main Karoo Basin in relation to the Windhoek Highlands, Cargonian Highlands, Southern Highlands and South America and Antarctica (after Scheffler et al., 2006).

1.3.2.1 Previous studies on the Karoo Supergroup of the Kalahari Karoo Basin

Green (1966) described the regional stratigraphy of the Karoo succession in Botswana (then called the Karoo System in Bechuanaland) and considered the sequence to be lithostratigraphically correlateable to the South African Karoo sequence. During the 1970s a reconnaissance aeromagnetic survey and geological interpretation of Botswana was undertaken to outline the depth and structure of basement rocks and to determine the nature and thickness of the overlying Kalahari Group and Karoo Supergroup with a view to assess the economic potential in the Kalahari Karoo Basin (Reeves, 1978).

Regional geophysical studies also played a further important role in the geological exploration of the Kalahari Karoo Basin in Botswana. The Botswana Geological Survey and Terra Surveys Limited reviewed geophysical data related to the broad geological structure of southern Africa looking for areas with high potential for economic mineralisation within the Kalahari Karoo Basin (Hutchins and Reeves, 1980).

Shell Coal Botswana carried out a reconnaissance drilling programme in the Ncojane area, southwest Botswana during the late 70's with the purpose of investigating the possible coal potential of this relatively unknown part of the Karoo sequence (Clark et al., 1986). This was followed by "The Kalahari Drilling Project" (1981-1982) in western and northern Botswana, where several boreholes were drilled, most of which penetrated the Karoo sequence and confirmed the existence of a relatively continuous coal-bearing Karoo sequence throughout western Botswana (Meixner and Peart, 1984).

More detailed lithostratigraphic studies of the Karoo Supergroup in Botswana was undertaken by Smith (1984), who compiled a report (Bulletin 26) based on the geophysical and geological results of follow-up drilling to the Aeromagnetic Survey of Botswana and also on coal exploration boreholes (Smith, 1984; Modie, 2000). Smith (1984) proposed seven sub-basins in the Kalahari Karoo Basin (Fig. 1.5), based on the geological setting related to the basement features and also to facies changes. The lithostratigraphy proposed by Smith (1984) now forms the basis for the stratigraphic correlation of the Karoo Supergroup in the Kalahari Karoo Basin of Botswana (Modie, 2007).

The stratigraphy of the Karoo Supergroup rocks in the Aranos Basin (Gemsbok Sub-basin, southeast Namibia) was also studied based on boreholes drilled for coal exploration during the early 1980's (Kingsley, 1985; Hegenberger, 1992). Kingsley (1985) provided a detailed sedimentological and stratigraphical analysis of the Ecca Group using 66 boreholes drilled by CDM Mineral Surveys, Gold Fields Prospecting Company (Pty) Limited, Agip Coal USA Inc and Impala Coal. The study provided information to build a sedimentological model of the Aranos Basin.

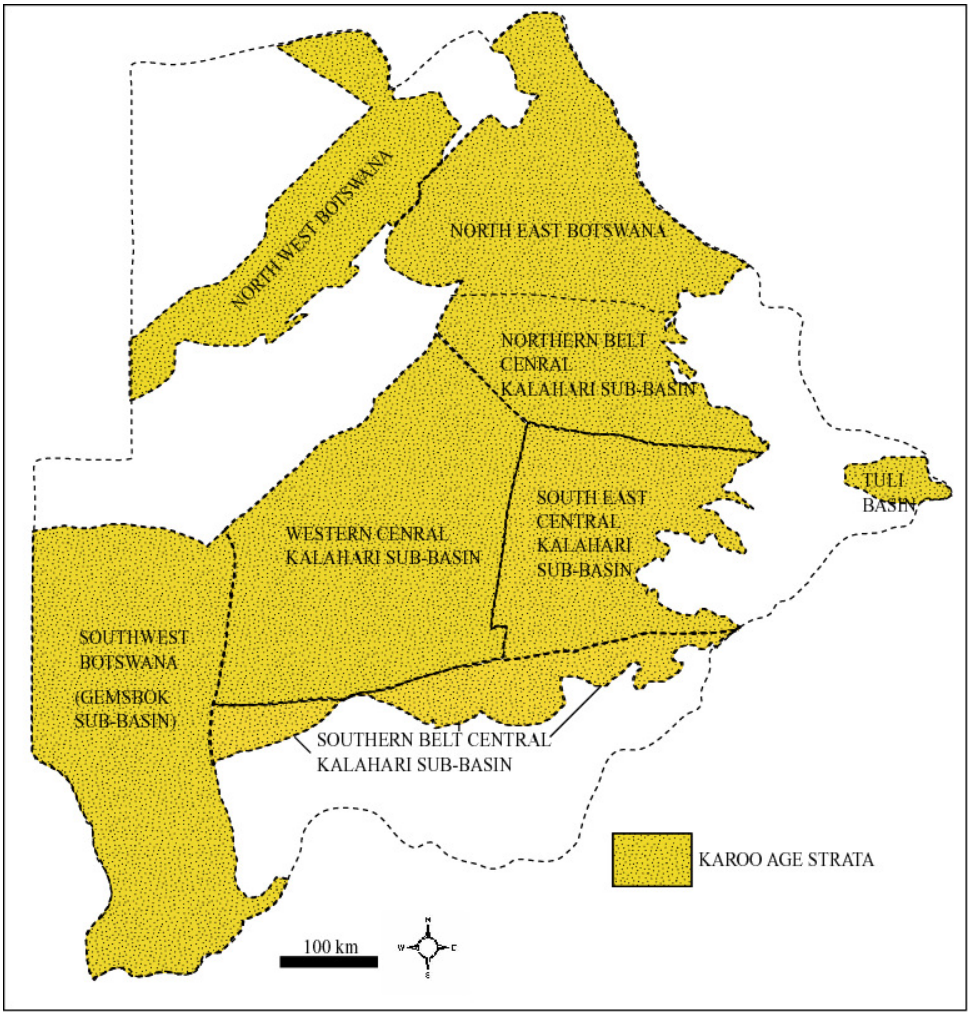


Figure 1.5 Karoo sub-divisions in Botswana (after Smith, 1984).

The Petro-Canada International Assistance Corporation conducted a reconnaissance seismic survey on behalf of the Botswana Government in 1987 and 1988. This survey was done in the Nossob-Ncojane Basin (Gemsbok Sub-basin) and Passarge Basin where five boreholes (W3, CKP8C-1, Vreda 281, CKP6 and CKP6A) in the area were used for seismic data collection. The seismic data interpretation and conclusion showed that the crust thickens towards the southeast as the Kalahari Line (a geophysical lineament along the 22°E meridian that separates the deep magnetic basement in the west from the shallow magnetic basement to the east [Reeves, 1978]) is approached. At the same time, the sedimentary cover progressively thins to the east suggesting that the western edge of the Kaapvaal Craton is a Precambrian, extended margin and that the thinned Kaapvaal crust extends westward under western Botswana at least as far as the Namibian border (Wright and Hall, 1990; Stoakes and McMaster, 1990).

Haverslew (1987) studied the petrography drill core samples from boreholes W2, W3, CKP8C-1, CKP6 and CKP6A, to evaluate primary composition and texture of sandstones, textural and compositional maturity of sediments, depositional environments, diagenetic mineralogy, lithology, porosity and permeability of the sandstones and useful parameters for future regional correlation.

Dolby (1990) contributed to the biostratigraphy of the Karoo Supergroup in the Gemsbok Sub-basin by studying palynology and micropalaeontology of one of the deepest boreholes (Masetlheng Pan-1 or MP1) drilled in southwest Botswana. The occurrence of two rich pollen-spore assemblages and rare foraminifera zones were recorded from the lower Karoo Supergroup (i.e., Dwyka to lower Ecca). The lower zone (Dwyka) is of Late Carboniferous (Gzhelian-Kasimovian) age and the upper zone (lower Ecca) is assigned to an Early Permian (Sakmarian-Asselian) age.

Haverslew (1990) studied the petrography of the chip samples from the MP1 borehole, and found that the Dwyka Group consisted mainly of tillites whereas the Ecca Group was dominated by arkosic and subarkosic sandstones which were capped by a dolerite sill. Stoakes and McMaster (1990) recorded a transitional sequence from the Dwyka Group into the Ecca Group in MP1 borehole, with two upward-coarsening sedimentary successions overlying the Dwyka Group (Key et al., 1998).

Grill (1997) undertook a detailed facies analysis of various sedimentary units exposed in outcrops and the Vreda 281 borehole. He developed a sequence stratigraphic framework and proposed depositional environments for the Permo-Carboniferous glacial to marine Karoo record in southern Namibia.

Exploration Consultants Limited (1998) developed a regional palynozonation scheme which was based on palynological analyses of borehole and field samples of Lower and Upper Karoo sequences from Namibia, Botswana, Zimbabwe and Zambia, and published literature on South African Karoo palynology. The palynomorphs indicated a Permian age for the Lower Karoo sequences (Exploration Consultants Limited, 1998). This company also carried out a technical evaluation of the petroleum potential of the Karoo sequence of

Botswana (Exploration Consultants Limited, 1998). This study resulted in the identification of the deepest parts of Karoo sub-basins such as Mmashoro and Lephephe Lows' which were identified for further petroleum and Coal Bed Methane exploration.

Key et al. (1998) presented palynological data from two boreholes drilled in southern Botswana (Tshabong area), which penetrated Lower Karoo strata. The palynological studies indicated that the Dwyka glaciation in the southeastern part of the Gemsbok Sub-basin lasted from ~303 Ma to about 280 Ma (Late Carboniferous to the Early Permian) and the age of the overlying Ecca Group ranges from Early to Late Permian. The Kwetla Formation in southern Botswana is correlated with the Beaufort Group in the Main Karoo Basin on the basis of palynological results (*Protohaploxypinus*, *Striatopodocarpites* and *Weylandites*), which show close correlation with the Biozone F, identified as Late Permian in the Mikambeni Formation of the Soutpansberg/Pafuri Basin (Key et al., 1998).

Bangert et al. (1999) published radiometric ages from ash-fall tuffs in the glaciogenic Carboniferous-Permian Dwyka Group of Namibia and South Africa, providing ages of 302 ± 3.0 Ma for the Namibian Dwyka and 288 ± 3.8 Ma for the Prince Albert Formation of South Africa.

Advanced Resources International in association with Scales Associates and the Department of Geological Survey of Botswana, undertook preliminary coalbed methane studies between 2001 and 2003. The main study investigated the availability and potential for development of natural gas resources associated with the coal-bearing sequences of the Kalahari Karoo Basin (Advanced Resources International, 2003). The major findings of this study indicated considerable coalbed methane and gas shale resources in the eastern part of the Kalahari Karoo Basin. In the western part of the Basin coal seams are thin and hence this area is not highly prospective for coalbed methane gas (Advanced Resources International, 2003).

Catuneanu et al. (2005) have established vertical profiles that define the sedimentary fill of the Karoo basins in the Kalahari Karoo Basin and other Karoo-aged basins in south-central

Africa (Fig. 1.6). These vertical profiles define the lithostratigraphic subdivisions of the Karoo Supergroup and their large-scale correlation.

Miller (2005) compiled a report, geological maps and borehole cross sections of the Stampriet Artisian Basin (SAB) which is considered part of the Aranos Basin. The report provides an outline of the post-Dwyka Karoo succession in the SAB recognising the Nossob Formation at the base followed by Mukorob Formation, Auob Formation, the Rietmond Formation, Neu Loore Formation, Kalkrand Basalt Formation, Karoo dolerites and the Kalahari Group sediments on top. In a subsequent publication, Miller (2008) presented all geological data such as geological maps and borehole cross-sections of the Stampriet Artisian Basin (SAB) and across the Aranos and Karasburg Basins. He presented an idealised stratigraphic section through the Dwyka Group of the Aranos and Karasburg Basins showing the four deglaciation sequences that make up the group, thus revising work done by Heath (1972), Grill (1997) and Bangert et al. (2000). Miller also provided a detailed description of the evolution of the Aranos and Karasburg Basins.

Modie and Le Hérissé (2009) studied and described palynomorphs for biostratigraphic classifications of Late Carboniferous to Permian strata of the Lower Karoo sequence in two borehole sections, STRAT 1 (in the southwest Botswana) and CKP 6 (in the Central Kalahari Karoo Basin). The two borehole sections contain well preserved pollen and spore palynomorphs. Three assemblage zones common to both sections were identified: the *Hamiapollenites bullaeformis* Biozone, the *Cyclogranisporites gondwanensis* Biozone and the *Platysaccus papilionis–Striatopodocarpites fusus* Biozone, in ascending order of stratigraphy. The three assemblages were compared and correlated with assemblages described from other Gondwana areas of Africa, Australia, Arabia, South America and Antarctica. Detailed analysis of taxa from the Kalahari Karoo Basin indicated a distinct similarity with assemblages from the Paraná Basin of South America and yielded age range from the Late Carboniferous (Kasimovian–Gzhelian) to latest Early or possibly earliest Middle Permian (Late Cisularian to Early Guadalupian).

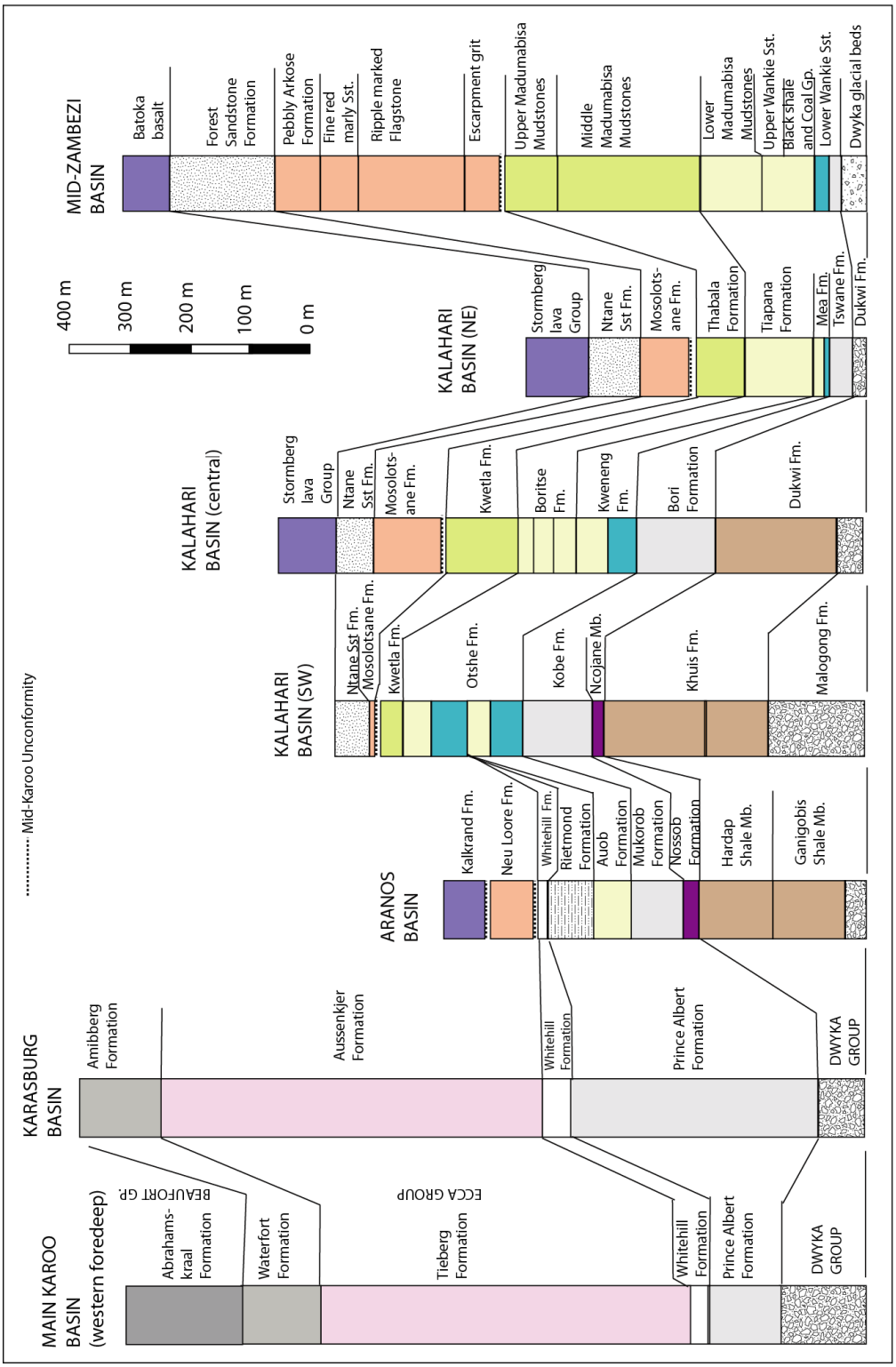


Figure 1.6 Correlation panel of the Karoo Supergroup lithostratigraphic units from the Main Karoo Basin (western foredeep) through the Aranos , Kalahari Karoo basins (modified after Catuneanu et al., 2005).

1.3.2.2 Stratigraphy of the Kalahari Karoo Basin

Large parts of the Karoo Supergroup rocks in the Kalahari Karoo Basin are covered by sedimentary rocks of the Cenozoic Kalahari Group (Smith, 1984). The extent of the Karoo rocks is known only from aeromagnetic surveys and water and mineral exploration boreholes (Smith, 1984; Modie, 2007; Miller, 2008). Due to a well-exposed and complete Karoo stratigraphy in the Main Karoo Basin and similarities between these sequences, the South African group nomenclature for the Karoo Supergroup (Dwyka, Ecca and Beaufort groups) has been utilised in the Kalahari Karoo Basin, although Formation names are different (Modie, 2007). Lithostratigraphically, the Kalahari Karoo Basin is informally sub-divided into the Lower and Upper Karoo, separated by a regional Mid-Karoo unconformity (Smith, 1984; Exploration Consultants Limited, 1998; Fig. 1.7).

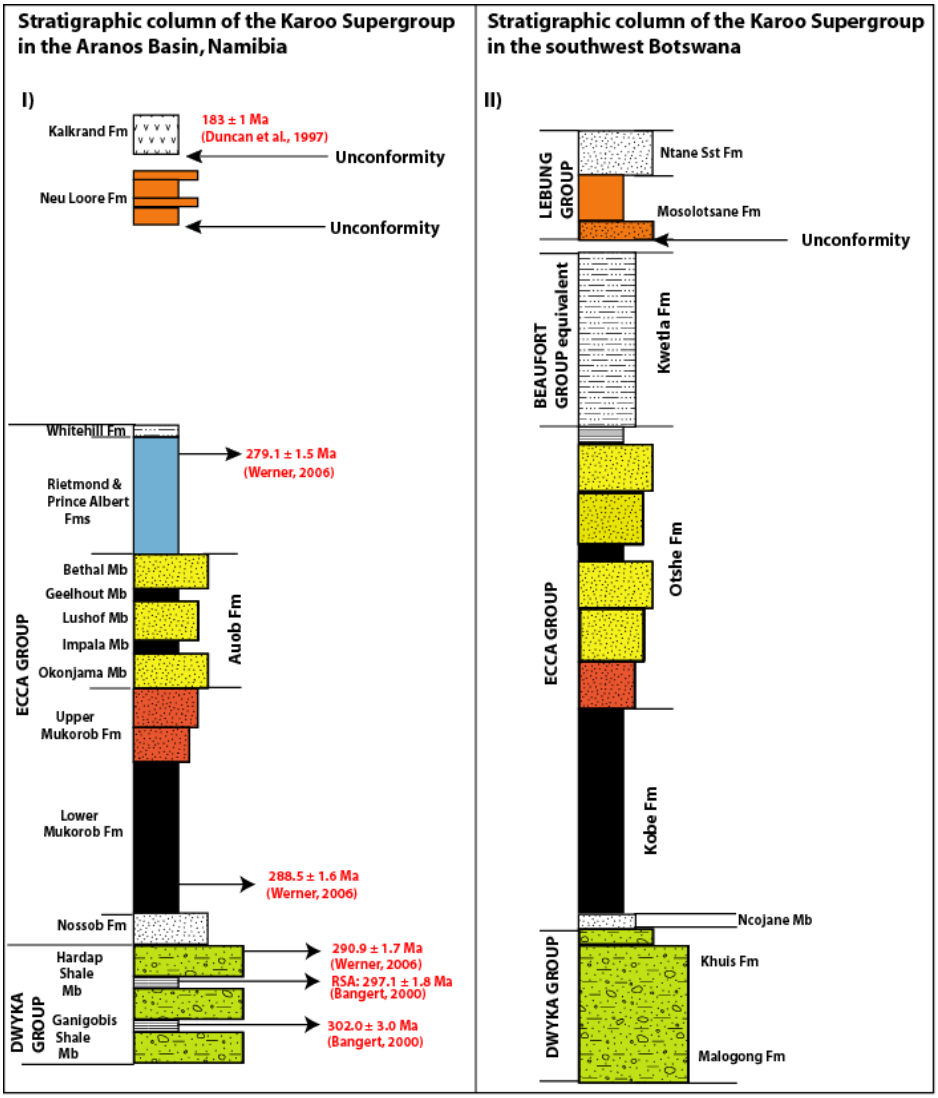


Figure 1.7 Generalised stratigraphic columns of the Karoo Supergroup in the Aranos Basin (I) and southwest Botswana (II) (modified after Key et al., 1998; Miller, 2008).

The Lower Karoo comprises the basal Dwyka Group, overlain by the Ecca Group and the Beaufort Group equivalent and the Upper Karoo comprises the Lebung Group followed by the Stormberg Lava Group (Smith, 1984; Exploration Consultants Limited, 1998). This succession records basal glacial diamictites of the Dwyka Group through fluvio-deltaic sandstone and mudrock units interbedded with coal beds of the Ecca Group, siltstone and mudrock lacustrine facies of the Beaufort Group equivalent, followed by the fluvial and aeolian red beds of the Lebung Group, and the basalt lava flows of the Stormberg Lava Group (Smith, 1984; Smith et al., 1993; Johnson et al., 1996; Modie, 2007; Bordy et al., 2010; Fig. 1.7).

1.3.2.3 Karoo Supergroup sub-divisions in Botswana

Smith (1984) spatially sub-divided the Karoo Supergroup in Botswana, along with the Tuli Basin (Zimbabwe and South Africa), into 7 sub-divisions based on geological setting and facies changes (Fig. 1.5, 1.8). These are: (1) western, (2) southeast, (3) southern and (4) northern belts of the Central Kalahari Sub-basin together with (5) southwest Botswana; (6) Northeast Botswana and (7) Northwest Botswana. Subtle lithostratigraphic differences were documented in each of these sub-divisions.

a) Central Kalahari Sub-basin

The Dwyka Group in the Central Kalahari Sub-basin is represented by the Dukwi Formation, which shows extreme thickness variations due to palaeotopographic influences (Green, 1966; Smith, 1984). Borehole data indicate a maximum thickness of 258 m for the Dukwi Formation. It has a basal unit which consists of stratified diamictites, conglomerates and sandstones (Smith, 1984). This is overlain by the fine-grained sandstone of the middle unit, while the uppermost unit consists of mudstones, siltstones, diamictites, fissile black shales and sandstones (Smith, 1984).

The Ecca Group comprises three formations. The basal Bori Formation is dominated by grey-black shale with intercalations of siltstone and sandstone in a upward-coarsenings sequence. The overlying Kweneng Formation consists of medium-to-coarse-grained feldspathic sandstone with dark grey siltstone and subordinate mudstone in a upward-

finings succession. The uppermost Boritse Formation is a sequence of alternating carbonaceous mudstones, coals, siltstones and coarse-grained sandstones (Smith, 1984).

The Kwetla Formation is conformably overlies the carbonaceous mudstones of the Boritse Formation and it is unconformably overlain by the Mosolotsane Formation (Smith, 1984). It consists of pale grey and greenish siltstone and mudstone which are commonly calcareous and non-carbonaceous (Smith, 1984).

The Lebung Group is divided into the lower Mosolotsane Formation and an upper Ntane Sandstone Formation. The Mosolotsane Formation is a fine- to medium-grained, well sorted, pinkish red to purplish grey sandstone unit with little mica and feldspar (Smith, 1984). The overlying Ntane Sandstone Formation is a fairly uniform sequence of pinkish to red-brown, fine- to medium-grained sandstone, primarily of aeolian origin. The two formations are covered by the basaltic lavas of the Stormberg Group (Smith, 1984).

<table>
<tr><th>GROUPS</th><th>SOUTH WEST BOTSWANA</th><th>KWENENG AND WESTERN CENTRAL KALAHARI</th><th>MMAMABULA</th><th>MORUPULE AND S.E. KALAHARI</th><th>NORTH EAST BOTSWANA AND NORTHERN BELT</th><th>NORTH WEST BOTSWANA</th><th>TULI BASIN, BOTSWANA</th></tr>
<tr><td>STORMBERG LAVA</td><td colspan="6">STORMBERG LAVA GROUP (undivided)</td><td>Bobonong Lava Formation</td></tr>
<tr><td rowspan="2">LEBUNG</td><td>Nakalatlou Sandstone.</td><td colspan="4">Ntane Sandstone Formation</td><td>Bodibeng Sandstone Formation</td><td>Tsheung Sandstone Formation</td></tr>
<tr><td>Dondong Fm.</td><td colspan="3">Mosolotsane Formation</td><td>Ngwasha Fm.
Pandamatenga Fm.</td><td>Savuti Formation</td><td>Thune Formation
Korebo Formation</td></tr>
<tr><td>BEAUFORT equivalent</td><td>Kule Fm.</td><td>Kwetla Fm.</td><td colspan="3">Tlhabala Formation</td><td>?</td><td rowspan="3">Seswe Formation</td></tr>
<tr><td rowspan="3">ECCA</td><td rowspan="2">Otshe Fm.</td><td rowspan="2">Boritse Fm.</td><td>Korotlo Fm.</td><td>Serowe Fm.</td><td rowspan="2">Tlapana Fm.</td><td rowspan="2">Marakwena Formation
Tale Formation</td></tr>
<tr><td>Mmamabula Fm.</td><td>Morupule Fm</td></tr>
<tr><td>Kweneng Fm.</td><td>Mosomane Fm.</td><td>Kamotaka Fm.</td><td>Mea Arkose Fm.</td><td>?</td></tr>
<tr><td>Kobe Fm.</td><td>Bori Fm.</td><td>Bori Fm.</td><td>Makoro Fm.</td><td>Tswane Fm.</td><td>?</td><td>Mofdiamogolo Formation</td></tr>
<tr><td rowspan="3">DWYKA</td><td>Middlepits Fm.</td><td colspan="3" rowspan="3">DUKWI FORMATION</td><td rowspan="3">?</td><td rowspan="3">?</td></tr>
<tr><td>Khuis Fm.</td></tr>
<tr><td>Mmalogong Fm.</td></tr>
</table>

Figure 1.8 Lithostratigraphy of the Karoo Supergroup in the Kalahari Karoo Basin of Botswana (modified after Smith, 1984; Bordy et al., 2010).Thick dashed line below the Lebung Group indicates the Mid-Karoo unconformity.

b) Northeast Botswana

The basal Karoo Supergroup in the northeast Kalahari Karoo Basin is represented by the Dukwi Formation which consists of diamictites (Smith, 1984). The Ecca Group is sub-divided into three formations; the lower Tswane Formation, middle Mea Formation and upper Tlhapana Formation. The Tswane Formation has been identified in several boreholes

in northeast Botswana; it comprises grey and black mudstones and siltstones that conformably overlies the Dukwi Formation. The Mea Arkose Formation is defined as the base of the coarse-grained feldspathic sandstones which overlies the Tswane mudrocks or the basement rocks (Smith, 1984). Overlying the Mea Arkose Formation is the Tlapana Formation which contains carbonaceous mudstones and coal seams with subordinate sandstone and grey-brown mudstones (Smith, 1984).

Overlying the Ecca Group in the northeast Kalahari Karoo Basin is the Beaufort Group equivalent consisting of the Tlhabala Formation, which is a 91 m thick unit, dominated by dark grey basal mudstone with minor carbonaceous partings, coaly streaks and siltstone lenses (Smith, 1984). The Lebung Group overlies the Tlhabala Formation and is represented by two sandstone formations: the underlying Mosolotsane Formation dominated by purplish muddy siltstones, sandstones, marls, and conglomerates and the overlying Ntane Sandstone Formation consisting of fine-grained, well sorted, porous sandstone representing a uniform, widespread aeolian unit. The Stormberg Lava Group overlies the Karoo Supergroup in the northeast Kalahari Karoo Basin (Smith, 1984).

c) Northwest Botswana

In northwest Botswana, the Karoo sequence is preserved in northeast-southwest trending grabens within the pre-Karoo basement (Smith, 1984). Owing to the lack of outcrop, the distribution of the Karoo sequence is not well known but borehole data shows it to comprise rocks of the Ecca Group, Lebung Group and the Stormberg Group (Smith, 1984). The Dwyka Group is confirmed to be absent. The Tale Formation at the base of the Ecca Group comprises conglomerates, coarse-grained sandstone and dark grey mudstones and is overlain by the Marakwena Formation consisting of bedded conglomerates and sandstones intercalated with minor silty mudstones (Smith, 1984).

The overlying Savuti Formation is a succession of red mudstones, poorly bedded pale-pink-brick red muddy siltstone (Smith, 1984). The basal part of the Formation contains white and pinkish calcite concretions which partly surround the few scattered extra-formational pebbles (Smith, 1984). The succeeding Bodibeng Sandstone Formation of the Lebung Group is dominated by fine-grained, well sorted and reddish sandstones with

subangular and subrounded detrital grains and it has been interpreted to represent aeolian deposits (Smith, 1984). This succession is overlain by the Stormberg Lava Group (Smith, 1984).

d) Tuli Basin

The Tuli Basin of the Kalahari Karoo Basin lies in eastern Botswana and extends eastward into Zimbabwe (the Mazunga Basin) and South Africa (Tuli-Sabi Trough) (Smith, 1984; Modie, 2000). The Karoo succession in the Tuli Basin is isolated from the Central Kalahari Sub-basin but it is believed to have been connected in earlier times to the Central Kalahari Sub-basin (Smith, 1984). In the Tuli Basin, the Karoo Supergroup overlies the Early Precambrian rocks of the Limpopo Mobile Belt (Smith, 1984). Post-Karoo fault systems trending east, northeast-west and south-west and parallel to the basin axis characterise the northern limit of the Karoo outcrop in the Tuli Basin (Smith, 1984). The Dwyka Group is absent in the Tuli Basin of Botswana, and as a result the Ecca Group rocks overlie an angular unconformity with the Precambrian basement (Smith, 1984). Two formations are recognised in the Ecca Group: the Mofdiahologolo Formation and Seswe Formation (Smith, 1984; Bordy and Catuneanu, 2002).

The Mofdiahologolo Formation comprises basal mudstones, argillaceous sandstones with 10% component of coarse sand and pebbles which coarsens towards the base, followed by grey-brown mudstones, fine-grained sandstones and silty mudstones (Smith, 1984). The Seswe Formation comprises carbonaceous and non-carbonaceous mudstone formations and thin coals and it is further divided into two members: the lower carbonaceous-rich member with thin coals and the upper non-carbonaceous member. Overlying the Ecca Group is the Lebung Group sedimentary rocks (Smith, 1984).

The Lebung Group commences with a conglomeratic horizon which is in turn overlain by the Korebo Formation's siltstones and fine-grained sandstones with 'red bed' characteristics (Smith, 1984). The Korebo Formation of the Lebung Group is overlain by the Thune Formation which is a transitional sequence of fine-grained sandstones and siltstones intercalated with coarse-grained sandstones (Smith, 1984). The lower part of the Thune Formation comprises alternation of fine-grained and silty, well sorted sandstones

which are greyish to brown in colour and the upper part includes zones with dark green mottling, calacerous cement and limestone concretions (Smith, 1984).

Sedimentary rocks of the Tsheung Formation overlie the Thune Formation rocks, which is in turn overlain by the Bobonong Lava Formation. The Tsheung Formation comprises fine-grained, well sorted, and pink-brown to pale grey, massive sandstones (Smith, 1984). The Bobonong Formation forms the uppermost part of the Karoo Supergroup in the Tuli Basin and contains some distinctive basalts which are intercalated with sedimentary rocks (Smith, 1984).

e) Southwest Botswana (Gemsbok Sub-basin)

The southwest Botswana Sub-basin (commonly referred to as the Gemsbok Sub-basin) extends south and west into South Africa and Namibia respectively (Smith, 1984). Because the Cenozoic Kalahari Group sediments cover much of the Gemsbok Sub-basin, the Sub-basin was identified by aeromagnetic surveys, seismic data and stratigraphic boreholes (Reeves, 1978; Smith, 1984; Exploration Consultants Limited, 1998). The Karoo Supergroup in the Gemsbok Sub-basin (southwest Botswana) is subdivided into the basal Dwyka Group, followed by the Ecca Group, Beaufort Group equivalent and the upper Stormberg Group (Smith, 1984; Key et al., 1998; Modie, 2007).

The Dwyka Group comprises basal massive tillite units of the Malogong Formation which is 183 m thick. Overlying the Malogong Formation is the Khuis Formation, a 202 m thick sequence consisting of pebbly mudstones, black to grey fissile shales, calcareous sandstone, banded calcareous siltstone, varves, and siltstone (Smith, 1984; Carney et al., 1994; Exploration Consultants Limited, 1998).

The Ecca Group consists of two formations: the lower Kobe and the upper Otshe Formation. Massive, argillaceous, dark grey siltstones characterise the 75 m thick Kobe Formation, which also contain thin lenses of sandstones, silty mudstones, and a few bands of bright coal. *Eurydesma* (a shallow marine bivalve) is present in the siltstones of this unit (Smith, 1984; Exploration Consultants Limited, 1998). Conformably overlying these sediments is the 218 m thick Otshe Formation (Smith, 1984; Exploration Consultants

Limited, 1998). It is dominated by micaceous, fine sandstone interbedded with dark grey siltstone, coal, sub-arkosic sandstone with dark grey siltstone and mudstone in a upward-finings sequence. The Ecca Group is interpreted to represent shallow-water deposition formed initially during marine transgression and later as prodelta mud (Smith, 1984).

The Kwetla Formation has only been recognised in boreholes in the Kule-Ncojane area of southwest Botswana and is considered the equivalent of the Beaufort Group in the Main Karoo Basin (Smith, 1984; Exploration Consultants Limited, 1998; Key et al., 1998). The Kwetla Formation comprises basal fine-grained sandstone of approximately 15 m in thickness, grading into dark grey mudstone, up to 25 m thick, with subordinate sideritic and limonitic banded siltstone. Some silty micaceous bands and calcareous nodules are also present (Smith, 1984; Exploration Consultants Limited, 1998).

A diachronous unconformity separates the Lebung Group from the underlying Kwetla or Otshe formations (Smith, 1984). It consists mainly of red clastics that were deposited under oxidizing continental conditions (Smith, 1984). The Lebung Group is divided into two formations. The 9 m thick Mosolotsane Formation which consists of conglomeratic sandstone grading into an upper, 4 m thick red brown mudstone, is considered to have been formed in a fluvial environment (Smith, 1984; Bordy et al., 2010). This is overlain by the arenaceous Ntane Sandstone Formation which is equivalent to the Clarens Formation in the Main Karoo Basin of South Africa (Smith, 1984; Bordy et al., 2010). The overlying Stormberg Lava Group is correlated with the Drakensberg Group of the Main Karoo Basin in South Africa. It represents the youngest unit of the Karoo sequence in southwest Botswana and consists of volcanic rocks such as finely crystalline dark grey, black, brown or purple amygdaloidal or massive basalts (Carney et al., 1994).

1.3.2.4 The Karoo Supergroup in the Kalahari (Aranos) Karoo Basin, Namibia

There are five known regions of Karoo-age strata in Namibia and these are located in western Damaraland, Kaokoveld, Owambo, Otjiwarongo (Omatako) and the Aranos Basin portion of the Kalahari Karoo Basin in Namibia and the Karasburg Basin (Cairncross, 2001). The Aranos Basin (referred to as Stampriet Artesian Basin) forms part of the Gemsbok Sub-basin and extends from southeastern Namibia east into southwest Botswana

and south into South Africa (Miller, 2008). The Aranos Basin shares an aquifer with Botswana (southwest Botswana) and South Africa (north-western regions of South Africa), which is hosted in the Ecca Group rocks of the Karoo Supergroup and the Kalahari Group sediments (Ndengu, 2004). The Karoo strata in this region are covered extensively by sands, gravels and calcretes of the Kalahari Group, but outcrop along the northern, western and southern margins of the basin (Miller, 2008). The thickness of the Karoo Supergroup in the Aranos Basin increases towards the centre with especial steep gradient from the north (the Ghanzi Ridge; Hegenberger, 1992; Cairncross, 2001). The Karoo Supergroup in the Aranos Basin is subdivided into the basal Dwyka Group, overlain by the Ecca Group consisting of Nossob, Mukorob, Auob, Rietmond and the uppermost Neu Loore and Kalkrand formations (Miller, 2005; Miller, 2008). The Dwyka Group reaches thicknesses up to 460 m and consists of a basal Gibeon Formation, followed by the Zwartbas, Sommerau and Grϋndorner formations (Miller, 2008). These formations consist of basal diamictite deposited initially under glacial environments overlain by a mudstone sequence containing dropstones and fossils (bivalves, crinoid remains, starfish and gastropods), which are deposited under marine conditions (Hegenberger, 1992; Cairncross, 2001).

The Ecca Group has been subdivided into three formations: the lower arenaceous Nossob Formation (ranging between 6 m and 15 m in thickness and consisting of two upward-coarsening sandstone units with an intercalated shale zone), the middle, shaly Mukorob Formation (consisting of 75 m to 160 m dark greenish-grey shale) and the uppermost sandstone–rich Auob Formation (ranging in thickness between 100 m and 150 m, comprising coal seams and upward-coarsening deltaic sequences of medium-coarse-grained, often micaceous, sandstone with local intercalations of sandy shale) (Miller, 2005; 2008). The Nossob and Auob formations are known to host groundwater in the Aranos Basin (Ndengu, 2004; Miller, 2005).

The Auob Formation is subdivided into five units consisting of three aquifer sandstone members: they are the lower arenaceous Okonjama Member, the middle arenaceous Lushof Member and the upper arenaceous Bethal Member, separated by two thin carbonaceous shale members associated with coal (Miller, 2005). The lower bituminous shale and coal horizon is called the Impala Member and the upper bituminous shale and coal horizon, the

Geelhout Member (Miller, 2005). The main coal seam is located ~30 m above the base of the Auob sandstone, and the Upper seam, 50 m above the main seam (Cairncross, 2001). The Rietmond Formation overlies the Auob Formation (Miller, 2008) and is dominated by laminated dark grey shale with minor thin sandstone bands. The Rietmond shale is interpreted to have been deposited during a major transgression over the entire Aranos Basin (Miller, 2008). The Whitehill Formation overlies the Rietmond Formation and is well developed in the southwestern part of the Aranos Basin (Miller, 2008). It consists mainly of dark carbonaceous shale and mudstone (Cairncross, 2001; Miller, 2008). Fossils such as *Mesosaurus tenuidens*, a small crustacean *Notocaris tapscotti*, *Eurydesma mytloides*, *Glossopteris* leaves and petrified wood have been found in the Whitehill Formation (Miller, 2008). A major unconformity separates the Rietmond Formation from the Neu Loore Formation, uppermost sedimentary unit of the Karoo Supergroup in the Aranos Basin (Miller, 2005). The Neu Loore Formation comprises alternating coarse- to fine-grained, orange-red to orange brown micaceous sandstones and shales (Miller, 2005). The Karoo Supergroup in the Aranos Basin is capped by basalts of the Kalkrand Formation which are associated with dolerites (Hegenberger, 1992; Miller, 1992; Cairncross, 2001; Miller, 2008).

1.4 Provenance of the rocks in the Kalahari Karoo Basin

Glacial striations recorded from exposures in the Molopo River bed, situated south of the Gemsbok Sub-basin, suggest that the ice sheet was moving from the Central Kalahari Sub-basin in a south-western direction during early Karoo times (Smith, 1984; Fig. 1.9). The massive tillites intersected by boreholes in the southwest Botswana contain rock clasts that include white, pale grey and reddish meta-arkoses and quartzites interpreted to originate from the Olifantshoek Supergroup, Waterberg Group or Transvaal Supergroup, which are located south-southeast of the Gemsbok Sub-basin (Smith, 1984). The larger boulders found in these massive tillites are commonly pink syenite, granite, dolerite and other plutonic type-rocks (Smith, 1984).

Smith (1984) suggested that the Precambrian granite and gneiss complex basement to the south probably acted as a source of detritus for the Ecca Group in the Central Kalahari Sub-

basin based on the angular feldspathic nature of the clasts and garnet and mica content of the sandstones. Reworked sediments from the Waterberg Group situated to the south of Botswana may also have contributed to the infilling of the Central Kalahari Sub-basin (Smith, 1984). The basement rocks located north of the Central Kalahari Sub-basin are also believed to have acted as a source of sediment filling the Sub-basin (Smith, 1984). The Ncojane Sandstone Member of the Ecca Group in southwest Botswana appears to thin considerably southwards and especially eastwards; therefore Smith (1984) suggested that the source might have been located to the north or northwest in Namibia (Fig. 1.9). The siliclastic debris of the Karoo Supergroup from the eastern Kalahari Karoo Basin was predominantly derived from the Cargonian Highlands in the south with minor contributions from the eastern and the northern highlands (Scheffler et al., 2006; Fig. 1.4). Postulated palaeocurrent directions for the fine-grained sandstones and siltstones of the Beaufort Group equivalent in the Central Kalahari Karoo Basin show source areas located in the south (Smith, 1984; Fig. 1.9).

In Namibia, Palaeo-ice flow directions for the lower tillites of the Dwyka Group in the Aranos Basin show southerly and southwesterly flow directions (Stollhofen et al., 2000; Scheffler et al., 2006; Fig. 1.10). The Dwyka Group tillites, deposited by early glaciation in the Aranos Basin, contain clasts of the red Fish River Subgroup of the Nama Group and were probably sourced from the Windhoek Highlands to the north (Miller, 2008). Rocks of the Dwyka Group deposited by the second glaciation in the Aranos Basin have clasts derived from the east, which were deposited by westerly flowing ice from the Cargonian Highlands positioned to the south and southeast (Miller, 2008). Palaeocurrent data obtained from the turbidite and fluvial bar deposits of the Nossob Member and Ecca Group show source directions from the north and the northwest (Stollhofen et al., 2000; Fig. 1.10).

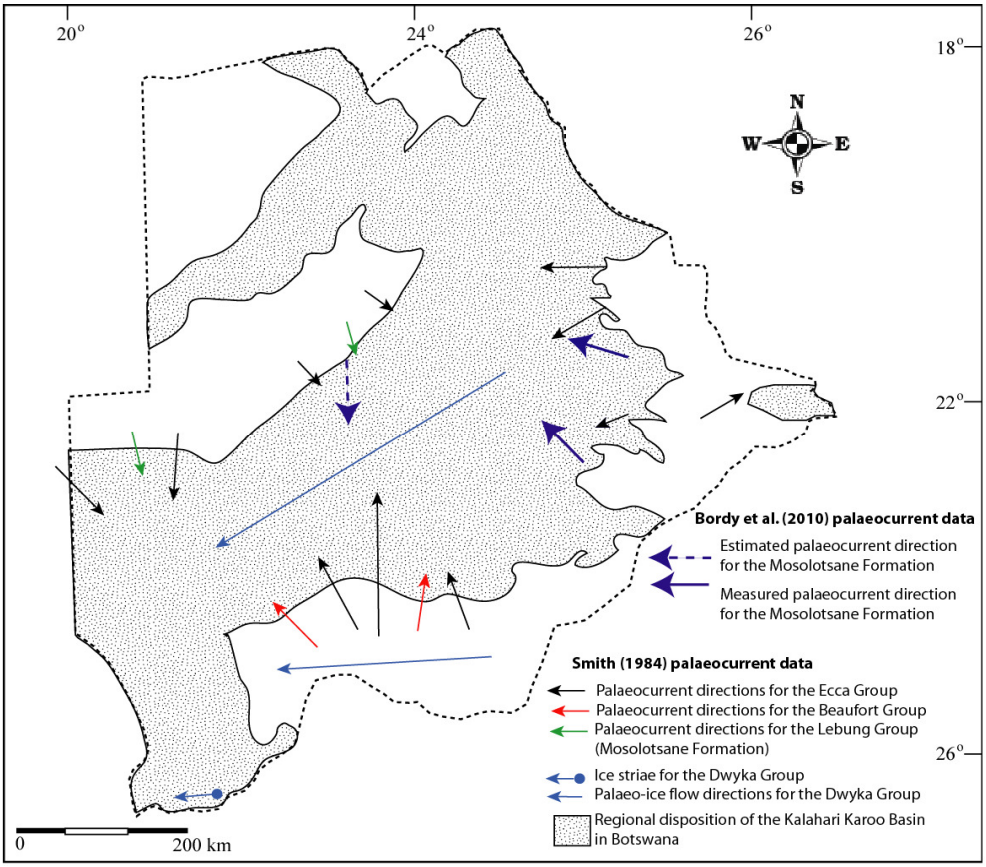


Figure 1.9 Palaeocurrent directions for the Dwyka Group, Ecca Group, Beaufort Group and the Lebung Group in the Kalahari Karoo Basin of Botswana (modified from Smith, 1984 and Bordy et al., 2010).

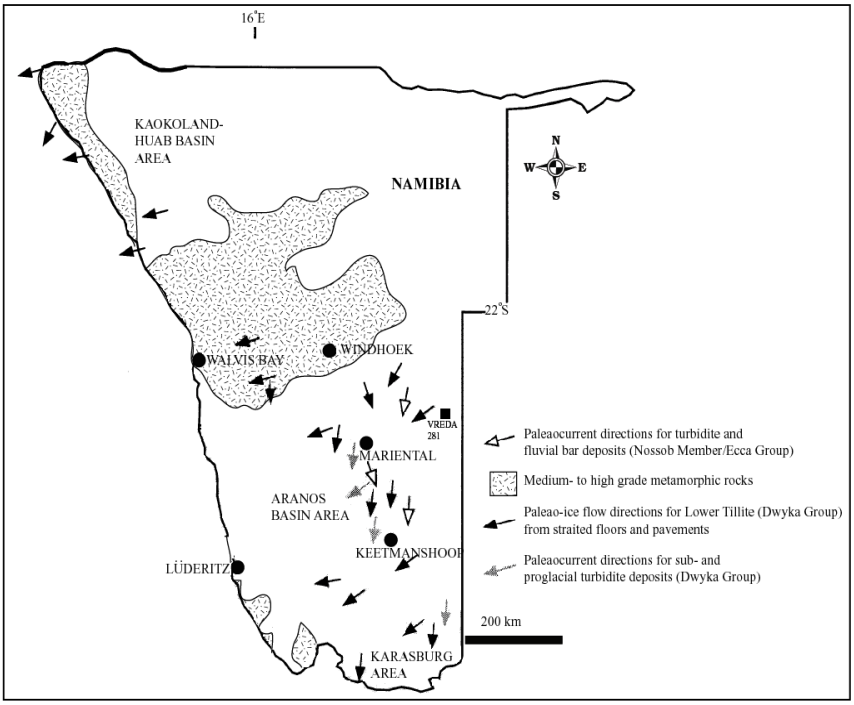


Figure 1.10 Palaeocurrent and palaeo-ice flow directions of the Ecca Group and the Dwyka Group in the Aranos Basin (after Stollhofen et al., 2000).

1.5 Structural framework of the Kalahari Karoo Basin

Most of the existing structural data of the Kalahari Karoo Basin has been obtained from geophysical data (i.e., aeromagnetic surveys and seismic profiles). The main structural features bounding the Kalahari Karoo Basin include: the Kalahari Line, Zoetfontein fault, Makgadikgadi Line, Ghanzi-Chobe Belt and the Damara Belt, Gariep Belt and the Karoo dolerite dyke swarm (Fig. 1.11). These major structures appear to have influenced the structural evolution and disposition of the Kalahari Karoo Basin as well as the distribution of the Karoo Supergroup within the basin (Exploration Consultants Limited, 1998; Modie, 2007).

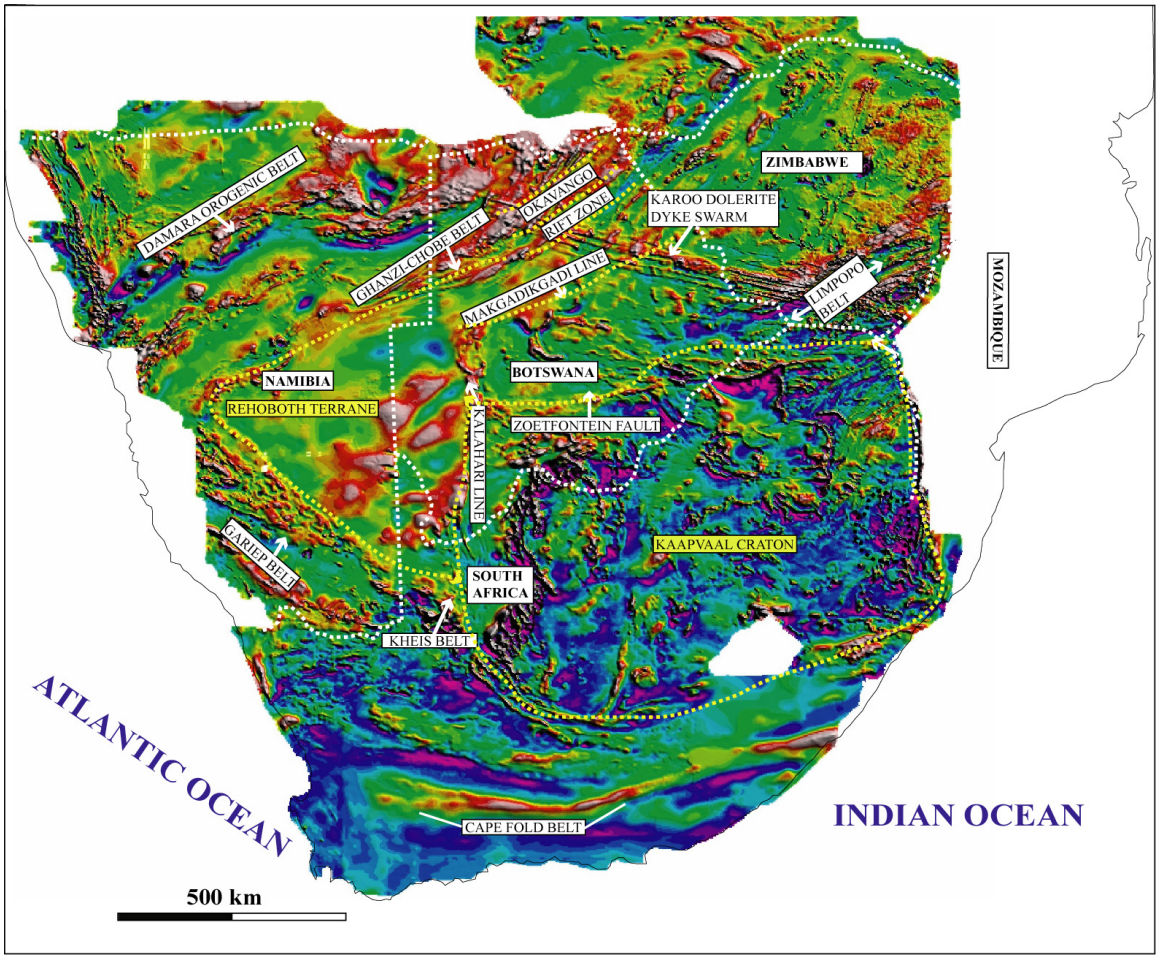


Figure 1.11 Geophysical map of southern Africa with major structural elements and cratons (source: Council for Geoscience).

1.6 Correlation of the Karoo Supergroup in the Kalahari Karoo Basin of Namibia and Botswana

Preliminary stratigraphic correlations between the Karoo Supergroup rocks of the Kalahari Karoo Basin and the Main Karoo Basin have been established (see Table 1).

The general lithostratigraphic correlation of the Karoo Supergroup in the Kalahari Karoo Basin has been made and is based on geological setting and facies changes (Smith, 1984). Seven sub-basins have been recognised, where Karoo Supergroup sequences were given local formation names and correlated across Botswana (Smith, 1984; Modie, 2007). The Dwyka Group in the Aranos Basin, Namibia is correlated with the Malogong and Khuis formations in southwest Botswana (Smith, 1984; Key et al., 1998). The Nossob Formation at the base of the Ecca Group in the Aranos Basin has been interpreted to be equivalent to the Ncojane Sandstone Member at the base of the Kobe Formation in southwest Botswana (Smith, 1984). The Kobe and Mukorob formations were correlated based on character similarities they share that represent deposition by similar sedimentary processes (Smith, 1984). Overlying the Kobe and Mukorob formations are the Otshe and Auob formations, respectively. Faulting interrupts the Otshe Formation in boreholes W2 and W3 in the southwest Botswana, therefore exact correlation is difficult (Miller, 2008). The uppermost part of the Otshe Formation in borehole W2, as described by Smith (1984), may correlate with much of the Auob Formation, even though it appears to lack a lateral equivalent of the Geelhout Member shale and coal (Miller, 2008).

The Beaufort Group equivalent sedimentary rocks (Kwetla Formation) and the aeolian Ntane Sandstone Formation have not been recognised in the Aranos Basin although sedimentary units interbedded with the Kalkrand basalts contain large amounts of well rounded aeolian quartz grains (Miller, 2008). The Neu Loore Formation exhibits the same characteristics as the Mosolotsane Formation in southwest Botswana. Deeply weathered erosional unconformities at the base of the Mosolotsane Formation and the unconformity at the top of the Auob Formation or at the top of Rietmond Formation support correlation of the Mosolotsane with the Neu Loore Formation in the Aranos Basin (Miller, 2008). Smith (1984) correlated the Mosolotsane Formation based on the red colour with the red beds of

the Elliot Formation in South Africa. Miller (2008) suggested that the Neu Loore Formation could correlate with any units ranging in age between Late Permian and Early Jurassic in South Africa. The Mosolotsane Formation (terrestrial red bed succession) in the Kalahari Karoo Basin of Botswana is lithologically correlated with the Late Triassic to Early Jurassic Molteno and Elliot formations in South Africa (Smith, 1984; Bordy et al., 2010). The Stormberg Lava Group in some parts of Botswana have ages of about 180 ± 10 Ma, which are comparable with the dates from the Karoo basalts in South Africa (Smith, 1984).

Table 1 Preliminary correlations of the Karoo Supergroup rocks in the Kalahari Karoo Basin, Aranos Basin and the Main Karoo Basin (after Miller, 2008).

Period	**Group**	**Kalahari Karoo Basin (Aranos, Namibia)**; (Miller, 2008)	**Kalahari Karoo Basin (Botswana)**; (Smith, 1984)	**Main Karoo Basin (South Africa)**; (SACS, 1980)
Jurassic		Kalkrand Formation	Stormberg Lava Group	Drakensberg Formation
Triassic			Ntane Formation	Clarens Formation
		Neu Loore Formation	Mosolotsane Formation	Elliot Formation Molteno Formation
Upper Permian			Kwetla & Kule formations	Burgersdorp Formation Katberg Formation?
				Wateford Formation
				Tierberg & Fort Brown formations
Lower Permian	Ecca	Whitehill Formation	Boritse Formation	Whitehill Formation
		Rietmond Formation		Prince Albert & Pietermaritzburg formations
		Auob Formation	Kweneng Formation: also upper Otshe Formation	
		Mukorob Formation	Bori Formation: also upper Kobe and lowest Otshe formations	
		Nossob Formation	Upper Ncojane Member	
Carboniferous	Dwyka	Dwyka Group	Top = basal Ncojane Member at the base of Kobe Formation; Malogong, Khuis, Middlepits, Dukwi formations	Dwyka Group

CHAPTER TWO: AIMS AND METHODS

2.1 Introduction

A basic correlative framework of southern African Karoo-age sequences was first established in the 1980's and early 1990's (Smith, 1984; Smith et al., 1993; Johnson et al., 1996). This was reviewed (Exploration Consultants Limited, 1998; Cairncross, 2001; Catuneanu et al., 2005) following the advancement of new basin development theories and as new data (from hydrocarbon exploration, seismic profiling and palynological studies) became available, but to date no detailed correlation between has been undertaken. The main aim of this project is to utilise all available cored borehole data and literature to analyse sedimentary rocks, correlate stratigraphy and infer depositional events across the Kalahari Karoo Basin with a major focus on the Gemsbok Sub-basin. Ultimately, the data from this study will be used in the development of a 3D stratigraphic model of the Gemsbok Sub-basin in the Kalahari Karoo Basin.

2.2 Location of the study area

The study area (the Gemsbok Sub-basin) is situated in the southwestern portion of the Kalahari Karoo Basin (Fig. 2.1). It extends west from longitude 22° E in the Kgalagadi District of Botswana to the eastern margin of Namibia (known as the Aranos Basin), longitude 20° E. The Karoo Supergroup rocks in the Gemsbok Sub-basin (study area) are not exposed due to extensive cover by Cenozoic Kalahari Group sediments and therefore this research is based on borehole data. Boreholes used in this study are located in the north (e.g., boreholes: W1, W2 and W3), east (e.g., boreholes: CKP8C-1, CKP8C and CKP8A), and west (e.g., boreholes ACP24, 19, 13, 3 and 4) of the Gemsbok Sub-basin. Previously logged sections from deep boreholes MP1 (drilled at the central part of the Gemsbok Sub-basin) and Vreda 281 (drilled 30 km west of the Namibia and Botswana international border line) were also used in this study.

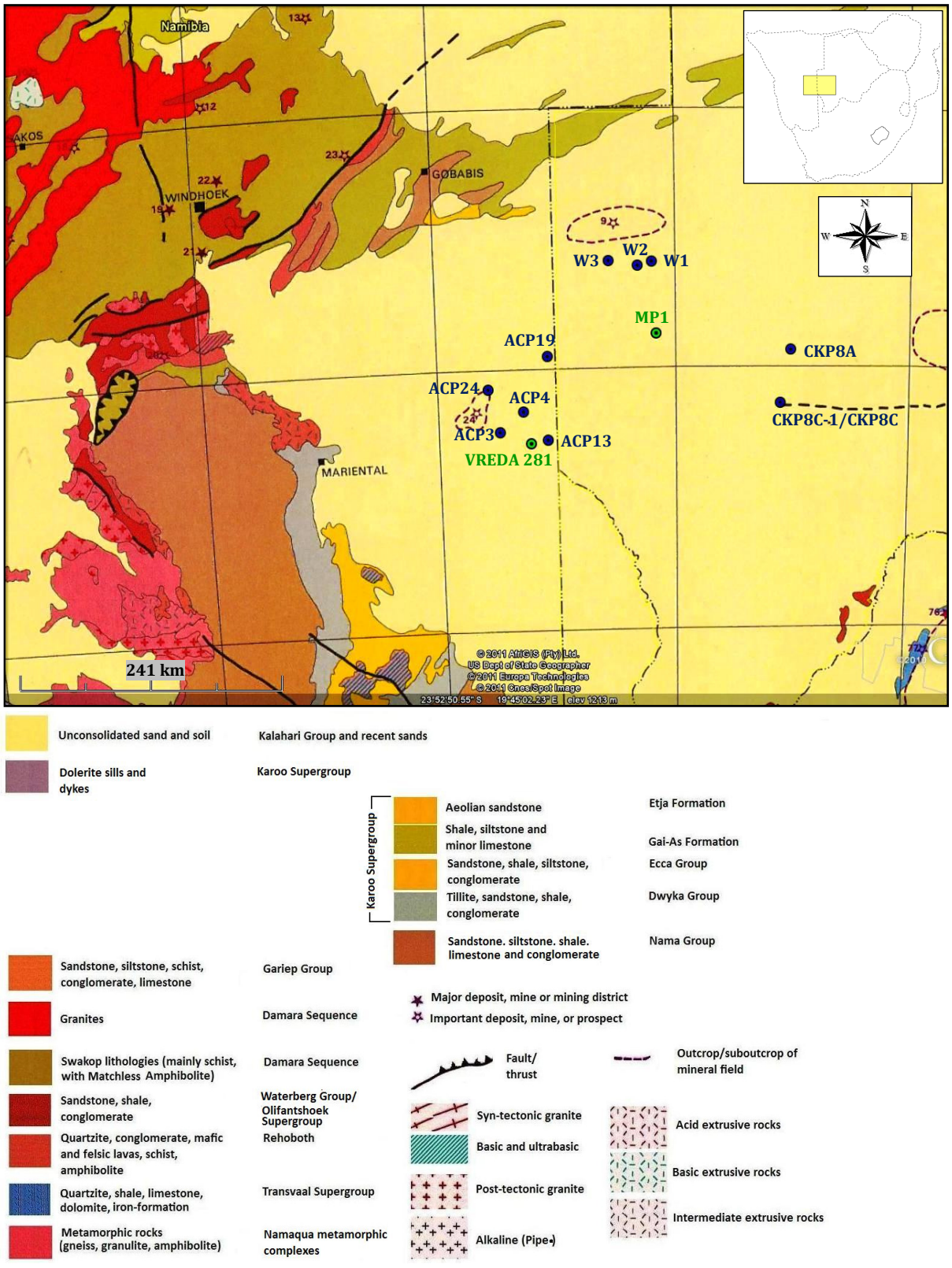


Figure 2.1 Geological map of the study area and the location of the boreholes used in this study (after Hammerbeck and Allcock, 1985).

2.2.1 The geological setting of the study area, the Gemsbok Sub-basin

The Gemsbok Sub-basin of Botswana and Namibia is bounded to the north and northwest by Precambrian rocks of the Ghanzi-Chobe Belt and the Damara Belt (Key et al., 1998; Ramokate et al., 2000). The Ghanzi-Chobe Belt marks both the southeastern limit of the Damara Fold Belt and the western margin of the Kalahari Karoo Basin in Botswana (Key et al., 1998). The Damara Belt consists of metamorphic rocks (schists, gneisses, phyllites and amphibolites), igneous rocks (granites), sedimentary and metasedimentary rocks (carbonates and quartzites). The Ghanzi-Chobe Belt comprises felsites, syenite, rhyolite, siliclastics (arkoses, meta-arkoses, and minor shales), metamorphic rocks (schists, gneisses and metadolerites) and granitiods (Meixner, 1983; Ramokate et al., 2000; Haddon, 2005). To the north of the Ghanzi-Chobe Belt, pre-Damaram basement rocks comprise gneisses, granites and schists (Carney et al., 1994).

The basement of the Karoo Supergroup in the Gemsbok Sub-basin is represented by the Neoproterozoic sedimentary or metasedimentary rocks of the Nama Group (Key and Ayers, 2000). The Nama Group rocks are in turn underlain by weakly metamorphosed siliclastic rocks of the Ghanzi Group (Key and Ayers, 2000), which forms part of the Ghanzi-Chobe Belt.

The western and south-western edge of the Gemsbok Sub-basin is mainly composed of the Nama Group basement rocks, Namibian metamorphic complexes (granitic gneisses, metasediments and felsic to mafic intrusions, granites and acidic extrusive rocks) and Namaqua-Natal metamorphic rocks (Hammerbeck and Allcock, 1985; Johnson et al., 2006). The rocks of the Olifantshoek Supergroup, Transvaal Supergroup and Waterberg Group outcrop along the southern margin of the Gemsbok Sub-basin where they contribute to the basement of the Karoo Supergroup. These rocks consist of sandstones, quartzites, ironstones, shale, dolomites, breccia and conglomerates (Meixner, 1983; Carney et al., 1994; Key and Ayres, 2000; Johnson et al., 2006). The Karoo Supergroup unconformably overlies Archaean granites and gneisses in the east and southeast of the Gemsbok Sub-basin (Meixner, 1983). To the northeast of the Gemsbok Sub-basin, the basement of the Karoo Supergroup is marked by felsic volcanic rocks, granitoids and granitic-gneiss rocks of the Okwa Complex (Meixner, 1983).

2.3 Methodology

This study utilises logs and cores of 11 previously drilled boreholes in the Gemsbok Sub-basin of Botswana and Namibia (Fig. 2.1). These boreholes were drilled either in the 1980's or else over the past 10 years and therefore comprise differing quality of descriptions of lithologies. The data found in the borehole logs have been used to construct Karoo Supergroup stratigraphy in the Kalahari Karoo Basin (Smith, 1984; Kingsley, 1985; Miller 2008). To supplement data obtained from the previously logged boreholes, visits to the geological surveys of Botswana and Namibia were made and the borehole cores were relogged in greater detail and photographed. A representative suite of samples were collected for detailed analyses.

2.3.1 Literature review

A literature review from scientific reports, exploration data, existing borehole logs, geophysical data and biostratigraphic data has been the primary source of information for this study. This data has been analysed and incorporated into basinal and correlative models that explain the distribution of the various stratigraphic units and deposits within the Kalahari Karoo Basin.

2.3.2 Borehole logging and facies analysis

A total of eleven boreholes from core libraries of the geological surveys of Namibia and Botswana (Fig. 2.1) were logged for this study. The aim of borehole logging was to identify lithofacies based on rock types and lithologic features such as sedimentary structures, texture, colour, grain size, composition and trace fossil content (ichnofacies). Detailed facies analysis was done using a modified version of Miall's (1977, 1983, 2000) lithofacies classification scheme. The lithofacies and ichnofacies were grouped into facies associations which represented different kinds of depositional environments of the Karoo Supergroup.

Drill cores with sandstone units were sampled for petrographic studies and geochemical analysis.

2.3.3 Borehole sampling

A total of thirty-five sandstone samples were collected for thin section analysis from 11 boreholes across the Gemsbok Sub-basin (borehole no: W1, W2, W3, CKP8C, CKP8C-1, CKP8A, ACP3, ACP4, ACP13, ACP19 and ACP24). Six of these sandstone samples are of coarse-grained sandstones, fifteen of medium-grained sandstones and thirteen samples of fine-grained sandstones. These sandstone samples were analysed to determine modal composition (point-count method) and other petrographical features (texture, grain shape, roundness). Sixteen sandstone samples from southwest Botswana were selected for geochemical analyses; however, there were no samples available for geochemical analyses from the southeast Namibia boreholes.

2.3.4 Petrographic studies of sandstones

Detrital modes of sandstone suites primarily reflect the different tectonic setting of provenance terranes, although other secondary factors i.e., relief, depositional environment, diagenetic change, transport mechanism, and climate also influence sandstone composition (Dickinson, 1985). Therefore, petrographic composition of sedimentary rocks is important when constraining provenance and identifying the tectonic settings of sedimentary basins. The quantitative detrital modes of sandstones can be calculated from point counts of thin sections (Dickinson, 1985). Transport history processes of sandstone suites can be obtained from careful examination of shape and roundness of grains, and textural and mineralogical maturity, which are easily determined in thin sections (Pettijohn et al., 1987).

The Gazzi-Dickinson's point-count method was applied for quantitative compositional analysis. A single coarse-grained crystal larger than (0.065mm) was counted as an individual mineral grain, while a fine-grained crystal (<0.065mm) was counted as a lithic fragment (Dickinson, 1985). In the point count method (Table 2), grains were grouped as Qm (Monocrystalline quartz), Qp (Ponocrystalline quartz), P (Plagioclase), K (K-spar), Lv (Volcanic or metavolcanic lithic fragments) and Ls (Sedimentary or metasedimentary lithic fragments). The detrital modes were then recalculated to 100%, excluding matrix, cement, micas, heavy minerals and carbonate grains (Dickinson, 1985). Values obtained are plotted on standard triangular diagrams (QFL) showing compositional fields associated with different provenances (i.e., continental block provenances, recycled orogen, magmatic arc

provenances, arc orogen sources, collision suture and thrust belt sources and circum-pacific volcanoplutonic suites [Dickinson, 1988]). The obtained values were also plotted on QFL diagrams (Folk, 1980), which show different sandstone types. For modal analysis, 350 points were counted per thin section.

Table 2 Classification and Symbols of Grain Types (after Dickinson 1985).

A.	Quartzose Grains (Qt or Q = Qm + Qp)
	Qt or Q = total quartzose grains Qm = monocrystalline quartz (> 0.625 mm) Qp = polycrystalline quartz (or chalcedony)
B.	Feldspar Grains (F = P + K)
	F = total feldspar grains P = plagioclase grains K = Kspar grains
C.	Unstable Lithic Fragments (L = Lv + Ls)
	L = total unstable lithic fragments Lv = volcanic or metavolcanic lithic fragments Ls = sedimentary or metasedimentary lithic fragments
D.	Total Lithic Fragments (Lt = L + Qp)
	Lc = extrabasinal detrital limeclasts (not included in L or Lt)

2.3.5 Geochemical analysis of sandstones

Major element geochemistry of sedimentary rocks is influenced by various factors such as source material, sedimentary processes within the depositional basin, transportation, diagenesis, physical sorting and weathering (Bhatia, 1983; Bhatia and Crook, 1986; Amstrong-Arltrin et al., 2004). Accordingly, the major and trace element geochemistry of sandstones can be used as a powerful tool to determine provenance and tectonic setting of sedimentary basins (Bhatia, 1983, Bhatia and Crook, 1986, Roser and Korsch, 1986). Several authors such as Pettijohn et al. (1972) and Herron (1988) have used the concentration ratios SiO_2/Al_2O_3 *vs.* Na_2O/K_2O, Fe_2O_3/K_2O to classify sandstones and the concentration ratios [Fe_2O_3* + MgO *vs.* TiO_2, Al_2O_3/SiO_2, K_2O/Na_2O and Al_2O_3/ (CaO + Na_2O), SiO_2 *vs.* K_2O/Na_2O] to discriminate tectonic settings of sandstones and sedimentary basins (Bhatia, 1983; Bhatia and Cook, 1986; Roser and Korsch, 1986;

Armstrong-Altrin et al., 2004; Armstrong-Altrin and Verma, 2005). Some trace element concentration ratios (La-Th-Sc, Th-Co-Zr/10, Th-Sc-Zr/10, La/Sc *vs.* Ti/Zr, Sc/Cr *vs.* La/Y) are also used to discriminate the provenance and tectonic setting of sandstones (Bhatia and Crook, 1986).

Sixteen fine to medium-grained sandstone samples from six boreholes in the southwest Botswana were selected for major and trace elements analyses. The major and trace element geochemistry of the sandstones was determined by X-ray fluorescence spectrometry (XRF) at the Council for Geoscience laboratory, Pretoria. Major and trace elements on fused glass discs and wax pellets were analysed using a PANanalytical Axios X-ray fluorescence spectrometer equipped with a 4 kW tube. Sandstone samples were milled at (<75 μ fraction) for major element analysis and roasted at 1000 °C for at least 3 hours to oxidize Fe^{2+} and S and to determine the loss of ignition (L.O.I). Glass disks for major element analysis were prepared by fusing 1 g roasted sample and 8 g of 12-22 flux consisting of 35% $LiBO_2$ and 64.71% $Li_2B_4O_7$ at 1050 °C. A 12 g milled sample wax was mixed with 3 g of Hoechst and pressed into powder briquette by hydraulic press at a pressure of 25 ton for trace element analysis. The XRF analyses were conducted by Mrs Corlien Cloete using XRF method documented in Cloete and Truter (2001).

2.3.6 3D geological modelling

Stratigraphic data collected from borehole core was analysed and used to create cross-sections and 3D block diagrams of the Karoo Supergroup. A 3D stratigraphic model of the Kalahari Karoo Basin in the Gemsbok Sub-basin was developed and provides information about the geographic distribution of lithostratigraphic units, facies associations and depositional environments.

CHAPTER THREE: SEDIMENTOLOGY

3.1 Introduction

This chapter presents detailed lithologic descriptions of sedimentary rocks of the Karoo Supergroup in the Gemsbok Sub-basin (study area) using existing borehole data and an extensive literature review on the Kalahari Karoo Basin. Eleven boreholes with depths ranging from 200 m to 795 m were used in this study (Fig. 2.1; App. Fig. 1 - 11). The major rock types identified in the studied boreholes include: diamictites, conglomerates, sandstones, siltstones and mudrocks. The study area covers the rocks of the Dwyka Group, the Ecca Group, the Beaufort Group equivalent, the Lebung Group (Mosolotsane Formation and Ntane Formation) and the Neu Loore Formation.

3.2 Facies analysis

Reconstruction of depositional environments of sedimentary rocks depends on a thorough characterisation of the lithofacies and sometimes biofacies (ichnofacies). A sedimentary facies is a body of sedimentary rock with specific characteristics and it is defined on basis of lithology, colour, bedding, composition, texture, grain size, sedimentary structures, palaeocurrent pattern and fossil content (Reading, 1996; Miall, 2000; Boggs, 2001). Description of sedimentary facies can be done in both outcrop and borehole sections (Reading, 1996).

It is very difficult to interpret depositional environments of sedimentary rocks based on individual and isolated facies (Reading, 1986; 1996; Miall, 2000). For instance, an individual facies (e.g., trough cross-bedded sandstone) can be formed by the same or different processes that are active in different depositional settings (e.g., beach or channel or aeolian). Accordingly, in order to make depositional environmental interpretations of sedimentary rock succession it is important to determine the relationship of facies to each other and to distinguish which facies tend to occur together (facies associations) (Reading, 1986; 1996). Facies associations are groups of facies that occur together and are considered to be genetically or environmentally related (Reading, 1986; Boggs,

2001). The association of facies provides additional evidence which makes environmental interpretation easier than treating each facies in isolation (Reading, 1986).

Sedimentary facies in this study were described based on the lithological characteristics, bed thickness, grain-size, colour, internal sedimentary structures and trace fossil assemblage (ichnofacies). Table 3 summarises the lithofacies recognised in the Karoo Supergroup of the Gemsbok Sub-basin. A modified version of Miall's (1977, 1983, 2000) lithofacies codes and interpretation were used for the Karoo Supergroup rocks in the study area in order to aid in interpretation of depositional environments. Stratification or bedding are characteristic feature of sedimentary rocks, and are produced mostly by changes in sedimentation patterns, sediment composition and/or grain size (Tucker, 1991). Here, bedding is defined as sedimentary layering thicker than 1 cm and any fine scale layering less than 1 cm thick is termed lamination. Fourteen lithofacies and thirteen ichnofossils were identified in the Karoo Supergroup rocks studied in the 11 logged boreholes in the study area (Gemsbok Sub-basin).

Table 3 Sedimentary lithofacies identified in the Karoo Supergroup boreholes in the Gemsbok Sub-basin (study area), modified from Miall (1977, 1983, 2000).

Facies code	Description
Gcm	Clast-supported, massive conglomerate
Dmm	Matrix-supported, massive diamictite
Dcm	Clast-supported, massive diamictite
Bc	Clast-supported, massive breccia
Sm	Massive or faint laminated sandstone
St	Trough cross-bedded sandstone
Sh	Horizontally laminated sandstone
Sr	Ripple cross-laminated sandstone
Sb	Bioturbated sandstone
Fl	Laminated sandstone, siltstone and mudrock
Fr	Bioturbated massive siltstone and mudrock
Fsm	Massive mudrock
Fc	Massive to laminated carbonaceous mudrock
C	Coal

3.3 Lithofacies description

3.3.1 Conglomerate lithofacies

3.3.1.1 Lithofacies Gcm - Clast-supported, massive conglomerate

The conglomerate lithofacies was recorded in borehole W1, at a depth between 101 m to 103 m (Fig. 3.1). It is clast-supported, well sorted, massive conglomerate with light grey (N7) to light pinkish grey (5 YR/8/1) colours. The matrix is composed of fine-grained sandstone and siltstone, whereas the clasts are subrounded to rounded (ranging from 0.1 cm to 1 cm diameter) and are dominantly quartz-rich in composition. In borehole W1 (App. Fig. 6), the conglomerate lithofacies is overlain by a moderate orange pink (5 YR/8/4)/ moderate red (5 R/4/6) mudrock and sandstone unit.

3.3.1.2 Lithofacies Dmm - Matrix-supported, massive diamictite

Lithofacies Dmm was recorded in four boreholes (ACP3, ACP4, W3 and CKP8C-1; App. Fig. 1, 2, 8 and 11) and comprises matrix-supported, massive diamictites. Matrix-supported, massive diamictites are poorly sorted and contain ± 80 percent mudrock (pale brown (5 YR/5/2), dark grey (N3), light olive-grey (5 Y/ 6/1) or light greenish grey (5 GY 8/1)) or sandstone (light grey (N7), medium grey (N5)) matrix (Fig. 3.2). The coarse detrital clasts include angular to subrounded sandstone, granite and quartzite which range in size between 0.1 cm and 2 cm.

3.3.1.3 Lithofacies Dcm - Clast-supported, massive diamictite

Lithofacies Dcm is a clast-supported, poorly sorted massive diamictite that has been recorded in borehole W3, at a depth between 364.40 m to 392.10 m (Fig. 3.3, App. Fig. 8). It displays massive texture and contains ± 10 percent fine- to medium-grained very light grey (N8) sandstone and muddy matrix. Lithofacies Dcm is characterised by angular, subrounded and rounded detrital clasts (ranging from 0.2 cm to 5 cm diameter) of different rock types (quartizites, ultramafic rocks such as dolerite and gabbro, granite, banded ironstones).

3.3.1.4 Lithofacies Bc – Clast-supported breccia

Lithofacies Bc is a clast-supported, poorly sorted breccia that is present in borehole CKP8A in the eastern part of the study area (Fig. 3.4, App. Fig. 9). It is contains ± 10 percent fine-grained to very coarse-grained matrix and composed of angular clasts (ranging from 0.1 cm to 7 cm in diameter) of coal, mudrocks, and sandstone. The difference between clast-supported, massive diamictites and clast-supported breccias, is that the latter is composed entirely of angular clasts.

3.3.2 Sandstone lithofacies

3.3.2.1 Lithofacies Sm – Massive or faint laminated sandstone

This lithofacies is common and occurs in all boreholes in the study area. It consists of massive (Fig. 3.5), fine to very coarse, in places pebbly, sandstones. The sandstones exhibit a variety of colours, i.e., light grey (N7), light grey white (N8-N9), very pale orange (10 YR 8/2), very light grey (N8) to yellowish grey (5 Y 7/2) and pale pink grey (5 YR 8/11). The sandstones are porous in places, micaceous and occasionally contain pyrite nodules. Carbonaceous mudrock stringers and mudrock rip-up clasts (ranging from 0.5 cm to 3.5 cm in diameter) were recorded within the sandstones. Massive sandstone units occur in packages up to 0.5 m thick and form sharp contacts with the overlying or underlying mudrocks or siltstones. These sandstones are sometimes interbedded with laminated, rippled cross-laminated siltstones and mudrocks.

3.3.2.2 Lithofacies St - Trough cross-bedded sandstone

Lithofacies St occurs in most boreholes in the study area, but it is not as common as other sandstone lithofacies. This lithofacies occurs as trough sets (ranging from 10 cm to 15 cm) in fine- to coarse-grained sandstones (Fig. 3.6). The sandstones are light grey (N7), yellowish grey (5 Y 7/2), light grey white (N8-N9), pale orange (10 YR 8/2) and pale pink grey (5 YR 8/1) in colour. They are commonly associated with lithofacies Sh and Sr and tend to be micaceous in places.



Figure 3.1 Clast-supported, massive conglomerate (lithofacies Gcm), borehole W1. Tape measure scale in centimeters.



Figure 3.2 Matrix-supported, massive diamictite (lithofacies Dmm), borehole W3. Tape measure scale in centimeters.



Figure 3.3 Clast-supported, massive diamictite (lithofacies Dcm), borehole W3. Tape measure scale in centimeters.



Figure 3.4 Clast-supported breccia (lithofacies Bc), borehole CKP8A. Tape measure scale in centimeters.

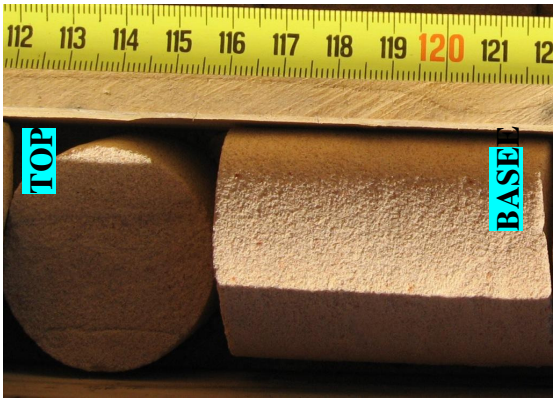


Figure 3.5 Massive or faint laminated sandstone (lithofacies Sm), borehole W1. Tape measure scale in centimeters.

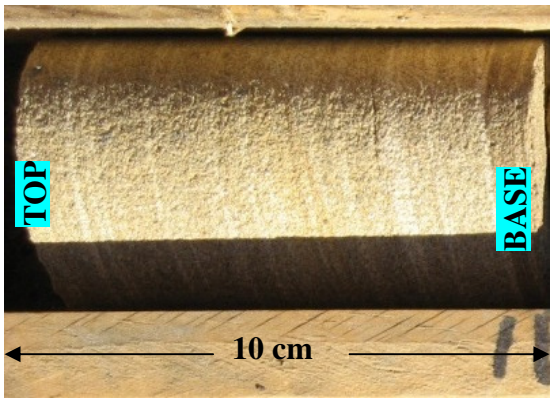


Figure 3.6 Trough cross-bedded sandstone (lithofacies St), borehole CKP8A.

3.3.2.3 Lithofacies Sh - Horizontally laminated sandstone

This lithofacies is common and was recorded in all the boreholes in the study area. It comprises very fine- to very coarse-grained sandstones, and in places even pebbly sandstones (Fig. 3.7). Horizontal laminated sandstones tend to be micaceous, poorly cemented and porous in places. Bioturbation, pale red (10 R 6/2, probably haematite) and sulphide nodules are present in places. The horizontally laminated sandstones are light grey (N7), light grey white (N8-N9), yellowish grey (5 Y 7/2) or pale pink grey (5 YR 8/1) in colour. This lithofacies commonly occurs in association with lithofacies St, Sm and occasionally is interbedded with fine-grained lithofacies.

3.3.2.4 Lithofacies Sr – Ripple cross-laminated sandstone

Ripple cross-laminated sandstone is very scarce within the boreholes in study area. This lithofacies occurs as medium-to fine-grained light grey (N7) to light pink grey (5 YR 8/1) sandstones (Fig. 3.8). Flaser and wavy bedding is common. Ripple cross-laminated sandstones are found associated with lithofacies Sm, St and Sh and mainly occurs towards the top of sandstone successions.

3.3.2.5 Lithofacies Sb – Bioturbated sandstone

Bioturbated sandstones are very scarce within the boreholes in the study area. Lithofacies Sb comprise sandstones which are massive and bioturbated (Fig. 3.9). These sandstones range from very fine-grained to fine-grained and are usually light grey in colour (N7).

Primary sedimentary structures are not easily identified due to presence of bioturbation stuctures. Lithofacies Sb is usually found in places associated with lithofacies Sm, Sh, St and Sr and it is present within thicker sandstone units (up to 55 m).



Figure 3.7 Horizontally laminated sandstone (lithofacies Sh), borehole CKP8C. Tape measure scale in centimeters.



Figure 3.8 Ripple cross-laminated sandstone (lithofacies Sr), borehole ACP24. Clinorule scale in centimeters.



Figure 3.9 Bioturbated sandstone (lithofacies Sb), borehole ACP24. Clinorule scale in centimeters.

3.3.3 Fine-grained lithofacies

3.3.3.1 Lithofacies Fl - Laminated sandstone, siltstone and mudrock or laminated siltstone and mudrock

Lithofacies Fl is very common in boreholes in the study area. It consists of interbedded layers of sandstone, siltstone and mudrock (Fig. 3.10). The sandstone layers that form this lithofacies are usually massive in texture and range from fine- to very fine-grained sand. Siltstone layers also show massive bedding, but may in places show horizontal lamination. Mudrock layers always have a massive texture. Individual sandstone, siltstone and mudrock layers range in thickness from 0.1 cm to 23 cm. The siltstone and sandstone layers range in colour from grey (N5) to light grey (N7), and in contrast the mudrock layers occur in a variety of colours, such as light green grey (5 G 8/1), pale red (10R 6/2), moderate reddish brown (10R 4/6), dark reddish brown (10R 3/4) and greyish red (10 R 4/2). Ripple cross-lamination structures, flaser, wavy and lenticular bedding, trace fossils and pale red nodules (probably haematite) are often associated with this lithofacies. This lithofacies is associated with the lithofacies Sm, St, Sh and Sr and has both sharp and gradational contacts with these lithofacies. In places, it has erosional contacts with the underlying and overlying sandstone lithofacies. Lithofacies Fl is also associated with lithofacies Fr and diamictites (Dmm).

3.3.3.2 Lithofacies Fr - Bioturbated massive siltstone and mudrock

Lithofacies Fr consists of bioturbated mudrocks and siltstones (Fig. 3.11). Primary sedimentary structures are destroyed or disturbed. The siltstones that form this lithofacies are light grey in colour (N7) and mudrocks are grey (N5), dark grey (N3) to black (N1) in colour. Lithofacies Fr is often transitional from lithofacies Fl to Fr and occasionally contains trace fossils. This lithofacies occurs mostly in the lower parts of upward-coarsening successions.

3.3.3.3 Lithofacies Fsm - Massive mudrock

Lithofacies Fsm consists of massive mudrocks (Fig. 3.12). It is uncommon in boreholes within the study-area. The mudrocks vary in colour and in most places consist of dark reddish brown (10R 3/4), light grey (N7) to dark grey (N3) and light greenish grey (5 G 8/1) colours. Lithofacies Fsm contains no primary sedimentary structures and occurs

typically as thin layers (ranging from 0.1 cm to 23 cm) associated or interbedded with lithofacies Sh, Sm and Fl.

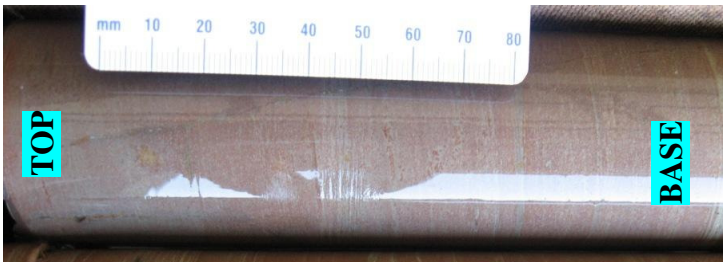


Figure 3.10 Fine laminated sandstone, siltstone and mudrock (lithofacies Fl), borehole ACP13. Ruler scale in millimeters.

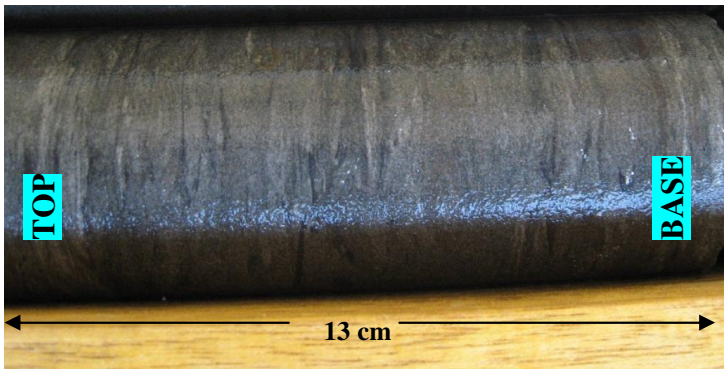


Figure 3.11 Bioturbated massive mudrock and siltstone (lithofacies Fr), borehole ACP19.

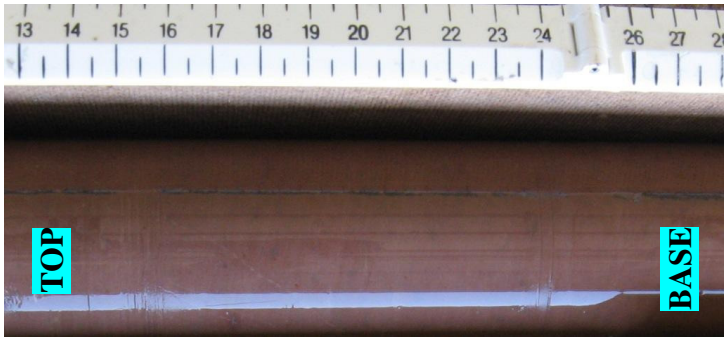


Figure 3.12 Massive mudrock (lithofacies Fsm), borehole ACP13. Clinorule scale in centimeters.

3.3.3.4 Lithofacies Fc - Massive to laminated carbonaceous mudstone

This lithofacies has been identified in most boreholes in the study area and occurs as massive to faint laminated grey to very dark grey (N3) and black (N1) carbonaceous or organic rich mudrocks (Fig. 3.13). Lithofacies Fc normally occurs in the lowermost part of a thick (ranging from 90 m to 109 m) upward-coarsening successions. Occasionally, this lithofacies sharply overlies sandstone lithofacies (Sm, Sh and St). Lithofacies Fc is

usually interbedded with fine-grained lithofacies (Fr, Fl, Fsm and C) and lithofacies Sh, Sm and St. The lithofacies Fc also occurs as rip-up clasts within massive sandstones (lithofacies Sm) in places.

3.3.3.5 Lithofacies C - Coal

Lithofacies C was documented in seven boreholes (Fig. 3.14; App. Fig. 2 -7, 9, 11) in the study area. This lithofacies is black (N1), in places is dull grey (~N1 and N2) and bright in colour. The thickest coal lithofacies horizon occurs in borehole CKP8C-1 (28 m) followed by coal horizons in borehole CKP8A (7 m) and boreholes W1 and W2 (± 4 m). In general the coal lithofacies (e.g., borehole ACP 13 and ACP24) are less than 0.5 m in thickness and are interbedded with carbonaceous mudrocks (Fc), siltstones and mudrocks (Fl, Fr). Coal lithofacies in borehole CPK8A and CKP8C-1 appears to have been baked as a result of dolerite sills. Most of the coal lithofacies sharply overlie sandstone successions.



Figure 3.13 Carbonaceous mudrocks (lithofacies Fc), borehole CKP8C. Tape measure scale in centimeters.



Figure 3.14 Coal (lithofacies C), borehole W1. Tape measure scale in centimeters.

3.4 Invertebrate Palaeontology

3.4.1 Trace Fossils

Trace fossils or ichnofossils are biologically produced sedimentary structures that include the tracks, trails, burrows or borings left by organisms as they move around, create holes for protection or sift nutrients from sediments (Frey, 1975; Nichols, 1999; Pemberton et al., 2007). Where body fossils are absent, trace fossils provide various alternatives to aid detailed environmental analysis and interpretation (Stanistreet et al., 1980). The study of trace fossils (ichnology) provides information on the behaviour of organisms, estimates of water depth, rate of sedimentation, criteria for the recognition of deltaic subenvironments, distinction between wave- and fluvial-dominated deltas, and criteria for the recognition of marine delta abandonment facies (Stanistreet et al., 1980; Nichols, 1999). In broad terms, certain trace fossils or suites of trace fossils (ichnofacies) are characteristic of a particular environment and in certain cases of a specific depth range (Tucker, 1991).

Trace fossils can be divided into two groups: 1) those formed on the sedimentary surface (mainly preserved in bedding planes and include tracks and trails) by epibenthic organisms and 2) those formed within the sediment (burrows and mainly seen on both horizontal and vertical sections) by endobenthic organisms (Tucker, 1991).

Kingsley (1985) reported trace fossil assemblages of *Skolithos* and *Cruziana* in borehole cores of the Karoo Supergroup in the Aranos Basin of Namibia. Trace fossils recorded by Kingsely (1985) included *Siphonichnus* (the retrusive upward movement of the burrower marked by the meniscate laminae around the central tube), *Diplocraterion* or *Teichichnus* (U-shaped burrows that migrated upwards [retrusively] in response to deposition), and *Diplocraterion* in shoreface beach sandstones. Smith (1984) noted the body fossil of a shallow marine bivalve *Eurydesma* in the lower part of the Ecca Group.

Borehole cores of the Karoo Supergroup in the study area are characterised by variety of trace fossils and include escape structures (fugichnia), *Siphonichnus*, *Diplocraterion*,

Rosselia , *Planolites*, *Thalassinoides*, *Pheobichnus*, *Teichichnus*, *Asterosoma*, *Zoophycos*, *Palaeophycus tubularis*, *Conichnus*, *Schaubcylindrichnus* and *Skolithos*.

1) Escape structures (fugichnia)

Escape structures are present in the boreholes situated in the western and northern parts of the study area (App. Fig. 5, 8). These structures are oriented perpendicular to the bedding and display concave-up laminae (Bhattacharya and Bhatthacharya, 2007). Escape structures have a length ranging from 2.5 cm to 8 cm and diameter ranging from 0.5 cm to 1 cm (Fig. 3.15).

2) *Siphonichnus*

Siphonichnus trace fossils are present in the boreholes situated in the western and northern parts of the study area (App. Fig. 1, 5, 8). These trace fossils are oriented perpendicular and oblique to the bedding (Fig. 3.15). *Siphonichnus* trace fossils show a much greater length (2.5 cm – 8 cm) compared to width (0.3 cm – 0.5 cm). They are characterised by backfill meniscate laminae which shows concave downward orientation (Stanistreet et al., 1980).

3) *Diplocraterion*

Diplocraterion trace fossils are preserved in borehole ACP24. They occur as vertical, U-shaped burrows containing concave-up laminae (spreiten), which are bounded by thin distinct wall linings (Chamberlain, 1978; Pemberton et al., 1992a). These trace fossils are oriented perpendicular to the bedding. *Diplocraterion* has an average length of 7 cm and a diameter of 1.5 cm (Fig. 3.16).

4) *Rosselia*

Rosselia was identified in borehole W3 and it is a vertical burrow with an upper opening like a bulb (Chamberlain, 1978; Pemberton et al., 1992a). The trace fossil is filled with fine-grained siltstone, which at the bottom has circular trace fossils (probably *Planolites*). The *Rosselia* trace fossil has a length of 4 cm and a bulbous opening diameter of 5 cm (Fig. 3.17).

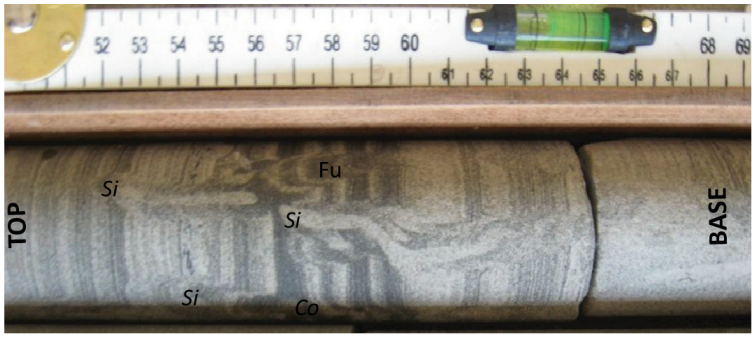


Figure 3.15 Horizontal laminated sandstone with fugichnia (Fu) and trace fossils *Siphonichnus* (Si) and *Conichnus* (Co), borehole ACP24. Clinorule scale in centimeters.

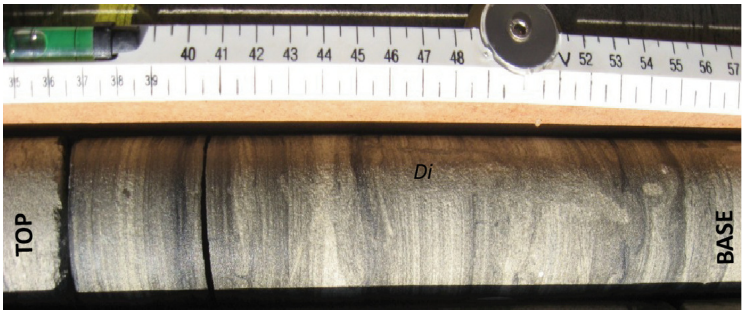


Figure 3.16 Horizontal laminated (Sh) sandstone with *Diplocratetion* (Di) trace fossil, borehole ACP24. Clinorule scale in centimeters.



Figure 3.17 Massive sandstone (Sm) and horizontal laminated (Sh) sandstone with *Rosselia* (Ro) trace fossil and fugichnia (Fu), borehole W3. Tape measure scale in centimeters.

5) *Planolites*

Planolites are burrows oriented approximately parallel to the bedding and sometimes occur in a circular and elliptical shape in boreholes (Pemberton et al., 1992a). *Planolites* burrows diameter range from 0.1 cm to 0.5 cm (Fig. 3.18). The lithology filling these trace fossils is different from the host rock lithology and *Planolites* do not have wall linings. These trace fossils are present in most boreholes in the study area (App. Fig. 1, 4, 5, 7, 8, 10, 11).

6) *Thalassinoides*

Thalassinoides trace fossils are circular and elliptical in cross-section, oriented parallel to the bedding and have diameters ranging from 0.6 cm to 1.5 cm (Fig. 3.18). These trace fossils have distinct thin boundary lining and are filled with lithology that is similar or different to the lithology of the host rock (Chamberlain, 1978; Rotnicka, 2005).

7) *Pheobichnus*

Pheobichnus trace fossils are circular in shape and oriented parallel to the bedding. These trace fossils are composed of a radial pattern around the core that is filled with massive, structureless, well sorted fine-grained sandstone (Gregory and Campbell, 2003; Fig. 3.18). *Pheobichnus* trace fossils have diameter range between 0.5 cm to 1 cm. These were only recognised in borehole ACP24, at depths between 211.39 m and 220.18 m (App. Fig. 5).

8) *Teichichnus*

Teichichnus trace fossils are vertical, tabular burrows, which are built as successively tightly stacked upward curving spreiten (Chamberlain, 1978; Pemberton et al., 1992a; Rotnicka, 2005). Individual *Teichichnus* trace fossils observed in this study have widths ranging from 2 cm to 2.25 cm, and lengths of about 0.5 cm (Fig. 3.19, 3.20). *Teichichnus* trace fossils were observed in boreholes ACP3, ACP4 and ACP24 (App. Fig. 1, 2, 5).

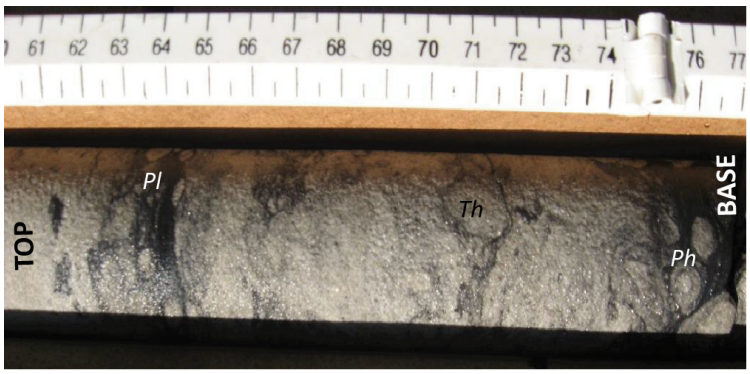


Figure 3.18 Massive sandstone (Sm) with *Planolites* (*Pl*), *Thalassinoides* (*Th*) and *Pheobichnus* (*Ph*) trace fossils, borehole ACP24. Clinorule scale in centimeters.

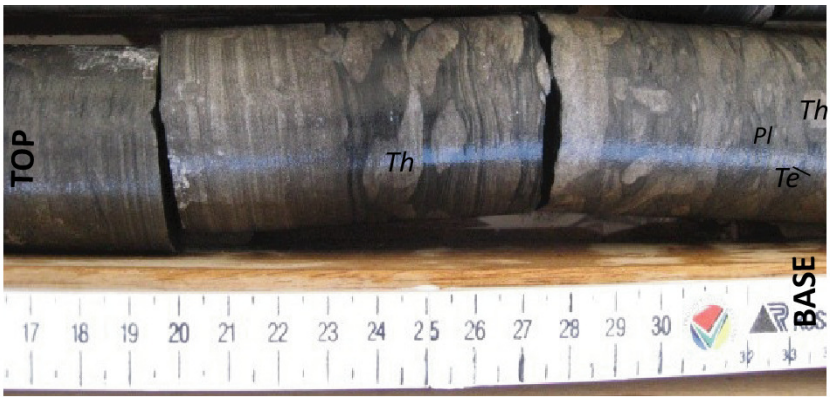


Figure 3.19 Laminated sandstone, siltstone and mudrock (Fl) with *Planolites* (*Pl*), *Thalassinoides* (*Th*) and *Teichichnus* (T*e*) trace fossils, borehole ACP4. Clinorule scale in centimeters.



Figure 3.20 Laminated sandstone, siltstone and mudrock (Fl) with *Teichichnus* (T*e*) trace fossil, borehole ACP24. Clinorule scale in centimeters.

9) *Asterosoma*

Asterosoma trace fossils are circular, composed of concentric rings, inner core filled with sandstone and the surrounding mudrock ball (Chamberlain, 1978; Rotnicka, 2005; Fig. 3.21). They have diameters ranging from 0.4 cm to 0.6 m.

10) *Zoophycos*

Zoophycos trace fossils occur as thin muddy lobes (range from 0.1 cm to 0.2 cm), which are multiple stacked (Chamberlain, 1978; Fig, 3.22).

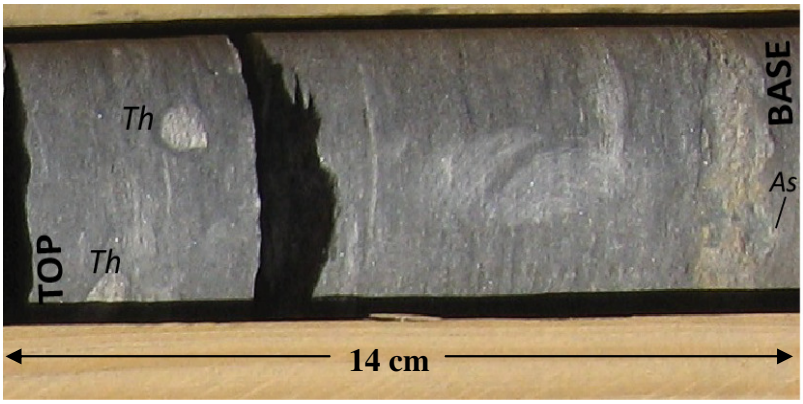


Figure 3.21 Massive carbonaceous mudrock (Fc) with *Asterosoma* (*As*) and *Thalassinoides* (*Th*) trace fossils, borehole W3.

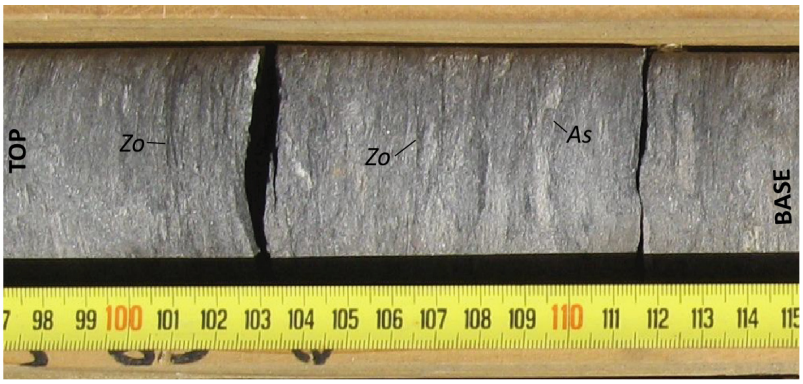


Figure 3.22 Bioturbated mudrock (Fr) with Zoophycos (*Zo*) and *Asterosoma* (*As*) trace fossils, borehole W3. Tape measure scale in centimeters.

11) *Palaeophycus tubularis*

Palaeophycus tubularis trace fossils are simple burrows oriented parallel to bedding. They occr as circular or elliptical structures which ranges in diameter from 0.2 cm to 0.6 cm (Fig. 3.23). The *Palaeophycus tubularis* have wall linings and filled with with the same lithology as the host rock (Kim et al., 2005).

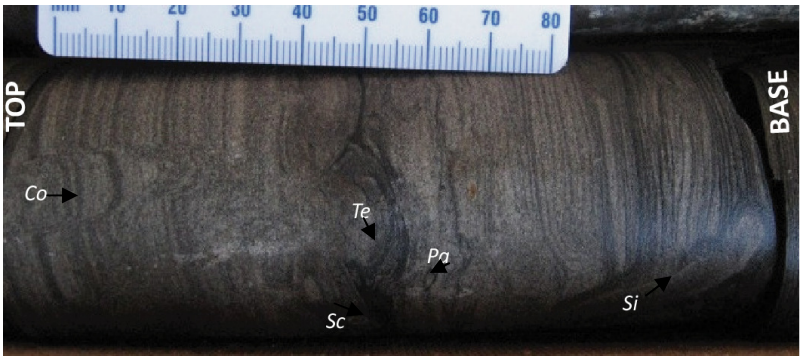


Figure 3.23 Laminated sandstone, silststone and mudrock (Fl) with *Palaeophycus tubularis* (*Pa*), *Schaubcylindrichnus* (*Sc*), *Conichnus* (*Co*), *Teichichnus* (*Te*) and *Siphonichnus* (*Si*) trace fossils, borehole ACP3. Ruler scale in millimeters.

12) *Conichnus*

Conichnus trace fossils are vertical oriented burrows with core that has U-shape laminae (Savrda, 2002). They range in length from 1.5 cm to 6 cm and have diameter range from 0.5 cm to 1 cm (Fig, 3.15, 3.23).

13) *Schaubcylindrichnus*

Schaubcylindrichnus trace fossil was identified only in borehole ACP3 at the depths between 415 m and 453 m (App. Fig. 1). It occurs in borehole section as an oval shape, which has a vertical axis (0.3 cm) greater than the horizontal axis (0.2 cm). The trace fossil filling is fine-grained and the wall consists of moderately sorted fine-grained sandstone (Nara, 2006; Fig. 3.23).

14) *Skolithos*

Skolithos trace fossils are vertical burrows that are oriented perpendicular to the bedding and typically show a much greater length compared to width (Chamberlain, 1978; Pemberton et al., 1992a). The length ranges from 0.2 cm to 0.5 cm and width is always less than 0.1 cm. The *Skolithos* ichnofossils were identified in borehole ACP4 at depths between 336 m and 362 m.

3.4.2 Association between lithofacies and ichnofossils

Ichnofacies is defined as the assemblage of trace fossils in association with lithological information (Nichols, 1999). Two types of ichnofacies exist in the boreholes of the Karoo Supergroup in the Gemsbok Sub-basin. 1) *Skolithos* ichnofacies and 2) *Cruziana* ichnofacies.

3.4.2.1 *Skolithos* ichnofacies

Skolithos ichnofacies is characterised by predominantly vertical and U-shaped burrows of *Siphonichnus*, *Conichnus*, *Diplocraterion*, *Rosselia* and escape structures (Ekdale et al., 1984; Pemberton et al., 1992; MacEachern et al., 2007). Few horizontal burrows are present and comprise *Thalassinoides*, *Palaeophycus tubularis*, *Pheobichnus* and *Planolites*. These ichnofacies is mainly associated with very clean sandstones (Fig. 3.15 –

3.18) showing horizontal laminations (Sh) and in places mica-sandstones with horizontal lamination (Sh).

3.4.2.2 *Cruziana* ichnofacies

Cruziana ichnofacies contains a moderately diverse and predominantly horizontal trace fossil assemblage including *Teichichnus, Schaubcylindrichnus, Palaeophycus tubularis*, *Planolites*, *Siphonichnus*, *Thalassinoides*, *Conichnus*, *Asterosoma*, *Zoophycos* and *Skolithos* (Ekdale et al., 1984; Pemberton et al., 1992; MacEachern et al., 2007). The *Cruziana* ichnofacies is mainly associated with laminated sandstones, siltstones and mudrocks (Fl) and fine-grained lithofacies (Fc, Fl, Fr; Fig. 3.19 – 3.23).

3.5 Facies associations

Eight facies associations (comprising fourteen lithofacies) and two trace fossil assemblages (assigned to the *Cruziana* and *Skolithos* ichnofacies) are present in the Karoo Supergroup rocks in the Gemsbok Sub-basin. The detailed descriptions of the eight identified facies associations has been given below and summarised in Table 4 and App. Fig. 1 -11.

3.5.1 Description: facies association 1

Facies association 1 consists of diamictite lithofacies (Dmm, Dcm) interbedded with sandstones (Sm), thin mudrock layers (ranging from 0.5 cm to 1 cm), bioturbated siltstones and mudrocks (Fr). This facies association is present in four boreholes which have intersected depths greater than 400 m (App. Fig. 1, 2, 8, 11) and forms the base of the Karoo Supergroup in the study area.

The diamictite lithofacies are present throughout the study area and are easily recognised by their poor sorting, massive mud and sandy matrix and the presence of scattered dropstones of variable lithologies.

Table 4 Facies associations identified in the boreholes of the Karoo Supergroup in the Gemsbok Sub-basin of Botswana and Namibia.

Facies associations (FAs)		Lithofacies in order of abundance	Sedimentary and biogenic structures
FA 8		Sm, St	Well sorted fine-grained sandstones. Non micaceous sandstones.
FA7		Fsm, Fl, Fr, Sm, Sr, Gcm	Reddish mudrocks.
FA6		Fl, Fr, Sr, Sh, Sm	Bioturbation structures. Rare upward-fining successions.
FA5		Sm, St, Sh, Sr, Fl, Fr, Fc, C, Fsm, Sb	Upward-fining successions (ranging from ± 0.3 m to 29 m). Erosive based sandstones. Mudrock clasts. Upward-coarsening successions (ranging from 3.5 m to 17.6 m). *Cruziana* ichnofacies (*Siphonichnus*, *Planolites* and *Thalassinoides*). Well sorted, clean sandstones with *Skolithos* ichnofacies (*Siphonichnus*, *Diplocraterion*, *Conichnus*, escape structures, *Phoebichnus*, *Planolites*, *Thalassinoides* and *Palaeophycus tubular*).
FA4	Upper part	Sh, Sm, St, Sr, Sb	Upward-coarsening successions (ranging from 22 m to 65 m). Well sorted and porous sandstones. Micaceous sandstones. *Cruziana* ichnofacies (*Thalassinoides*, *Planolites*, *Asterosoma*, *Teichichnus*, *Palaeophycus tubularis*, *Conichnus*, *Zoophycos* and *Skolithos*). *Skolithos* ichnofacies (*Conichnus*, *Rosselia*, *Siphonichnus* and escape structures)
	Lower part	Fl, Fc, Fr	
FA3		Fl, Fc, Fsm, Sm	Thinly laminated mudrocks, intercalated with thin massive sandstone layers.
FA2		Sm, Sh, Sr, Fsm, Fc	Upward-fining Bouma cycles.
FA1		Dmm, Fl, Sm, Sh, Sr, Dcm, Fc	Soft-sediment deformation structures. *Cruziana* ichnofacies (*Conichnus*, *Teichichnus*, *Siphonichnus*, *Schaubcylindrichnus* and *Palaeophycus tubularis*) in borehole ACP3.

Facies association 1 in the western part of the study area (i.e., boreholes ACP3 and ACP4), is dominated by matrix-supported diamictites (Dmm, Fig. 3.24). In borehole ACP3, facies association 1 starts at the base with a laminated sandstone, siltstone and mudrock unit (Fl) with light grey and dark grey to black colours, and evidence for *Cruziana* ichnofacies (*Conichnus*, *Teichichnus*, *Siphonichnus*, *Schaubcylindrichnus* and *Palaeophycus tubularis*; Fig. 3.23). The laminated sandstone, siltstone and mudrock lithofacies grade upwards into a 12 m thick sandstone unit, composed of sandstones interbedded with thin (range in size between 0.1 cm to 1 cm) mudrock layers and also

dominated by soft sediment deformation structures (consisting of small-scale folds; Fig. 3.25). Sedimentary structures within the sandstones include massive bedding, horizontal bedding, ripple cross lamination and load structures. Upward-fining cycles (ranging between 2 cm to 10 cm) are present within these sandstones. At a depth of 403.12 m a gradational contact separates the sandstone dominated unit from the overlying massive, matrix-supported diamictites (Dmm). Facies association 1 in borehole ACP4 consists of bioturbated dark grey mudrocks (Fl), with minor siltstone lenses (Fl), which grade upwards into matrix-supported diamictites (Dmm). No trace fossils were identified in facies association 1 of borehole ACP4.

In the northern part of the study area (i.e., borehole W3), facies association 1 is dominated by medium-grained sandstone units (range in thickness between 1.5 m to 5 m) interbedded with both matrix- and clasts-supported diamictites (Dmm, Dcm; Fig. 3.2, 3.3). Here the sandstone units of facies association 1 are moderately sorted, clean and occasionally are interbedded with thin carbonaceous mudrock (Fc) layers ranging in thickness from 0.1 cm to 1 cm. Sedimentary structures present within these sandstone units include ripple cross-lamination (Sr), soft sediment deformation structures (micro folds; Fig. 3.25), massive bedding (Sm), contorted bedding and load casts. Upward-fining cycles (ranging in thickness between 0.5 cm and 5 cm) are present within the sandstone units. Alternating mudrock and sandstone layers overlie the diamictite and sandstone units in borehole W3 (Fig. 3.26). These alternating mudrock and sandstone layers range in thickness from 0.5 cm to 2.5 cm and display upward-fining trends. Horizontal laminations and cross-laminations are common sedimentary structures in facies association 1 sedimentary rocks in the northern part of the study area.

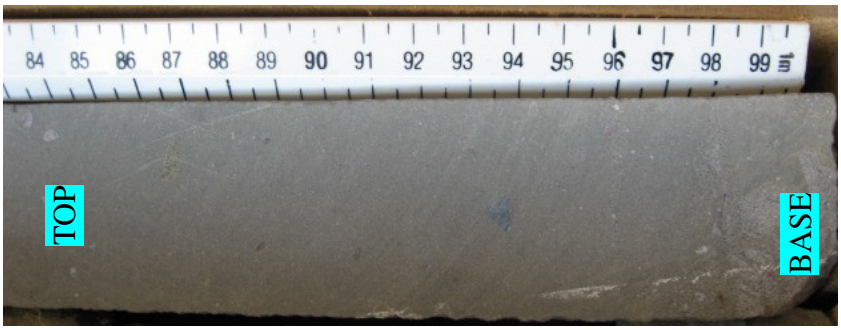


Figure 3.24 Matrix-supported, massive diamictite (Dmm), borehole ACP3. Clinorule scale in centimeters.



Figure 3.25 Soft-sediment deformation structures (micro-folds), borehole W3. Tape measure scale in centimeters.



Figure 3.26 Clast-supported diamictite (Dcm) and alternating layers of sandstones and mudrocks displaying upward-fining cycles, borehole W3. Tape measure scale in centimeters.

In the eastern part of the study area (only borehole CKP8C-1; App. Fig. 11), facies association 1 lies above a sharp contact, which separates it from the basement coarse-grained gabbroic rocks. Facies association 1 in CKP8C-1 borehole is characterised by bioturbated grey-greenish mudrocks at the base which grade into fine- to medium-grained sandstones interbedded with thin dark grey mudrock layers (ranging in thickness from 0.2 cm to 1 cm). Overlying the fine- to medium-grained sandstone is a sharp contact with a 3.5 cm thick pink granite boulder. The granite boulder is sharply overlain by dark grey mudrocks with thin siltstone intervals (ranging between 0.5 cm and 1 cm). Cross-laminations are present within the dark grey mudrocks. The dark grey mudrock unit

grades upwards into a sandstone-rich unit. The sandstone unit consists of light grey white sandstones with massive bedding and scattered rock clasts. Overlying the sandstone unit are laminated light grey, dark grey and light brown siltstones and mudrocks (Fl). These are characterised by upward-fining trends (1 cm thick) and the presence of cross-laminations. The uppermost part of facies association 1 in borehole CKP8C-1 is mainly formed by laminated light grey and dark grey mudrocks and siltstones with rare cross laminations and displays upward-fining trends.

3.5.2 Description: facies association 2

Facies association 2 has only documented in the western and northern parts of the study area. It is dominated by various sandstone lithofacies (Sm, Sh and Sr), which are interbedded with massive mudrocks and carbonaceous mudrocks (Fsm and Fc). In most places, sandstone lithofacies that characterise facies association 2 are moderately sorted and clean.

In the western part of the study area, facies association 2 overlies the matrix-dominated diamictites of facies association 1 with a sharp contact. Facies association 2 was observed only in boreholes ACP3 and ACP4 (App. Fig. 1, 2). It consists of sandstones, which are moderately sorted, clean and interbedded with alternating layers of siltstones (range in thickness from 0.3 cm to 3.5 cm) and massive carbonaceous mudrocks (range in thickness from 0.1 cm to 1.5 cm). Sandstones of facies association 2 show repetitive upward-fining trends (Fig. 3.27). These upward-fining successions range in thickness from 1.5 cm to 5 cm (e.g., borehole ACP4) and consist of medium-grained massive sandstones with sharp bases, grading upwards into horizontal laminated, fine-grained sandstones, ripple cross-laminated, fine-grained sandstones and capped by carbonaceous mudrocks. Sometimes these upward-fining successions consist of horizontal laminated sandstones or siltstones with a sharp base and grade upwards into carbonaceous mudrocks.

In the northern part of the study area, facies association 2 is separated by a sharp contact from the underlying alternating sandstone and mudrock unit of facies association 1 (e.g., borehole W3; App. Fig. 8). It consists predominantly of moderately-sorted, medium-

grained and clean sandstones (Fig. 3.28), which are interbedded with thin black mudrocks (up to 1 cm thick), bioturbated siltstones (greater than 0.5 m thick) and pale-green mudrocks (up to 0.5 m thick). Sedimentary structures, such as massive structures, horizontal laminations, cross-laminations and in places contorted laminations are common. Upward-fining cycles (ranging from 5 cm to 15 cm), comprising massive, medium-grained sandstones with erosive bases and rip-up mudrock clasts at the base, succeeded by laminated and cross-laminated, fine-grained sandstones and finally black mudrocks are recorded (Fig. 3.29). Pale-green mudrocks, which occur interbedded with the medium-grained, clean sandstones, contain carbonate bands and calcareous nodules in places.



Figure 3.27 Upward-fining cycles within sandstones of facies association 2 in borehole ACP4. Clinorule scale in centimeters.



Figure 3.28 Facies association 2 in borehole W3. Tape measure scale in centimeters.

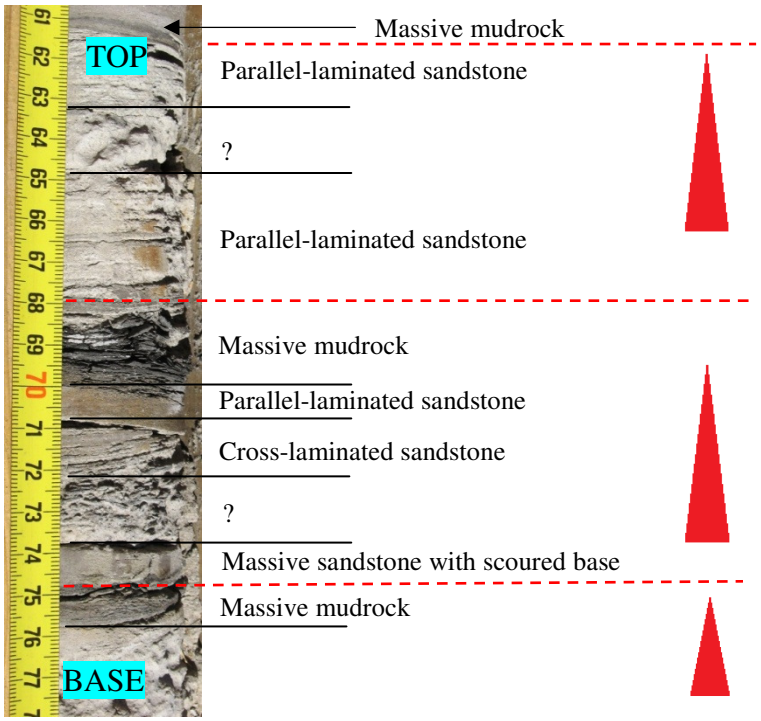


Figure 3.29 Upward-fining cycles (red triangles) within the sandstone-dominated facies association 2 in borehole W3. Red dotted lines show break between two upward-fining cycles and **?** indicates unidentified sedimentary structures. Tape measure scale in centimeters.

3.5.3 Description: facies association 3

Facies association 3 sharply overlies facies association 2 in the western and northern parts of the study area, and facies association 1 in the east. Facies association 3 is present in six of the studied boreholes in the study area (boreholes ACP3, ACP4, ACP19, ACP24, W3 and CKP8C-1). It is characterised by a thick argillaceous succession, which in the western part of the study area reaches thickness of up to 50 m (App. Fig. 1, 2, 4, 5, 7, 8, 11, 12, 13), and to the northern (App. Fig. 8) and the eastern (App. Fig. 11) parts of the study area, thicknesses of about 55 m and 124 m respectively. The argillaceous succession of facies association 3 comprises massive and laminated dark grey, black and greenish grey mudrocks (Fsm, Fl, Fc) which display a fissile texture in places (Fig. 3.30, 3.31). Thin (less than 1 cm) light grey siltstone units were observed within the mudrocks and they tend to display lenticular bedding structures. Clean sandstone (Sm) layers of about 5 cm thick are also present within facies association 3 mudrocks (Fig. 3.31).

In the western part of the study area, facies association 3 is dominated by dark grey and greenish grey mudrocks (Fl and Fsm) which are laminated and massive and occasionally contain soft sediment deformation structures. In borehole ACP4 in the western part of the study area, facies association 3 mudrocks are interbedded with sandy units of about 1 cm thick (Fig.3.30).



Figure 3.30 Facies association 3 in borehole ACP4. Clinorule scale in centimeters.

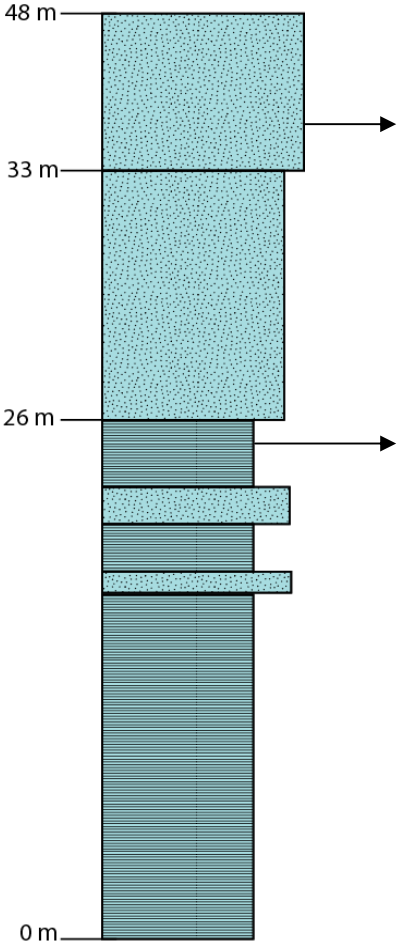
In the northern and eastern part of the study area, most of the facies association 3 mudrocks are dark grey and black in colour with finely-laminated, massive bedding, lenticular bedding and slump structures in places (Fig. 3.31). Thin (range from 1 cm to 5 cm) clean and moderately sandstone units were observed within the black mudrocks of facies association 3 in borehole W3 in the northern part of the study area. Dolerite sills have intruded facies association 3 mudrocks in the eastern part of the study area. Throughout the basin, facies association 3 mudrocks transition upwards into arenaceous-rich units of facies association 4.

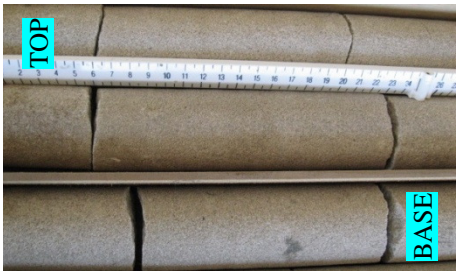


Figure 3.31 Facies association31 in borehole W3. Tape measure scale in centimeters.

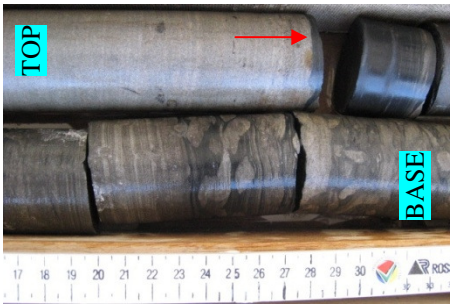
3.5.4 Description: facies association 4

Facies association 4 is present in all boreholes in the study area. It consists of a upward-coarsening succession comprising interbedded ripple cross-laminated siltstones and sandstones (Sr) and laminated sandstones, siltstones and mudrocks (Fl), which transition upwards into sandstone-stacked units (Fig. 3.32, 3.33, 3.34). The rocks of facies association 4 conformably overlie facies association 3 rocks (App. Fig. 1-2, 4-5, 7-8, 11). Facies association 4 is easily distinguished from the underlying facies association 3 and overlying facies association 5 because of the dominant arenaceous units, ripple cross-laminations, and thick upward-coarsening trends (ranging from 22 m to 65 m). In places, facies association 4 shows an upward transition from *Cruziana* ichnofacies at the base to *Skolithos* ichnofacies at the top.





Well sorted, massive (Sm) and porous sandstones of the upper facies association 4. Clinorule scale in centimeters.



Sharp contact (red arrow) between lower facies association 4 and upper facies association 4. Laminated sandstones, siltstones and mudrocks (Fl) of lower part of facies association 4 with *Cruziana* ichnofacies. Clinorule scale in centimeters.

Figure 3.32 Upward-coarsening succession of facies association 4 in borehole ACP4.

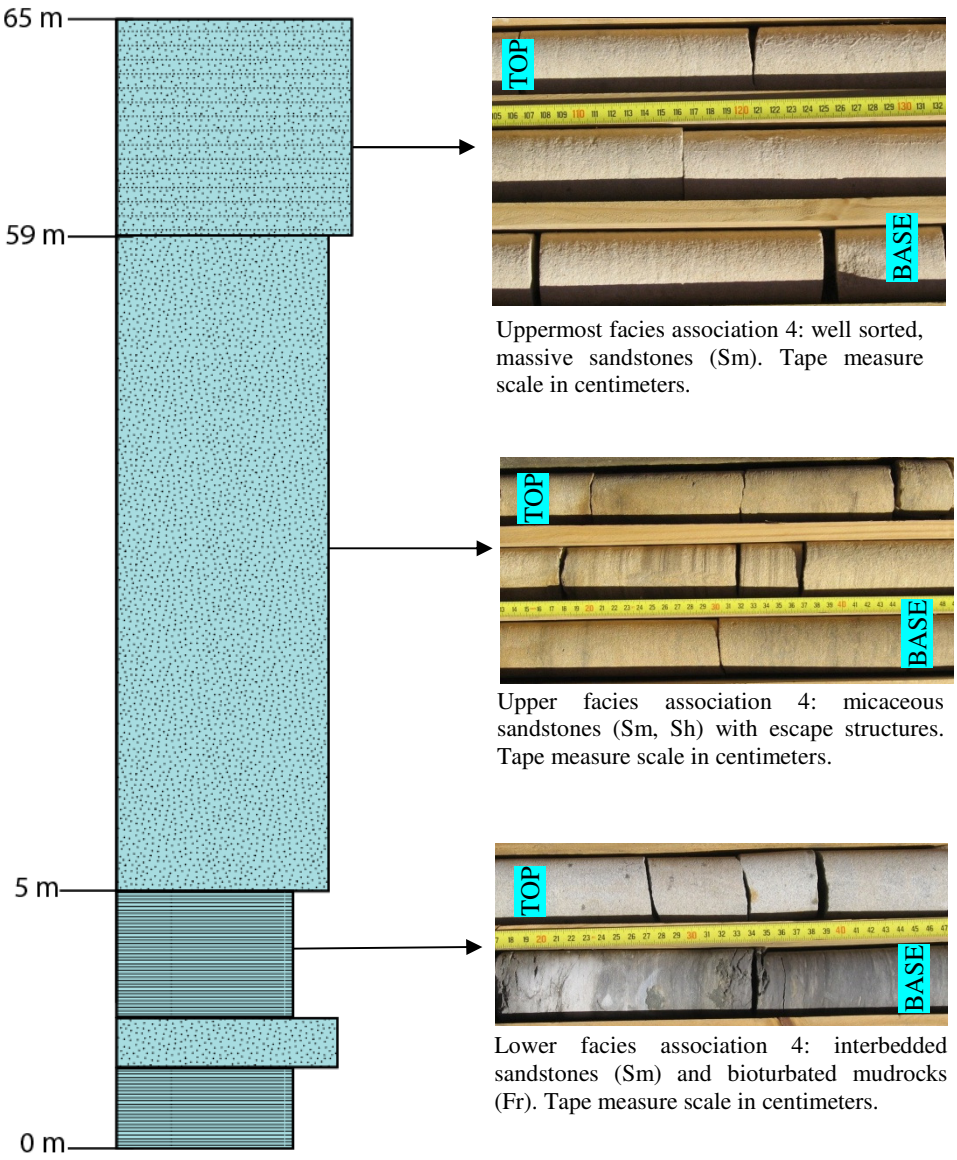
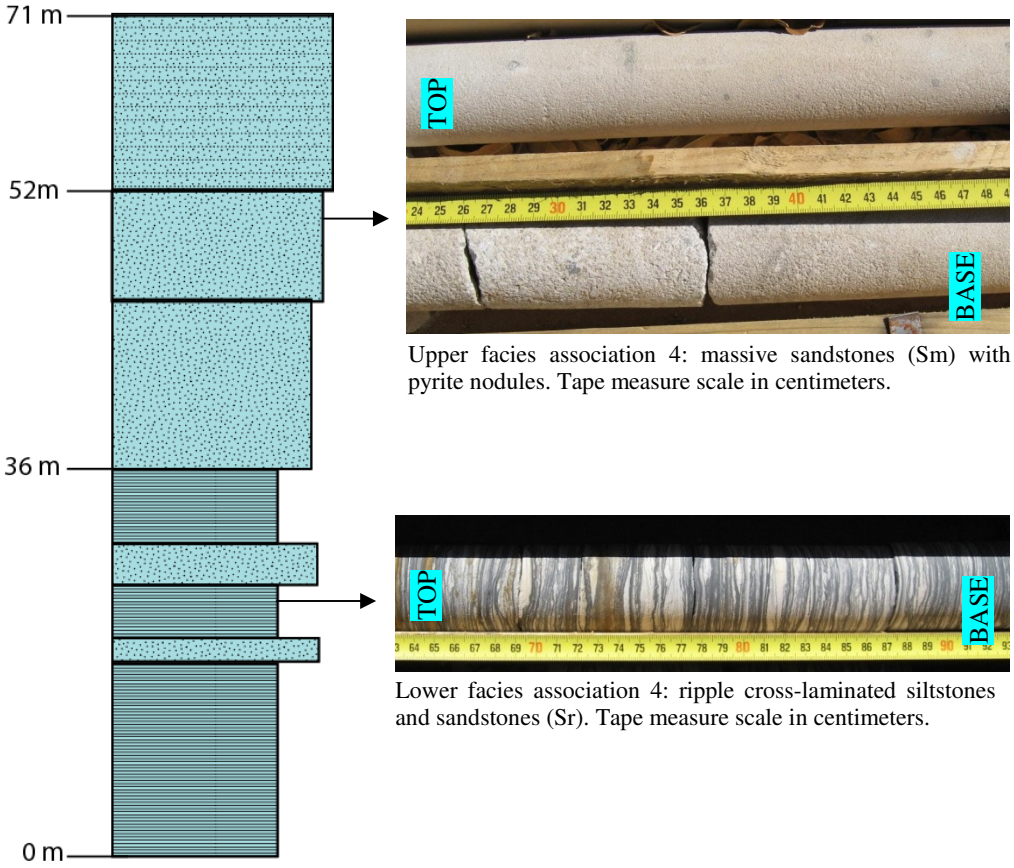


Figure 3.33 Upward-coarsening succession of facies association 4 in borehole W3.

In the western part of the study area, the lower part of facies association 4 is dominated by laminated sandstones, siltstones and mudrocks (Fl), which are often associated with *Cruziana* ichnofacies (dominated by *Thalassinoides*, *Teichichnus*, *Palaeophycus tubularis*, *Planolites*, *Zoophycos*, *Asterosoma*, *Skolithos* and *Conichnus*; Fig. 3.32).

In borehole W3 of the northern part of the study area, the lower part of facies association 4 consists of a 13 m thick succession composed of interbedded siltstones, mudrocks with subordinate sandstones. The base of the lower facies association 4 consists of interbedded

carbonaceous mudrocks (Fc), laminated siltstones and mudrocks (Fl) and bioturbated mudrocks (Fr; Fig. 3.33). Lenticular bedding is preserved within the mudrocks. Laminated siltstones and mudrocks (Fl) and bioturbated mudrocks (Fr) are characterised by a diverse suite of trace fossils (mainly of the *Cruziana* ichnofacies). Sandstone units range in thickness from 0.3 m to 0.5 m and are often interbedded with these mudrocks and are characterised by sharp bases, massive texture (Sm) and the presence of pyrite nodules. The top of the lower facies association 4 is dominated by micaceous laminated siltstones and mudrocks (Fl), which display lenticular bedding and bioturbation structures (Fr; Fig. 3.33). Trace fossils present within the lower part of facies association 4 in borehole W3 include *Thalassinoides*, *Planolites*, *Asterosoma* and *Zoophycos*.



Upper facies association 4: massive sandstones (Sm) with pyrite nodules. Tape measure scale in centimeters.

Lower facies association 4: ripple cross-laminated siltstones and sandstones (Sr). Tape measure scale in centimeters.

Figure 3.34 Upward-coarsening succession of facies association 4 in borehole CKP8C-1.

In the eastern part of the study area, the lower part of facies association 4 consists of laminated sandstones, siltstones and mudrocks (Fl), with plentiful ripple cross-lamination and few bioturbation structures (*Planolites* trace fossils; Fig. 3.34). These laminated sandstones, siltstones and mudrocks are interbedded with coarse-grained sandstones with sharp or erosive basal contacts.

The lower part of facies association 4 grades upwards into the arenaceous-rich upper facies association 4. Thick sandstone units (accumulated thickness range from 5 m to 60 m), consisting of lithofacies Sh, Sm, St and Sb dominate the upper portion of facies association 4. Medium- to fine-grained sandstones dominate, although rare units of coarse-grained to pebbly sandstones were also recorded.

In the boreholes situated in the western part of the study area, accumulated sandstone units of facies association 4 reach thicknesses up to 36 m, whereas the sandstone units of the northern part of the study area reach maximum thicknesses of up to 60 m. In the east of the study-area, these sandstone units do not exceed 35 m thickness.

In the western part of the study area, the upper part of facies association 4 consists of fine- to medium-grained sandstones that are massive or display horizontal bedding. Internally the sandstones are well sorted, porous and clean, although mica-rich sandstone lithofacies occur. Bioturbation structures within the sandstones tend to destroy bedding in most of the horizontally laminated sandstones (Sh). These sandstones locally contain mudrock clasts, pyrite nodules, traces of the *Skolithos* ichnofacies (dominated by *Conichnus* trace fossils) and often interbedded with pebble-sized sandstone layers (5 cm to 15 cm in thickness).

Sandstone units observed in the northern part of the study area are medium- to fine-grained, micaceous, horizontally laminated (Sh) and may contain trace fossils assigned to the *Skolithos* ichnofacies (dominated by escape structures, *Siphonichnus* and *Rosselia* isp.). In most cases, mica minerals tend to be aligned parallel to the orientation to the bedding within these sandstone lithofacies. The medium- to fine-grained micaceous

sandstones grade upwards into cleaner, porous, well sorted, medium- to fine-grained sandstones characterised by massive-, horizontal- and trough cross-bedding (Sm, Sh, St).

Sandstone lithofacies that dominate the upper parts of facies association 4 in the eastern part of the study area consists of medium- to fine-grained, clean and well sorted to moderately sorted sandstones. These sandstones are micaceous and poorly cemented in places. The sandstones of facies association 4 are usually massive, horizontally laminated, and porous and in places contain mudrock clasts and pyrite nodules. Coarse-grained to pebbly-sized sandstone layers (2 cm to 10 cm in thickness) sometimes were recorded with the medium- to fine-grained sandstones. No trace fossils are recorded from the sandstones of the upper facies association 4 in the eastern part of the study area.

Two cycles of upward-coarsening (App. Fig. 7, 8) trends produced by facies association 3 and 4 are present in the northern part and the central part of the study area (i.e., reference borehole MP1). An individual upward-coarsening succession in the northern part of the study area range in size from 100 m to 109 m.

3.5.5 Description: facies association 5

Facies association 5 is present in all boreholes in the study area and it is dominated by sandstone lithofacies and fine-grained lithofacies arranged in upward-fining cycles. Locally, upward-coarsening successions (3.5 m to 17.6 m thick) produced by these lithofacies were also documented. Individual upward-fining successions of facies association 5 ranges in thickness from ± 0.3 m to 29 m and stacked upward-fining successions vary from 5 m to 67 m across the Sub-basin. Cyclic upward-fining successions are dominant in the western and eastern parts of the study area compared to the northern part of the study area (App. Fig. 1, 2, 3, 4, 6, 7, 8, 10, 11). Facies association 5 in the western and eastern parts of the study area is dominated by more than three upward-fining cycles. In the northern part of the study area, facies association 5 consists of two to three upward-fining cycles.

Upward-fining successions observed are mainly characterised by sharp or erosive bases, coarse-grained to pebbly massive sandstones, which grades upwards into medium- to

fine-grained horizontally laminated (Sh), trough cross-bedded (St) and rippled cross-laminated (Sr) sandstones, and eventually fine-grained lithofacies (Fl, Fr, Fsm, Fc and C) at the top (Fig. 3.35, 3.36). The coarse-grained or pebbly sandstones that form the basal parts of the upward-fining successions are normally massive, poorly-sorted and in places contain rip-up clasts of mudrock and coal (Fig. 3.37). Pyrite and pale red (probably haematite) nodules were also observed within these poorly-sorted sandstones. No trace fossils were found associated with sandstones of facies association 5 within the study area. Occasionally, the massive, poorly sorted sandstones are abruptly capped by fine-grained lithofacies. Fine-grained lithofacies that cap most sandstone units are usually bioturbated, and often display wavy, flaser and lenticular bedding. Few trace fossils (*Planolites*) were found within the fine-grained lithofacies.

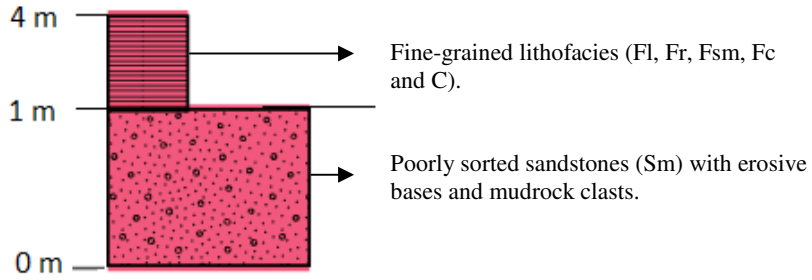


Figure 3.35 Upward-fining successions of facies association 5.



Figure 3.36 Upward-fining succession from sandstones (Sh, St, Sb) at the base grading upwards into bioturbated siltstone and mudrock (Fr) and carbonaceous mudrocks (Fc) interbedded with thin coals (C). Borehole CKP8C. Tape measure scale in centimeters.



Figure 3.37 Poorly sorted, pebbly massive sandstones (Sm) with carbonaceous mudrock clast sharply overlain by laminated sandstone, siltstone and mudrock lithofacies (Fl). Borehole CKP8C. Tape measure scale in centimeters.

Upward-coarsening successions identified in facies association 5 consist of laminated siltstones and mudrocks (Fl), bioturbated massive mudrocks and siltstones (Fr) and carbonaceous mudrocks (Fc) at the base which grades upwards into rippled cross-laminated (Sr) and horizontally laminated (Sh) sandstones (Fig. 3.38). The mudrocks and siltstones that form the basal parts of these upward-coarsening successions, in places display lenticular, wavy and flaser bedding, traces of *Planolites*, *Siphonichnus* and *Thalassinoides*, which are of *Cruziana* ichnofacies (Fig. 3.39). Most of the sandstone units that form the upper parts of the upward-coarsening successions contain lot of mica minerals. The upward-coarsening successions were mainly observed in the western part of the study area. Here, thick, porous, well sorted medium- to fine-grained sandstones (29 m to 50 m thick) are present within facies association 5. These thick sandstone units mainly overlie fine-grained lithofacies (Fc, C, Fl) or occasionally poorly sorted coarse-grained sandstones. Trace fossils assigned to the *Skolithos* ichnofacies (mainly *Siphonichnus*, *Diplocraterion*, *Conichnus*, escape structures, *Phoebichnus*, *Planolites*, *Thalassinoides* and *Palaeophycus tubularis*) were observed in borehole ACP24 (depth 211.39 m – 220.18 m) and associated with well sorted, clean, thick medium-grained sandstone units.

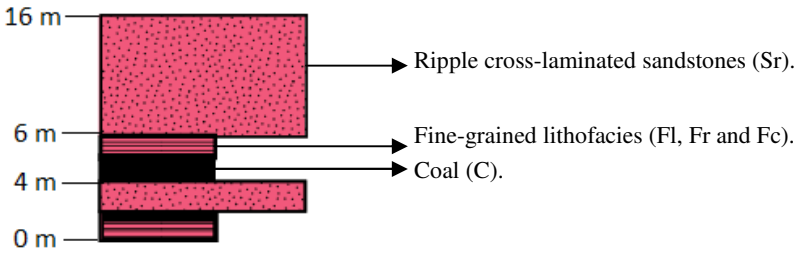


Figure 3.38 Upward-coarsening successions of facies association 5.

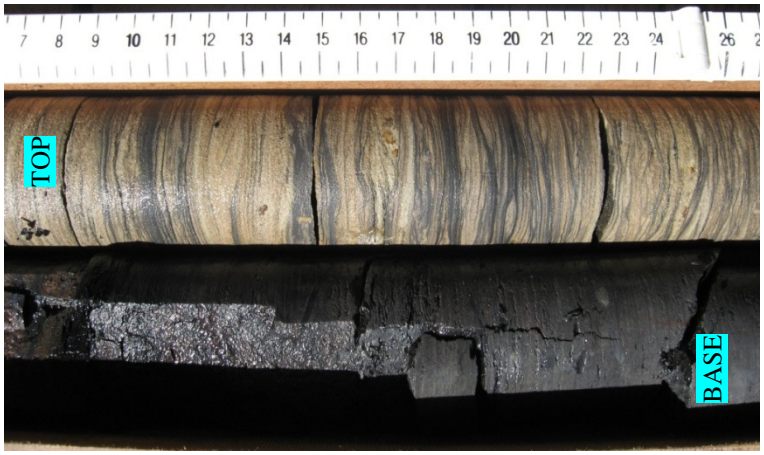


Figure 3.39 Carbonaceous mudrocks (Fc) with *Planolites* trace fossil grading upwards into ripple cross-laminated sandstones (Sr) of facies association 4, borehole ACP24. Clinorule scale in centimeters.

Coal lithofacies within the study area are mainly associated with carbonaceous mudrocks (Fc), laminated siltstones and mudrocks (Fl) and bioturbated mudrocks (Fr). Coal normally occurs on top of massive, coarse-grained sandstone units (App. Fig. 2, 3, 4, 10, 11) with a sharp contact, and in places overlies upward-fining successions (i.e., W1). Coals in places are in turn overlain by upward-coarsening successions (ranging in thickness from 3.5 m to 17.6 m) and by massive sandstones and fine-grained lithofacies (Fl, Fr, Fc). The thickness of coal lithofacies varies from one borehole to the other.

Coals in the western part of the study area are relatively thin (ranging in thickness between 10 cm to 80 cm). These coals occur interbedded with sandstone units, which are bounded at the base and on top by sharp contacts and in places occur above thick sandstone units of facies association 4 and below upward-coarsening successions (ranging from 3.5 m to 17.6 m) of facies association 5 (App. Fig. 4). In borehole ACP19, coal lithofacies are interbedded with pebbly, sharp-based sandstones (Sm). Coal lithofacies in boreholes ACP4 and ACP13 underlie facies association 4 sandstones units and are overlain by upward-coarsening successions, which in places are in turn overlain by thick (29 m) well sorted sandstones (App. Fig. 2, 3). In borehole ACP24 (App. Fig. 5), coal deposits occur between stacked upward-coarsening successions (ranging from 3 m to 8 m), which underlie thick (50 m) sandstone units.

In the northern part of the study area, coal lithofacies range in thickness between 3 m and 4.82 m. Two coal horizons (lower and upper) have been identified within the boreholes in the northern part of the study area (App. Fig. 6 – 8). The lower coals occur above the first or lower upward-coarsening cycle produced by facies association 3 and 4 and the upper coals occur above the second or upper upward-coarsening cycle.

In borehole W2 and W3, coals have an average thickness of 3 m and occur above fine-grained lithofacies or coarse-grained sandstones, which are in turn underlain by sandstone lithofacies of facies association 5 and facies association 4 (App. Fig. 7, 8). The coals in these two boreholes are overlain by sandstones (Sm) or fine-grained lithofacies (Fl, Fr, Fc), and occur below or above the thick (100 m to 105 m) upward-coarsening cycle produced by facies association 3 and 4. In borehole W1, coals (up to 4.82 m thick) occur above the second delta cycle and overlain at least by one upward-fining cycle (App. Fig. 6).

Within the study area, the thickest coals occur in the eastern part of the study area (i.e., CKP8C and CKP8C-1; App. Fig. 10, 11), where they are up to 28 m thick. Dolerite sills intruded most of the coal lithofacies in the eastern part of the study area. Coal lithofacies in the eastern part of the study area occur above coarse-grained sandstones in a sharp contact and are overlain sharply by fine-grained lithofacies (Fl, Fr, Fc) interbedded with thin (less than 0.2 m) medium-grained sandstone units, which are in turn overlain by stacked upward-fining successions with no coals.

3.5.6 Description: facies association 6

Facies association 6 has been identified only in the northern and eastern parts of the study area. It is dominated by homogeneous non-carbonaceous siltstone successions (Fig. 3.40) ranging between 32 m to 164 m in thickness. This facies association conformably overlies facies association 5 (App. Fig. 6, 7, 10, 11).

Siltstone (Fl) successions of facies association 6 are interbedded with thin mudrocks (less than 0.5 m in thickness) and fine-grained massive (Sm), horizontally laminated (Sh) and ripple cross-laminated (Sr) sandstones (normally less than 0.5 m thick, rarely up to 3 m

thick). The siltstones are mainly light grey in colour with few greyish orange pink, moderate reddish brown, light pink grey and very pale orange colours. Bioturbation structures (see lithofacies Fr; Fig. 3.40), calcareous nodules and pale red (probably haematite) nodules (Fig 3.41) were observed.

Upward-fining successions (ranging from 0.3 m to 4 m) are locally present within facies association 6 and comprise sandy siltstones with rip-up clasts of carbonaceous mudrocks at the base, which grades upward into sandy siltstones and siltstones (e.g., borehole W2; App. Fig. 7).



Figure 3.40 Bioturbated siltstones (Fr) of facies association 6 in borehole CKP8A. Tape measure scale in centimeters.



Figure 3.41 Siltstones (Fsm) with pale red nodules (probably heamatite), borehole CKP8A. Tape measure scale in centimeters.

3.5.7 Description: facies association 7

Facies association 7 was only observed in four boreholes (App. Fig. 3, 4, 6, 7) in the western and northern parts of study area. It overlies facies association 5 in the western part of the study area and facies association 6 rocks in the northern part of the study area. This

facies association in the western study area has an average thickness of approximately 56 m, and in the northern part of the study area ranges in thickness from 5 m to 21 m.

In the western part of the study area, facies association 7 comprises mudrocks and siltstones which are dark reddish brown, pale red, greyish red and light grey in colour, massive and laminated (lithofacies Fsm and Fl) with calcareous nodules (Fig. 3.42). Dolerites intruded facies association 7 mudrock successions in borehole ACP13 (western part of the study area; App. Fig. 3). In the northern part of the study area, facies association 7 is characterised by a basal conglomerate (Gcm), which grades upward into medium-grained, reddish sandstones (Sm, Sr) and laminated to massive moderate reddish brown mudrocks (Fl, Fsm) arranged in a upward-fining character (i.e., borehole W1; Fig. 3.43, 3.44; App. Fig. 6).

3.5.8 Description: facies association 8

This facies association occurs only in the northern and eastern parts of the study area (App. Fig. 6, 8, 9, 10, 11). Facies association 8 overlies facies association 6 in the northern part of the study area and in the eastern part of the study area it overlies facies association 6. Facies association 8 is characterised by fine-grained sandstones, which are clean, moderately to well sorted and massive in texture (Fig. 3.45). Cross-bedding (St) is also present within these sandstones but is not prevalent as massive bedding (Sm). The sandstone lithofacies characterising this facies association do not contain any mica minerals and are light brown, very pale orange and very light grey.



Figure 3.42 Reddish mudrocks (Fsm) of facies association 7 in borehole ACP13. Core tray caring 6.02 m of core.

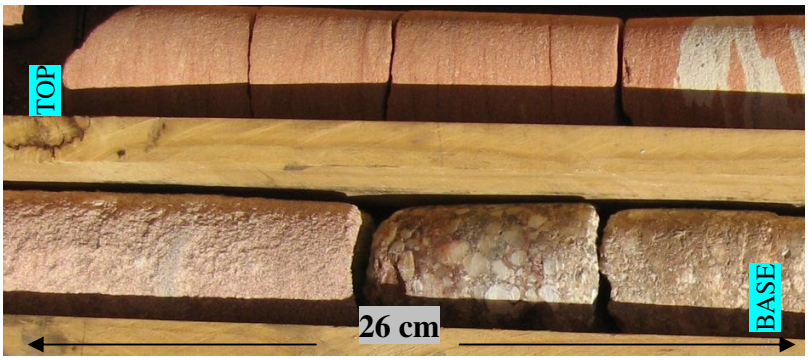


Figure 3.43 Basal clast-supported conglomerate (Gcm) overlain by sandstones (Sm, Sr) of facies association 7 in borehole W1.



Figure 3.44 Reddish mudrocks of facies association 7 sharply overlain (erosive contact) by well sorted, fine-grained sandstones (Sm) of facies association 8 in borehole W1. Tape measure scale in centimeters.



Figure 3.45 Facies association 8 massive(Sm), mica-free sandstones in borehole W1. Tape measure scale in centimeters.

CHAPTER FOUR: SANDSTONE PETROLOGY, GEOCHEMISTRY AND PROVENANCE

4.1 Introduction

In order to understand and reconstruct the palaeodepositional history of sedimentary rocks within a basin, a petrographic analysis of sandstone suites should be conducted. The petrography of sandstone suites generally reflects the provenance of the detritus, although various other sedimentological factors (weathering, transportation and diagenesis) also influence their original compositions (Dickinson, 1985). Therefore, petrographic analyses were done in order to understand the palaeoenvironments and the probable source rocks for the Karoo Supergroup in the Gemsbok Sub-basin. Thirty-five sandstone samples were collected from well-developed or thick sandstone bodies in eleven boreholes consisting of well-cemented fine to medium sandstones, which were subsequently found in facies associations 4, 5 and 8. Sandstone samples which begin with prefix **B** are those which have been sampled from the boreholes situated in the northern and eastern Gemsbok Sub-basin (southwest Botswana) and those that begin with prefix **N** were sampled from the western part of the Gemsbok Sub-basin (the Aranos Basin). Thin sections were prepared of all sandstone samples for petrographic analysis. The sandstone thin sections were examined in detailed and counted for modal composition using the Gazzi-Dickinson point count method (Dickinson, 1985). The results of the detailed petrographic studies and point counts of all the sandstone samples are presented and summarised in Appendix A and Tables 5 and 6.

4.2 Sandstone petrography

This section presents detailed petrographic descriptions of representative sandstone samples of facies association 4 (sample N8, B7 and B20), facies association 5 (sample N11 and B17) and facies association 8 (sample B1) in different locations in the study area.

Table 5 Detrital modes of the Ecca Group facies association 4 and 5 sandstones in the western part of the Gemsbok Sub-basin.

Facies association (FA)	Sample No:	Borehole No:	Depth (m) From (m)	Depth (m) To (m)	Qm	Qp	Qt	K	P	F=K+P	L	M + C	QFL (%) Q	QFL (%) F	QFL (%) L	QmFLt (%) Qm	QmFLt (%) F	QmFLt (%) Lt
FA5	N1	ACP4	234.17	234.24	144	13	157	27	32	59	13	103	69	26	6	63	26	11
FA5	N2	ACP4	245.06	245.14	151	13	164	29	31	60	7	102	71	26	3	65	26	9
FA4	N3	ACP4	328.65	328.76	114	13	127	31	35	66	7	118	64	33	4	57	33	10
FA5	N4	ACP3	166.07	166.13	158	44	202	18	42	60	1	85	77	23	0	60	23	17
FA5	N5	ACP3	245.99	246.05	185	35	220	33	32	65	0	61	77	23	0	65	23	12
FA5	N6	ACP3	265.06	265.11	142	30	172	22	32	54	1	126	76	24	0	63	24	14
FA5	N7	ACP19	261.59	261.64	143	27	170	35	34	69	3	106	70	29	1	59	29	12
FA4	N8	ACP19	324.92	325	131	22	153	25	32	57	9	126	70	26	4	60	26	14
FA5	N9	ACP24	170.84	170.89	134	16	150	36	46	82	4	112	64	35	2	57	35	8
FA5	N10	ACP24	230	230.07	180	8	188	25	45	70	7	100	71	26	3	68	26	6
FA5	N11	ACP13	244.3	244.37	157	32	189	31	45	76	7	73	69	28	3	58	28	14
FA5	N12	ACP13	271.42	271.47	145	30	175	40	27	67	1	109	72	28	0	60	28	13
FA5	N13	ACP13	226.56	226.61	129	30	159	34	31	65	2	124	70	29	1	57	29	14

Qm: monocrystalline quartz, Qp: polycrystalline quartz, Qt: quartz total, K: potassium feldspar or Kspar, P: plagioclase, F: total feldspar, L: lithic fragment, M: matrix, C: cement, Q: quartz, Lt: total lithic fragments.

Table 6 Detrital modes of the Ecca Group facies association 4 and 5 and Ntane Sandstone Formation facies association 8 in the northern and eastern parts of the Gemsbok Sub-basin.

Facies association (FA)	Sample No:	Borehole No:	Depth (m) From (m)	Depth (m) To (m)	Qm	Qp	Qt	K	P	F=K+P	Lsi	M + C	QFL (%) Q	QFL (%) F	QFL (%) L	QmFLt (%) Qm	QmFLt (%) F	QmFLt (%) Lt
FA8	B1	WI	96.81	96.9	180	10	190	3	14	17	6	20	89	8	3	85	8	8
FA4	B2	WI	169.29	169.39	117	18	135	37	10	47	20	60	67	23	10	58	23	19
FA4	B3	W2	154.69	154.79	157	10	167	42	20	62	16	59	68	25	7	64	25	11
FA4	B4	W2	152.18	152.26	148	12	160	38	34	72	6	110	67	30	3	62	30	8
FA4	B5	W2	170.2	170.24	60	3	63	33	32	65	8	41	46	48	6	44	48	8
FA4	B6	W2	230.69	230.77	170	12	182	59	18	77	6	81	69	29	2	64	29	7
FA4	B7	W3	206.8	206.16	169	11	180	17	25	42	3	121	80	19	1	75	19	6
FA4	B8	W3	130.24	130.34	125	10	135	56	21	77	4	98	63	36	2	58	36	6
FA4	B9	W3	97.25	97.34	183	7	190	14	30	44	6	30	79	18	3	76	18	5
FA4	B10	CKP8C-1	415	415.91	120	7	127	7	18	25	3	111	82	16	2	77	16	6
FA5	B11	CKP8A	277.4	277.86	113	23	136	13	7	20	12	156	81	12	7	67	12	21
FA5	B12	CKP8A	283.74	283.89	166	18	184	18	31	49	21	141	72	19	8	65	19	15
FA5	B14	CKP8C-1	261.74	261.9	156	40	196	28	36	64	11	32	72	24	4	58	24	19
FA5	B15	CKP8C-1	411.25	411.31	168	8	176	10	30	40	8	130	79	18	4	75	18	7
FA5	B16	CKP8C-1	321.1	321.32	96	20	116	20	46	66	9	133	61	35	5	50	35	15
FA5	B17	CKP8C-1	278.19	278.35	179	9	188	11	29	40	13	109	78	17	5	74	17	9
FA5	B18	CKP8C-1	320.76	320.83	117	5	122	20	33	53	3	153	69	30	2	66	30	4
FA5	B19	CKP8C-1	320.83	320.93	117	5	122	20	33	53	3	153	69	30	2	66	30	4
FA4	B20	CKP8C-1	474.63	474.73	173	1	174	29	20	49	4	110	77	22	2	76	22	2
FA5	BA	CKP8C	277.35	277.51	131	5	136	25	11	36	7	148	76	20	4	73	20	7
FA5	BB	CKP8C	298.93	299	135	46	181	23	24	47	9	110	76	20	4	57	20	23
FA5	BC	CKP8C	326	326.09	174	12	186	28	39	67	8	72	71	26	3	67	26	8

Qm: monocrystalline quartz, Qp: polycrystalline quartz, Qt: quartz total, K: potassium feldspar or Kspar, P: plagioclase, F: total feldspar, L: lithic fragment, M: matrix, C: cement, Q: quartz, Lt: total lithic fragments.

Sample N8

Sample N8 was sampled from borehole ACP19 (western part of the study area) at depths between 324.92 m and 325.00 m (Fig. 4.1). The sample is moderately to well sorted and fine- to coarse-grained (0.125 mm – 1 mm). Fine detrital grains dominate the sandstone. This sample comprises subangular to subrounded detrital framework grains. Framework

grains include quartz (both monocrystalline and polycrystalline quartz), feldspar (plagioclase, microcline and other potassium-feldspars) and quartzo-feldspathic rock fragments. Most of the polycrystalline quartz grains are formed by three to four non-sutured crystals and more than five sutured and non-sutured quartz crystals. Mica grains are present in the sample and consist of muscovite with a lesser amount of biotite. Muscovite grains are deformed in places. Sandstone sample N8 is poorly cemented by calcite and contains a detrital clay matrix. Accessory minerals present include tourmaline, garnet, subrounded zircons and pyrite.

Sample N11

Sandstone sample N11 was sampled from borehole ACP24 (western part of the study area) at depths between 244.30 m and 244.37 m (Fig. 4.2). It is a poorly sorted, medium-grained (0.30 mm - 0.56 mm) sandstone, composed of subangular to subrounded detrital grains. Sandstone sample N11 is poorly cemented by calcite. Framework grains comprise quartz, feldspar and rock fragments (quartz-feldspar). Quartz grains occur as both monocrystalline and polycrystalline quartz, with lesser amounts of polycrystalline quartz. The most commonly observed polycrystalline quartz grains are those comprising four to more than five non-sutured quartz crystals. Feldspar grains are dominated by microcline and lesser amounts of plagioclase and other potassium-feldspars. Rock fragments comprise quartz-feldspar and argillaceous rock fragments. The sandstone sample N11 is characterised by a clay matrix with abundant micaceous minerals and it is poorly cemented by calcite. Accessory framework grains comprise trace amounts of mica (muscovite), tourmaline (green), garnet, subrounded zircon and pyrite.

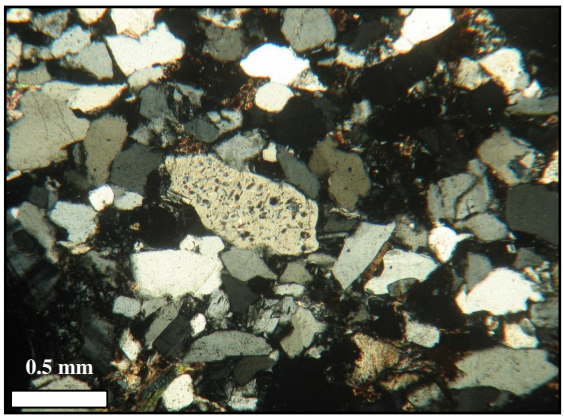


Figure 4.1 Photomicrograph of sample N8, Facies association 4, western part of the study area.

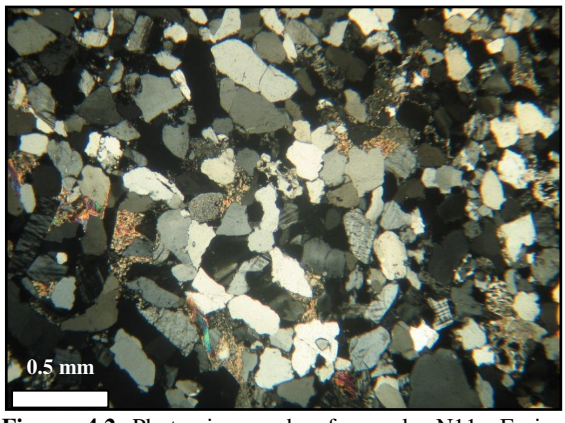


Figure 4.2 Photomicrograph of sample N11. Facies association 5, western part of the study area.

Sample B7

Sample B7 was sampled from borehole W3 (northern part of the study area) at depths between 206.08 m and 206.16 m (Fig. 4.3). It is a moderately sorted, medium-grained (0.25 mm – 0.50 mm) sandstone. The sandstone has angular to subangular grains, with the latter being dominant. Quartz, feldspar and rock fragments are the main detritus in the sandstone sample B7. The most abundant quartz grains are the monocrystalline quartz with only trace amounts of polycrystalline quartz. Polycrystalline quartz grains consist of five non-sutured quartz crystals. Feldspar grains consist of microcline, plagioclase and potassium feldspars. Rock fragments are present and comprise argillaceous rock fragments and quartz-feldspar rock fragments. Mica is present and includes muscovite, which is deformed in places. The sample is partially cemented with calcite. Detrital clay constitutes the matrix. Accessory framework grains include zircon (subrounded and rounded), mica, rutile, tourmaline (rounded, elongate green tourmaline) and garnet (light pink). Rounded tourmaline and zircon inclusions within the quartz grains were observed.

Sample B20

Sample B20 was sampled from depths between 474.63 m and 474.73 m in borehole CKP8C-1 (eastern part of the study area) (Fig. 4.5). Sandstone sample B20 is poorly sorted, medium-grained (0.25 mm – 0.40 mm) and consists of subangular to subrounded detrital grains. Major detrital framework grains present include quartz, feldspar and rock fragments. Quartz grains include monocrystalline and polycrystalline quartz. Polycrystalline quartz occurs in lesser amounts and consists of two (non-sutured) and more than five (sutured) crystals of quartz. Feldspars present in the sample include microcline, plagioclase and other potassium-feldspars. Rock fragments consist of quartz-feldspar and argillaceous rock fragments. The sample consists of lesser amounts of mica and muscovite occurs in larger quantities compared to biotite. The muscovite mica grains appear bent adjacent to quartz and feldspar grains. Accessory minerals include zircon (subrounded), garnet, rutile, tourmaline (brown and green) and pyrite. Apatite and tourmaline are common as inclusions within quartz grains.

Sample B17

Sample B17 is from borehole CKP8C-1 (eastern part of the study area) and was sampled between depths of 278.19 m and 278.35 m (Fig. 4.4). The sandstone sample is moderately to well sorted and fine- to medium-grained (0.20 mm - 0.30 mm) in size. This sandstone consists of subangular to subrounded detrital framework grains of quartz (monocrystalline and polycrystalline quartz), feldspar and rock fragments. Different types of polycrystalline quartz grains were identified in this thin section and are composed of more than two quartz crystals. Feldspar grains include plagioclase, microcline and other potassium-feldspars. Microcline is the most abundant feldspar. Rock fragments include argillaceous rock fragments, which in places have been replaced by calcite. Sample B17 is poorly-cemented by calcite and contains up to 1% mica minerals (muscovite and biotite). Accessory grains comprise trace amounts of zircon (irregular and subrounded), tourmaline, rutile, apatite (as rounded inclusions within quartz grains) and angular garnets.

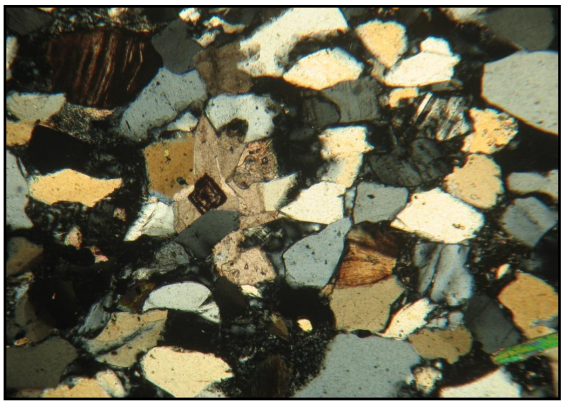


Figure 4.3 Photomicrograph of sample B7, Facies association 4 northern part of the study area.

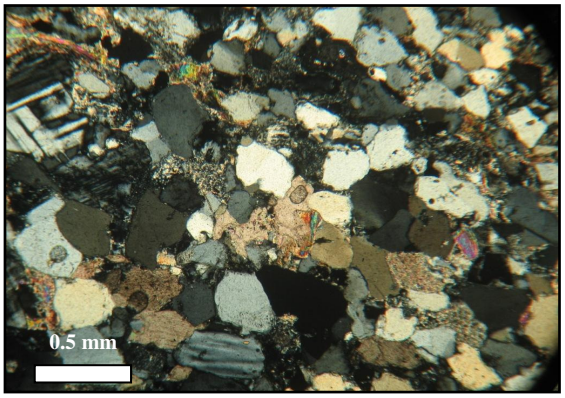


Figure 4.4 Photomicrograph of sample B20, Facies association 4 eastern part of the study area.

Sample B1

Sample B1 is from borehole W1 (northern part of the study area) and was sampled at depths between 96.81 m and 96.90 m (Fig. 4.6). The sandstone sample is well sorted and fine-grained (0.125 mm - 0.25 mm). Detrital grains that make up this sample are subangular to subrounded. The sample is dominated by detrital grains of quartz followed by feldspar grains and lithic fragments. The quartz component of this sandstone comprises monocrystalline quartz and polycrystalline quartz, with the monocrystalline quartz content being greater. Polycrystalline quartz is formed by more than five non-

sutured quartz crystals. Subrounded quartz grains with inclusions of subrounded and elongate shape apatite were observed. The sandstone sample contains lesser amount of feldspar. Feldspar grains include microcline and plagioclase. The sample contains minor amounts of rock fragments (argillaceous and polycrystalline quartz). Carbonate cement and clay matrix are present in lesser amounts. No mica minerals were found in this thin section. Accessory minerals include zircons (zoned and subrounded), rutile (subrounded), tourmaline (green in colour, zoned and subrounded) and garnet (angular).

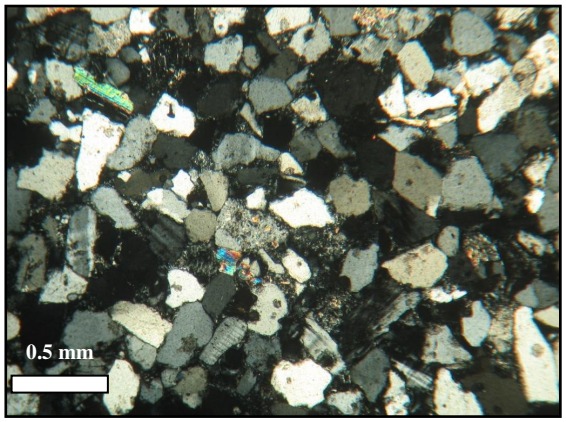


Figure 4.5 Photomicrograph of sample B17, Facies association 5 eastern part of the study area.

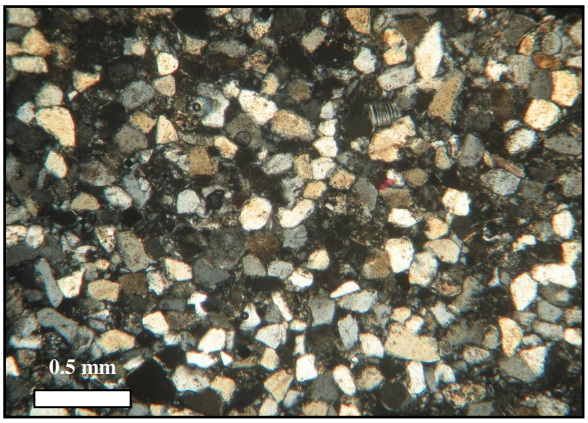


Figure 4.6 Photomicrograph of sample B1, Facies association 8 northern part of the study area.

4.3 Detrital framework grains

The sandstone samples of facies association 4 and 5 in the western, northern and eastern parts of the study area comprise the following framework grains: quartz, feldspars, rock fragments, micas, heavy minerals (zircon, tourmaline, garnet, rutile and apatite), pyrite, matrix and cement. Facies association 8 sandstone sample B1 does not contain mica minerals, but has all the other framework grains. All analysed sandstones are characterised by subrounded to subangular detrital grains, with the latter being dominant. The sandstones tend to be moderately sorted and poorly cemented. In a few of the analysed sandstone samples, subrounded to rounded grains of zircon, tourmaline, apatite, pyrite minerals and quartz have been noted.

Quartz

Petrographic studies of sandstones from facies association 4, 5 and 8 from the Gemsbok Sub-basin reveal that quartz is the most abundant framework grain with lesser feldspar grains and rock fragments. Quartz occurs as both monocrystalline quartz (Qm) and polycrystalline quartz (Qp) (see Table 2; Fig. 4.7, 4.8), with monocrystalline quartz being more abundant. Different types of polycrystalline quartz grains are present within the sandstones. Observed polycrystalline quartz grains are composed of three to more than five crystals of quartz, which may be sutured or non-sutured. The detrital quartz grains are mainly angular to subangular with subrounded to rounded grains being much rarer.

Feldspar

Feldspar grains include microcline, plagioclase and potassium-feldspar (Fig. 4.9). Microcline and other potassium feldspars are more abundant than plagioclase in most of the studied sandstone samples in the western, eastern and the northern parts of the study area.

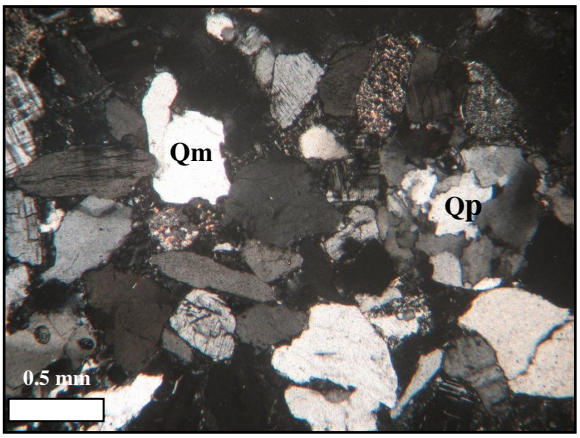


Figure 4.7 Photomicrograph of sample BB, facies association 5, borehole CKP8C, depth 298.93 m – 299.00 m. Polycrystalline quartz (Qp) with more than five non-sutured quartz crystals (Cross Polarised Light).

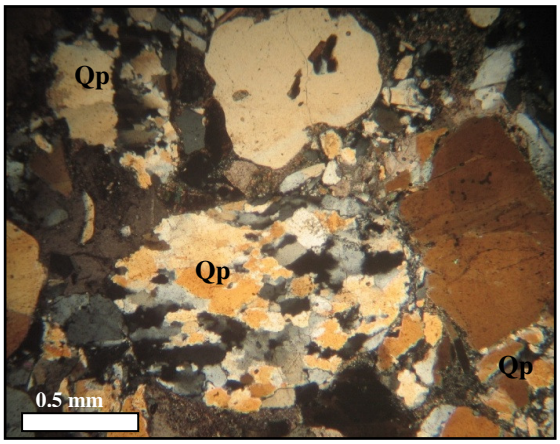


Figure 4.8 Photomicrograph of sample B15, facies association 5, borehole CKP8C-1, depth 411.25 m – 411.31 m. Polycrystalline quartz (Qp) with more than five sutured quartz crystals (Cross Polarised Light).

Rock fragments

Rock fragments observed in thin sections are of sedimentary, igneous and metamorphic (Fig. 4.9, 4.10) origin. The sedimentary rock fragments consist mainly of fine-grained, argillaceous rock fragments, whereas igneous rock fragments comprise quartz-feldspar grains. Metamorphic rock fragments are represented by polycrystalline quartz grains composed of more than five crystals of quartz, which display sutured boundaries.

Sandstone samples of facies association 4, 5 and 8 in the Gemsbok Sub-basin contain only a small amount of rock fragments.

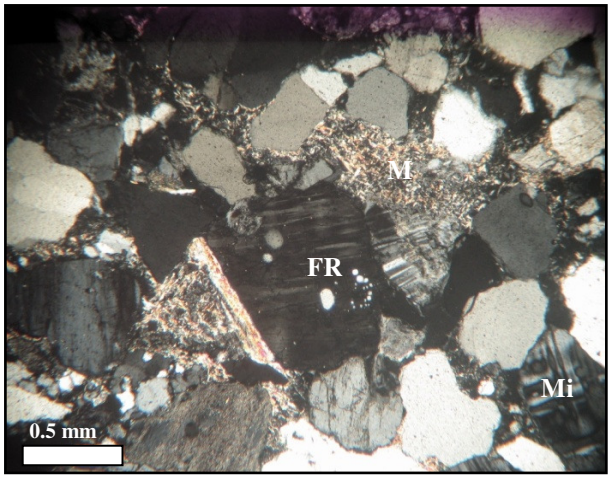


Figure 4.9 Photomicrograph of sample N13, facies association 5, borehole ACP13, depth 226.56 m – 226.61 m. Angular to subangular quartz-feldspar rock fragment (FR), microcline (Mi) grains and matrix (M) (Cross Polarised Light).

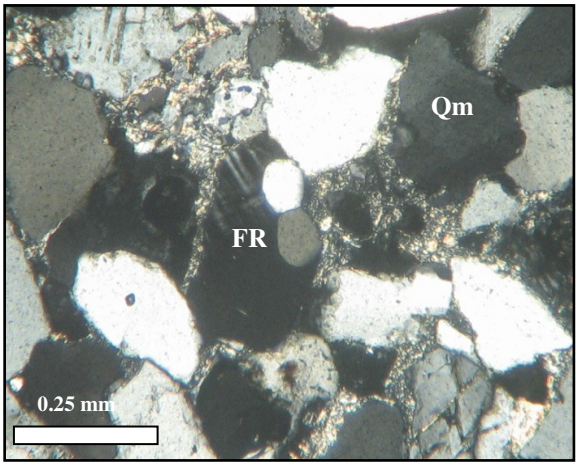


Figure 4.10 Photomicrograph of sample N6, facies association 5, borehole ACP3, depth 265.06 – 265.11 m. Quartz-feldspar rock fragment (RF), quartz grain (Qm) showing undulatory extinction and fine-grained matrix (Cross Polarised Light).

Micas

The sandstone samples of facies association 4 and 5 in the northern, eastern and western parts of the study area exhibit abundant micaceous minerals (muscovite and biotite) aligned parallel to bedding planes (Fig. 4.11). Many of these micaceous grains have been altered to clay minerals and in places to chlorite. Most of these micaceous minerals in the studied thin sections are associated with fine- to medium-grained sandstones. Bent mica minerals are common within the sandstones. Sample B1 of facies association 8 is the only sample analysed which does not contain any mica minerals (Fig. 4.6).

Matrix

The matrix of the sandstones is generally composed of fine-grained material comprising microcrystalline quartz, mica and feldspar grains (Fig. 4.9).

Cement

Calcite cement was recognised in most of the sandstone samples (Fig. 4.12). Calcite cement tends to form poikilitic textures and envelops some of the detrital grains within the sandstone thin sections. Most of the studied sandstones are partially cemented by

calcite; however there are a few sandstone samples, which are well cemented by calcite (Fig. 4.12).

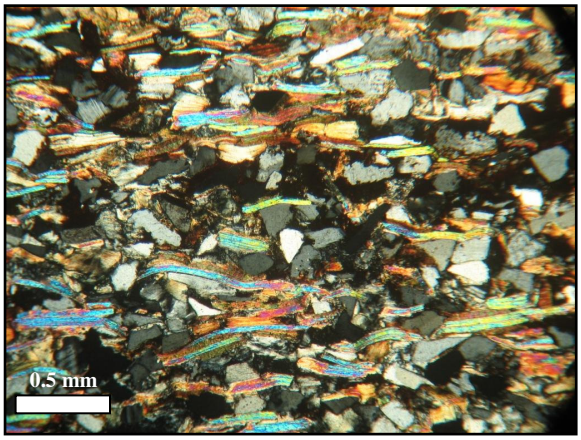


Figure 4.11 Photomicrograph of sample B5, facies association 4, borehole W2, depth 170.20 m – 170.24 m. Micaceous sandstone with bent mica minerals (Cross Polarised Light).

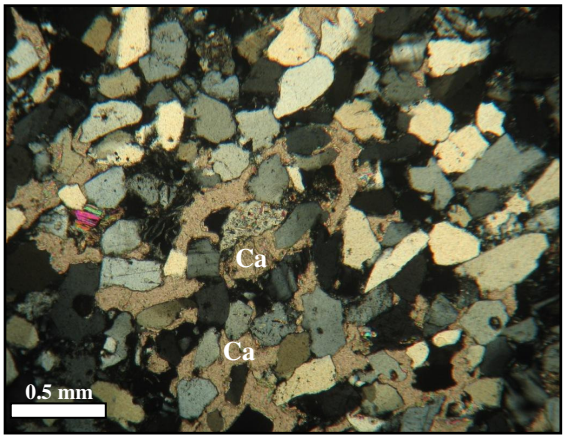


Figure 4.12 Photomicrograph of sample B17, facies association 5, borehole CKP8C-1, depth 278.19 – 278.35 m. Calcite (Ca) cement (Cross Polarised Light).

Heavy Minerals

Heavy minerals identified in the sandstones studied include tourmaline, zircon, rutile, garnet, apatite (subrounded to rounded and elongate shapes) and pyrite minerals. Zircons occur as subrounded, rounded and euhedral grains (Fig. 4.13, 4.14). The euhedral zircon grains tend to show a lot of zonation. Tourmaline occurs as rounded, subrounded, irregular and euhedral grains (Fig. 4.15, 4.16) and zoned tourmaline is present within the sandstones. Rutile mineral grains are deep red and mostly occur in euhedral form but subrounded rutile grains were also observed (Fig. 4.17, 4.18). Garnet is dominant within the sandstones; it occurs in irregular shape having colourless and light pink colours in thin sections (Fig. 4.19, 4.20). Apatite grains occur as inclusions within quartz grains and are often colourless in plane polarised light (Fig. 4.21). Pyrite grains are present in trace amounts within the sandstone samples and mainly occur as subrounded grains, but angular grains are also present (Fig. 4.22).

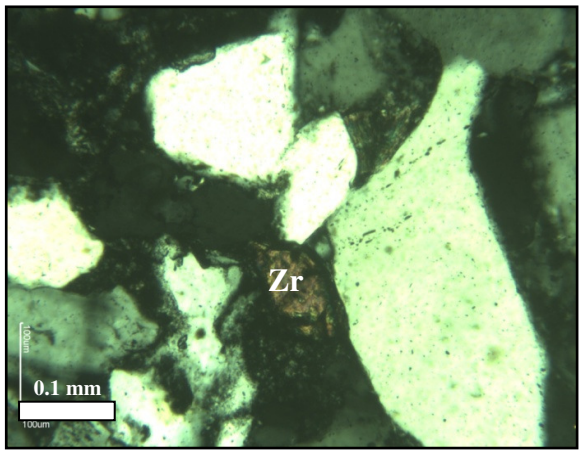


Figure 4.13 Photomicrograph of sample B17, facies association 5, borehole CKP8C-1, depth 278.19 m – 278.35 m. Euhedral zircon (Zr) grain (Cross Polarised Light).

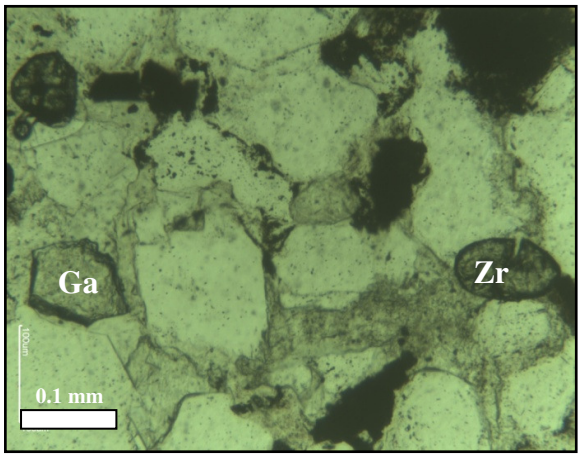


Figure 4.14 Photomicrograph of sample N1, facies association 5, borehole ACP4, depth 234.17 m – 234.24 m. Angular garnet (Ga) grain and rounded zircon (Zr) grain (Plane Polarised Light).

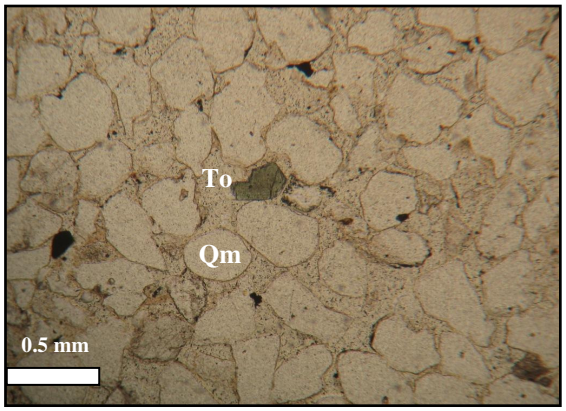


Figure 4.15 Photomicrograph of sample B6, facies association 4, borehole W2, depth 230.69 m – 230.77 m. Sandstone with subrounded quartz (Qm) grains and partially euhedral green tourmaline (To) grain (Plane Polarised Light).

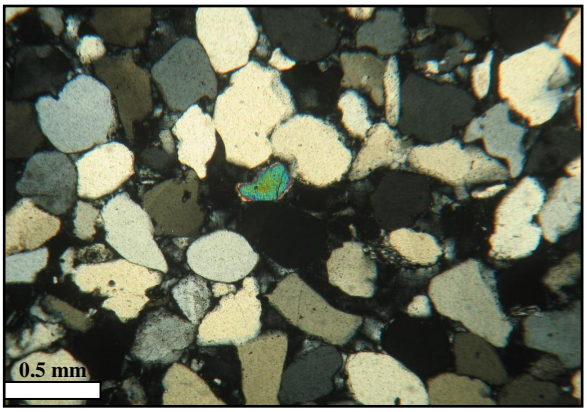


Figure 4.16 Photomicrograph of sample B6, facies association 4, borehole W2, depth 230.69 m – 230.77 m. Tourmaline grain showing zonation (Cross Polarised Light).

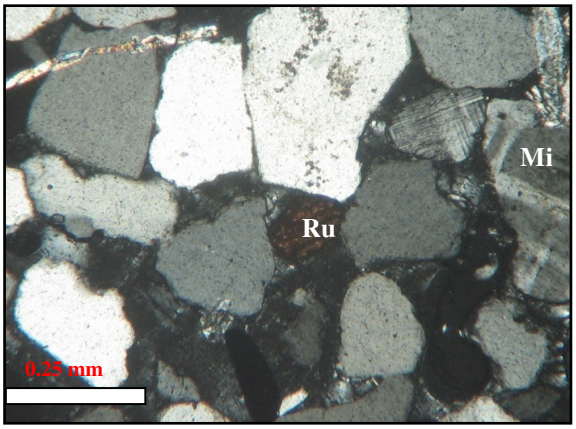


Figure 4.17 Photomicrograph of sample B6, facies association 4, borehole W2, depth 230.69 m – 230.77 m. Rutile grain (Ru) with irregular cleavage fractures (Cross Polarised Light).

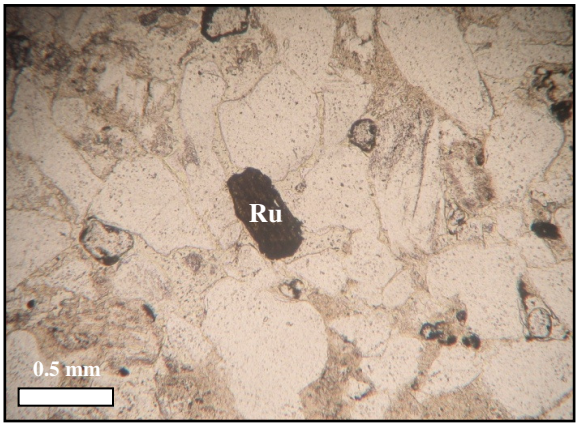


Figure 4.18 Photomicrograph of sample N13, facies association 5, borehole ACP13, depth 226.56 m – 226.61 m. Rutile (Ru) grain (Plane Polarised Light).

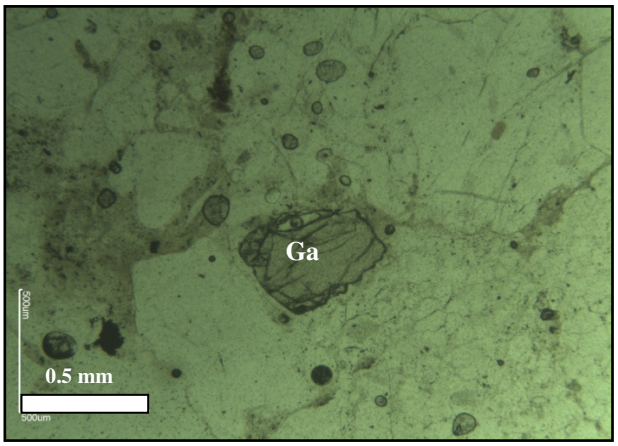


Figure 4.19 Photomicrograph of sample B15, facies association 5, borehole CKP8C-1, depth 411.25 m – 411.31 m. Garnet (Ga) grain with irregular fractures (Plane Polarised Light).

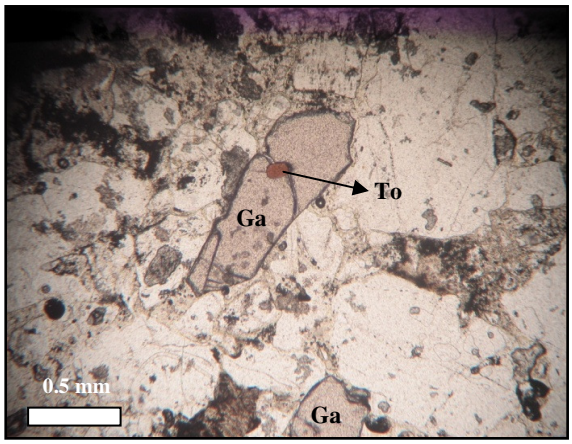


Figure 4.20 Photomicrograph of sample B12, facies association 5, borehole CKP8A, depth 283.74 m – 283.89 m. Garnet (Ga) grains and subrounded brown tourmaline (To) grain (Plane Polarised Light).

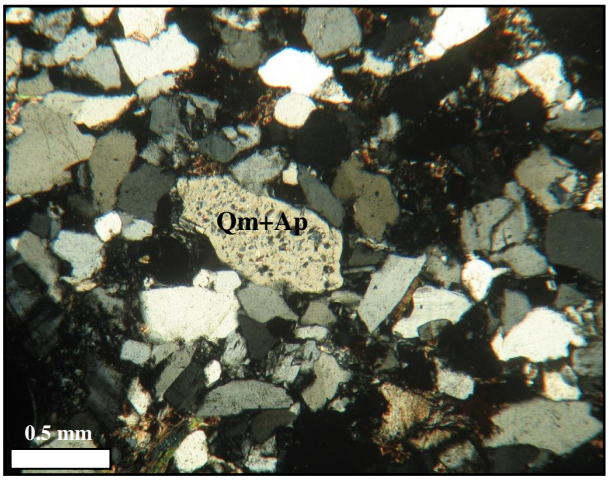


Figure 4.21 Photomicrograph of sample N8, facies association 4, borehole ACP19, depth 324.92 m – 325.00 m. Sandstone with angular to subangular detrital grains, apatite (Ap) minerals occur as inclusions within the monocrystalline quartz grain (Cross Polarised Light).

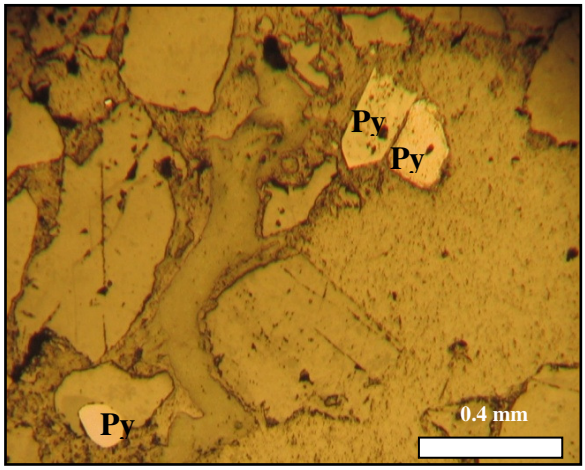


Figure 4.22 Photomicrograph of sample B17, facies association 5, borehole CKP8C-1, depth 278.19 – 278.35 m. Pyrite (Py) grains (Plane Polarised Light).

4.4 Detrital modes

For modal analysis, three hundred and fifty framework grains were counted from each studied thin section (Tables 5, 6). Matrix, cement, micas, heavy minerals and pyrite grains were not counted. Thin section point counts were done using the Gazzi-Dickinson point count method (refer to Chapter 2, Dickinson, 1985) and were then plotted on QFL diagrams for sandstone classification (Folk, 1980) and also plotted on Dickinson and Suczek (1979) tectonic provenance diagrams (Fig. 4.23, 4.24, 4.25, 4.26).

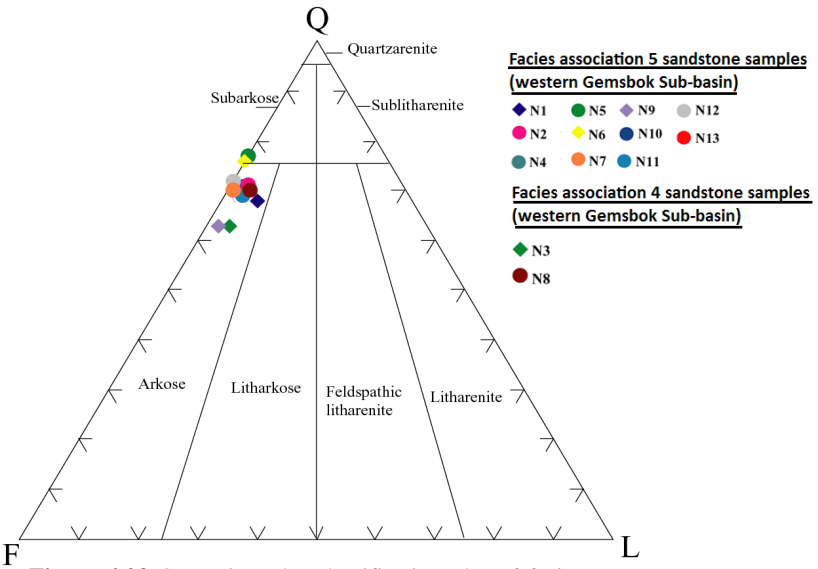


Figure 4.23 QFL triangular classification plot of facies associations 4 and 5 sandstones in the western part of the study area (after Folk, 1980).

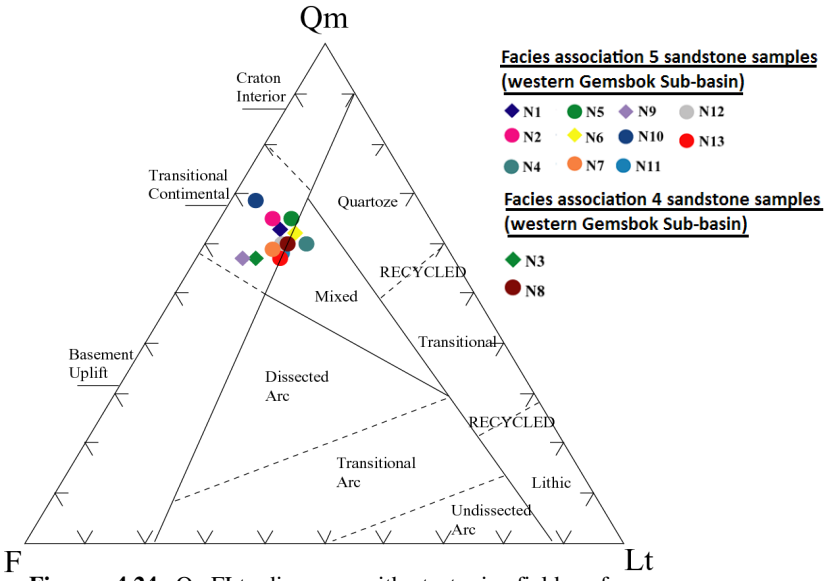
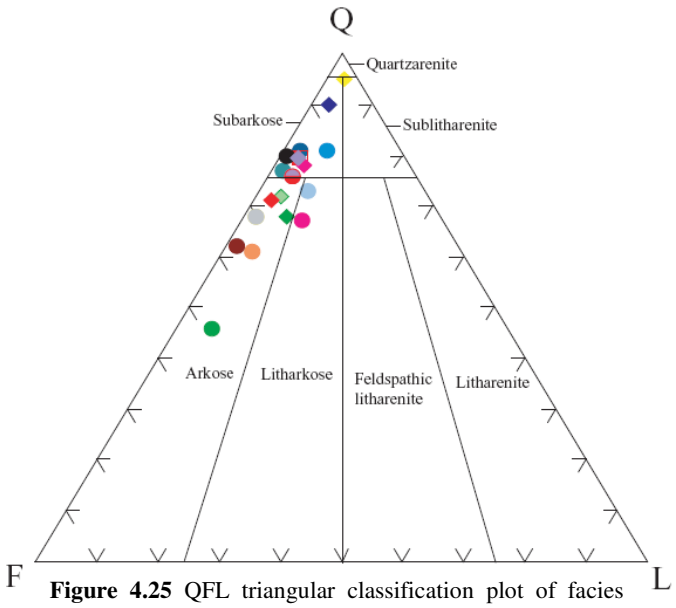


Figure 4.24 QmFLt diagram with tectonic fields of Dickinson and Suczek (1979) for facies associations 4 and 5 sandstones in the western part of the study area.



Facies association 8 sandstone sample (northern Gemsbok Sub-basin)

B1

Facies association 5 sandstone samples (eastern Gemsbok Sub-basin)

B11 B17
B12 B18/B19
B14 BA
B15 BB
B16 BC

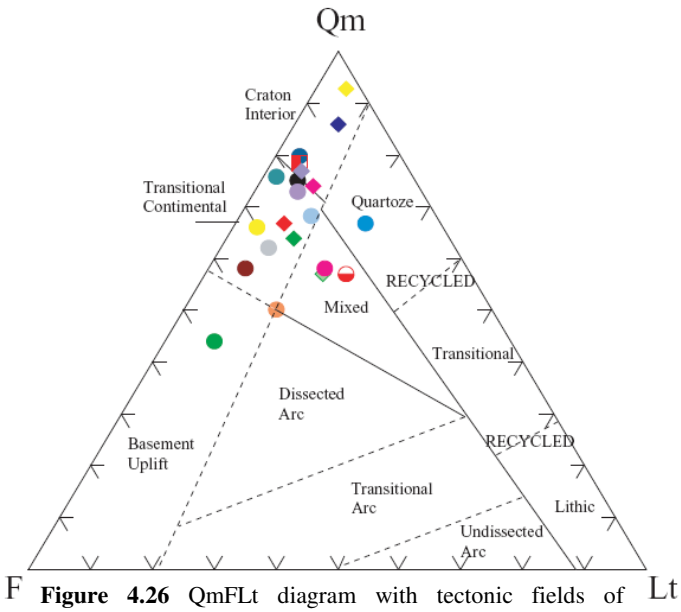
Facies association 4 sandstone samples (northern Gemsbok Sub-basin)

B2 B6
B3 B7
B4 B8
B5 B9

Facies association 4 sandstone samples (eastern Gemsbok Sub-basin)

B10
B20

Figure 4.25 QFL triangular classification plot of facies associations 4, 5 and 8 sandstones in the northern and eastern parts of the study area (after Folk, 1980).



Facies association 8 sandstone sample (northern Gemsbok Sub-basin)

B1

Facies association 5 sandstone samples (eastern Gemsbok Sub-basin)

B11 B17
B12 B18/B19
B14 BA
B15 BB
B16 BC

Facies association 4 sandstone samples (northern Gemsbok Sub-basin)

B2 B6
B3 B7
B4 B8
B5 B9

Facies association 4 sandstone samples (eastern Gemsbok Sub-basin)

B10
B20

Figure 4.26 QmFLt diagram with tectonic fields of Dickinson and Suczek (1979) for facies associations 4, 5 and 8 sandstones in the northern and eastern parts of the study area.

4.4.1 Western part of the Gemsbok Sub-basin

4.4.1.1 Facies association 4

Sandstone samples (sample N3 and N8) from facies association 4 in the western part of the study area are predominantly medium-grained, with grain sizes ranging from 0.125 mm to 0.25 mm. The average quartz-feldspar-lithic fragment ratio is $Q_{67}F_{30}L_4$. Facies association 4 sandstone samples are classified as arkose in a QFL diagram (Fig. 4.23) (Folk, 1980). Facies association 4 sandstones in the western part of the study area plot within the field of transitional continental provenance with one sample plotting in between the transitional continental and mixed provenance fields (Fig. 4.24).

4.4.1.2 Facies association 5

This facies association consists of fine-grained sandstones (0.125 mm - 0.25 mm), medium-grained sandstones (0.25 mm - 0.57 mm), and a lesser number of coarse-grained sandstones (0.57 mm – 0.7 mm). The sandstones are typically arkosic sands (number of samples = 9) with lesser amount of subarkosic sands (number of samples = 2) and have an average modal value of $Q_{71}F_{27}L_2$ (Fig. 4.23). Eighty percent of detrital modes of facies association 5 sandstones in QmFLt diagrams plot within the transitional continental provenance field with 20% in the mixed provenance field (Fig. 4.24).

4.4.2 Northern and eastern part of the Gemsbok Sub-basin

4.4.2.1 Facies association 4

All studied thin sections from facies association 4 in the northern and eastern part of the study area are predominantly fine- (0.125 mm - 0.25 mm) and medium-grained (0.25 mm – 0.5 mm) sandstones. The average framework grain modes of facies association 4 sandstones in the northern part of the study area are $Q_{67}F_{29}L_4$ and in the eastern part of the study area are $Q_{79}F_{19}L_2$. In the northern part of the study area, facies association 4 sandstones are mainly classified as arkose, with lesser amounts of subarkose, litharkose and sublitharenite (Fig. 4.25). Point count values for these sandstones reveal that the source was predominantly from a transitional continental provenance, with some contributions from a craton interior provenance as well as from mixed and basement uplift sources (Fig. 4.26). Two sandstone samples of the facies association 4 in the

eastern part of the study area are classified as subarkose and fall within craton interior and transitional continental provenance fields.

4.4.2.2 Facies association 5

Facies association 5 in the eastern part of the study area consists of fine-grained sandstones (0.125 mm – 0.25 mm), medium-grained sandstones (0.25 mm – 0.50 mm), coarse-grained sandstones (0.50 mm – 1 mm) and very coarse-grained sandstones (1 mm – 2 mm). QFL percentages documented in this study for the sandstones in the eastern part of the study area are commonly $Q_{74}F_{22}L_4$. Sandstones of facies association 5 in the eastern part of the study area have less quartz than those of facies association 4 in the eastern part of the study area. On the basis of the framework grains, facies association 5 sandstones are classified as subarkose (number of samples = 5) and arkose (number of samples = 5) with lesser amount of litharkose (number of samples = 1), (see Fig. 4.25). The QmFLt plots for the facies association 5 sandstone samples falls within the transitional continental field (number of samples = 6), craton interior (number of samples = 2) and mixed provenance field (number of samples = 2) and one sample plots in the quartoze recycled orogen provenance field (Fig. 4.26).

4.4.2.3 Facies association 8

Sandstone sample B1 of facies association 8 is predominantly fine-grained (0.125 mm – 0.25 mm) and contains high amounts of quartz grains, constituting average 89% of rock volume. The sandstone sampled contains minor amounts of feldspar (average of 8%) and lithic fragments (average of 3%). It is classified as subarkose (Fig. 4.25) and plots within the craton interior field in the QmFLt diagram (Fig. 4.26).

4.5 Geochemistry of sandstones

Geochemical analyses were performed only on the sandstone samples from the boreholes in the northern and eastern parts of the study area (Tables 7 and 8) to supplement the petrographic data and making interpretations of source areas. In the western part of the study area, no core was available for geochemical analyses.

Table 7 Chemical composition (major element concentrations) in weight percent (Wt%) of the Ntane Sandstone Formation (facies association 8) and the Ecca Group (facies association s 4 and 5) sandstones in the northern and eastern parts of the study area.

Facies association (FA)	**FA4**	**FA4**	**FA4**	**FA4**	**FA4**	**FA4**	**FA4**	**FA4**	**Average**	**FA5**	**FA5**	**FA5**	**FA5**	**FA5**	**FA5**	**FA5**	**Average**	**FA8**	**Average**
BH No:	**W1**	**W2**	**W2**	**W2**	**W3**	**W3**	**CKP8C-1**	**CKP8C-1**		**CKP8A**	**CKP8C-1**	**CKP8C-1**	**CKP8C-1**	**CKP8C-1**	**CKP8C**	**CKP8C**		**W1**	
Sample No:	**B2**	**B3**	**B5**	**B6**	**B8**	**B9**	**B10**	**B20**		**B11**	**B14**	**B16**	**B17**	**B18**	**BA**	**BC**		**B1**	
SiO_2	62.56	76.87	57.99	94.93	78.97	75.81	68.87	72.40	73.55	75.43	78.80	74.28	77.50	64.67	69.95	77.93	74.08	89.83	89.83
TiO_2	0.49	0.30	0.74	0.33	0.56	0.24	1.11	0.60	0.55	1.17	0.57	0.68	0.37	0.74	0.76	0.44	0.68	0.16	0.16
Al_2O_3	13.18	13.45	23.37	2.42	12.33	12.26	20.34	10.84	13.52	14.45	10.12	13.61	7.40	14.43	9.02	13.37	11.77	5.71	5.71
$Fe_2O_3(t)$	1.85	0.99	3.99	0.84	1.13	0.79	0.87	6.80	2.16	2.18	2.39	2.78	0.51	8.74	1.27	1.77	2.81	0.88	0.88
MnO	0.14	0.01	0.03	0.01	0.02	0.02	0.01	0.08	0.04	0.02	0.06	0.02	0.09	0.05	0.10	0.02	0.05	0.06	0.06
MgO	0.61	0.29	1.37	0.15	0.27	0.23	0.24	1.04	0.53	0.68	0.44	0.80	0.18	1.13	0.39	0.39	0.57	0.32	0.32
CaO	7.87	0.19	0.23	0.14	0.11	1.78	0.09	1.26	1.46	0.15	1.07	0.49	5.36	0.60	7.83	0.62	2.30	0.17	0.17
Na_2O	0.92	1.19	0.82	0.24	0.32	1.04	0.66	0.94	0.77	0.38	1.51	1.96	1.35	2.02	1.31	2.14	1.52	0.62	0.62
K_2O	3.14	4.70	4.85	0.71	3.21	4.62	3.15	2.60	3.37	3.40	3.10	3.57	2.66	3.72	2.38	3.22	3.15	3.06	3.06
P_2O_5	0.05	0.02	0.03	0.01	0.07	0.02	0.03	0.05	0.03	0.08	0.05	0.04	0.03	0.06	0.05	0.03	0.05	0.08	0.08
Cr_2O_3	0.03	0.01	0.02	0.01	0.01	0.01	0.02	0.01	0.01	0.01	0.01	0.01	0.01	0.01	0.01	0.01	0.01	0.00	0.00
L.O.I.	9.63	2.13	6.31	0.51	2.97	3.25	3.87	3.31	4.00	2.13	2.06	1.86	4.64	3.91	7.95	1.55	3.44	0.45	0.45
K_2O/Na_2O	3.41	3.94	5.92	2.97	9.88	4.43	4.81	2.78	4.77	8.96	2.05	1.82	1.97	1.84	1.82	1.51	2.85	4.91	4.91
Total	100.47	100.15	99.76	100.30	99.96	100.07	99.26	99.93	99.99	100.09	100.20	100.09	100.09	100.08	101.02	101.49	100.44	101.33	101.33
$Fe_2O_3(t)+MgO$	2.47	1.28	5.37	0.99	1.40	1.02	1.11	7.84	2.68	2.87	2.83	3.58	0.69	9.87	1.66	2.16	3.38	1.19	1.19
H_2O^-	0.75	0.41	1.08	0.17	0.28	0.31	1.60	0.45	0.63	0.51	0.20	0.64	0.22	0.62	0.34	0.57	0.44	0.52	0.52
Al_2O_3/SiO_2	0.21	0.18	0.40	0.03	0.16	0.16	0.30	0.15	0.20	0.19	0.13	0.18	0.10	0.22	0.13	0.17	0.16	0.06	0.06
Na_2O/K_2O	0.29	0.25	0.17	0.34	0.10	0.23	0.21	0.36	0.24	0.11	0.49	0.55	0.51	0.54	0.55	0.66	0.49	0.20	0.20
SiO_2/Al_2O_3	4.75	5.71	2.48	39.30	6.40	6.18	3.39	6.68	9.36	5.22	7.79	5.46	10.48	4.48	7.75	5.83	6.72	15.74	15.74
log Na_2O/K_2O	-0.53	-0.60	-0.77	-0.47	-0.99	-0.65	-0.68	-0.44	-0.64	-0.95	-0.31	-0.26	-0.30	-0.26	-0.26	-0.18	-0.36	-0.69	-0.69
log SiO_2/Al_2O_3	0.68	0.76	0.39	1.59	0.81	0.79	0.53	0.82	0.80	0.72	0.89	0.74	1.02	0.65	0.89	0.77	0.81	1.20	1.20
Fe_2O_3/K_2O	0.59	0.21	0.82	1.19	0.35	0.17	0.28	2.61	0.78	0.64	0.77	0.78	0.19	2.35	0.53	0.55	0.83	0.29	0.29
log Fe_2O_3/K_2O	-0.23	-0.68	-0.08	0.08	-0.45	-0.77	-0.56	0.42	-0.28	-0.19	-0.11	-0.11	-0.72	0.37	-0.27	-0.26	-0.18	-0.54	-0.54

Table 8 Chemical composition (trace element concentrations) in parts per million (ppm) of the sandstones of the Ntane Sandstone Formation (facies association 8) and the Ecca Group (facies association 4 and 5) in the northern and eastern parts of the study area.

Facies association (FA)	FA4	FA4	FA4	FA4	FA4	FA4	FA4	FA4	Average	FA5	FA5	FA5	FA5	FA5	FA5	FA5	Average	FA8	Average
BH No:	W1	W2	W2	W2	W3	W3	CKP8C-1	CKP8C-1		CKP8A	CKP8C-1	CKP8C-1	CKP8C-1	CKP8C-1	CKP8C	CKP8C		W1	
Sample No:	B2	B3	B5	B6	B8	B9	B10	B20		B11	B14	B16	B17	B18	BA	BC		B1	
As	<4	<4	<4	<4	<4	<4	<4	<4	-	<4	4.2	<4	<4	<4	<4	<4	-	<4	-
Ba	549	787	676	160	700	785	500	484	580	808	765	626	569	690	550	731	677	489	489
Bi	<3	<3	<3	<3	<3	<3	<3	<3	-	<3	<3	<3	<3	<3	<3	<3	-	<3	-
Br	<2	<2	<2	<2	<2	<2	<2	<2	-	<2	<2	<2	<2	<2	<2	<2	-	<2	-
Ce	41	15	43	<10	32	<10	40	29	33	67	43	54	25	78	49	27	49	26	26
Co	8.6	6.9	20	4.6	8.2	8.7	9.5	11	16	10	6.2	8.6	3.6	17	6.0	7.8	14	4.3	-
Cr	50	24	112	13	46	22	96	54	52	82	42	49	32	56	42	34	48	9.4	-
Cs	<5	<5	12	<5	<5	<5	<5	8.9	12	<5	<5	5.3	<5	7.1	<5	5.6	-	<5	-
Cu	10	15	15	48	14	23	14	13	19	9.7	8.5	11	13	17	9.9	15	14	11	11
Ga	14	13	29	2.0	13	12	27	14	17	21	11	18	7.4	20	11	15	16	5.1	-
Ge	<1	<1	<1	<1	<1	<1	<1	<1	-	<1	<1	<1	<1	<1	<1	<1	-	<1	-
Hf	<3	3.0	<3	<3	4.0	<3	4.4	6.6	-	7.7	5.7	5.6	3.0	6.9	8.0	4.3	-	3.1	-
La	24	<10	23	<10	17	11	30	15	20	33	25	30	15	36	26	15	26	17	17
Mo	<2	<2	<2	<2	<2	<2	<2	<2	-	<2	<2	<2	<2	<2	<2	<2	-	<2	-
Nb	14	10	22	8.2	14	8.5	26	16	17	26	14	17	8.7	19	17	14	18	4.7	-
Nd	19	<10	17	<10	21	<10	28	17	20	37	19	27	13	33	26	13	24	22	22
Ni	19	9.6	53	5.2	15	6.9	24	24	27	25	10	13	3.6	32	12	13	18	5.0	-
Pb	17	23	25	6.8	20	24	23	18	21	19	18	21	14	23	14	21	19	13	13
Rb	113	121	202	20	96	119	95	87	107	123	102	151	82	158	86	127	118	66	66
Sc	8.3	4.1	11	<3	11	5.0	17	17	14	13	6.4	8.3	<3	12	4.2	5.5	13	<3	-
Se	<1	<1	<1	<1	<1	<1	<1	<1	-	<1	<1	<1	<1	<1	<1	<1	-	<1	-
Sm	<10	<10	<10	<10	<10	<10	<10	<10	-	<10	<10	<10	<10	<10	<10	<10	-	<10	-
Sr	134	114	95	24	82	110	60	90	89	73	145	144	376	150	790	171	264	54	54
Ta	<2	<2	<2	<2	<2	<2	<2	<2	-	2.1	<2	<2	<2	<2	<2	<2	-	<2	-
Th	6.5	3.6	6.1	<3	4.8	<3	11	8.4	11	13	9.1	12	4.9	14	15	5.4	14	<3	-
Tl	<3	<3	<3	<3	<3	<3	<3	<3	-	<3	<3	<3	<3	<3	<3	<3	-	<3	-
U	2.7	<2	2.6	<2	<2	<2	3.2	<2	-	3.8	<2	2.2	<2	3.4	<2	<2	-	<2	-
V	54	39	85	10	57	25	115	75	58	98	33	45	22	57	43	28	47	13	13
W	<3	<3	<3	<3	<3	<3	<3	<3	-	<3	<3	<3	<3	<3	<3	<3	-	<3	-
Y	15	5.5	11	2.5	21	6.3	23	17	17	29	13	15	12	18	24	10	17	13	13
Yb	<2	<2	<2	<2	<2	<2	<2	<2	-	3.7	<2	<2	<2	<2	<2	<2	-	<2	-
Zn	57	25	117	21	36	29	131	50	58	87	28	45	12	60	17	27	39	9.0	-
Zr	126	71	94	151	174	58	257	224	144	561	307	347	178	406	491	148	348	196	196

4.5.1 Major element geochemistry

4.5.1.1 Facies association 4 (northern Gemsbok Sub-basin)

The sandstone samples of facies association 4 in the northern part of the study area (number of samples, n = 6) have SiO_2 contents averaging at 74.52 wt%. Exceptions include sample B5 and B6 from borehole W2, which exhibit relatively low concentration of SiO_2 (57.99 wt%) and high SiO_2 concentration (up to 95 wt %) respectively. The sandstones of facies association 4 show high concentrations of Al_2O_3 (mean: 12.84 wt%) compared to an average (8.7 wt%) arkose composition (Pettijohn *et al*., 1987). Sample B5 has the highest Al_2O_3 (23.37 wt%) concentration compared to the mean value (8.7 wt%) (Pettijohn *et al*., 1987). Sample B6 from borehole W2 shows low concentrations of Al_2O_3 (2.42 wt%). Concentrations of TiO_2, $Fe_2O_{3(t)}$, MnO, MgO, Na_2O, P_2O_5 and Cr_2O_3 are very low in the sandstone samples of facies association 4 in the northern part of the study area. CaO concentrations are also low (less than 1 wt%) in most sandstone samples. Sample B2 (7.87 wt%) and B9 (1.78 wt%) have higher CaO concentrations which is consistent with the mineral calcite. The sandstones of facies association 4 in the northern part of the study area have a K_2O content with an average of 3.54 wt%. The concentrations of Na_2O within the sandstones (mean: 0.76 wt%) is less than the concentrations of K_2O (mean: 3.54 wt%). Sample B8 of borehole W1 and sample B5 of borehole W2 have higher K_2O/Na_2O ratios (9.88 and 5.92, respectively). The ratio of SiO_2 to Al_2O_3 is also high within the sandstones (average: 10.80). Sample B6 of borehole W2 has the highest SiO_2/Al_2O_3 (39.30).

4.5.1.2 Facies association 4 (eastern Gemsbok Sub-basin)

The two sandstone samples of facies association 4 in the eastern part of the study area have an average SiO_2 content of 70.63 wt%. The sandstones show high concentrations of Al_2O_3 (mean: 15.59 wt %) compared to an average (8.7 wt %) arkose composition (Pettijohn *et al*., 1987). Sample B10 from borehole CKP8C-1 shows high concentration of Al_2O_3 (20.34 wt%) compared to an average (8.7 wt%) arkose composition (Pettijohn *et al*., 1987). Concentrations of TiO_2, $Fe_2O_{3(t)}$, MnO, MgO, Na_2O, P_2O_5 and Cr_2O_3 are very low in the sandstone samples of facies association 4 in the eastern part of the study area. CaO concentrations are low (less than 1 wt%) in most sandstone samples in the eastern

part of the study area. Sample B20 in the eastern Gemsbok Sub-basin has slightly higher CaO concentrations (1.26 wt%), which is consistent with the mineral calcite. The sandstone samples of facies association 4 in the eastern part of the study area have an average K_2O value of 2.88 wt% and show K_2O/Na_2O ratios between 2.78 and 4.81. The concentrations of Na_2O (mean: 0.80 wt%) is less than K_2O concentrations (mean: 2.88 wt%) in the sandstone samples in the eastern part of the study area. The average ratio of SiO_2 to Al_2O_3 within these sandstones is 5.03.

4.5.1.3 Facies association 5 (eastern Gemsbok Sub-basin)

The sandstone samples of facies association 5 (number of samples, n = 7) in the eastern Gemsbok Sub-basin have a slightly higher SiO_2 content averaging at 73 wt%. Al_2O_3 content in these sandstones is slightly higher (average of 11.05 wt%) compared to an average (8.7 wt%) arkose composition (Pettijohn *et al*., 1987). Most of the sandstone samples (n=7) show low concentrations of $Fe_2O_{3(t)}$. Sample B18 has slightly higher concentration of $Fe_2O_{3(t)}$ (8.74 wt%). Concentrations of TiO_2, MnO, MgO, Na_2O, P_2O_5 and Cr_2O_3 are very low within the sandstone samples of facies association 5. CaO concentrations in these samples have an average of 2.30 wt% and two samples (B17 and BA) have slightly higher concentrations. The concentrations of Na_2O are greater than 1 wt% except in sample B11 of borehole CKP8A. The sandstone samples of facies association 5 show high K_2O content (range: 2.38 wt% – 3.72 wt%) compared to Na_2O content. Average K_2O/Na_2O ratio in these sandstones is 2.85 and sample B11 from borehole CKP8A shows higher K_2O/Na_2O ratio (8.96). The SiO_2/Al_2O_3 ratio mean value for seven sandstone samples of facies association 5 is 6.72.

4.5.1.4 Facies association 8 (northern Gemsbok Sub-basin)

A geochemical analysis of facies association 8 is based only on one sandstone sample (B1) from borehole W1. The sandstone is very rich in silica (SiO_2), with a value of 89.83 wt%. Al_2O_3 concentration measures at 5.71 wt% and is less than the average (8.7 wt%) arkose composition (Pettijohn *et al*., 1987). The concentrations of TiO_2, Fe_2O_3, MnO, MgO, CaO, Na_2O, P_2O_5 and Cr_2O_3 are very low (less than 1 wt%). The K_2O value is 3.06 wt% which is greater than the N_2O value (0.62 wt%). The average K_2O/Na_2O ratio in

sandstone sample B1 is very high (4.91 wt%). The SiO_2/Al_2O_3 ratio (15.74) is higher than the K_2O/Na_2O ratio.

4.5.2 Trace element geochemistry

4.5.2.1 Facies association 4 (northern Gemsbok Sub-basin)

The concentrations of Ba are high in the sandstone samples of facies association 4 in the northern part of the study area with an average of 610 ppm. Samples B3 and B5 from borehole W2 and samples B8 and B9 from borehole W3 have higher Ba concentrations. Sample B6 from borehole W2 has the lowest concentration value of Ba. Rubidium (Rb) concentrations within the sandstones are moderately high (mean: 112 ppm). Sample B5 in borehole W2 shows very high concentrations of Rb, up to 202 ppm. The concentrations of Sr in sandstone samples of facies association 4 are less than 100 ppm, with an average of 93 ppm. Sample B2 (134 ppm) and B3 (114 ppm) from borehole W2 and sample B9 (110 ppm) from borehole W3 show higher concentrations of Sr. Zr concentration in the sandstones is moderately high with a mean of 112 ppm. Sandstone sample B6 from borehole W2 and sample B8 from borehole W3 have Zr values greater than 100 ppm. The concentrations of other trace elements such as Bi, Br, Ce, Co and Ni are very low with an average less than 100 ppm.

4.5.2.2 Facies association 4 (eastern Gemsbok Sub-basin)

The Barium (Ba) concentrations of the sandstone samples of facies association 4 in the eastern part of the study area have an average of 492 ppm. Sample B10 has a Barium concentration of 500 ppm. Rubidium (Rb) concentration in the sandstones has a mean value of 91ppm. The concentrations of Sr in sandstone samples of facies association 4 are less than 100 ppm, with an average of 75 ppm. Zr concentration in the sandstones is moderately high with a mean of 241 ppm. Sample B10 from borehole CKP8C-1 has Zr values greater than 241 ppm. Most elements such as Bi, Br, Ce, Cr, Co and Ni are relatively low and have mean values less than 100 ppm.

4.5.2.3 Facies association 5 (eastern Gemsbok Sub-basin)

The concentrations of Ba are very high in the sandstone samples of facies association 5 (mean: 677 ppm, number of samples = 7). Four sandstone samples from borehole CKP8A

(sample B11), borehole CKP8C-1 (sample B14 and sample B18) and borehole CKP8C (sample BC) have higher concentrations of Ba. Rb concentration within the sandstones range from 82 ppm to 151 ppm, with an average of 118 ppm. The sandstones of facies association 5 show slightly higher concentrations of Sr (average: 264 ppm). Sample BA from borehole CKP8C has a Sr value of 790 ppm. Zr content in the sandstones of facies association 5 is very high with a mean value of 348 ppm. Samples B11, B18 and BA have zirconium concentrations of more than 348 ppm. The mean values of other trace elements such as Ni, Cr, Pb, Co and Cu are very low (below 100 ppm).

4.5.2.4 Facies association 8 (northern Gemsbok Sub-basin)

The concentration of Ba is slightly higher in the sandstone sample B1 of facies association 8 (mean: 489 ppm). Zr content is also high with a mean value of 196 ppm. Concentrations of other trace elements are very low and are less than 70 ppm.

4.6 Sandstone classification using geochemistry

Using the Herron (1988) geochemical classification diagram, most of the sandstone samples of facies association 4 in the northern part of the study area are classified as arkose (number of samples, n = 4) with a small number of samples classified as wacke and sublitharenite (Fig. 4.27). In the eastern part of the study area, one sandstone sample of facies association 4 is classified as litharenite in the Herron (1988) diagram (Fig. 4.27). The sandstone samples of facies association 5 in the eastern part of the study area are classified as arkose (n = 5) with one (n = 1) plotting in the shale field (Fig. 4.27). In the "SandClass System" diagram of Herron (1988), the facies association 8 sandstone is classified as a subarkose (Fig.4.27).

4.7 Sandstone provenance and tectonic settings

A summary table for the provenance and tectonic setting of the Ecca Group and Ntane Sandstone Formation sandstones is given in Table 9.

4.7.1 Facies association 4 (northern and eastern Gemsbok Sub-basin)

According to the TiO_2-Ni diagram of Floyd et al. (1989), the source area for facies association 4 sandstone samples in the northern and eastern part of the study area was of a predominantly acidic magmatic nature (Fig. 4. 28). Sandstone sample B5 of facies association 4 in the northern part of the study area, shows a provenance from mature sedimentary rocks (Fig. 4. 28).

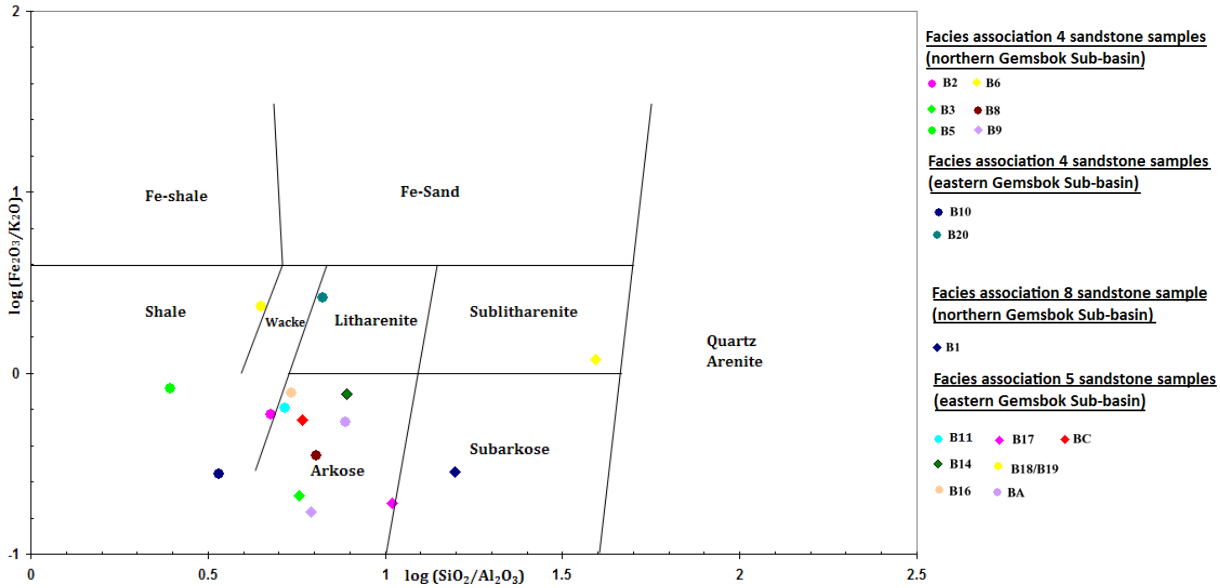


Figure 4.27 Chemical classification scheme of sandstones from facies associations 4, 5 and 8 in the northern and eastern parts of the study area based on log (SiO_2/Al_2O_3) *vs.* log (Fe_2O_3/K_2O) diagram of Herron (1988).

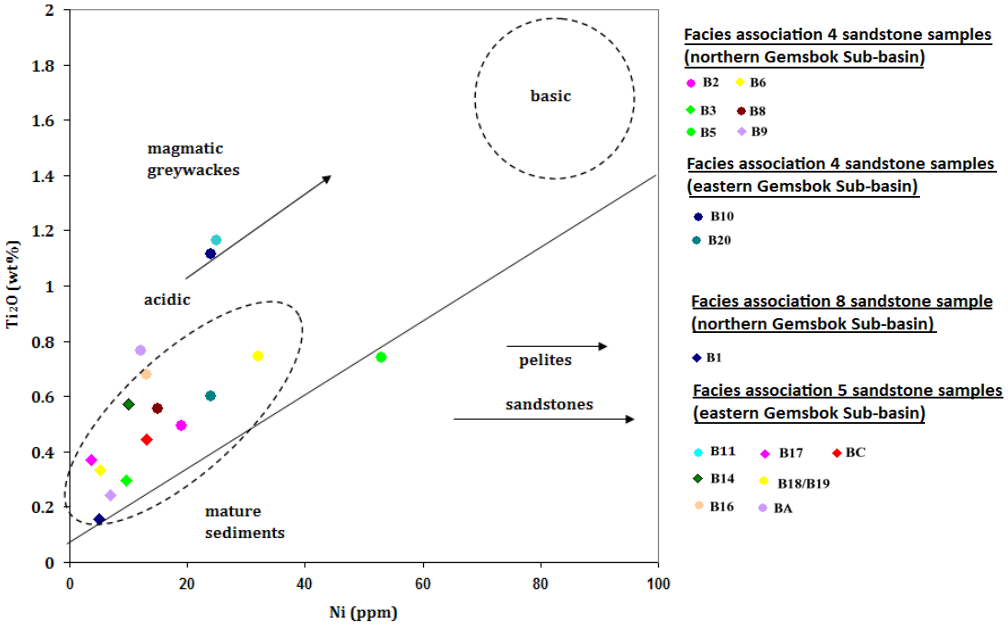


Figure 4.28 Characterisation of source rock composition based on Ni *vs.* TiO_2 diagram for the facies association 4, 5 and 8 sandstones in the northern and eastern parts of the study area (after Floyd et al., 1989).

The provenance discrimination diagrams of Roser and Korsch (1988) are based on major element data and have four different sedimentary provenance fields. The sedimentary provenance fields include: P1 (mainly mafic and lesser intermediate igneous provenance); P2 (primarily intermediate igneous provenance, represented by lithic volcanogenic greywacke and argillites); P3 (felsic (volcanic and plutonic) igneous provenance represented by quartzofeldspathic sandstones (greywackes) and P4 (quartoze sedimentary rocks of mature continental provenance, e.g., sandstones and argillites, poor feldspar and rock fragment content and quartz-rich sandstones). Most of the facies association 4 sandstones in the northern and eastern part of the study area fall within a quartzose sedimentary field, with a small number of sandstone samples plotting in the field of felsic igneous rocks (Fig. 4.29). In the Th-Sc-Zr/10 tectonic discrimination diagram by Bhatia and Crook (1986), facies association 4 sandstones plot within the continental island arc field (Fig. 4.30).

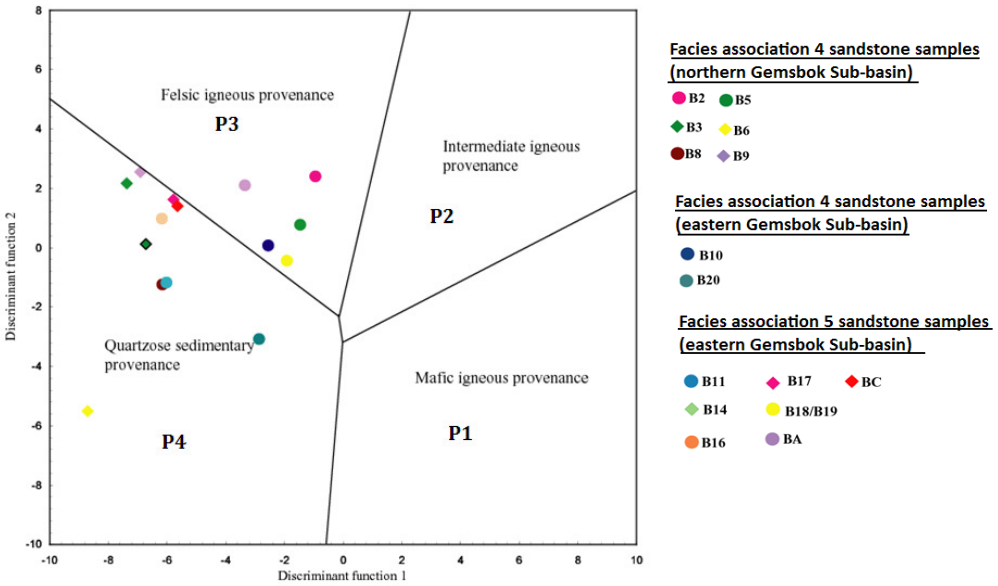


Figure 4.29 Facies associations 4, 5 and 8 sandstones in the northern and eastern parts of the study area, based on the discrimination function diagram of Roser and Korsch (1988).

4.7.2 Facies association 5 (eastern Gemsbok Sub-basin)

The Floyd et al. (1989) source rock composition diagram (Fig. 4.28) indicates that the sandstone samples from facies association 5 were derived mainly from acidic magmatic source rocks. According to the provenance discrimination diagram of Roser and Korch (1988), the sandstone samples were mainly derived from a quartzose sedimentary

provenance with some contribution from a felsic igneous source area (Fig. 29). Two sandstone samples (sample BC and B18) of facies association 5 plot in the continental island arc field in the Th-Sc-Zr/10 tectonic discrimination diagram (Fig. 4.30) of Bhatia and Crook (1986) and one sample (sample BA) plots in the passive margin field. The other three samples (sample B11, B14 and B16) of facies association 5 sandstones plot between the passive margin and continental island arc fields.

4.7.3 Facies association 8 (northern Gemsbok Sub-basin)

In the source rock composition binary diagram by Floyd et al. (1989), the sandstone sample from facies association 8 indicates derivation from acidic magmatic source rocks (Fig. 4.28).

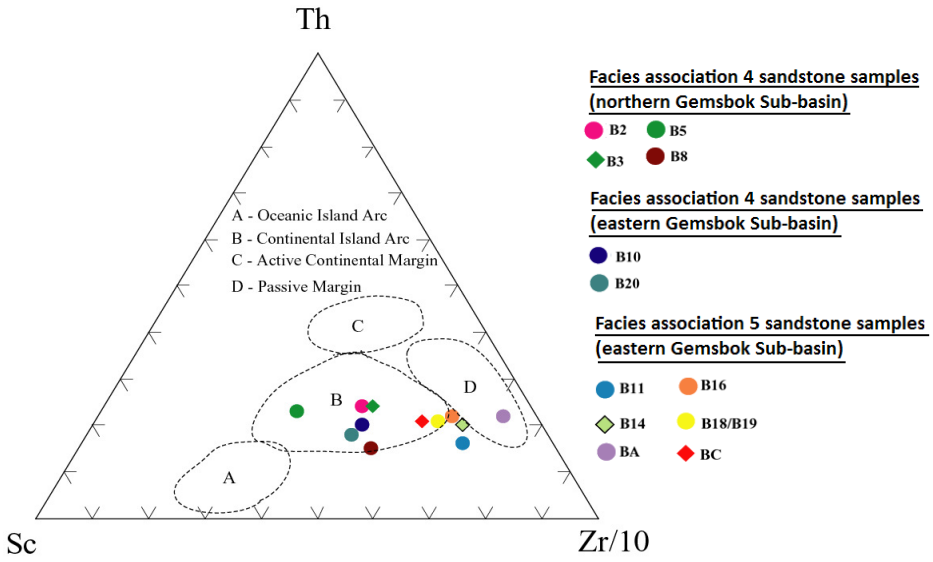


Figure 4.30 Facies associations 4, 5 and 8 sandstones in the northern and eastern parts of the study area, based on Th-Sc-Zr/10 tectonic discrimination diagram of Bhatia and Crook (1986).

Table 9 Summary table for provenances of the Ntane Sandstone Formation and the Ecca Group sandstones in the Gemsbok Sub-basin.

STUDY AREA	FAs	PROVENANCES			
		Dickinson and Suczek, (1979) diagram	Floyd et al, (1989) diagram	Roser and Korsch, (1988) diagram	Bhatia and Crook, (1986) diagram
Western part of the study area	FA4	Transitional continental provenances	-	-	-
	FA5	Transitional continental provenances with some contributions from mixed provenances	-	-	-
Northern part of the study area	FA4	Transitional continental with some contributions from craton interior, mixed and basement uplifted sources	Acidic magmatic sources with some contribution from mature sedimentary rock sources	Quartzose sedimentary field with some contribution from felsic igneous rocks	Continental island arc sources
	FA8	Craton interior provenances	Acidic magmatic sources		
Eastern part of the study area	FA4	Craton interior and transitional continental provenances	Acidic magmatic sources	Quartzose sedimentary field with some contribution from felsic igneous rocks	Continental island arc sources
	FA5	Transitional continental with some contributions from craton interior, mixed and quartzose recycled orogen provenances	Acidic magmatic sources	Quartzose sedimentary provenances with some contribution from felsic igneous source areas	Continental island arc with some contribution from passive margin sources

CHAPTER FIVE: DISCUSSION

5.1 Stratigraphy

The Karoo Supergroup in the Gemsbok Sub-basin of Botswana and Namibia (study area) is poorly exposed and largely covered by the Cenozoic Kalahari Group. Thirteen (including two reference boreholes VREDA 281 and MP1; App. Fig. 1 - 13) borehole cores across the Sub-basin confirm the existence of a thick (up to 1056 m) sedimentary succession of the Karoo Supergroup. The Karoo Supergroup in the study area comprises the Dwyka Group, Ecca Group, Beaufort Group equivalent, Lebung Group and the Neu Loore Formation (Fig. 5.1). The Dwyka Group forms the base of the Karoo Supergroup in the study area, and is overlain by the Ecca Group. In the In the northern and eastern parts of the study area, the Beaufort Group equivalent conformably overlies the Ecca Group, but in the western part of the study area, the Neu Loore Formation unconformably overlies the Ecca Group. The Beaufort Group equivalent or Ecca Group rocks in the northern and eastern parts of the study area are unconformably overlain by the Lebung Group rocks.

Based on detailed sedimentological and ichnological analysis of eleven borehole (App. Fig. 1 – 11) cores of the Karoo Supergroup in the Gemsbok Sub-basin of Botswana and Namibia, fourteen lithofacies and two trace fossil assemblages (assigned to the *Cruziana* and *Skolithos* ichnofacies) were identified. These have been grouped into eight broadly defined facies associations (facies association 1 to facies association 8) which correspond to the lithostratigraphic subdivisions (the Dwyka Group, Ecca Group, Beaufort Group equivalent, Lebung Group [Mosolotsane and Ntane formations] and Neu Loore Formation) of the Karoo Supergroup. The Dwyka Group consists of facies association 1; the Ecca Group comprises facies association 2, 3, 4 and 5; the Beaufort Group equivalent includes facies association 6, the Neu Loore Formation and the Mosolotsane Formation comprises facies association 7, and facies association 8 corresponds to the Ntane Sandstone Formation.

Accumulated Thickness (m)		Lithostratigraphy	Facies associations (FAs)	Depositional interpretation
1056		Ntane Sandstone Formation	FA8	Aeolian, fluvial (arid to semi-arid)
996		Mosolotsane Formation or Neu Loore Formation	FA7	Fluvial (semi-arid)
934		Beaufort Group equivalent	FA6	Large floodplain with shallow lakes, ponds
770		Ecca Group	FA5	Delta plain with floodplains, distributaries, fluvial systems
		Ecca Group	FA4	Delta front
		Ecca Group	FA3	Prodelta
		Ecca Group	FA2	Deeper water turbidites (sea or lake)
334		Dwyka Group	FA1	Glaciomarine or glaciolacustrine
0				

Figure 5.1 Vertical distribution and preliminary interpretation of the eight different facies associations of the Karoo Supergroup in the Gemsbok Sub-basin.

5.1.1 Dwyka Group

The Dwyka Group forms the basal unit of the Karoo Supergroup and was identified in only four boreholes (ACP3, ACP4, W3 and CKP8C-1; App. Fig. 1, 2, 8, 11) in the study area. It ranges in thickness from 28 m – 134 m in the studied boreholes but show much greater thickness of 461 m and 441 m in the reference boreholes (MP1 and Vreda 281) respectively from the centre and the south of the study area (Fig. 5.2, 5.3, 5.4, 5.5, 5.6, 5.7). This study showed the Dwyka Group in the Gemsbok Sub-basin to consist of a variety of lithofacies that are assigned to facies association 1. The Dwyka Group comprises diamictites (Dmm and Dmc) interbedded with massive sandstones (Sm), laminated sandstone, siltstone and mudrock (Fl), bioturbated mudrocks (Fr), and alternating layers of sandstones (Sh) and mudrocks (Fc, Fl). Massive sandstones within facies association 1 are interbedded with thin mudrock (Fc) layers and in places display soft-sediment deformation structures. Trace fossils that belong to the *Cruziana* ichnofacies (*Conichnus*, *Teichichnus*, *Siphonichnus*, *Schaubcylindrichnus* and *Palaeophycus tubularis*) are present within the Dwyka Group facies association 1 in the western part of the study area.

The lithofacies of the Dwyka Group in the study area are the same as described by Smith (1984) and Kingsley (1985). Kingsley (1985) recognised *Cruziana* ichnofacies within the Dwyka Group in borehole ACP3. Smith (1984) described a varved sequence that marks the top of the Dwyka Group in the northern and eastern margins of the Gemsbok Sub-basin. This varved sequence was not recognised in this study, but alternating mudrock and sandstone layers with cross lamination and displaying upward-fining trends (ranging from 0.5 cm to 2.5 cm in thickness) are present at the top of facies association 1 (Dwyka Group) in the northern part of the study area. In the eastern part of the study area, the top of the Dwyka Group facies association 1 is marked by laminated light grey and dark grey mudrocks and siltstones with upward-fining trends and cross laminations. Facies association 1 of the Dwyka Group is overlain by facies association 2 of the Ecca Group with a sharp contact in the western and northern parts of study area.

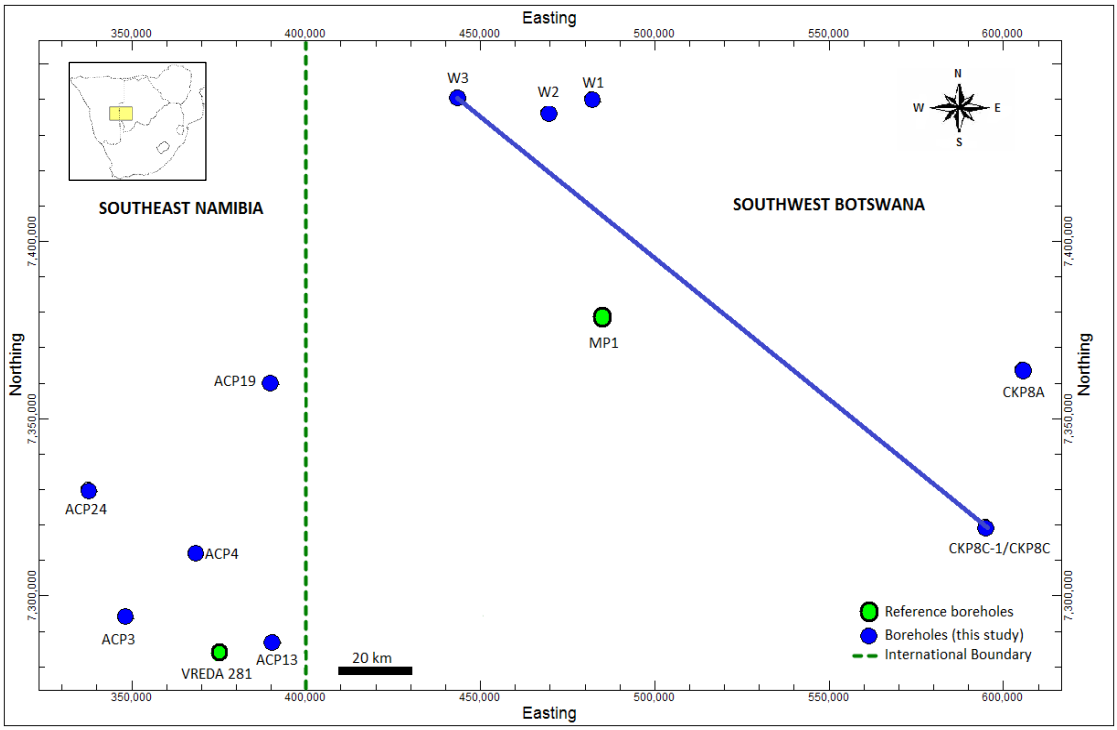


Figure 5.2 Cross-section line W3 – CKP8C-1/CKP8C in the northern and eastern part of the Gemsbok Sub-basin.

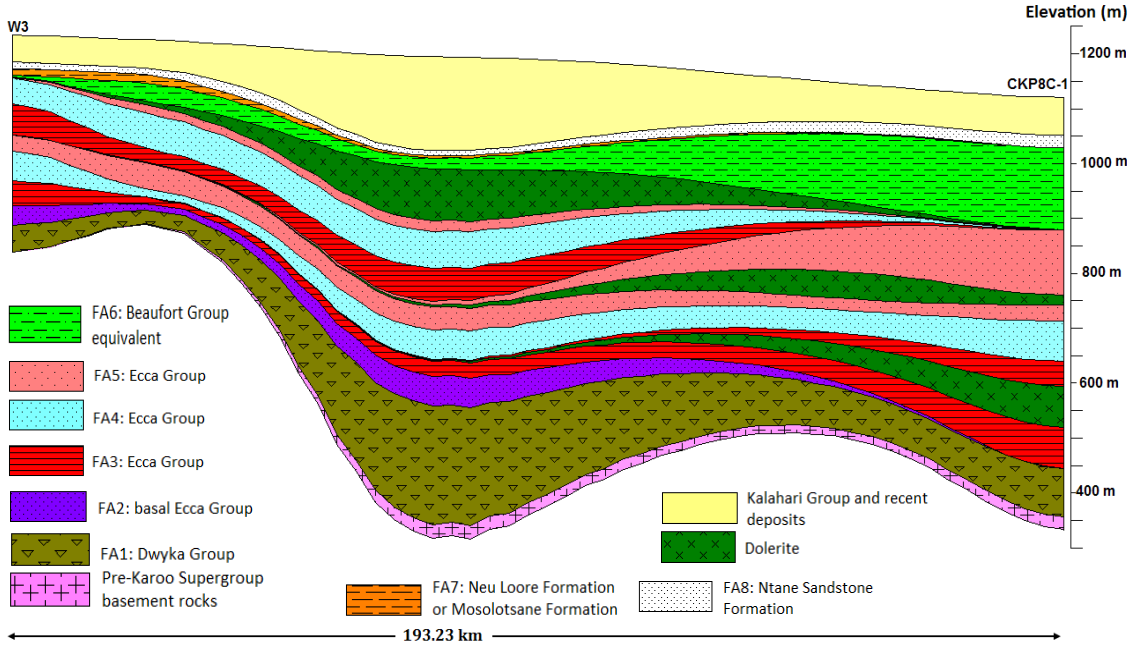


Figure 5.3 Cross-section W3- CKP8C-1/CKP8C showing thickness variations of different facies associations.

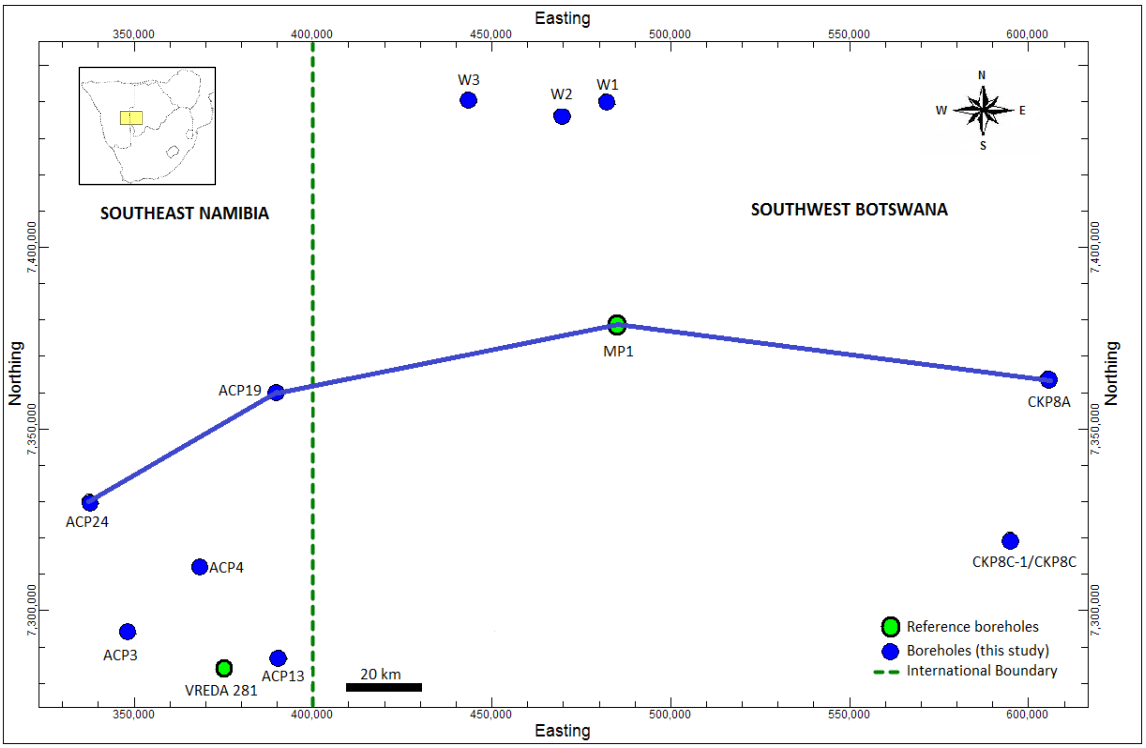


Figure 5.4 Cross-section line across the Gemsbok Sub-basin (from west to east direction).

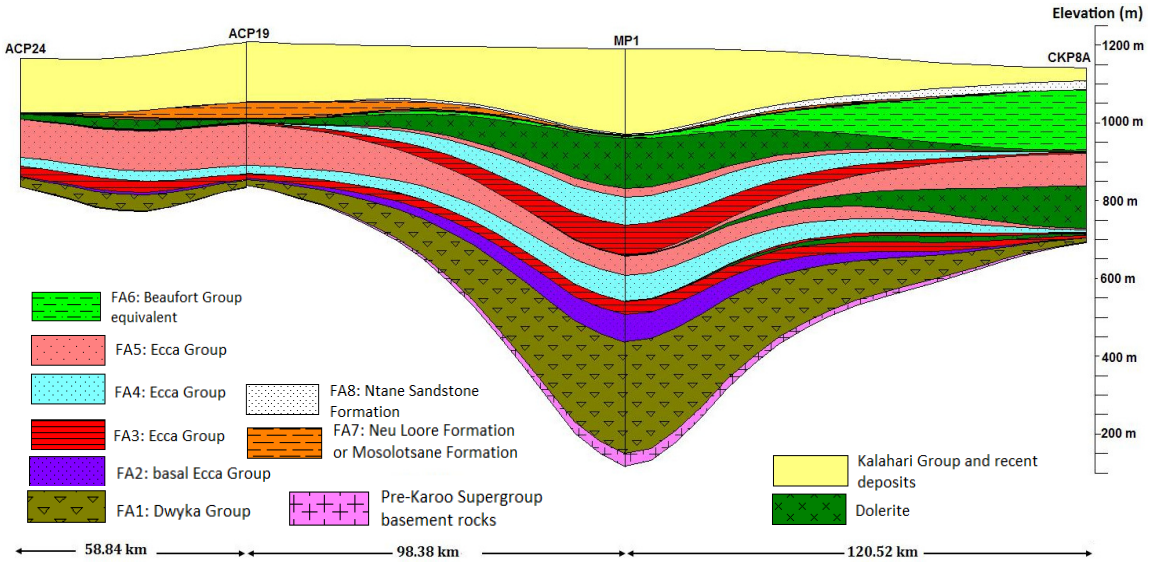


Figure 5.5 Cross-section from the west to the east direction showing thickness variations of different facies associations across the Gembok Sub-basin.

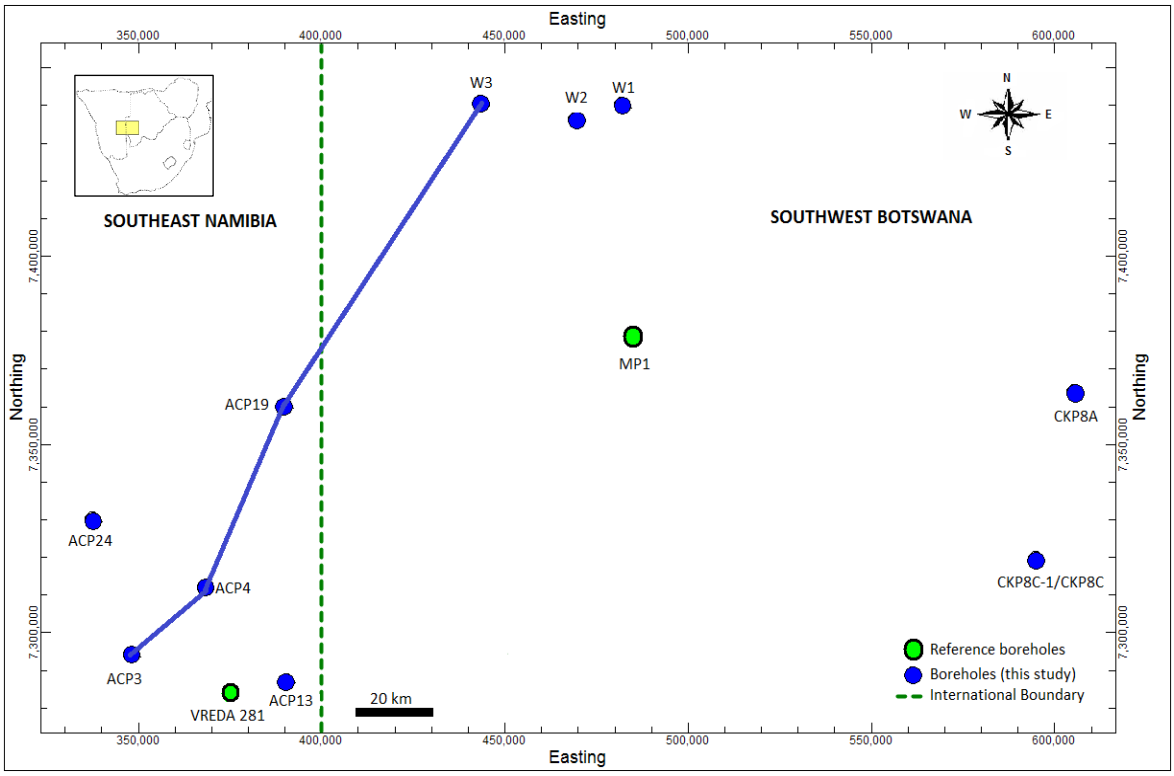


Figure 5.6 Cross-section line W3 – ACP19 – ACP4 – ACP3 from the northern part to the western part of the Gemsbok Sub-basin.

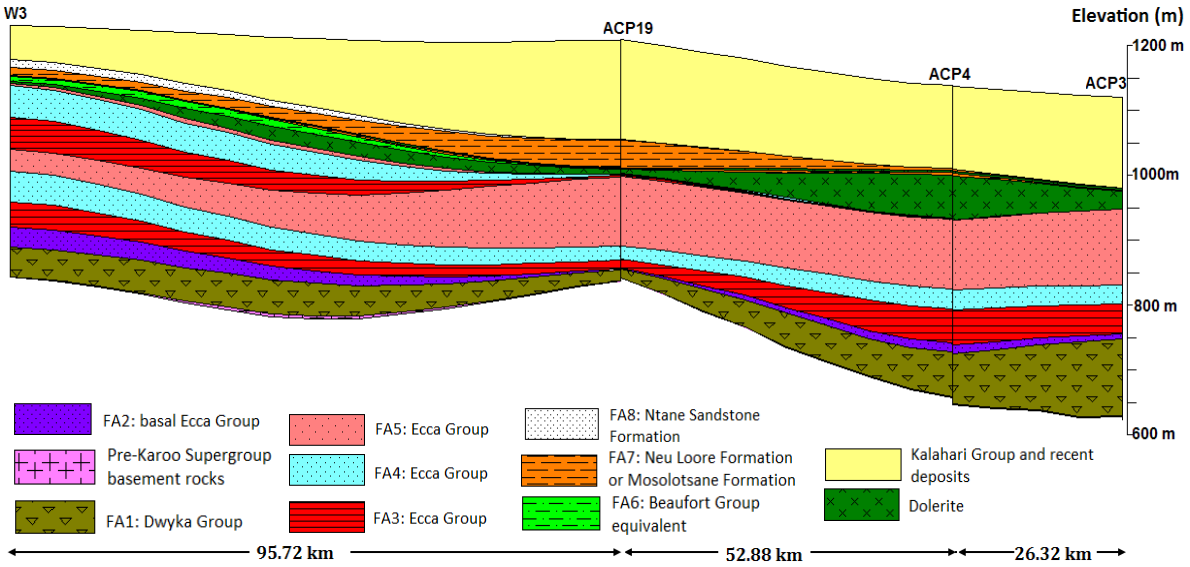


Figure 5.7 Cross-section W3 – ACP19 – ACP4 – ACP3 showing thickness variations of different facies associations.

5.1.2 Ecca Group

The Ecca Group occurs in all boreholes in the study area, but only a few boreholes have a complete stratigraphic succession of the Ecca Group (i.e., CKP8C-1 and W3). The Ecca Group overlies facies association 1 sedimentary rocks in boreholes which have intersected the Dwyka Group in the study area. A complete sedimentary succession of the Ecca Group in the study area consists of four facies associations (facies association 2, 3, 4 and 5). The Ecca Group in the study area ranges in thickness from 288 m in the north, 349 m in the east, 240 m in the west and 436 m at the center of the basin (Fig 5.2, 5.3, 5.4, 5.5).

5.1.2.1 Facies association 2

Facies association 2 was observed only in the boreholes situated in the western (i.e., boreholes ACP3 and ACP4) and northern (borehole W3) parts of the study area. The rock units of facies association 2 range in thickness from 26 m in the western part of the study area to 47 m in the northern part of the study area. Here, the sedimentary rocks of facies association 2 form the base of the Ecca Group and conformably overlie facies association 1 sedimentary rocks of the Dwyka Group. Facies association 2 corresponds with both the Nossob Formation (in the western part of the study area) and the Ncojane Sandstone Member (in the northern part of the study area). In the western and northern parts of the study area, facies association 2 is dominated by sandstone units, which are interbedded with thin mudrock layers and siltstones. Stacked upward-fining cycles (Fig. 3.29) produced by sandstones, siltstones and mudrocks were observed within facies association 2. Facies association 2 in the western part of the study area thickens considerably towards the north and from the northern part of the study area thins towards the east and southeast (Fig. 5.2, 5.3). Smith (1984) and Kingsley (1985) have also noted the thinning of Ncojane Member and Nossob Formation towards the south and east of the Sub-basin.

5.1.2.2 Facies association 3

Facies association 3 (Ecca Group) overlies facies association 2 (basal Ecca Group) in the western and northern parts of the study area, and facies association 1 (Dwyka Group) in the eastern part of the study area (App. Fig. 1, 2, 8, 11). Thick argillaceous units (up to 55 m) dominated by dark grey to grey greenish finely laminated and massive mudrocks

characterise facies association 3 in the western part of the study area. In the northern and eastern part of the study area facies association 3 is characterised by thick argillaceous unit (up to 124 m in thickness) consisting of dark grey and black mudrocks. The lithology of facies association 3 is the same as that described for the lower Mukorob Formation in the western part of the Gemsbok Sub-basin (Aranos Basin) and the Kobe Formation in the northern and eastern Gemsbok Sub-basin (southwest Botswana, Smith, 1984; Key et al., 1998; Miller, 2008).

5.1.2.3 Facies association 4

Overlying the argillaceous unit of facies association 3 (Ecca Group) in the study area is an arenaceous unit comprising facies association 4 (Ecca Group). In the study area, facies association 4 exhibits upward-coarsening character from laminated sandstones, siltstones and mudrocks (Fl), interbedded with sandstones (Sm, Sr), mudrocks (Fc, Fsm) and siltstones (Fsm), which transition upwards into thick (ranging from 5 m to 60 m) sandstone-rich (Sm, Sh, St) units. In places, facies association 4 shows an upward transition from *Cruziana* ichnofacies (dominated by *Thalassinoides*, *Teichichnus*, *Palaeophycus tubularis*, *Planolites*, *Zoophycos*, *Asterosoma*, *Skolithos* and *Conichnus*) to *Skolithos* ichnofacies (dominated by *Conichnus*, escape structures, *Siphonichnus* and *Rosselia*).

Sandstone lithofacies of facies association 4 in the study area are dominantly arkose and subarkose in composition (Fig. 4.23, 4.25, 4.27) with subangular detrital grains dominating over subrounded detrital grains. The sandstones of facies association 4 of the Ecca Group in the study area indicate transitional continental provenance and craton interior with minor contributions from mixed sources and basement uplifted sources (Fig. 4.24, 4.26). The geochemistry of facies association 4 sandstones from the northern and eastern study area reveals quartzose sedimentary (mature rocks) and acidic magmatic or felsic igneous rocks as source rocks, derived from a continental island arc tectonic setting with minor contributions from the passive margin settings (Fig. 4.28, 4.29, 4.30).

The lithofacies and some of the ichnofacies of facies association 4 are the same as those described by Kingsely (1985) for the upper Mokorob and Auob formations in the western

part of the study area (Miller, 2008). In the northern and eastern parts of the study area, facies association 4 correspond to the Otshe Formation, which has been described by Smith (1984). Detailed sedimentological facies analyses of facies association 4 in the northern and eastern parts of the study area documented for the first time fourteen recurring lithofacies and trace fossil assemblages attributed to *Cruziana* and *Skolithos* ichnofacies.

5.1.2.4 Facies association 5

In the study area, sedimentary rocks of facies association 5 overlie a upward-coarsening succession produced by facies association 4. Facies association 5 displays an overall upward-fining trend and in places has sharp or erosive based coarse-grained to pebbly massive sandstones (Sm) and medium- to fine-grained sandstones (Sm, St, Sh, Sr, Sb) which grade upward into or capped by fine-grained lithofacies associated (Fsm, Fc, Fl and Fr) with coals. Upward-coarsening successions (3.5 m to 17.6 m thick) are also recorded in facies association 5, but mainly in the boreholes situated in the western part of the study area. A trace fossil assemblage consisting of *Planolites*, *Siphonichnus* and *Thalassinoides* of the *Cruziana* ichnofacies are mainly associated with fine-grained lithofacies that form the base of the upward-coarsening successions in the western part of the study area. Thick (up to 60 m), well sorted fine- to medium-grained sandstones are present within facies association 5 in the western part of the study area and contain the *Skolithos* ichnofacies (dominated by *Conichnus*, *Siphonichnus*, escape structures, *Planolites*, *Phoebichnus*, *Palaeophycus tubularis* and *Thalassinoides*).

Sandstone lithofacies of facies association 5 are predominantly arkose and subarkose in composition (Fig. 4.23, 4.25, 4.27). These sandstones contain dominantly subangular grains and lesser amounts of subangular detrital grains. The sandstones samples from facies association 5 in the eastern and western part of the Gemsbok Sub-basin suggest transitional continental provenance and craton interior as the dominant sources and few contributions from the mixed and recycled orogen sources (Fig. 4.24, 4.26). The geochemistry of the facies association 5 sandstones in the eastern part of the Gemsbok Sub-basin reveals acidic magmatic or felsic igneous provenance and quartzose sedimentary provenance derived from continental island arc and passive margin tectonic

settings (Fig. 4.28, 4.29, 4.30). Facies association 5 is here interpreted to equate to part of the Auob and Otshe formations in the western and eastern parts of the study area respectively (Smith, 1984; Grill, 1997; Key et al., 1998; Miller, 2008).

5.1.3 Beaufort Group equivalent

The Beaufort Group equivalent in the Gemsbok Sub-basin occurs only in the northern and eastern parts of the study area and there are no equivalents of this Group in the western part of the study area (Fig. 5.2, 5.3). In the study area, it conformably overlies facies association 5 sedimentary rocks of the Ecca Group (Fig. 5.1). The Beaufort Group equivalent in the study area is defined by facies association 6 which comprises thick (ranging from 32 m and 165 m) siltstone packages which are interbedded with thin mudrocks (up to 10 cm) and sandstones (up to 3 m). Facies association 6 thins to the north and northwest and thickens towards the east and southeast (Fig. 5.2, 5.3) of the study area. A upward-fining succession comprising sandstones with rip-up mudrock clasts at the base and grading upwards into thick non-carbonaceous siltstone and sandstone successions was recorded in borehole W2 in the northern part of the study area. Calcareous and pale red (probably haematite) nodules were observed in these thick siltstone successions. The Beaufort Group equivalent sedimentary rocks show bioturbation structures. The siltstones, mudrocks and sandstones of the Beaufort Group equivalent range in colour from light grey to light grey pink with few pale red layers.

Smith (1984) interpreted the Beaufort Group equivalent in the southwest Botswana to conformably overlie carbonaceous and coaly successions of the Ecca Group. The Beaufort Group equivalent in the southwest Botswana is known to be represented by non-carbonaceous siltstones and mudstones of the Kwetla Formation which consists of basal fine-grained sandstones and dominated of dark grey mudstones with sideric and limonitic banded siltstones (Smith, 1984). Calcareous nodules and some silty micaceous bands are present (Smith, 1984; Exploration Consultants Limited, 1998). A regional unconformity has been recorded at the top of the Beaufort Group equivalent in the southwest Botswana and it forms the basal part of the overlying Lebung Group (Smith, 1984; Exploration Consultants Limited, 1998).

5.1.4 Lebung Group

The Lebung Group in the northern and eastern part of the study area is defined by two formations, the Mosolotsane and the Ntane formations (Smith, 1984). The equivalent of the Mosolotsane Formation in the western part of the study area was recently discovered and assigned to the Neu Loore Formation (Miller, 2008). Smith (1984) and Miller (2008) respectively defined the base of Mosolotsane and Neu Loore formations as an intra-Karoo unconformity.

5.1.4.1 Mosolotsane Formation

The Mosolotsane Formation occurs in two boreholes in the northern part of the study area (i.e., W1 and W2; App. Fig. 6, 7) and ranges in thickness from 5 m to 21 m. It consists of rocks of facies association 7 and is dominated by reddish mudrocks. In borehole W1, it consists of a upward-fining succession of less than a meter thick, composed of conglomerate (Gcm) at the base, which grade upwards into medium-grained, reddish sandstones and laminated to massive moderate reddish brown mudrocks.

5.1.4.2 Neu Loore Formation

The Neu Loore Formation in the western part of the study area is also characterised by facies association 7 sedimentary rocks and show similar characteristics as the Mosolotsane Formation in the northern part of the study area. The facies association 7 in the Neu Loore Formation consists of approximately 50 to 62 m thick dark reddish brown, greyish red and pale red mudrocks which are interbedded thin light grey siltstones (App. Fig. 3). Calcareous nodules are present within the mudrocks and siltstones of the Neu Loore Formation.

5.1.4.3 Ntane Sandstone Formation

The Ntane Sandstone Formation conformably overlies the Mosolotsane Formation in the northern part of the study area and occurs in five boreholes located in the northern and eastern parts of the study area (App. Fig. 6, 8, 9, 10, 11). This Formation comprises well sorted, fine- to medium-grained, mica-free sandstones of facies association 8 and ranges in thickness from 0.5 to 60 m. The sandstone lithofacies that was analysed from facies association 8 of the Ntane Sandstone Formation shows an average quartz content of 89%,

feldspar content of 8% and rock fragments content of 3% (Table 6). The analysed sandstone sample from facies association 8 is dominated by subangular and subrounded grain shapes and it is classified as a subarkose which plots within the craton interior provenance field (Fig. 4.25, 4.26).

5.2 Depositional Environments

Detailed sedimentological analysis (this study) of borehole cores from across the Gemsbok Sub-basin revealed a variety of depositional environments which existed during Karoo times. The inferred depositional environments (this study) are in agreement with the previous documented depositional environments by Smith (1984), Kingsley (1985), Grill (1997), Key et al. (1998) and Miller (2008). The results obtained from this investigation demonstrate detailed facies associations and different depositional environments present within the Karoo Supergroup in the Gemsbok Sub-basin of Botswana and Namibia.

5.2.1 Dwyka Group

The Dwyka Group is mainly represented by diamictites (Dmm, Dcm), with interbedded sandstone (Sm, Sr) units, thin mudrock (Fc) layers, laminated sandstone, siltstones and mudrocks (Fl), and bioturbated mudrocks (Fr). Diamictites of the Dwyka Group consists of dropstones, which are clasts of different rock types that were dropped into finer sediment by floating melting ice (Reading, 1986). Matrix-supported, massive diamictites are interpreted as a product of rainout and debris flow processes (Eyles et al., 2007). The massive, clast-supported diamictites and sandstones can be interpreted as deposits of high concentration turbidity currents or debris flows (Pickering et al., 1989). Dropstones within the diamictite lithofacies (Dmm, Dcm) provide a strong evidence of ice rafting in the Dwyka Group sedimentary rocks (Reading, 1986). The clast-supported, massive diamictites with angular and subrounded clasts and interbedded massive sandstones resemble “Facies Class A” deep marine disorganised gravels and sands of Pickering et al. (1989). The roundness of the dropstones found in lithofacies Dcm (borehole W3) might have been due to glaciofluvial transport either on or below icesheets.

Sandstone units interbedded with diamictites normally display upward-fining trends (ranging between 1 cm and 10 cm), intercalated with thin mudrocks and consist of sedimentary structures (massive bedding, ripple cross-laminations, convolute lamination and load casts), and which point to deposition by turbidity currents (Boggs, 2001). The massive sandstones indicate rapid deposition from turbidity currents, and massive sandstones are interpreted as Bouma-type 'A' divisions (Eyles and Eyles, 2000). Soft-sediment deformation structures within the sandstones of the Dwyka Group include micro-faults and micro-folds and are interpreted as slump structures, which represent terrigenous deposits that have been emplaced downslope by mass-wasting processes (Tucker, 1991; Boggs, 2001).

The presence of the *Cruziana* ichnofacies (dominated by *Conichnus*, *Teichichnus*, *Siphonichnus*, *Schaubcylindrichnus* and *Palaeophycus tubularis* trace fossils) suggests a feeding pattern most characteristic of quiet-water, shelf marine deposits (Frey, 1975; Winters, 1990/1991, Miller, 2007; Galloway and Hobday, 1996). Massive, bioturbated grey-green mudrocks and laminated siltstones and mudrocks represent fine-grained turbidites or pelagic deposits deposited in suspension under low-energy environment and relatively slow rates of sedimentation indicated by the bioturbation structures within these mudrocks in borehole CKP8C-1 (Eyles and Eyles, 2000).

Grill (1997) has interpreted the palaeoenvironments of Dwyka Group in the western part of the study area to have been dominantly continental glacial and subglacial environments, with marine glacial, proglacial and interglacial deposits also occurring. Palynological studies of the Dwyka Group in the southwest Botswana (e.g., borehole MP1, Fig 2.1) have suggested mixed marine, marginal marine and continental environments (Stoakes and McMaster, 1990; Key et al., 1998). The current study shows that the Dwyka Group in Gemsbok Sub-basin was deposited by deep-water glaciomarine or glaciolacustrine environments. This interpretation is supported by the presence of a wide variety of deep-water siliclastic sedimentary rocks, which include turbidites, glaciomarine or glaciolacustrine lithofacies (diamictites), soft-sediment deformation structures and *Cruziana* ichnofacies (Boggs, 2001).

5.2.2 Ecca Group

Based on the differences in sedimentary structures, lithofacies, and trace fossils, the Ecca Group is subdivided into four facies associations (facies associations 2, 3, 4 and 5) and depositional environments.

5.2.2.1 Facies association 2

Facies association 2 forms the base of the Ecca Group in the study area and it is dominated by thick sandstone units that are characterised by Bouma turbidite sequence sedimentary intervals A, B, C, D and E. The classic Bouma turbidite sequence for medium-grained sand and mud is represented by upward-fining successions (ranging in thickness between 1.5 cm to 15 cm) comprising massive, medium-grained sandstones (Sm) with erosive bases and in places rip-up mudrock clasts at the base, succeeded by laminated or cross-laminated, fine-grained sandstones (Sh or Sr) and finally mudrocks (Fc). Massive sandstones at the base of these upward-fining successions lack sedimentary structures and represent rapid deposited sandstones by high concentration turbidity currents and can be classified as Bouma A subdivision (Shepard, 1964; Boggs, 1987; Pickering et al., 1989; Reading, 1996; Wild et al., 2009; Figueiredo et al., 2010). The upward-fining successions might have resulted from flows of decreasing energy (Reading, 1996) or they have resulted from high concentration turbidity currentss (Pickering et al., 1989; Wild et al., 2009). Internal structures associated with the sandstones of facies association 2 in the study area include horizontal lamination, ripple cross-lamination, and contorted bedding in places. These internal structures together with upward-fining cycles suggest deposits by deep-water turbidity currents (Bouma et al., 1962; Reading, 1996; Boggs, 2001; 2006). Alternating layers of siltstones and mudrocks displaying upward-fining trends in borehole ACP4 are also interpreted as fine-grained turbidite facies dominated by C, D and E intervals of Bouma, and resulting from low concentration turbidity currents (Shepard, 1964; Pickering et al., 1989; Reading, 1996; Hodgson, 2009; Wild et al., 2009). The pale green mudrocks in borehole W3 might represent hemipelagic or pelagic mudrocks deposited in reducing, low energy environments (Reading, 1996; Wild et al., 2009).

The base of the Ecca Group in the western part of the study area is believed to be marked by a major sand input into the basin and represented by Nossob Formation which indicates deposition by turbidity currents (Kingsley, 1985; Grill, 1997). Smith (1984) defined the base of the Ecca Group in the northern part of the study area, as the bedding surface above which glacial characteristics are absent and a plane at which massive siltstones conformably overlie the varved sequence of the Dwyka Group and represented by the Ncojane Sandstone Member, which reflects distal deltaic sands and deposition during marine transgression.

Based on the described lithofacies and sedimentary structures within facies association 2 and the stratigraphic position above the glaciomarine or glaciolacustrine deposits of the Dwyka Group, the lower Ecca Group (facies association 2 of the Nossob Formation and Ncojane Sandstone Member) is interpreted as deep-water (sea or lake) turbidite deposits.

It has been frequently suggested that thick-bedded turbidite deposits are deposited in areas near the turbidite source and thin-bedded turbidites in more distal regions to the source (Boggs, 1987). The cross-section W3- CKP8C-1/CKP8C (Fig. 5.2, 5.3) shows facies association 2 thickening towards the north and northwest of the study area, which might indicate that the source for facies association 2 was located in the north and northwest. Kingsley (1985) has also observed and interpreted the Nossob Formation as the delta front sand which thickens northwards but pinches out toward the south. Smith (1984) interpreted the Ncojane Sandstone Member which is equivalent to the Nossob Formation to have probably been derived from the northwest.

5.2.2.2 Facies association 3

Massive and laminated mudrocks dominate facies association 3 in the study area and indicate deposition in quiet-water environments (Coleman and Prior, 1980; Galloway and Hobday, 1996; Miall, 2000). Massive mudrocks can be interpreted as suspended sediments deposited by rapid sedimentation (Coleman and Prior, 1980). Soft-sediment deformation structures (micro-faults and micro-folds) within facies association 3 mudrocks are indicative of rapid sedimentation, which result in sediment instability and are typical for sediments deposited in the delta front and prodelta settings (Tucker, 1991; Galloway and

Hobday, 1996; Reading, 1996). Dark colour (dark grey and black) within these mudrocks is due to high organic content (Coleman and Prior, 1980; Tucker, 1991; Galloway and Hobday, 1996). The grey greenish colour of the massive mudrocks of facies association 3 in the western part of the study area indicates that the rocks were deposited in reducing conditions (Johnson et al., 2006).

Within the borehole sections in the study area, facies association 3 shows an upward increase in sandstone content into facies association 4. Therefore, the abundance of finely-laminated and massive mudrocks, lenticular bedding, slump structures, together with an upward increase in sandstone interbeds into the overlying facies association 4 points to a depositional settings below the wave base in prodelta environments (Coleman and Prior, 1980; Reading, 1996). This interpretation agrees with that of Smith (1984), Kingsley (1985) and Grill (1997).

5.2.2.3 Facies association 4

Facies association 4 is dominated by arenaceous lithofacies and conformably overlies facies association 3 in the study area. Lithofacies within facies association 4 reflect a upward-coarsening character, from argillaceous rocks at the base to arenaceous units at the top.

Lower part of facies association 4

The lower part of facies association 4 consists of laminated sandstones, siltstones and mudrocks (Fl) interbedded in places with massive sandstones (Sm), ripple cross-laminated sandstones (Sr), carbonaceous mudrocks (Fc) and bioturbated mudrocks (Fr). Internal sedimentary structures in the lower part of facies association 4 include ripple cross-laminations (wavy, lenticular and flaser bedding), horizontal laminations and bioturbation. The abundant ripple cross-laminations (Sr) record the alteration of quiet-water mud sedimentation and higher-energy flow conditions under which rippled sandstones were deposited (Miall, 2000). Interbedded sandstone, siltstone and mudrock lithofacies reflect fluctuations in sedimentation conditions, whereby there were periods of suspension settling (mud) followed by periods of high energy traction sedimentation (silt and sand) (Boggs, 1987). Massive sandstones (Sm) lithofacies within the lower part of

facies association 4 indicate rapid deposition (Boggs, 2001) and pyrite nodules found within these sandstones indicate replacement of plant debris (Coleman and Prior, 1980).

A trace fossil assemblage of the *Cruziana* ichnofacies (dominated by *Thalassinoides*, *Teichichnus*, *Palaeophycus tubularis*, *Planolites*, *Zoophycos*, *Asterosoma*, *Skolithos* and *Conichnus*) is present within the lower parts of facies association 4 in several boreholes (W3, ACP4, ACP3 and ACP24), which suggests a shallow marine settings below the minimum wave base, but above the storm wave base (Ekdale et al., 1984; Pemberton et al., 1992; MacEachern et al., 2007). The observed lithofacies (Fl, Fc, Fr, Sm), the *Cruziana* ichnofacies and sedimentary structures (i.e., ripple cross-lamination, erosive structures within the sandstones and horizontal bedding) within the lower part of facies association 4 and the stratigraphic position above the prodelta facies of facies association 3 suggest a distal bar depositional setting (Reineck and Singh, 1973; Coleman and Prior, 1980; Reading, 1996).

Upper part of facies association 4

In a fluvial-dominated delta, distal bar deposits grades upwards into distributary mouth bar deposits, whereas in a wave-dominated delta, the delta front deposits comprise thick sand units deposited in distal bar, shoreface, beach and distributary mouth bar environments (Galloway and Hobday, 1996; Reading, 1996; Nichols, 2009). Where wave energy dominates, the subaqueous delta front is a shoreface modified by fluvial processes around active channel mouths (Galloway and Hobday, 1996). The upper part of facies association 4 is dominated by sandstone lithofacies, which are interpreted to have been deposited in the proximal mouth bars, shoreface and beach environments in the delta front setting.

The upper part of facies association 4 in the western and eastern parts of the study area show similar characteristics. It is dominated by 35 m to 36 m thick sandstones units which are well sorted, porous, micaceous, fine- to medium-grained sandstones (Sm, Sh, St) and are locally interbedded with pebble-sized sandstone (Sm) layers. These sandstones locally contain mudrock clasts and pyrite nodules. Fine- and medium-grained, micaceous and well sorted sandstones within the upper part of facies association 4 reflect

deposition in high-energy environments where sediments are reworked by wave currents (Reineck and Singh, 1973; Kingsley, 1985). The massive bedding within the sandstones might represent rapid deposition in high-energy settings (Boggs, 1987). Horizontal laminated sandstones indicate deposition form rapid flows under upper (high) flow regime conditions (Reineck and Singh, 1973). Trough cross-bedding might have been produced by migration of three-dimensional dunes in high-energy depositional environments (Reading, 1996). The presence of pyrite nodules within the massive sandstones suggests replacement of organic rich plant debris through pyritisation processes in reducing environments (Coleman and Prior, 1980; Tucker, 1991). Mudrock clasts within the medium-grained and pebble-sized sandstones suggest high-energy erosive currents (Rubidge et al., 2000). Porous sandstones dominate upper parts of facies association 4 and are characteristics of the distributary mouth bar deposits (Coleman and Prior, 1980). Sandstone units of the upper part of facies association 4 in the western and eastern parts of the study area resemble those deposited in the delta front of fluvial-dominated deltas, whereby fluvial processes are more dominant than wave or tidal processes (Reading, 1996).

A well-preserved trace fossil assemblage of the *Skolithos* ichnofacies (dominated by escape structures*, Siphonichnus* and *Rosselia*), thick (up to 60 m) clean, fine- to medium-grained sandstone units in the northern part of the study area (borehole W3), indicate a well-developed beach environment in delta front setting (Frey, 1975; Miall, 1979; Pemberton et al., 1992; Boggs, 2001; MacEarchern et al., 2007). Traces of the *Skolithos* ichnofacies are indicative of high wave or current energy settings and are mainly associated with well sorted, loose or shifting substrates (Pemberton et al., 1992; MacEachern et al., 2007). They commonly occur in sandy shoreface of beaches and sheltered foreshore environments, and they have also been observed in proximal wave-dominated delta fronts (Pemberton et al., 1992; MacEachern et al., 2007). The trace fossil-rich sandstones of the upper facies association 4 in borehole W3 are normally overlain by clean, moderately fine- to medium-grained porous sandstones, which have been deposited in a foreshore beach environments where wave energy and current energy extremely is high (Frey, 1975; Pemberton et al., 1992; Boggs, 2001, MacEarchern et al., 2007). The upper part of facies association 4 in the northern part of the study area

suggests deposition in a wave-dominated delta front (shoreface and beach environments) with frequent reworking of sediments during storms (Reineck and Singh, 1973; Johnson et al., 2006).

Previous studies on the Ecca Group in the Gemsbok Sub-basin (Smith, 1984; Kingsley, 1985; Grill, 1997) have interpreted it to have been deposited by prograding deltas in the northern and the eastern parts of the study area and to have been deposited by both fluvial and wave-dominated deltas in the western part of the study area. The morphology and sedimentary facies of deltaic deposits depend on the interaction of various factors, including fluvial sediment input, climate, river-mouth processes, waves, tides, slope of the shelf, rates of subsidence, geometry of the depositional basin and the tectonics of the receiving basin (Miall, 1979; Reading, 1986; Galloway and Hobday, 1996; Boggs, 2001). Among these variables, fluvial sediment input, wave-energy flux and tide flux are the most important processes that control the geometry, trend, and internal feature of the progradational delta front sand bodies (Boggs, 2001).

Deltaic successions comprise two basic components and that includes the subaerial delta plain and the subaqueous delta front. The delta plain is subdivided into upper delta plain and lower delta plain. The former is little affected by marine processes and it is dominated by fluvial processes such as distributary channel migration, channel and point bar deposition, overbank flooding and crevassing into lake basins (Boggs, 2001). The main depositional environments in the upper delta plain include both braided and meandering channels, backswamps, marshes and swamps, freshwater lakes and lacustrine delta fills (Reading, 1996; Boggs, 2001). The lower delta plain is an area that is affected by both continental fluvial and marine processes. It consists of active and abandoned distributary channels, natural levees, interdistributary bays, crevasse splays, marshes and swamps (Reading, 1996; Boggs, 2001). The delta front comprises an area that lies seaward and actively receives fluvial sedimentation (Boggs, 2001). It consists of the distributary mouth bar deposits, prodeltaic (offshore) deposits and slump deposits (Reading, 1996; Boggs, 2001).

Deltas can be classified according to a four-fold scheme based on the relative influence of fluvial processes versus marine (waves and tides) processes and based on the dominant grain size of the sediments (Galloway and Hobday, 1996; Boggs, 2001; Fig 5.8). The physical stratigraphic framework of a fluvial-dominated delta and wave-dominated delta is broadly similar; they both comprise an upward-coarsening succession that passes upward from muddy, offshore or prodelta deposits into continental, fluvial facies (Miall, 1979; Galloway and Hobday, 1996; Reading, 1996). This upward-coarsening succession of facies is the distinctive feature of deltaic deposits (Tucker, 1991; Boggs, 2001; Nichols, 2009). The main distinctive features of a wave-dominated delta are thick stacked beach-ridge deposits and mouth bar deposits which form a continuous sand sheet in vertical section like that of the prograding marine shoreface (Galloway and Hobday, 1996). These beach-ridge sands are deposited along the front and margins of the delta (Galloway and Hobday, 1996). In fluvial-dominated deltas, delta front sand sheets are relatively thin compared to those of the wave-dominated deltas. Tide-dominated deltas consist of a progradational, upward-coarsening prodelta mud and tidal sand ridge sequence overlain by aggradational, delta plain tidal-flat, tidal channel, and marsh or swamp deposits (Galloway and Hobday, 1996).

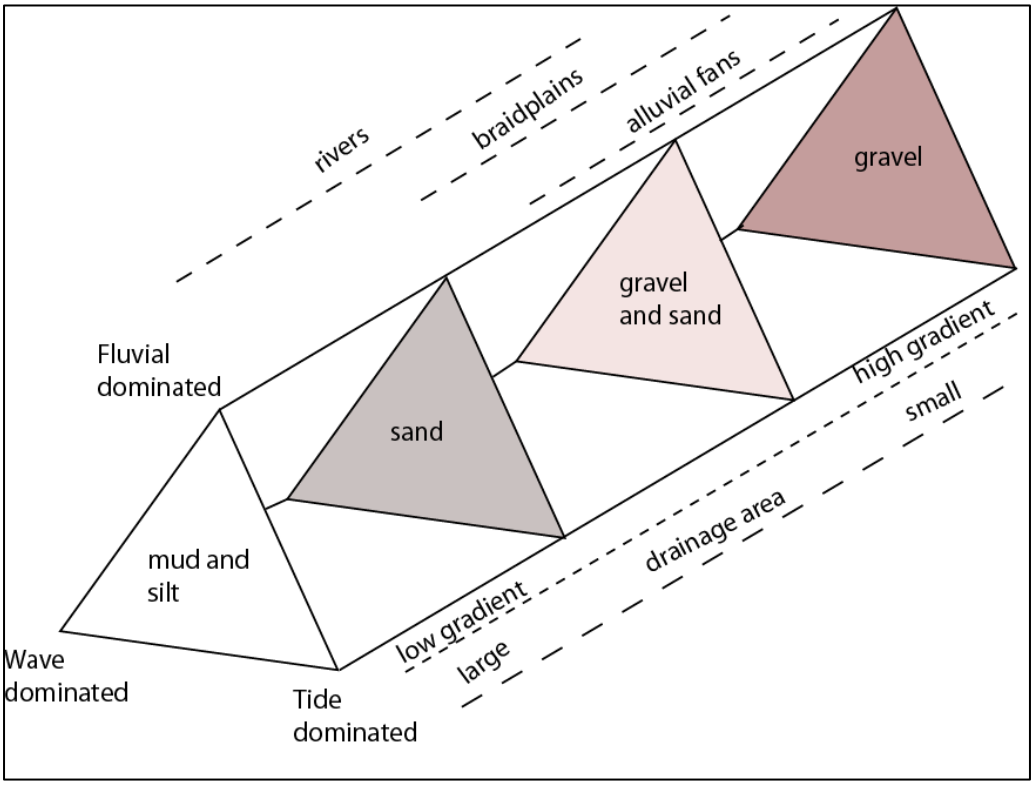


Figure 5.8 Classification of deltas based on grain size and on sediment supply mechanism. (Modified after Orton and Reading, 1993; Nichols, 2009).

Progradation of deltas seemed to have become dominant during deposition of the Ecca Group in the Gemsbok Sub-basin. Facies association 3 and 4 of the Ecca Group are arranged in an upward-coarsening character, which resemble that of prograding deltaic systems. Deltaic deposits have been recognised in all studied boreholes in the study area and display an upward-coarsening, continuous vertical succession of marine facies associations (prodelta and distal bars) at the base, shallow-marine facies associations (mouth bars and beach face) at the top. These upward-coarsening successions of facies associations are interpreted to represent the deposition by prograding deltaic systems during regressions.

Upward-coarsening cycles produced by facies association 3 and 4

Boreholes in the northern (boreholes W2 and W3; App. Fig. 7, 8) and the central parts of the study area (reference borehole MP1; App. Fig. 12) consist of two stacked upward-coarsening wave-dominated delta cycles. Individual delta cycle range in thickness from 100 m to 109 m and comprise prodelta mudrocks (facies association 3) at the base and shoreface or foreshore (beach) deposits (facies association 4) at the top. Evidence of beach face (shoreface and foreshore) deposition within these borehole is supported by the presence of vertical, U-shaped burrows, which belong to the *Skolithos* ichnofacies and thick, well sorted, clean, medium- to fine-grained sandstone units (Boggs, 2001; MacEachern et al., 2007). The trace fossil evidence makes it easier to distinguish sedimentary rocks deposited in shoreface and foreshore environments from the ones deposited in the shallow-marine, offshore regions (Stanistreet et al., 1980).

Two deltaic cycles represent progradation and abandonment of two wave-dominated delta lobes (Galloway and Hobday, 1996). In actively subsiding basins, cyclic wave-dominated delta lobe progradation and abandonment might generate repetitive stacked upward-coarsening beach-ridge deposits (Galloway and Hobday, 1996). Therefore, the first deltaic cycle observed in boreholes W3 (App. Fig. 8) is interpreted to represent progradation of wave-dominated deltaic system which was abandoned and followed by relative sea level rise (transgression) due to a combination of factors such as sediment compaction, local basin subsidence and climate change (Galloway and Hobday, 1996;

Catuneanu, 2002; Nichols, 2009). These two large scale delta cycles were previously recorded by Smith (1984) in the northern part of the study area.

5.2.2.4 Facies association 5

Facies association 5 overlies facies association 4 (delta front deposits) in a sharp contact in the study area. It is characterised by upward-fining profiles with poorly sorted, coarse-grained to pebbly massive sandstones (with mudrock clasts) at the base, grading upwards into medium- to fine-grained horizontally laminated (Sh), trough cross-bedded (St) and rippled cross-laminated (Sr) sandstones, and eventually capped by fine-grained lithofacies (Fl, Fr, Fsm, Fc and C). The base of the basal sandstone succession is erosive into the underlying rocks. In all the boreholes, facies association 5 directly overlies the delta front deposits of facies association 4 (App. Fig. 1 to 13).

Facies association 5 is interpreted to represent deposits on the delta plain. This interpretation is based on the stratigraphic position (immediately overlying the delta front deposits of facies association 4), dominance of upward-fining successions, presence of erosional or sharp basal contacts within the sandstone lithofacies, as well as the association of sedimentary structures in the sandstones (lithofacies Sm, St, Sh, and Sr) containing intraformational mudrock or coal clasts. Depositional subenvironments recognised within the delta plain facies association 5 in the study area include distributary channel deposits, floodplain deposits, interdistributary bay deposits, crevasse splays as well as trangressive shoreface (beach face) deposits.

Distributary channel deposits

In the study area, distributary channel deposits comprise poorly sorted, pebbly, very coarse- or coarse-grained sandstones with sharp or erosive bases and mudrock or coal clasts. Poor sorting within the pebbly- and coarse-grained sandstones suggest rapid deposition without reworking (Boggs, 2001). The intraformational mudrock and coal clasts suggest high-energy flow (Reading, 1996; Rubidge et al., 2000). The poorly sorted channel sandstones are normally coarse and massive (lithofacies Sm) at the base and fine upwards into medium- to fine-grained lithofacies Sh, St and Sr. Massive sandstones (lithofacies Sm) are interpreted to have formed in conditions where rapid sedimentation

of high-density gravity flows occurred (Tucker, 1982; Boggs, 1987). Lithofacies St probably resulted from the migration of three-dimensional dunes within the channels (Miall, 1977), whereas horizontally laminated sandstones (lithofacies Sh) have been resulted from plane-bed flow under upper flow regimes (Miall, 1977; Reading, 1996). Ripple cross-laminated sandstones are indicative of deposition of sand in a low energy shallow-water environment (Miall, 1977; Reading, 1996). Pyrite nodules indicate the replacement of plant debris (Coleman and Prior, 1980), whereas the pale-red (probably haematite) nodules might point out to subaerially exposed and well-drained environments where pedogenic nodules formed (Rubidge et al., 2000).

Floodplain deposits

Floodplain deposits mostly comprise fine-grained lithofacies (Fl, Fr, Fsc, Fsm, Fc and C) and indicate deposition of fine material from suspension in the delta plain subenvironments during flooding events (Reineck and Singh, 1973; Collinson, 1986). These fine-grained lithofacies overlie channel sandstones and are interpreted as channel-fill or overbank deposits that fill the channel during flooding and channel abandonment stages (Miall, 1985; Bhattacharya and Walker, 1992; Miall, 1996). Bioturbated mudrocks and siltstones (Fr) are characteristic features of channel-fill and overbank deposits (Coleman and Prior, 1980). Laminated sandstones, siltstones and mudstones (Fl) are interpreted as backswamp deposits or shallow lake or pond deposits (Miall, 1977; 1996, Roberts, 2007). Carbonaceous mudrocks, coals and associated lithofacies suggest poorly drained swamps with luxuriant vegetation within the delta plain environments (Reineck and Singh, 1973; Reading, 1986).

Upward-fining trends produced by sandstone lithofacies (Sm, Sh, St and Sr) indicate decrease in flow energy during deposition (Reading, 1996; Boggs, 2001). Vertically stacked upward-fining cycles within delta plain deposits of facies association 5 indicate multiple periods of channel aggradation and channel abandonment due to episodes of channel migration (Miall, 1977; 1982; Boggs, 2006). These multiple stacked upward-fining successions also indicate varying patterns of subsidence rates in the Gemsbok Sub-basin (Coleman and Prior, 1980). Therefore, the cyclic upward-fining successions (more than three) in the western and eastern parts of the study area are typical for fluvial-

dominated deltas, whereas in the northern part of the study area, delta plain facies association consisted of fewer upward-fining cycles (channel and overbank deposits), which points out to a wave-dominated delta environment (Galloway and Hobday, 1996; Reading, 1996).

Interdistributary bay deposits and crevasse splays

Upward-coarsening successions within the delta plain environment produced by fine-grained lithofacies and sandstone lithofacies are typical for interdistributary bay filling processes, whereby interdistributary bay fine-grained lithofacies are punctuated by crevasse splay or channel deposits (Coleman and Prior, 1980; Boggs, 1987; Bhattacharya and Walker, 1992; Boggs, 2001; Catuneanu, 2002; Nichols, 2009). Interdistributary bays are areas surrounded by levees, marshes or channels and open to a body of water (e.g., a large lake or sea) (Reineck and Singh, 1973; Coleman and Prior, 1980), and occur mostly in the lower delta plain environments of fluvial-dominated deltas (Reading, 1996; Boggs, 2001). Deposition in interdistributary bays is mainly from suspension, mostly when there is no wave activity. Coarse-grained sediments are usually deposited by crevasse channels (Reineck and Singh, 1973). Lenticular bedding is abundant, and bioturbation, paralle and current ripple cross- lamination are common (Reineck and Singh, 1973; Coleman and Prior, 1980).

Upward-coarsening successions (ranging from 3.5 m to 17.6 m in thickness) within facies association 5 grade from fine-grained lithofacies (Fl, Fr, Fc) upwards into sandstones (Sr, Sh). Fine-grained lithofacies (Fl, Fr, Fc) in the lower parts of upward-coarsening successions result from low energy suspension deposition in a quiet area (Reineck and Singh, 1973; Rubidge, 1988). These fine-grained lithofacies probably represent a low energy, distal, interdistributary bay environment (Rubidge, 1988). They might also indicate overbank deposits, which have spilled from the river channels during flooding events, and fill the interdistributary bays (Miall, 1982; Bhattacharya and Walker, 1992; Catuneanu, 2002). In places, the fine-grained lithofacies show presence of wavy, flaser and lenticular bedding and *Cruziana* ichnofacies (consisting of *Planolites*, *Siphonichnus* and *Thalassinoides*), suggesting that the interdistributary bays were affected by waves (Reineck and Singh, 1973; Reading, 1996; Catuneanu, 2002; Roberts, 2007). Ripple

cross-lamination, horizontal bedding and bioturbation is common within the sandstone lithofacies in the upper parts of the upward-coarsening successions and indicate deposition during floods on natural levees and deposition under lower flow regime conditions (Miall, 2000). The ripple cross-laminated and horizontal laminated sandstones represent crevasse splays and channel deposits (Reineck and Singh, 1973). The upward-coarsening successions within facies association 5 are therefore interpreted to represent interdistributary bay and crevasse splay deposits in a fluvial-dominated deltas.

Transgressive shoreface and foreshore (beach) deposits

Thick (29 m to 50 m), well sorted medium- to fine-grained sandstones are present within the delta plain deposits of facies association 5 in the western part of the study (i.e., boreholes ACP3, ACP13 and ACP24; App. Fig. 1, 3, 5) and indicate transgressive shoreface and beach deposits (Galloway and Hobday, 1996; Catuneanu, 2002). Borehole ACP24 displays a well-developed thick beach face deposit ~50 m thick. Trace fossils belonging to the *Skolithos* ichnofacies are present within these thick sandstone units and they provide strong evidence of shoreface deposition (MacEachern et al., 2007). The transgressive shoreface and beach deposits within the delta plain deposits of facies association 5 in the western part of the study area might have resulted from major changes in the hydrologic and sediment regime due to local tectonism (differential subsidence or uplift), major diversions of rivers upstream, or changes in relative sea level (Boggs, 2001; Catuneanu, 2006).

Fluvial-wave interaction deltas such as Rhône and Ebro have similar sequences as those of fluvial-dominated deltas, although there is difference in the degree of wave reworking towards the top (Reading, 1996). A conclusion can be drawn that the delta plain deposits in several boreholes in the western part of the study area were dominated by wave processes, which resulted in the deposition of well sorted, shoreface and beach face deposits. Therefore, deltas in the western part of the study area included both fluvial-dominated (as evidenced by well-developed floodplains and channels in the delta plain) and fluvial-wave interaction (as evidenced by transgressive beach deposits) deltas. Kingsley (1985) interpreted the Ecca Group in the western part of the study area to have been dominated by fluvial and at other times by wave agencies.

Coal distribution and thickness

The geology of the coal deposits in the western part of the study area differs from the northern and eastern parts of the study area. Coals in the western part are generally thin (less than 1 m) and are associated with lithofacies and ichnofacies interpreted as lower delta plain deposits (interdistributary bay, bay fill deposits, channels and trangressive shoreface or beach deposits). In the northern part of the study area, coal deposits are slightly thicker (range from 3 m to 4.82 m) and are associated with stacked upward-coarsening, wave-dominated delta deposits, upper delta plain (upward-fining successions) and delta abandonment facies (lithofacies Fr, Fl and Fc). Coals in the eastern part are up to 28 m in thickness and occurred in upper delta plain environments, associated with channels and delta abandonment facies (lithofacies Fr, Fl and Fc).

Thick coal deposits are known to develop in areas where the climate is humid, vegetation is abundant, the water table is at a high level relative to the topography and within high accommodation system tracts where the rates of creation of accommodation was high relative to the sediment input (Reineck and Singh, 1973; Miall, 1982; Catuneanu, 2006). Such areas included delta plains, floodplains with backswamps and swamps in the subaerial environments (Reineck and Singh, 1973). Where vegetation in less abundant or where the rates of sediment input is high, thick peat accumulation is less important and complex lakes and swamps result (Reading, 1986). The distribution, lateral extent, thickness and maceral content of coal deposits are primarily controlled by basin tectonics and differential subsidence (Cadle et al., 1993; Johnson et al., 2006).

Tectonics (i.e., subsidence rates) and variable sediment influx seemed to have controlled the thickness of the coals in the western and northern parts of the study area. The thin coal deposits in the western part of the study area are associated with channel deposits, interdistributary bays and beach deposits. High rates of sedimentation in the western part of the study area are represented by two features: 1.) stacked sharp-based pebbly sandstones interbedded with coals (e.g., ACP19) and 2.) upward-coarsening successions (interdistributary bay and crevasse splays), which overlie coal deposits (i.e., borehole ACP4, ACP13 and ACP24). The stacked sharp-based pebbly sandstones are interpreted as channel deposits with a high rate of avulsion (Smith et al., 1989). Therefore, channel

avulsions resulted in erosion of coal deposits and produced extremely thin coals in the western part of the study area (i.e., borehole ADP19). Peat formation in boreholes ACP4 and ACP13 was probably accompanied by sediment influx from the distributaries (bay fill deposits) and marine incursions (presence of *Cruziana* ichnofacies) as a result of the compaction of the delta front and prodelta deposits (Cadle et al., 1993), therefore resulting in extremely thin coals. In borehole ACP 24, coal swamps were terminated by an increase in clastic sedimentation (Kingsley, 1985). In the western part of the study area, peat-forming environments seemed to be restricted to backswamp, floodplain or backshore environments of the lower delta plain (Kingsley, 1985; Galloway and Hobday, 1996).

Coal deposits in the northern part of the study area were located in a tectonically active portion of the basin where rapid subsidence and sedimentation took place (Cadle et al, 1993). This is evidenced by the presence of two stacked regressive deltaic cycles in this part of the study area (App. Fig. 8). Coal deposits occur in two horizons (lower and upper) and associated with the delta abandonment stage. The lower coals are relatively thin compared to the upper coals, and this might have resulted from rapid subsidence, differential compaction of the underlying wave-dominated delta cycle, which caused the drowning of coals hence termination of peat formation. High sediment influx (represented by the overlying, second wave-dominated delta cycle) might also have contributed in the thining of coals, resulting in termination of peat formation. The upper coals above the second wave-dominated delta cycle are overlain by at least one upward-fining succession. The accumulation of the upper coals occurred when clastic influx was less vigorous in the Sub-basin (Cadle et al., 1993) and resulted in coals up to 4.82 m thick. This study concludes that rates of clastic sedimentation seemed to have controlled the thickness of coal deposits in the northern part of the study area.

In the eastern part of the study area, the coals are underlain by thick delta front and channel sandstone units and overlain by delta abandonment facies (Fl, Fr, Fc). These coals are relatively thicker than the ones developed in the western and northern parts of the study area. In this area, the coals are associated with the final stage of delta progradation and low rates of sediment influx. Therefore, thicker coals in the eastern part

of the Sub-basin might have developed within an area where the rates of creation of accommodation was high relative to the sediment input and where the water table was at its highest level relative to the topography in a low energy depositional environment (Catuneanu, 2006). The succession above the coal horizon in boreholes CKP8C and CKP8C-1 reveal high rates of avulsion by the multiple stacking of upward-fining successions (Smith et al., 1989). Coal horizons in the eastern side of the study area have been disturbed by intrusions of dolerite sills, therefore the coals have high ash content and they have been degraded by the heat from the dolerite intrusions and are known to be uneconomic (Meixner and Peart, 1984).

5.2.3 Beaufort Group equivalent

5.2.3.1 Facies association 6

The progradation of both wave- and fluvial-dominated deltas of the Ecca Group in the northern and eastern parts of the study area was followed by the deposition of a thick homogeneous successions of siltstones with minor sandstone units and rare upward-fining successions (facies association 6) of the Beaufort Group equivalent. Thick successions of homogenous siltstones are typical for floodplain deposition mostly in the lakes (Miall, 1982). The presence of rare upward-fining sequences indicates deposition by fluvial channels (Boggs, 2001). In boreholes W1 and W2 (northern part of study area), the evidence of fluvial channel deposition is indicated by the upward-fining successions (ranging from 0.3 m to 4 m) comprising at the base, sandy siltstones with rip-up carbonaceous mudrock clasts which grades upwards into sandy siltstones (St and Sr) and siltstones. Bioturbation structures within the siltstones of facies association 6 indicate processes which destroy and modify primary sedimentary structures through the activity of organisms, which were living in it (Bromely, 1990). Calcareous nodules dominate the thick siltstone units of the Beaufort Group equivalent and are indicative of semi-arid floodplain environments (Reineck and Singh, 1973; Miall, 1982; Tucker, 1991; Rubidge et al., 2000). The dominance of light grey pink and subordinate pale red colours in the siltstones may also be considered to semi-arid fluvial environments (Reineck and Singh, 1973; Johnson et al., 2006).

An open lacustrine environment has been suggested for Beaufort Group equivalent in the northern and eastern parts of the study area Smith (1984). The Beaufort Group equivalent can therefore be interpreted to represent deposition by shallow lakes or ponds in the floodplain setting (Miall, 1996).

5.2.4 Mosolotsane Formation and Neu Loore Formation

5.2.4.1 Facies association 7

Red mudrocks (Fl, Fsm) are common in both the Mosolotsane and the Neu Loore formations. The laminated and massive mudrocks indicate deposition from suspension on the distal floodplains (Miall, 1977; Johnson et al., 2006). In borehole W1, the Mosolotsane Formation shows characteristics of fluvial channels, as is indicated by a upward-fining succession consisting of conglomerate lithofacies (Gcm) at the base, overlain by sandstone lithofacies (Sm) and mudrock lithofacies (Fl, Fsm) (Collinson, 1986). Clast-supported conglomerate (Gcm) suggests deposition by a debris flow or turbulent flow (Miall, 1977; 1996). Therefore, the upward-fining succession indicates deposition by fluvial channels (Reineck and Singh, 1973; Tucker, 1982).

The presence of calcareous nodules within the Neu Loore Formation (borehole ACP13) supports the evidence of deposition under dry climates (Tucker, 1991). The dominance of red colour within the mudrocks of facies association 7 suggests deposition under oxidising conditions in semi-arid environments (Tucker, 1982; Collinson, 1986; Johnson et al., 2006). Bordy et al. (2010) interpreted the Mosolotsane Formation in the eastern Botswana to have been deposited in a relatively low-sinuosity meandering river system that drained from southeast and east-southeast to northwest and west-northwest in a possibly semi-arid environment. The palaeo-environmental interpretation of the Mosolotsane in the eastern part of Botswana by Bordy et al. (2010) corresponds with that one of the Neu Loore Formation and the Mosolotsane Formation in the Gemsbok Sub-basin (this study).

5.2.5 Ntane Sandstone Formation

5.2.5.1 Facies association 8

The Ntane Sandstone Formation predominantly comprises clean, well sorted, fine-grained sandstone units with no mica minerals. This Formation was observed in the northern and eastern part of the study area (boreholes W1, W3, CKP8C and CKP8C-1). Sandstones of the Ntane Sandstone Formation show a high degree of sorting and lack of micas and clay minerals, which are the characteristics of sediment deposits in an aeolian environment (Smith, 1984; Reading, 1986; Nichols, 2009).

5.3 Geographic distribution of facies associations

As stated on previous chapters, the Gemsbok Sub-basin is poorly exposed due to much cover by Cenozoic Kalahari Group; therefore the basin development model is likely to be more complex than can be discerned in the available borehole core. Nonetheless, an attempt was made to reconstruct the development of the basin based on available evidence. Thirteen boreholes were used to construct stratigraphic cross-sections and block diagrams (Fig. 5.3, 5.5, 5.7, 5.9, 5.10), which demonstrate thickness variations and geographic distribution of the eight facies associations of the Karoo Supergroup in the Gemsbok Sub-basin of Botswana and Namibia. The Karoo Supergroup rocks in the Gemsbok Sub-basin have been intruded by thick dolerite sills at varying stratigraphic horizons, which complicates thickness comparisons.

The Dwyka Group glacial deposits form the basal unit of the Karoo Supergroup (Fig. 5.3, 5.5, 5.7) and thicken towards the centre of the Sub-basin (Fig. 5.3, 5.5). These are conformably overlain by the Ecca Group turbidites (facies association 2) and delta deposits (facies association 3, 4 and 5). The turbidite deposits make up the Nossob Formation and the Ncojane Sandstone Member and forms the base of the Ecca Group. These deposits thin towards the east of the Sub-basin and the source might have been located to the north and northwest. The delta deposits of the Ecca Group (facies association 3, 4 and 5) occur throughout the Gemsbok Sub-basin and thicken towards the centre of the basin. Two cycles of delta progradation are present in the northern and the central parts of the Gemsbok Sub-basin but are not present in the western and eastern

parts of the study area. This might suggest that the northern and central parts of the study area were subjected to base level changes either due to variable (tectonic) subsidence rates or lake/sea level changes during the Ecca Group times (Catuneanu et al., 2006).

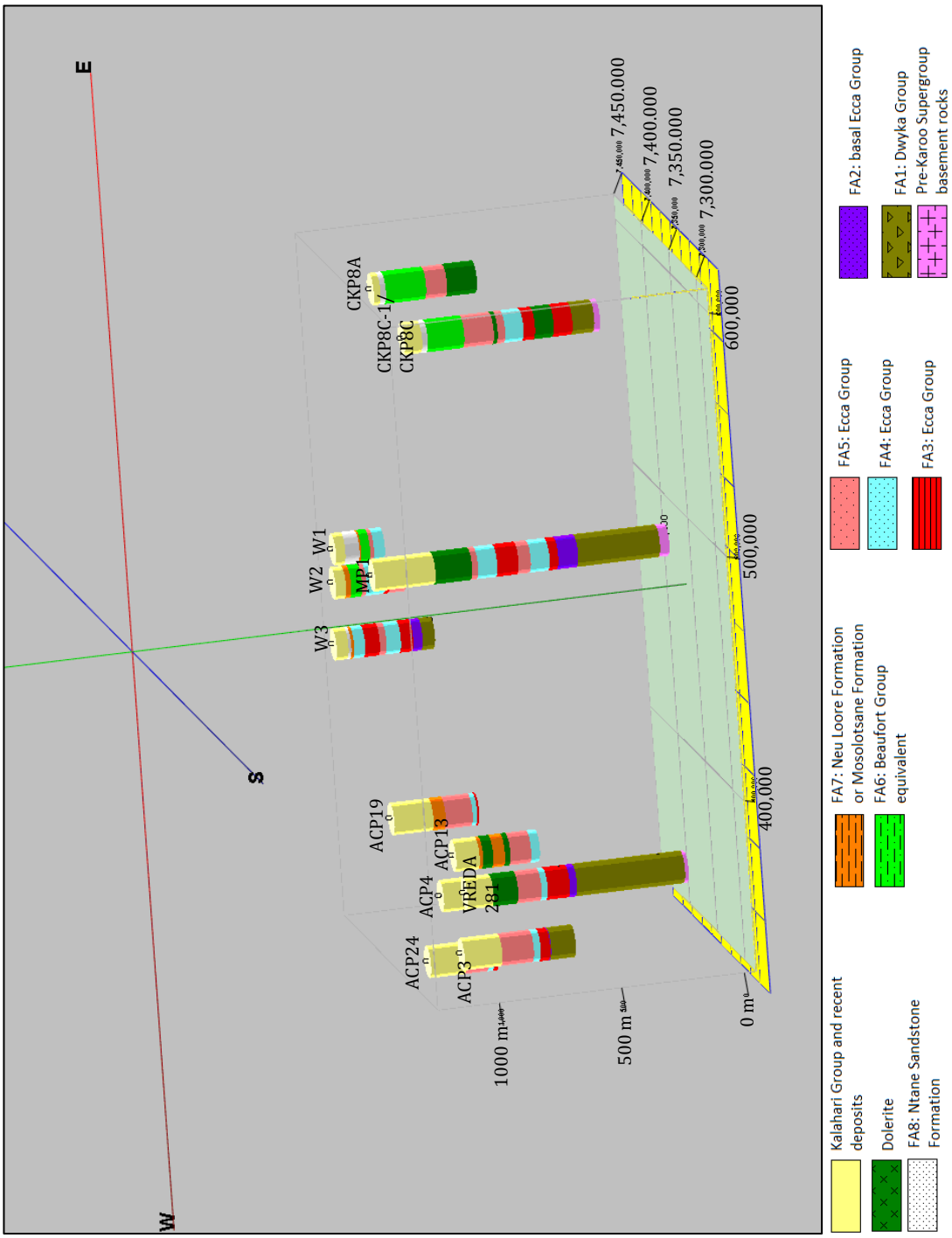


Figure 5.9 3D diagram of the Karoo Supergroup boreholes in the Gemsbok Sub-basin showing different facies associations.

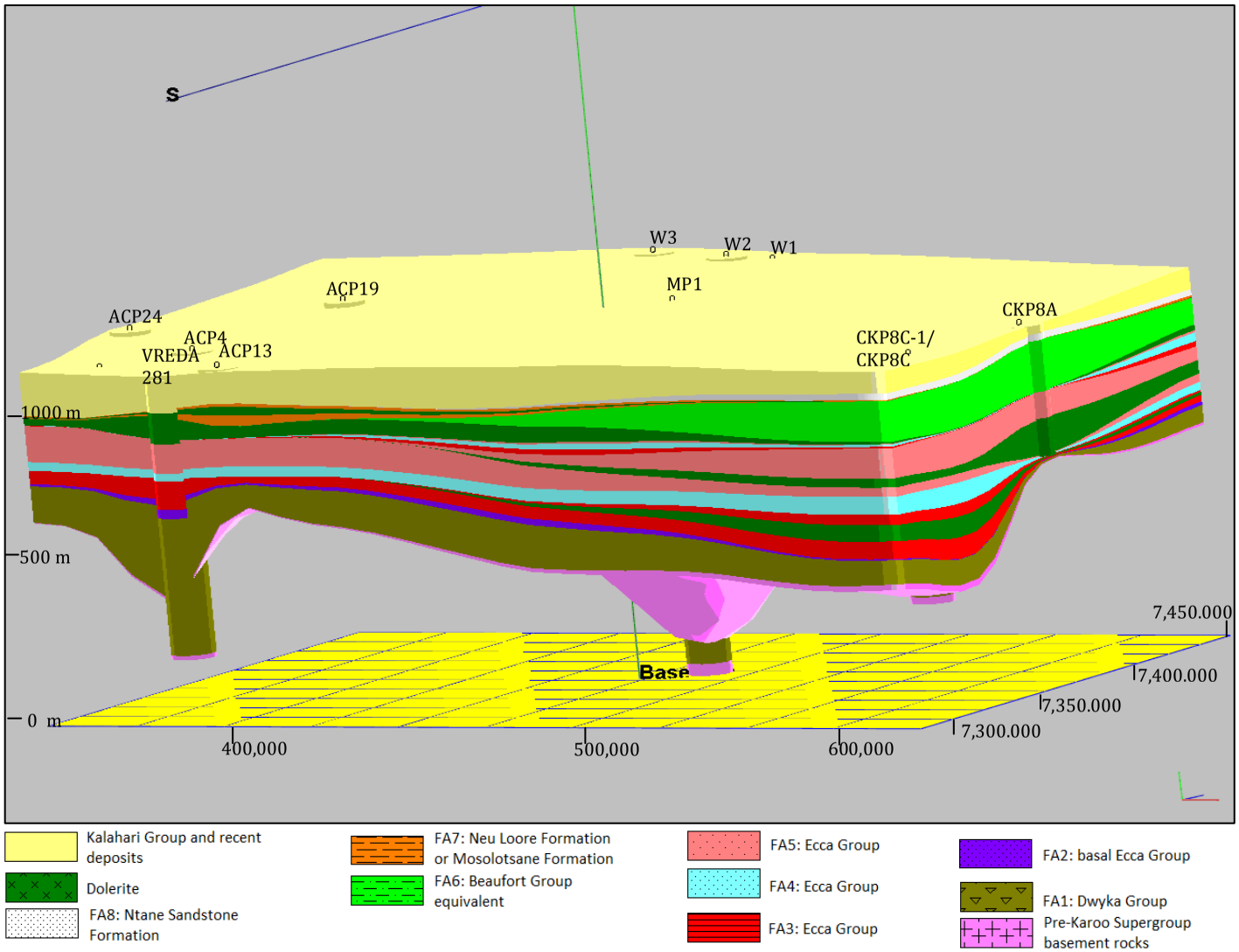


Figure 5.10 3D stratigraphic model of the Karoo Supergroup facies associations in the Gemsbok Sub-basin.

The Beaufort Group equivalent floodplain deposits (i.e., channels and shallow lakes) are present in the eastern and northern parts of the Gemsbok Sub-basin and thicken towards the east (Fig. 5.3, 5.5, 5.10). The Neu Loore Formation floodplain deposits (probably deposited in semi-arid environments) occur in northern and some parts of the western Gemsbok Sub-basin. The Ntane Sandstone Formation (aeolian deposits) is present only in the northern and eastern parts of the study area (Fig. 5.3, 5.5, 5.7) and does not show any significant thickness variations.

5.4 Geological history of the Gemsbok Sub-basin

Petrographic and geochemical studies of sandstones of the Karoo Supergroup, their provenances and relationships to the tectonic settings in the Gemsbok Sub-basin have not been investigated previously. Accordingly, petrography and geochemistry of the sandstones of the Ecca Group and the Ntane Sandstone Formation were studied in order to better understand the geological history of the Gemsbok Sub-basin in Botswana and Namibia.

5.4.1 Sandstone petrography and geochemistry

The sandstones studied from the Ecca Group in the study area consist of compositionally immature arkoses, subarkoses with lesser amounts of litharkose and sublitharenites (Fig. 4.23, 4.25). The Ntane Sandstone Formation consists of compositionally immature subarkoses (Fig. 4.25). Angular to subangular feldspars dominate the sandstones of the Ecca Group and the Ntane Sandstone Formation and imply richly feldspathic source areas dominated of granites and gneisses (Pettijohn et al., 1987). The petrographical classification of sandstones of the Ecca Group (i.e., facies association 4 and 5) in the northern and eastern parts of the study area agrees with the geochemical data (Fig. 4.27). According to the Herron (1988) diagram, the sandstone sample B1 of the Ntane Sandstone Formation is classified as subarkose, which is in agreement with the petrographical data.

The presence of arkoses and subarkoses suggest basement uplifted source areas with high relief, where there is rapid transportation, deposition and rapid burial before extensive weathering can occur (Dickinson and Suczek, 1979; Blatt et al., 1980; Dickinson et al., 1983; Boggs, 2001). The angular to subangular nature of detrital grains in the sandstones of the Ecca Group (i.e., facies association 4, 5) and the Ntane Formation (i.e., facies association 8) suggest source areas nearby (Folk, 1980; Pettijohn et al., 1987).

5.4.2 Provenance of the sandstones from the Ecca Group and the Ntane Sandstone Formation

The combination of sandstone petrography and geochemistry studies has been used to identify provenance and ancient tectonic environment characteristics of the sedimentary basins, although relief, climate, transport mechanism, depositional environment and diagenetic change may all be important secondary factors affecting the original composition of the sediment (Bhatia, 1983; Dickinson, 1985; Bhatia and Crook, 1986).

5.4.2.1 Evidence from petrography

The presence of subrounded or rounded quartz, pyrite, rutile, tourmaline, apatite, zircon grains and argillaceous rock fragments within the sandstones of the Ecca Group (facies association 4 and 5) and the Ntane Sandstone Formation (facies association 8) suggest a sedimentary source (Pettijohn et al., 1987; Boggs, 2001). Polycrystalline quartz grains with more than five sutured quartz crystals within the Ecca Group and Ntane Sandstone Formation sandstones suggest that the sedimentary rocks were derived from metamorphic rocks such as gneisses (Blatt et al., 1980; Boggs, 2001). Polycrystalline quartz grains with three and than five non-sutured crystals within the Ecca Group sandstones suggest a plutonic igneous source (Blatt et al., 1980). High proportions of Qm than Qp and low percentages of lithic fragments and feldspars within the Ecca Group and the Ntane Sandstone Formation sandstones indicate acidic plutonic rocks or recycled sedimentary rocks as the source (Dickinson, 1988). K-feldspar grains are more abundant than plagioclase grains in most of the studied sandstones and high feldspar proportion might suggest uplifted continental basement or eroded arc plutons as source areas (Dickinson, 1988). The high mica content in facies associations 4 and 5 sandstones of the Ecca Group might have been derived from metamorphic provenances located nearby and dominated

by schists and gneisses (Pettijohn et al., 1987). The quartz-feldspar rock fragments might suggest derivation from plutonic igneous or metamorphic terrains (Blatt et al., 1980). Heavy mineral garnet (angular in shape) was found in all sandstone samples in the study area and might have been derived from metamorphic source rocks (Folk, 1980; Deer et al., 1992; Boggs, 2001). All studied sandstones contain a few sedimentary and metamorphic rock fragments; this suggests that their source area is of sedimentary and metamorphic origin. The heavy mineral assemblage comprising rutile (euhedral), tourmaline (euhedral and subangular), zircon (euhedral, showing zonation) and apatite (angular) suggests alkaline igneous source rocks (Pettijohn et al., 1987; Boggs, 2001).

Dickinson and Suczek (1979) classified all provenances and sandstone detritus suites into 1) continental block, which includes stable cratons and basement uplifts; 2) magmatic arc, which includes dissected and undissected arcs; and 3) recycled orogen. Continental block provenances are located within continental masses, which may be bounded on one side by a passive margin and on the other by an orogenic belt. The source rocks from the continental block provenances consist of plutonic igneous, metamorphic and sedimentary rocks but include limited volcanic rocks (Boggs, 2001). Dickinson and Suczek (1979) defined the transitional continental provenance as the provenance that lies between the craton interior and uplifted basement suites. This means that transitional continental sandstones have characteristics of both craton interior and basement uplift source areas. Craton interior sandstones are well known of their high quartz content (mature detritus), whereas the basement uplift sandstones are of arkosic nature (Dickinson and Suczek, 1979; Dickinson et al., 1983). Magmatic arc provenances are situated where plates converge and where sediment is eroded mainly from volcanic debris sources (Boggs, 2001). Recycled orogen provenances forms where there is a collision of major plates, which creates an uplifted source area next to the collision suture belt and the source rocks tend to be sedimentary and metamorphic rocks (Boggs, 2001). Sources from recycled orogens include sedimentary strata (metasedimentary or sedimentary rocks) and subordinate volcanic rocks, partly metamorphosed and exposed to erosion by orogenic uplifted fold belts (Dickinson et al., 1983).

The petrographic study of sandstones of the Ecca Group (facies association 4 and 5) in

the western, northern and eastern parts of the study area revealed the main source areas representing a transitional continental setting, with minor contributions from a craton interior and recycled orogen, as well as mixed and basement uplift suites (Fig. 4.24, 4.26). Most of these sandstones are arkosic and subarkosic in composition (Fig. 4.23, 4.26) and are likely to have been derived from the uplifted granite-gneiss or gneiss and schist basement and uplifted metasedimentary basement (Dickinson et al., 1983).
The sandstone sample from the Ntane Sandstone Formation (sample B1 of facies association 8) falls within the craton interior provenance (Fig. 4.26) and it is classified as a subarkose (Fig. 4.25), which might indicate that it has been derived from uplifted basement rocks (granite-gneiss or metasedimentary rocks) (Dickinson et al., 1983).

5.4.2.2 Evidence from geochemistry

The high concentration of Al_2O_3, K_2O and Ba and high K_2O/Na_2O ratio within the sandstones of the Ecca Group in the northern and eastern parts of the study area indicate a high proportion of feldspars (Pettijohn et al., 1987; Rollinson, 1993). The zirconium (Zr) concentrations of more than 100 ppm within the sandstones of the Ecca Group and the Ntane Sandstone Formation indicate the presence of the mineral zircon and also suggest a granitic or recycled detritus source (Bhatia and Crook, 1986).

The source rock composition diagram of Floyd et al. (1989) suggests an acidic magmatic nature source rock for most of the sandstone samples from the Ecca Group (facies associations 4 and 5) and the Ntane Sandstone Formation (facies association 8) in the northern and eastern Gemsbok Sub-basin (Fig. 4.28). One sandstone sample from the Ecca Group (facies association 4) in the northern part of the study area indicated source areas from mature sedimentary rocks (Fig. 4.28).

The provenance discrimination diagrams of Roser and Korsch (1988) of the northern and eastern Gemsbok Sub-basin sandstones suggest a quartzose sedimentary provenance for most of the Ecca Group (facies associations 4 and 5) sandstones as well as felsic igneous provenance (Fig. 4.29). The quartzose sedimentary provenance has source rocks which include granitic-gneissic or pre-existing sedimentary terranes (Roser and Korsch, 1988). Sediment deposited at passive continental margins, intracratonic sedimentary basins, and

recycled orogenic provenances will commonly exhibit P4 (quartzose sedimentary provenance) signatures (Roser and Korsch, 1988). A felsic igneous provenance is associated with sediments derived from mature continental margin arcs (plutonic-volcanic rocks) and continental transform boundaries (Roser and Korsch, 1988).

Selected trace elements, such as La, Ce, Nd, Y, Th, Zr, Hf, Nb, Sc, Co and Ti are useful in discriminating provenance and tectonic setting of sedimentary basins because of their relative immobility during sedimentary processes (Bhatia and Crook, 1986; Rollinson, 1993). These elements are present in very low concentrations in sea and river water, are chiefly transported as particulate matter, and reflect the signature of the parent material (Bhatia, 1983; Bhatia and Crook, 1986; Rollinson, 1993).

Triangular Th-Sc-Zr/10 plots by Bhatia and Crook (1986) suggest continental island arc source with a minor contribution from a passive continental margin source for the sandstones of the Ecca Group in the northern and eastern parts of the study area (Fig. 4.30). Sedimentary basins plotting in the continental island arc tectonic setting in the Th-Sc-Zr/10 diagram are developed adjacent to island arcs formed on well-developed continental crust or on thin continental margins (Bhatia, 1983). Sediments in this tectonic setting are deposited in inter-arc, back-arc and fore-arc basins and the provenance type is dissected magmatic arc or recycled orogen consisting of felsic volcanic rocks (Bhatia, 1983; Bhatia and Crook, 1986). A passive margin tectonic setting is characterised by highly mineralogically mature sandstones, which are derived by the recycling of older sedimentary and metamorphic rocks (Bhatia, 1983; Roser and Korsch, 1986). Passive margin sandstones are also recognised by their K_2O/Na_2O ratio being greater than 1 (Bhatia, 1983; Roser and Korsch, 1986). The sandstones analysed from the Ecca Group and the Ntane Sandstone Formation have a K_2O/Na_2O ratio of more than 1 and are mineralogically immature sandstones. This suggests that most of the Ecca Group and the Ntane Formation sandstones were not derived from the passive margin source areas, but rather derived from basement uplifted source areas.

5.4.3 Probable source rocks for the Karoo Supergroup and tectonic setting of the Gemsbok Sub-basin

The petrography and geochemistry of the Ecca Group (facies associations 4 and 5) sandstones in the western, northern and eastern parts of the study area suggest nearby source areas dominantly composed of plutonic (granites) and metamorphic (gneisses and schists) rocks with a component from a sedimentary (quartzites, shales, arkoses and metarkoses) rocks. These source areas might have been from adjacent areas and include the Damara Belt (metamorphic, plutonic and sedimentary rocks), the Ghanzi-Chobe Belt, the Nama Group and metamorphic basement rocks in the north and northwest as well as the basement uplifted rocks (consisting of the granitic-gneisses and schists of the Kaapvaal Craton and the metasedimentary rocks of the Transvaal Supergroup, Olifantshoek Supergroup and Waterberg Group) located in the southeastern margins of the Gemsbok Sub-basin. This interpretation is in agreement with the measured and postulated palaeocurrent data from previous studies (Smith, 1984; Grill, 1997).

Petrographic and geochemical results of the facies association 8 sandstone of the Ntane Sandstone Formation suggest uplifted basement source areas dominated by sedimentary rocks and/or granite-gneiss rocks. The source rocks for the Ntane Sandstone Formation might have been the recycled pre-Ntane Karoo Supergroup rocks located in the Gemsbok Sub-basin or the pre-Damaran basement rocks (granites and gneisses) located further to the north of the Sub-basin.

CHAPTER SIX: CONCLUSIONS

Since the establishment of a basic correlative framework of the Karoo Supergroup rocks in the Kalahari Karoo Basin (Green, 1966; Smith, 1984), theories of basin development in the Main Karoo Basin in South Africa (the reference basin of all Karoo-aged basins in southern Africa) have been reviewed. In addition, new geological data on the Karoo Supergroup in the Kalahari Karoo Basin has became available from different sources (e.g., hydrocarbon exploration and seismic profiling) but the correlations have not been updated.

The main aim of this project has been to analyse sedimentary rocks, correlate stratigraphy and infer depositional environments of the Karoo Supergroup across the Kalahari Karoo Basin, with a major focus on the poorly understood Gemsbok Sub-basin of Botswana and Namibia. In the region the Karoo Supergroup is overlain and largely covered by the Cenozoic Kalahari Group with the result that this research has been limited to borehole data.

This study, using eleven borehole cores and two reference borehole logs, has shown that it is possible to correlate sedimentary facies associations of the Karoo Supergroup across the Gemsbok Sub-basin by applying detailed facies analysis. Eight facies associations (FAs) comprising fourteen lithofacies and two trace fossil assemblages (*Cruziana* and *Skolithos* ichnofacies) were identified for the first time and correlated across the Gemsbok Sub-basin. The eight facies associations (FA1 to FA8) correspond to the lithostratigraphic subdivisions (the Dwyka Group, Ecca Group, Beaufort Group equivalent, Lebung Group [Mosolotsane and Ntane formations] and Neu Loore Formation) of the Karoo Supergroup. Sedimentological and ichnological characteristics of the identified facies associations indicate the following depositional environments: glaciomarine or glaciolacustrine (FA1, Dwyka Group), deep-water (lake or sea) (FA2, Ecca Group), prodelta (FA3, Ecca Group), delta front (FA4, Ecca Group), delta plain (FA5, Ecca Group), floodplain with shallow lakes (FA6, Beaufort Group equivalent),

fluvial (FA7, Mosolotsane and Neu Loore formations) and aeolian (FA8, Ntane Formation).

The Dwyka Group (FA1) forms the base of the Karoo Supergroup in the Gemsbok Sub-basin and is overlain by the Ecca Group comprising FAs 2, 3, 4 and 5. FA2 forms the base of the Ecca Group and is dominated by sandstone units which display Bouma cycles. This unit which thickens to the north and pinches out to the east is considered to have been the result of subaqueous turbidite deposition. FA3 and FA4 show an overall upward-coarsening trend, suggesting deposition in prograding delta environment.

Delta deposits have been previously classified in the western part of the Gemsbok Sub-basin (Kingsley, 1985; Grill, 1997) but no work has been done in the northern and eastern parts. This current study has revealed the presence of three delta types (fluvial-wave interaction, wave- and fluvial-dominated deltas) across the Gemsbok Sub-basin. The western part is characterised by fluvial-dominated and fluvial-wave interaction deltas, whereas the northern part is characterised by wave-dominated deltas. Deltas in the eastern part of the Gemsbok Sub-basin were fluvially dominated.

An unconformity above the Beaufort Group equivalent is present in the north and east. In the western part of the Sub-basin this unconformity occurs above the Ecca Group. The Mosolotsane Formation (in the northern Gemsbok Sub-basin) and Neu Loore Formation (in the western Gemsbok Sub-basin) are characterised by similar lithologies (FA7) pointing to deposition in a subaerially exposed fluvial environments. The Ntane Sandstone Formation (FA8) is the uppermost stratigraphic unit of the Karoo Supergroup and conformably overlies the Mosolotsane Formation in the northern and eastern parts of the Gemsbok Sub-basin.

Petrography and geochemical studies on sandstones of the Ecca Group suggest that the source areas were dominated by metamorphic and felsic igneous or acidic magmatic rocks with lesser influence from sedimentary source rocks located adjacent to the Gemsbok Sub-basin in the north, northwest and southeast. Similar studies on the Ntane Sandstone Formation revealed sources areas dominated by sedimentary and granite-

gneiss rocks, which are located in the Gemsbok Sub-basin and far north of the Gemsbok Sub-basin, respectively.

This study has provided a lithostratigraphic and palaeoenvironmental framework for the Karoo-aged basins in the southwest Botswana and southeast Namibia and will therefore form a sound platform for future basin history models of the Karoo Supergroup in the Kalahari Karoo Basin.

CHAPTER SEVEN: REFERENCES

7.1 List of References

Advanced Resources International (ARI), Inc. Arlington, VA USA, 2003. Results of the Central Kalahari Karoo Basin Coalbed Methane Feasibility Study. Executive Summary Report, Volume I, Geological Survey of Botswana, Report GC 154/1/1.

Armstrong-Altrin, J.S., Lee, Y.I., Verma, S.P., Ramasamy, S. 2004. Geochemistry of sandstones from the Upper Miocene Kudankulam Formation, southern India: implication for provenance, weathering and tectonic setting. Journal of Sedimentary Research, 74(2), 285–297.

Armstrong-Altrin, J.S., Verma, S.P. 2005. Critical evaluation of six tectonic setting discrimination diagrams using geochemical data of Neogene sediments from known tectonic settings. Sedimentary Geology, 177, 115–129.

Bangert, B., Stollhofen, H., Geiger, M., Lorenz, V. 2000. Fossil record and high-resolution tephrostratigraphy of Carboniferous glaciomarine mudstones, Dwyka Group, southern Namibia. Communications of the Geological Survey of Namibia 12, 235–245.

Bangert, B., Stollhofen, H., Lorenz, V., Armstrong, R. 1999. The geochronology and significance of ash-fall tuffs in the glaciogenic Carboniferous-Permian Dwyka Group of Namibia and South Africa. Journal of African Earth Sciences, 29, 33–49.

Bhatia, M.R. 1983. Plate tectonics and geochemical composition of sandstones. Journal of Geology, 91, 611–627.

Bhatia, M.R., Crook, K.A.W. 1986. Trace element characteristics of greywackes and tectonic setting discrimination of sedimentary basins. Contributions to Mineralogy and Petrology, 92, 181–193.

Bhattacharya, B., Bhattacharya, H.N., 2007. Implications of trace fossil assemblages from Late Paleozoic Glaciomarine Talchir Formation, Raniganj Basin, India. Gondwana Research, 12, 509–524.

Bhattacharya, J.P., Walker, R.G. 1992. Deltas. In: R.G. Walker, N.P. James (Editors). Facies Models: Response to Sea Level Change. Geological Association of Canada, 157–177.

Blatt, H., Middleton, G., Murray, R. 1980. Origin of sedimentary rocks, (2nd edition). Prentice Hall, New Jersey. 782pp.

Boggs, S. (Jr). 1987. Principles of sedimentology and stratigraphy. Merrill, Columbus, Ohio, 784pp.

Boggs, S. (Jr.). 2001. Principles of sedimentology and stratigraphy, (3rd edition). Prentice Hall, Upper Saddle River, New Jersey, 726pp.

Boggs, S. (Jr.). 2006. Principles of sedimentology and stratigraphy, (4th edition). Prentice Hall, Upper Saddle River, New Jersey, 662pp.

Bordy, E.M., Catuneanu, O. 2002. Sedimentology of the Beaufort-Molteno Karoo fluvial strata in the Tuli Basin, South Africa. South African Journal of Geology, 105, 51–66.

Bordy, E.M., Hancox, P.J., Rubidge, B.S. 2005. The contact of the Molteno and Elliot formations through the main Karoo Basin, South Africa: a second-order sequence boundary. South African Journal of Geology, 108, 351-364.

Bordy, E.M., Segwabe, T., Makuke, B. 2010. Sedimentology of the Upper Triassic - Lower Jurassic (?) Mosolotsane Formation (Karoo Supergroup), Kalahari Karoo Basin, Botswana. Journal of African Earth Sciences, doi:10.1016/j.jafrearsci.2010.02.006

Bouma, A. H. 1962. Sedimentology of some flysch deposits, a graphic approach to facies interpretation. Elsevier, Amsterdam, 168pp.

Bromley, R.G. 1990. Trace fossils: biology and taphonomy. Unwin Hyman Ltd, London, 280 pp.

Bumby, A.J., Guiraud, R. 2005.The geodynamic setting of the Phanerozoic basins of Africa. Journal of African Earth Sciences, 43, 1–12.

Cadle, A.B., Cairncross, B., Christie, A.D.M., Roberts, D.L. 1993. The Karoo Basin of South Africa: type basin for the coal-bearing deposits of southern Africa. International Journal of Coal Geology, 23, 117-157.

Cairncross, B. 1995. A geological overview of the coal-bearing strata in South Africa and the potential for coalbed methane. Abstract: Coal Bed Methane Exploration Trends and Potential for South Africa. Joint Sponsors – Geological Society of South Africa and Brown and Root, Rosebank, Johannesburg.

Cairncross, B. 2001. An overview of Permian (Karoo) coal deposits of southern Africa. Journal of African Earth Sciences, 33, 529-562.

Carney, J. N., Aldis, D. T., Lock, N. P. 1994. The Geology of Botswana. Bulletin 37, Geological Survey Department, Botswana, 37, 113pp.

Catuneanu, O. 2002. Sequence stratigraphy of clastic systems: concepts, merits, and pitfalls. Journal of African Earth Sciences, 35, 1–43.

Catuneanu, O. 2006. Principles of sequence stratigraphy. Elsevier, Amsterdam. 375pp.

Catuneanu, O., Elango, H.N. 2001. Tectonic control on fluvial styles: the Balfour Formation of the Karoo Basin, South Africa. Sedimentary Geology, 140, 291-313.

Catuneanu, O., Wopfner, H., Eriksson, P. G., Cairncross, B., Rubidge, B. S., Smith, R. M. H., Hancox, P. J. 2005. The Karoo basins of south-central Africa. Journal of African Earth Sciences, 43, 211-253.

Chamberlain, C.K. 1978. Recognition of trace fossils in cores. In: P.B. Basan (Editor). Trace Fossil Concepts. Society of Economic Paleontologists and Mineralogists, Short Course Notes 5, 133–183.

Clark, G. C., Lock, N. P., Smith, R. A. 1986. Coal resources of Botswana. In: C. R. Anhaeusser, S. Maske (Editors.). Mineral Deposits of Southern Africa. Geological Society of South Africa, Johannesburg, pp. 2071 – 2085.

Cloete, H.C.C., Truter, J. 2001. Major and Trace Element Analysis by X-ray Fluorescence Spectrometry at the Council for Geoscience. Council for Geoscience, Open file report 2001-0074.

Coleman, J.M., Prior, D.B. 1980. Deltaic Sand Bodies: A 1980 Short Course. Education Course Note Series # 15. American Association of Petroleum Geologist, Coastal Studies Institute, Louisiana State University, 171pp.

Collinson, J.D. 1986. Alluvial sediments. In: H.G. Reading (Editor). Sedimentary environments and facies, (2nd edition). Blackwell Scientific Publications, Oxford, pp. 20-62.

Deer, W. A., Howie, R. A., Zussman, J. 1992. An Introduction to the Rock-Forming Minerals, (2nd edition). Longman Scientific and Technical, Wiley in Harlow, Essex, England, New York, NY, 696pp

Dickinson, W.R. 1985. Interpreting provenance relation from detrital modes of sandstones. In: G.G. Zuffa (Editor). Provenance of Arenites. D. Reidel Publishing Company, Dordrecht, pp. 333–361.

Dickinson, W.R. 1988. Provenance and sediment dispersal in relation to paleotectonics and paleogeography of sedimentary basins. In: K.L. Kleinspehn, C. Paola (Editors). New Perspectives in Basin Analysis. Springer-Verlag, New York, pp. 3–25.

Dickinson, W.R., Beard, L.S., Brakenridge, G.R., Erjavec, J.L., Ferguson, R.C., Inman, K.F., Knepp, R.A., Lindberg, F.A., Ryberg, P.T. 1983. Provenance of North American Phanerozoic sandstones in relation to tectonic setting. Geological Society of America Bulletin, 94, 222-235.

Dickinson, W.R., Suczek, C.A. 1979. Plate tectonics and sandstone compositions. American Association of Petroleum Geologist, 63, 2164–2182.

Dolby, G. 1990. The biostratigraphy of the G.S.D./P.C.I.A.C Masetlheng Pan-1 well, Botswana. Department of Geological Survey, Botswana, 23pp.

Ekdale, A.A., Bromely, R.G., Pemberton, S.G. 1984. Ichnology: the use of trace fossils in sedimentology and stratigraphy. Society of Economic Paleontologists and Mineralogists, SEPM Short Course Notes no. 15, 317pp.

Exploration Consultants Limited, 1998. Petroleum Potential of the Karoo of Botswana. Report - Volume 1. Department of Geological Survey, Botswana, GC 122/2/1a.

Eyles, C.H., Eyles, N. 2000. Subaqueous mass flow origin for Lower Permian diamictites and associated facies of the Grant Group, Barbwire Terrace, Canning Basin, Western Australia. Sedimentology, 47, 343–356.

Eyles, C.H., Eyles, N., Grey, K. 2007. Palaeoclimate implications from deep drilling of Neoproterozoic strata in the Officer Basin and Adelaide Rift Complex of Australia; a marine record of wet-based glaciers. Palaeogeography, Palaeoclimatology, Palaeoecology, 248, 291–312.

Figueiredo, J.J.P., Hodgson, D.M., Flint, S.S., Kavanagh, J.P. 2010. Depositional environments and sequence stratigraphy of an Exhumed Permian Mud-dominated Submarine Slope Succession, Karoo Basin, South Africa. Journal of Sedimentary Research, 80, 97–118.

Floyd, P. A., Winchester, J. A., Park, R. G. 1989. Geochemistry and tectonic setting of Lewisian clastic metasediments from the early Proterozoic Loch Maree Group of Gairloch, N. W. Scotland. Precambrian Research, 45, 203-214.

Folk, R.L. 1980. Petrology of Sedimentary Rocks. Hemphill, Austin, Texas, 159pp.

Frey, R.W. 1975. The study of trace fossils: a synthesis of principles, problems, and procedures in ichnology. Springer-Verlag, New York, 562pp.

Galloway, W.E., Hobday, D.K. 1996. Terregeneous clastic depositional systems: Application to fossil fuel and groundwater resources, (2nd revised edition). Springer-Verlag, Berlin Heidelberg, 489pp.

Green, D. 1966. The Karoo System in Bechuanaland. Bulletin. Geological Survey of Bechuanaland, 2, 74pp.

Gregory, M.R., Campbell, K.A. 2003. A '*Phoebichnus* look-alike': a fossilised root system from Quaternary coastal dune sediments, New Zealand. Palaeogeography, Palaeoclimatology, Palaeoecology, 192, 247–258.

Grill, H. 1997. The Permo-Carboniferous glacial to marine Karoo record in southern Namibia: sedimentary facies and sequence stratigraphy. Beringeria 19, 1–98.

Haddon I.G. 2005. The Sub-Kalahari geology and tectonic evolution of the Kalahari Basin, Southern Africa. Unpublished Ph.D thesis, University of the Witwatersrand, Johannesburg, South Africa, 343pp.

Haddon, I.G., McCarthy, T.S. 2005. The Mesozoic–Cenozoic interior sag basins of Central Africa: The Late-Cretaceous–Cenozoic Kalahari and Okavango basins. Journal of African Earth Sciences, 43, 316–333.

Hammerbeck, E.C.I., Allcock, R.J. 1985. Geological map of Southern Africa (1: 4 000 000 scale). Geological Society of South Africa.

Hancox, P.J. 2000. The Continental Triassic of South Africa. Zentralblatt für Geologie und Paläontologie, Teil I, 1998, 1285-1324.

Hancox, P.J., Rubidge, B.S. 2001. Breakthroughs in the biodiversity, biogeography, biostratigraphy and basin analysis of the Beaufort group. Journal of African Earth Sciences, 33, 563-577.

Haverslew, B. 1987. Petrography of diamond drill core samples from boreholes W3, W2, CKP8C-1, CKP6 and CKP6A from west-central and southwest Botswana. Petro-Canada International Assistance Corporation, Calgary, Alberta, 59pp.

Haverslew, B.1990. Petrographic analysis of core, sidewall core, and cuttings samples from Masetlheng pan 1 Botswana. Petro-Canada International Assistance Corporation, Gc 47/5/1, 74pp.

Heath, D.C. 1972. Die geologie van die Sisteem Karoo in die gebied Mariental-Asab, Suidwes-Afrika, with a summary in English. Memoir 61, Geological Survey of South Africa, 44pp.

Hegenberger, W. 1992. Coal. In: The Mineral Resources of Namibia. Geological Survey of Namibia, Windhoek, 7.21-1 – 7.2-29.

Herron, M.M. 1988. Geochemical classification of terrigenous sands and shales from core or log data: Journal of Sedimentary Petrology, 58, 820–829.

Hodgson, D.M. 2009. Distribution and origin of hybrid beds in sand-rich submarine fans of the Tanqua depocenter, Karoo Basin, South Africa. Marine and Petroleum Geology, 26, 1940–1956.

Hutchins, D.G., Reeves, C.V. 1980. Regional Geophysical Exploration of the Kalahari in Botswana. Tectonophysics, 69, 201-220.

Johnson, M. R., van Vuuren, C. J., Hengenberger, W. F., Key, R., Shoko, U. 1996. Stratigraphy of the Karoo Supergroup in southern Africa: an overview. Journal of African Earth Sciences, 23 (1), 3-15.

Johnson, M. R., van Vuuren, C. J., Visser, J. N. J., Wickens, H. deV., Christe, A. D. M., Roberts, D.L. 1997. The foreland Karoo Basin, South Africa. In: R.C. Selley (Editor). African Basins-Sedimentary Basins of the World. Elsevier, Amsterdam, 269-317.

Johnson, M.R., van Vuuren C.J., Visser, J.N.J., Cole, D.I., Wickens, H. de V., Roberts, D.L., Brandl, D. 2006. Sedimentary Rocks of the Karoo Supergroup. In: M.R. Johnson, C.R. Anhaeusser, R.J. Thomas (Editors). The Geology of South Africa. Geological Society of South Africa, 461-499.

Key, R. M., Tidi, J., Mc George, I., Aitken, G., Cadman, A., Anscombe, J. 1998. The lower Karoo Supergroup geology of the southwestern part of the Gemsbok sub-basin of the Kalahari Basin, Botswana. South African Journal of Geology, 101, 225-236.

Key, R.M., Ayres, N. 2000. The 1998 edition of the National Geological Map of Botswana. Journal of African Earth Sciences, 30 (3), 427-451.

Kim, J.Y., Keighley, D. G., Pickerill, R.K., Hwang, W, Kim, K. S. 2005. Trace fossils from marginal lacustrine deposits of the Cretaceous Jinju Formation, southern coast of Korea. Palaeogeography, Palaeoclimatology, Palaeoecology, 218, (1-2), 105-124.

Kingsley, C. S. 1985. Sedimentological aspects of the Ecca Sequence in the Kalahari basin, South West Africa/Namibia. CDM Mineral Surveys, Open File Report, 13/175/510/85/277. Geological Survey, Windhoek, Namibia, 35pp.

MacEachern, J.A., Pemberton, S.G., Gingras, M.K., Bann, K.L. 2007. The ichnofacies paradigm: a fifty-year retrospective. In W. Miller (Editor). Trace Fossils, Concepts, Problems, Prospects. Elsevier. Amsterdam, pp. 52-77.

Meixner, H. M., Peart, R. J. 1984. The Kalahari Drilling Project. Bulletin 27, Geological Survey Department, Botswana, 27, 224pp.

Meixner, H.M. 1983. Geological framework of western Botswana and adjacent areas (1: 2 000 000 scale), Map. Geological Survey, Botswana.

Miall, A.D. 1977. A review of the braided-river depositional environment. Earth Science. Reviews, 13, 1–62.

Miall, A.D. 1979. Deltas. In R.G. Walker (Editor). Facies models. Geoscience Canada Reprint Series, 1. Geological Association of Canada Publications, Toronto, 211pp.

Miall, A.D. 1982. Analysis of fluvial depositional systems. Education Course Note Series no. 20. American Association of Petroleum Geologists, 75pp.

Miall, A.D. 1983. Glaciomarine sedimentation in the Gowganda Formation (Huronian), northern Ontario. Journal of Sedimentary Petrology, 53 (2), 477-491.

Miall, A.D. 1985. Architectural-element analysis: a new method of facies analysis applied to fluvial deposits. Earth Science Reviews, 22, 261–308.

Miall, A.D. 1996. The geology of fluvial deposits: sedimentary facies, basin analysis, and petroleum geology. Springer Verlag, Berlin, 582pp.

Miall, A.D. 2000. Principles of Sedimentary Basin Analysis, (3rd edition). Springer-Verlag, Berlin-Heidelberg, 616pp.

Miller, R. McG. 2005. Complilation of geological maps of the Stampriet Artisian Basin. Final Report. Ministry of Agriculture, Water and Rural Development, Department of Water Affairs, Republic of Namibia, 20pp.

Miller, R. McG. 2008. The Geology of Namibia. Palaeozoic to Cenozoic (Volume 3). Ministry of Mines and Energy, Geological Survey, Namibia. 16:1 – 28:13.

Modie, B. N. 2000. The Karoo Supergroup of the Kalahari Basin: report on field visit to exposures in the Kalahari Karoo basin of Botswana. Internal Report BNM/5/2000. Department of Geological Survey, Botswana, 57pp.

Modie, B.N. 2007. The Palaeozoic Palynostratigraphy of the Karoo Supergroup and palynofacies insight into palaeoenvironmental interpretations, Kalahari Karoo Basin, Botswana. Unpublished PhD thesis, Universite de Bretagne Occidentale, France, 300pp.

Modie, B.N., Le Hérissé, A. 2009. Late Palaeozoic palynomorph assemblages from the Karoo Supergroup and their potential for biostratigraphic correlation, Kalahari Karoo Basin, Botswana. Bulletin of Geosciences, 84(2), 337–358.

Nara, M. 2006. Reappraisal of *Schaubcylindrichnus*: A probable dwelling/feeding structure of a solitary funnel feeder. Palaeogeography, Palaeoclimatology, Palaeoecology, 240, 439–452.

Ndengu, S. 2004. International shared aquifers in Namibia. In: B. Appelgren (Editor). ISARM-AFRICA: Managing Shared Aquifer Resources in Africa. IHP-VI, Series on Groundwater, NO. 8. United Nations Educational, Scientific and Cultural Organization, Paris, France, pp. 117 – 122.

Neveling, J. 2002. Biostratigraphy and sedimentological investigation of the contact between the Lystrosaurus and Cynognathus Assemblage Zones (Beaufort Group: Karoo Supergroup). Unpublished PhD thesis, University of the Witwatersrand, Johannesburg, South Africa, 232pp.

Nichols, G. 1999. Sedimentology and stratigraphy. Blackwell Science Ltd, London, 355pp.

Nichols, G. 2009. Sedimentology and stratigraphy, (2nd edition). John Wiley and Sons Ltd, UK, 419pp.

Orton, G.J., Reading, H.G., 1993. Variability of deltaic processes in terms of sediment supply, with particular emphasis on grain size. Sedimentology, 40, 475–512.

Pemberton, S. G., MacEachern, J. A., Gingras, M. K. 2007. The antecedents of invertebrate ichnology in North America: The Canadian and Cincinnati schools. In: W. Miller (Editor). Trace Fossils, Concepts, Problems, Prospects. Elsevier, Amsterdam, pp. 14-31.

Pemberton, S.G., MacEachern, J.A., Frey, R.W. 1992. Trace fossil facies models: Environmental and Allostratigraphic significance. In: R.G. Walker and N.P. James (Editors). Facies Models: Response to Sea Level Change. Geological Association of Canada, pp. 47–71.

Pemberton, S.G., van Wagoner, J.C., Wach, G.D. 1992a. Ichnofacies of a wave-dominated shoreline. In: S.G. Pemberton (Editor). Application of ichnology to petroleum exploration. Society of Economic Palaeontologists and Mineralogist Core Workshop, 17, 339–382.

Pettijohn, F.J., Potter, P.E., Siever, R. 1987. Sand and Sandstones. Springer-Verlag, New York, 553pp.

Pickering, K.T., Hiscott, R.N., Hein, F.J. 1989. Deep marine environments: clastic sedimentation and tectonics. Unwin Hyman Ltd, London, 416pp.

Pinetown, K.L., Ward, C. R., van der Westhuizen, W.A. 2007. Quantitative evaluation of minerals in coal deposits in the Witbank and Highveld Coalfields, and the potential impact on acid mine drainage. International Journal of Coal Geology 70, 166–183.

Ramokate, L.V., Mapeo, R.B.M., Corfu, F., Kampunzu, A.B. 2000. Proterozoic geology and regional correlation of the Ghanzi-Makunda area, western Botswana. Journal of African Earth Sciences, 30 (3), 453-466.

Reading, H.G. 1986. Sedimentary environments and facies, (2nd edition). Blackwell Scientific Publications, Oxford, London, 615pp.

Reading, H.G. 1996. Sedimentary Environments: Processes, Facies and Stratigraphy, (3rd edition). Blackwell Science Ltd, Oxford, London, 688pp.

Reeves, C. V. 1978. Reconnaissance Aeromagnetic survey of Botswana 1975 – 1977. Final Interpretation Report. Geological Survey Department, Botswana, 84 pp.

Reineck, H.-E., Singh, I.B. 1973. Depositional sedimentary environments. Springer - Verlag, Berlin, Heidelberg, 439pp.

Roberts, E.M. 2007. Facies architecture and depositional environments of the Upper Cretaceous Kaiparowits Formation, southern Utah. Sedimentary Geology, 197, 207–233.

Rollinson, H.R. 1993. Using Geochemical Data: Evaluation, Presentation, Interpretation. Longman, UK. 352pp.

Roser, B.P., Korsch, R.J. 1986. Determination of tectonic setting of sandstone– mudstone suites using SiO_2 content and K_2O/Na_2O ratio. Journal of Geology, 94, 635–650.

Roser, B.P., Korsch, R.J. 1988. Provenance signatures of sandstone–mudstone suites determined using discriminant function analysis of major-element data. Chemical Geology, 67, 119–139.

Rotnicka, J., 2005. Ichnofabrics of the Upper Cretaceous fine-grained rocks from the Stołowe Mountains (Sudetes, SW Poland). Geological Quarterly, 49(1), 15–30.

Rubidge, B.S. 1988. A palaeontological and palaeoenvironmental synthesis of the Permian Ecca-Beaufort in the southern Karoo between Prince Albert and Rietbron, Cape Province, South Africa. Unpublished PhD thesis, University of Port Elizabeth, South Africa, 347pp.

Rubidge, B.S. 2005. Reuniting lost continents - fossil reptiles from the ancient Karoo and their wanderlust. South African Journal of Geology, 108, 135–172.

Rubidge, B.S., Hancox, P.J., Catuneanu, O. 2000. Sequence analysis of the Ecca-Beaufort contact in the southern Karoo of South Africa. South African Journal of Geology, 103 (1), 81–96.

Rust, I.C. 1975. Tectonic and sedimentary framework of Gondwana basins in southern Africa. In: K.S.W. Campbell (Editor). Gondwana Geology (3rd Gondwana Symposium). Australian National University Press, Canberra, pp. 537–564.

SACS (South African Commitee for Stratigraphy), 1980. Lithostratigraphy of the Republic of South Africa, South-West Africa/Namibia and the Republics of Bophuthatswana, Transkei and Venda (Kent, L.E. comp.). Handbook of the Geological Survey of South Africa, 8, 690pp.

Savrda, C.E. 2002. Equilibrium responses reflected in a large *Conichnus* (Upper Cretaceous Eutaw Formation, Alabama, USA). Ichnos, 9, 33–40.

Scheffler, K., Buhmann, D., Schwark, L. 2006. Analysis of late Palaeozoic glacial to postglacial sedimentary successions in South Africa by geochemical proxies – Response to climate evolution and sedimentary environment. Palaeogeography, Palaeoclimatology, Palaeoecology, 240, 184–203.

Shepard, F.P. 1964. Criteria in modern sediments useful in recognizing ancient sedimentary environments. In L.M.J.U. Van Straaten (Editor). Developments in Sedimentology (Volume 1). Deltaic and Shallow Marine Environments, Proceedings of the sixth International Sedimentological Congress, the Netherlands and Belgium, Elsevier Publishing Company, Amsterdam, London, New York, pp. 1-25.

Smith, N.D., Cross, T.A., Dufficy, J.P., Clough, S.R. 1989. Anatomy of an avulsion. Sedimentology, 36 (1). 1 – 23.

Smith, R. A. 1984. The lithostratigraphy of the Karoo Supergroup in Botswana. Bulletin 26. Geological Survey Department, Botswana, 26, 239pp.

Smith, R. M. H. 1990. A review of the stratigraphy and sedimentary environments of the Karoo basin of South Africa. Journal of African Earth Sciences, 10, 117-137.

Smith, R. M. H., Eriksson, P. G., Botha, W. J. 1993. A review of stratigraphy and sedimentary environments of the Karoo-aged basins of southern Africa. Journal of African Earth Sciences, 16, 143-169.

Stanistreet, I.G., Smith, G. L., Cadle, A.B. 1980. Trace fossils as sedimentological and palaeoenvironmental indices in Ecca Group (Lower Permian) of Transvaal. Transactions of the Geological Society of South Africa, 83, 333 – 334.

Stoakes F.A., McMaster D.W. 1990. Interpretation of the results of stratigraphic well Masetlheng Pan-1 in the Nosop-Ncojane Basin of southwest Botswana. Final Technical Report Botswana Project. Department of Geological Survey, Botswana, GC47/26/1, 129pp.

Stollhofen, H., Stanistreet, I. G., Bangert, B., Grill, H. 2000. Tuffs, tectonism and glacially related sea-level changes, Carboniferous–Permian, southern Namibia. Palaeogeography, Palaeoclimatology, Palaeoecology 161, 127–150.

Tucker, M.E. 1982. The field description of sedimentary rocks. John Wiley and Sons, Geological Society of London Handbook Series, 112pp.

Tucker, M.E. 1991. Sedimentary petrology: an introduction to the origin of sedimentary rocks, (2nd edition). Geoscience Texts. Blackwell Science Ltd, 260pp.

Turner, B.R. 1999. Tectonostratigraphic development of the upper Karoo foreland basin: orogenic unloading versus thermally-induced Gondwana rifting. Journal of African Earth Sciences, 28, 215-238.

Visser, J.N.J. 1995. Post-glacial Permian stratigraphy and geography of southern and central Africa: boundary conditions for climatic modelling. Palaeogeography, Palaeoclimatology, Palaeoecology, 118, 213-243.

Wild, R., Flint, S.S., Hodgson, D.M. 2009. Stratigraphic evolution of the upper slope and shelf edge in the Karoo Basin, South Africa. Basin Research, 21, 502–527.

Winters, L.J.M. 1990/1991. Trace fossils and sedimentary successions of the Vryheid Formation, Ecca Group, South Africa. Final year honours field study report. Department of Geology, University of Manchester, 71pp.

Wopfner, H. 2002. Tectonic and climatic events controlling deposition in Tanzanian Karoo basins. Journal of African Earth Sciences, 34, 167–177.

Wright, J.A., Hall J. 1990. Deep seismic profiling in the Nosop Basin, Botswana: cratons, mobile belts and sedimentary basins. Tectonophysics, 173, 333–343.

APPENDICES

APPENDIX A

Sandstone descriptions for facies associations 4, 5 and 8

1. Facies association 4 sandstones (western Gemsbok Sub-basin)

Facies association 4 in the western part of the study area consists of sandstones numbered N3 and N8.

Descriptions of facies association 4 sandstones in the western Gemsbok Sub-basin:

Sample N3

Sample N3 was sampled from borehole ACP4 at depths between 328.65 m and 328.76 m (App. Fig. 2). The sample is poorly sorted and medium- rained (0.25 mm – 0.50 mm). This sandstone sample comprises subangular to subrounded detrital framework grains. The dominant framework grains are quartz followed by feldspar, rock fragments and mica. Quartz occurs as both monocrystalline and polycrystalline quartz. Polycrystalline quartz types include ones composed of four, five and more than five non-sutured quartz crystals. Feldspar framework grains include plagioclase, microcline and other potassium-feldspars. Microcline is more dominant than other feldspar grains. Rock fragments consist of quartz-feldspar grains. Mica grains are present and include muscovite, biotite and chlorite. Some mica grains are deformed in places. The sample is poorly cemented by calcite and exhibits a clay matrix. Accessory minerals include zircons, garnets, tourmaline and very few pyrite grains.

Sample N8

Sample N8 was sampled from borehole ACP19 at depths between 324.92 m and 325.00 m (App. Fig. 4). The sample is moderately to well sorted and fine- to coarse-grained (0.125 mm – 1 mm). Fine detrital grains dominate the sandstone. This sample comprises subangular to subrounded detrital framework grains. Framework grains include quartz

(both monocrystalline and polycrystalline quartz), feldspar (plagioclase, microcline and other potassium-feldspars) and quartzo-feldspathic rock fragments grains. Most of the polycrystalline quartz grains are formed by three to four non-sutured crystals and more than five sutured and non-sutured quartz crystals. Mica grains are present in the sample and consist of muscovite with a lesser amount of biotite. Muscovite grains occur deformed in places. Sandstone sample N8 is poorly cemented by calcite and contains a detrital clay matrix. Accessory minerals present include tourmaline, garnet, subrounded zircons and pyrite.

2. Facies association 5 sandstones (western Gemsbok Sub-basin)

Sandstone samples numbered N1, N2, N4, N5, N6, N7, N9, N10, N11, N12 and N13 were all sampled from facies association 5 in the western part of the study area.

Descriptions of facies association 5 sandstones in the western Gemsbok Sub-basin:

Sample N1

Sample N1 was sampled from borehole ACP4 at depths between 234.17 m and 234.24 m (App. Fig. 2). It is a well sorted, fine-grained (0.125 mm - 0.25 mm), micaceous sandstone with subangular to subrounded detrital grains. Framework grains consist of quartz, feldspar, mica and rock fragments. Monocrystalline quartz grains are more abundant than polycrystalline quartz. The observed polycrystalline quartz grain types are composed of two non-sutured and more than five sutured and non-sutured quartz crystals. Feldspar grains include plagioclase, microcline and other potassium-feldspars. Mica grains are present in the sample and comprise biotite and muscovite. Most of the mica grains are aligned parallel to the bedding and some mica grains are deformed. Rock fragments are quartz-feldspar grains. Sandstone ample N1 is poorly cemented by calcite and contains clay matrix. Accessory minerals include zircons (subrounded and euhedral in shape), garnets, tourmalines and pyrite.

Sample N2

Sample N2 was sampled from borehole ACP4 at depths between 245.06 m and 245.14 m (App. Fig. 2). It is a moderately to well sorted, fine-grained (0.125 mm - 0.25 mm) sandstone with subangular to subrounded detrital framework grains. Framework grains include quartz (both monocrystalline and polycrystalline quartz, with monocrystalline grains being the dominant quart type), feldspar (plagioclase, microcline and other potassium-feldspars) and rock fragments. Polycrystalline quartz types are formed by two to five quartz crystals. Microcline is the dominant feldspar in the sample. Rock fragments consist of quartzo-feldspathic grains. The sandstone sample is entirely cemented with calcite. Mica minerals are present and include deformed muscovite grains. Accessory minerals present include zircons (subrounded and rounded grains), garnets, tourmaline (green), rutile and apatite (as inclusions within the quartz grains).

Sample N4

Sample N4 sandstone was sampled from borehole ACP3 at depths between 166.07 m and 166.13 m (App. Fig. 1). The sandstone is poorly sorted, coarse-grained (0.57 mm – 0.70 mm) and composed of subrounded to subangular detrital grains. Framework grains consist of quartz (monocrystalline and polycrystalline quartz with lesser amounts of polycrystalline quartz), feldspar (dominantly microcline with lesser amounts of plagioclase and other potassium-feldspars) and less amounts of rock fragments (quartz-feldspar). The grains of polycrystalline quartz are composed of three non-sutured quartz crystals and more than five (non-sutured and sutured) quartz crystals. Mica (muscovite) is present in minor amounts. Deformed muscovite was observed in the thin section and some of the micas have fibrous texture. Accessory framework grains include heavy mineral zircon, tourmaline, garnet and pyrite. Some of the zircon grains are subrounded and some show zonation.

Sample N5

Sample N5 was sampled from borehole ACP3 at depths between 245.99 m and 246.05 m (App. Fig. 1). It is a well sorted, medium-grained sandstone with a grain size range of 0.25 mm – 0.30 mm. The sandstone consists of subangular to subrounded detrital grains. Framework grains consist of quartz, feldspar and rock fragments. Quartz grains include

both monocrystalline and polycrystalline quartz. Polycrystalline quartz grains consist of three to more than five quartz crystals with non-sutured boundaries. Feldspars include plagioclase, microcline and other potassium-feldspars. Rock fragments are present comprising mainly quartz-feldspar grains. Mica constitutes up to 2% of the sample and consists of biotite and muscovite. Some of the muscovite grains are deformed or bent. Sandstone sample N5 is poorly cemented with calcite. Accessory minerals include zircons, garnets, tourmaline, rutile, apatite and pyrite. Inclusions of subrounded tourmalines (green), apatite and zircons were observed within the quartz grains.

Sample N6

Sample N6 was sampled from borehole ACP3 at depths between 265.06 m and 265.11 m (App. Fig. 1). It is moderately sorted, medium- to coarse-grained sandstone (0.25 mm – 1.00 mm) and consists of subangular to subrounded detrital framework grains. Framework grains include quartz, feldspar and rock fragments. Quartz grains comprise both monocrystalline and polycrystalline quartz with monocrystalline quartz being more plentiful. Polycrystalline quartz grains composed of more than five sutured and non-sutured crystal boundaries were commonly observed. Feldspars comprise plagioclase, microcline and other potassium-feldspars. Rock fragments consist of quartz-feldspar grains. Mica is present in the rock sample and consists of biotite and muscovite. Biotite alteration to chlorite occurs within the sample. The sandstone sample is partially cemented by calcite. Subrounded zircon grains are present in trace amounts together with garnet grains and pyrite.

Sample N7

Sample N7 is from borehole ACP19 and was sampled at depths between 261.59 m and 261.64 m (App. Fig. 4). Sandstone sample N7 is poorly sorted and medium-grained (0.30 mm - 0.57 mm). Framework grains that make up the sample include monocrystalline quartz and polycrystalline quartz, feldspar and quartz-feldspar rock fragments. Polycrystalline quartz grains include those composed of four to more than five non-sutured crystals and those composed of more than five sutured crystals. Feldspars present include plagioclase, microcline and other potassium-feldspars. Rock fragments occur as quartz-feldspar grains. The thin section contains lesser amount of mica grains.

Mica includes deformed and undeformed muscovite. The sample is poorly cemented with calcite and has clay matrix. Accessory minerals include zircon, garnet, chlorite and pyrite.

Sample N9

Sample N9 sandstone was sampled from borehole ACP24 at depths between 170.84 m and 170.89 m (App. Fig. 5). The sandstone is well sorted and fine-grained (0.13 mm - 0.25 mm). It consists of subangular to subrounded detrital grains. Framework grains include quartz, feldspars and rock fragments. Quartz grains are both monocrystalline and polycrystalline. Polycrystalline quartz grains with three non-sutured crystals and more than five non-sutured crystals were observed in this thin section. Feldspars include microcline, plagioclase and other potassium-feldspars. Rock fragments present are quartz-feldspar grains and argillaceous rock fragments. The sandstone is dominated by a matrix of fine-grained material consisting of small-sized micas, quartz and feldspar grains. Accessory minerals include subrounded zircons, tourmalines (green), mica (mainly muscovite), rutile, garnet and pyrite. Some of the mica grains are deformed.

Sample N10

Sandstone sample N10 was sampled in borehole ACP24 at depths between 230.00 m and 230.07 m (App. Fig. 5). The sandstone sample is well sorted and consists of fine-grained (0.125 mm - 0.25 mm) subangular to subrounded detrital grains. Framework grains making up this sandstone include quartz (both monocrystalline and polycrystalline quartz, with monocrystalline being more abundant), feldspar (plagioclase and potassium-feldspars) and rock fragments (quartzo-feldspathic). Polycrystalline quartz grains are formed by three to four non-sutured quartz crystals and more than five non-sutured quartz crystals. Mica is present and consists of muscovite and chlorite. Most of the mica mineral grains are aligned parallel to the bedding. The sandstone is poorly cemented with calcite and exhibits a matrix dominated by clay minerals. Deformed or bent muscovite was observed in thin section. Accessory minerals include subrounded and angular zircons, tourmalines, rutile grains and pyrite.

Sample N11

Sandstone sample N11 was sampled from borehole ACP24 at depths between 244.30 m and 244.37 m (Fig. 4.2). It is a poorly sorted, medium-grained (0.30 mm - 0.56 mm) sandstone, composed of subangular to subrounded detrital grains. Sandstone sample N11 is poorly cemented by calcite. Framework grains comprise quartz, feldspar and rock fragments (quartz-feldspar). Quartz grains occur as both monocrystalline and polycrystalline quartz, with lesser amounts of polycrystalline quartz. The most commonly observed polycrystalline quartz grains are those comprising four to more than five non-sutured quartz crystals. Feldspar grains are dominated by microcline and lesser amounts of plagioclase and other potassium-feldspars. Rock fragments comprise quartz-feldspar and argillaceous rock fragments. The sandstone sample N11 is characterised by a clay matrix with abundant micaceous minerals and it is poorly cemented by calcite. Accessory framework grains comprise trace amounts of mica (muscovite), tourmaline (green), garnet, subrounded zircon and pyrite.

Sample N12

Sandstone sample N12 was sampled from borehole ACP13 at depths between 271.42 m and 271.47 m (App. Fig. 3). It is a well sorted, medium-grained (0.30 mm - 0.5 mm) sandstone with subangular to subrounded detrital grains. Framework grains comprise quartz, feldspar and lesser amounts of rock fragments. Quartz grains include both monocrystalline and polycrystalline quartz. Feldspar grains comprise plagioclase; microcline and other potassium-feldspars. Polycrystalline quartz grains with more than five sutured crystals and with less than five non-sutured crystals were observed in this sandstone sample. Microcline is the dominant feldspar in the sample. Rock fragments include quartz-feldspar grains and polycrystalline quartz. The sandstone is poorly cemented by calcite. Accessory mineral grains include zircon, tourmaline (green), mica, garnet and pyrite. Mica present is muscovite and it is deformed in places.

Sample N13

Sample N13 was sampled from borehole ACP13 at depths between 226.56 m and 226.61 m (App. Fig. 3). It is a well sorted, medium- to very coarse-grained sandstone (0.30 mm - 1.50 mm grain size). The sandstone is composed of subrounded to subangular detrital

grains. Framework grains consist of quartz (both monocrystalline and polycrystalline quartz with monocrystalline dominant), feldspar (dominantly microcline and lesser amounts of plagioclase and other potassium-feldspars) and lesser amounts of quartz-feldspar rock fragments. Two types of polycrystalline quartz grains were observed which include polycrystalline quartz with three to four non-sutured crystals and polycrystalline quartz with more than five non-sutured crystals. Mica minerals (muscovite) are present in lesser amounts and deformed muscovite was observed in thin section. The sandstone is poorly cemented by calcite and consists of a clay-rich matrix. Accessory phases include zircon, garnet, rutile, tourmaline (green), mica and pyrite.

3. Facies association 4 sandstones (northern and eastern Gemsbok Sub-basin)

Facies association 4 in the northern part of the study area consists of sandstones numbered B2, B3, B4, B5, B6, B7, B8, B9 and in the eastern part of the study area consists of sandstones numbered B10 and B20.

Descriptions of facies association 4 sandstones (northern Gemsbok Sub-basin):

Sample B2

Sample B2 was sampled from borehole W1 at a depth between 169.29 m and 169.39 m (App. Fig. 6). Internally, it is moderately to well sorted, fine-grained with grain size ranging from 0.20 mm to 0.25 mm. The sandstone sample contains detrital framework grains of quartz, feldspar and mica. These grains are subrounded to subangular, although the latter predominates. Quartz is the more abundant followed by feldspar and mica. Monocrystalline and polycrystalline quartz are present. Polycrystalline quartz grains are composed of two and more than five non-sutured crystals. Grains of polycrystalline quartz with more than five sutured crystals are present within this sandstone sample. Plagioclase, microcline and other potassium-feldspars are common. Sample B2 is rich in mica (biotite and muscovite) and most of the mica is aligned parallel with bedding. Most of the mica minerals alter to chlorite. Bent mica was observed in this thin section. Lithic fragments are rare and compries argillaceous rock fragments. The sandstone sample is poorly cemented by calcite. Accessory minerals include subrounded zircons and angular to subangular garnets.

Sample B3

Sample B3 was sampled from borehole W2 at a depth of 154.69 m to 154.79 m (App. Fig. 7). This sandstone sample is well sorted and fine-grained (range between 0.125 mm and 0.25 mm). The major detrital grains include quartz, feldspar and argillaceous rock fragments. The detrital grains within sample B3 are subrounded to subangular. Quartz grains dominate and occur as both monocrystalline and polycrystalline (three to more than five non-sutured crystals). Plagioclase, microcline and potassium-feldspar make up the total feldspar content. Argillaceous fragments are rare. Biotite and muscovite are also present within this sandstone sample and are usually concentrated along bedding planes. The observed muscovite appears to have been bent. The matrix comprises fine-grained quartz, mica and clay minerals. Accessory minerals include zircon (subrounded), tourmaline (green in colour and irregular shape), apatite (as inclusions in quartz) and pyrite.

Sample B4

Sample B4 is from borehole W2 and sampled at a depth between 152.18 m and 152.26 m (App. Fig. 7). The sandstone sample is moderately to poorly sorted and is dominated by medium-grained (0.3 mm to 0.5 mm) angular to subangular grains with minor amounts of subrounded grains. Major framework grains include quartz and feldspar. Monocrystalline quartz dominates over polycrystalline quartz. Polycrystalline quartz grains are composed of three to five and more than five crystals. Both sutured and non-sutured quartz crystals within the polycrystalline quartz grains (consisting of more than five crystals) are present. Inclusions of mica and subrounded and elongate apatite grains are common within the monocrystalline quartz grains. Feldspars present include plagioclase, microcline and potassium-feldspars. Rock fragments are present in small numbers and consist of quartz-feldspar grains and other argillaceous rocks fragments. Mica is present in this sample, although rare and consists of muscovite which normally alters to chlorite. Bent micas were observed in this thin section. Calcite is present as a cement, but the sandstone is poorly cemented. The matrix consists of altered mica and clay. Subrounded zircon grains, apatite grains, tourmaline and garnet were observed in this thin section and occur as accessory minerals together with some pyrite.

Sample B5

Sample B5 sandstone was sampled from borehole W2 at depths between 170.20 m and 170.24 m (App. Fig. 7). It is a moderately to poorly sorted, fine-grained (0.125 - 0.25 mm) sandstone. The framework grains of the B5 sandstone are monocrystalline quartz, polycrystalline quartz (with two to five non-sutured crystals), potassium -feldspar, plagioclase, mica and rock fragments. The detrital grains are subangular to subrounded. Quartz grains dominate over feldspar grains (potassium -feldspar and plagioclase). Some of the quartz grains have inclusions of mica and apatite. Biotite and muscovite are dominant and are confined to the bedding planes or laminations of the sandstone. Some of the mica is bent and squashed between the quartz grains. The matrix of sample B5 sandstone is generally composed of argillaceous matrix. Few rock fragments are present comprising quartz- feldspar grains and argillaceous rock fragments. Accessory minerals include subrounded zircons, apatite grains and chlorite.

Sample B6

Sandstone sample B6 is from borehole W2 and sampled at depths between 230.69 m and 230.77 m (App. Fig. 7). It is a fine-grained (0.25 mm - 0.5 mm), moderately to well sorted sandstone consisting of quartz, feldspar and rock fragments as major framework grains. Quartz grains are more abundant than feldspar grains and rock fragments in the thin section. Quartz occurs as both polycrystalline and monocrystalline grains. Grains of polycrystalline quartz are composed mainly of two, three and greater than five non-sutured crystals. Polycrystalline quartz with more than five sutured crystals was observed within this thin section. Quartz grains with apatite mineral inclusions were also observed. Feldspar grains occur as plagioclase, microcline and potassium feldspars. Rock fragments are rare and include polycrystalline quartz grains. Muscovite grains are present in the sample, but in lesser amounts. Calcite is present in a form of cement, but the sandstone sample is poorly cemented. Accessory minerals include subangular and subrounded zircons, rutile (rounded in places), green tourmaline grains (subrounded to euhedral in shape and zoned in places) and garnets (angular in shape). Some of the zircon grains show zonation.

Sample B7

Sample B7 was sampled from borehole W3 at depths between 206.08 m and 206.16 m (Fig. 4.3). It is a moderately sorted, medium-grained (0.25 mm – 0.50 mm) sandstone. The sandstone has angular to subangular grains, with the latter being dominant. Quartz, feldspar and rock fragments are the main detritus in the sandstone sample B7. The most abundant quartz grains are the monocrystalline quartz with only trace amounts of polycrystalline quartz. Polycrystalline quartz grains consist of five non-sutured quartz crystals. Feldspar grains consist of microcline, plagioclase and potassium feldspars. Rock fragments are present and comprise argillaceous rock fragments and quartz-feldspar rock fragments. Mica is present and includes muscovite, which is deformed in places. The sample is partially cemented with calcite. Detrital clay constitutes the matrix. Accessory framework grains include zircon (subrounded and rounded), mica, rutile, tourmaline (rounded, elongate green tourmaline) and garnet (light pink). Rounded tourmaline and zircon inclusions within the quartz grains were observed.

Sample B8

Sample B8 was sampled from borehole W1 at depths between 130.24 m and 130.34 m (App. Fig. 6). The sample is a moderately sorted, medium-grained (0.25 mm – 0.30 mm) sandstone. It is composed of angular to subangular detrital grains with lesser amounts of subrounded grains. Framework grains consist of quartz, feldspar and rock fragments. Quartz grains occur as both monocrystalline and polycrystalline quartz with lesser amounts of polycrystalline quartz. Observed polycrystalline quartz grains are composed of more than five sutured quartz crystals and less than five non-sutured crystals. The sample is dominated by feldspar grains, which include plagioclase, microcline and other potassium feldspar. Rock fragments include quartz-feldspar, polycrystalline quartz and altered argillaceous rock fragments. Biotite, muscovite and chlorite micas are present. Deformed muscovite has been observed in the thin section. Accessory framework grains include trace amounts of zircon (subrounded and euhedral), tourmaline (subrounded) and pyrite.

Sample B9

Sample B9 was sampled from borehole W3 at depths between 97.25 m and 97.34 m (App. Fig. 8). The sample is moderately to well sorted and fine-grained (0.130 mm - 0.25 mm) in size. It is composed of subangular to subrounded detrital framework grains with subangular grains dominated. Quartz is the dominating framework grain in sandstone sample B9 and consist of both monocrystalline and polycrystalline (three and more than five non-sutured quartz crystals) quartz grains. Other framework grains making-up sample B9 include feldspar grains (plagioclase, microcline and other potassium-feldspars), mica and rock fragments (argillaceous, polycrystalline quartz). Mica grains are more abundant than the rock fragments and consist of muscovite grains. Some muscovite grains appear deformed in places. The sample is poorly cemented by calcite. Detrital clay occurs as a matrix and comprise fine-grained quartz, mica and feldspar grains. Accessory minerals include zircon, tourmaline, apatite and opaque minerals.

Descriptions of facies association 4 sandstones (eastern Gemsbok Sub-basin):

Sample B10

Sample B10 is from borehole CKP8C-1 and sampled from depths between 415.71 m and 415.91 m (App. Fig. 11). Sandstone sample B10 is a moderately sorted and fine-grained (0.125 mm - 0.25 mm). The sample is very altered (sericitisation) and micaceous. Framework grains include monocrystalline quartz, polycrystalline quartz, feldspar, mica and rock fragments (argillaceous). Quartz occurs in two forms, monocrystalline and polycrystalline grains. Polycrystalline quartz grains are composed of three to five non-sutured quartz crystals. Feldspars include potassium feldspars and the mica grains consists of both biotite and muscovite, which are altered in places. Deformed mica was observed within the thin section. The matrix is mainly composed of clay minerals. Accessory minerals include zircon, tourmaline, apatite and pyrite.

Sample B20

Sample B20 was sampled from depths between 474.63 m and 474.73 m in borehole CKP8C-1 (Fig. 4.5). Sandstone sample B20 is poorly sorted, medium-grained (0.25 mm

– 0.40 mm) and consists of subangular to subrounded detrital grains. Major detrital framework grains present include quartz, feldspar and rock fragments. Quartz grains include monocrystalline and polycrystalline quartz. Polycrystalline quartz occurs in lesser amounts and consists of two (non-sutured) and more than five (sutured) crystals of quartz. Feldspars present in the sample include microcline, plagioclase and other potassium-feldspars. Rock fragments consist of quartz-feldspar and argillaceous rock fragments. The sample consists of lesser amounts of mica and muscovite occurs in larger quantities compared to biotite. The muscovite mica grains appear bent adjacent to quartz and feldspar grains. Accessory minerals include zircon (subrounded), garnet, rutile, tourmaline (brown and green) and pyrite. Apatite and tourmaline are common as inclusions within quartz grains.

4. Facies association 5 sandstones (eastern Gemsbok Sub-basin)

Facies association 5 in the eastern part of the study area consists of sandstones numbered B11, B12, B14, B15, B16, B17, B18, B19, BA, BB and BC.

Descriptions of facies association 5 sandstones (eastern Gemsbok Sub-basin):

Sample B11

Sample B11 sandstone was sampled from borehole CKP8A at depths between 277.40 m and 277.86 m (App. Fig. 9). It is a fine-grained (0.125 mm – 0.25 mm), moderately to well sorted sandstone. The sandstone sample consists of subangular to subrounded framework grains. Framework grains include quartz, feldspar and rock fragments. Quartz grains consist of both monocrystalline and polycrystalline quartz with high amounts of monocrystalline quartz grains. Polycrystalline quartz grains are formed by two to five and more than five crystals of quartz, which are non-sutured. Feldspars present include microcline, plagioclase and other potassium-feldspars. Rock fragments are made up of quartz-feldspar and polycrystalline quartz. The sandstone is poorly cemented and consists of fine-grained matrix composed mainly of small grains of mica. Deformed muscovite grains have been observed in this thin section. Accessory framework grains include trace amounts of heavy mineral zircon, rutile, garnet and pyrite.

Sample B12

Sample B12 was sampled from depths between 283.74 m and 283.89 m in borehole CKP8A (App. Fig. 9). The sandstone sample is poorly sorted and coarse-grained (0.50 mm – 1.00 mm). It consists of angular to subangular detrital framework grains of quartz, feldspar and rock fragments. Quartz grains include both monocrystalline and polycrystalline quartz. Polycrystalline quartz grains consist mainly of three and more than five quartz crystals. The quartz crystal boundaries are sutured in polycrystalline quartz grains consisting of more than five crystals, but non-sutured quartz crystals are also present. Feldspars present are microcline and plagioclase. Rock fragments consist of quartz-feldspar and polycrystalline quartz rock fragments. Biotite and muscovite are present in the sandstone sample and tend to alter to chlorite. Small quantities of deformed muscovite are present in the sample. The sandstone is poorly cemented with calcite and consists of clay matrix. Zircon (subrounded), rutile, tourmaline (irregular, subrounded and rounded) and garnet occur as accessory minerals.

Sample B14

Sample B14 was taken from borehole CKP8C-1 at depths between 261.74 m and 261.90 m (App. Fig. 11). The sandstone sample is moderately to well sorted, fine-grained (0.125 mm - 0.25 mm), and consists of angular to subangular detrital grains. Major framework grains comprise quartz, feldspar, mica and rock fragments. Grains of both monocrystalline and polycrystalline quartz were observed, with monocrystalline quartz dominant. Polycrystalline quartz grains composed of two to four crystals of quartz are present. Plagioclase, microcline and potassium-feldspar make the total spectrum of feldspar in the sample. Mica grains consist of altered and non-altered biotite, muscovite and chlorite. Some bent mica grains were observed in this sandstone sample. Rock fragments consists quartz-feldspar rock fragments. The sandstone is poorly cemented by calcite. Subrounded to rounded zircon, apatite (subrounded) tourmaline (green) and pyrite have been observed in thin section and occur in trace amounts. Apatite occurs as inclusions within the quartz grains.

Sample B15

Sample B15 was sampled from borehole CKP8C-1 at depths between 411.25 m and 411.31 m (App. Fig. 11). It is poorly sorted, coarse- to very coarse-grained sandstone (0.50 mm – 2.00 mm) and consists of subangular to subrounded framework grains. Framework grains include quartz, feldspar and rock fragments. The total quartz grains comprise both monocrystalline quartz and polycrystalline quartz. Monocrystalline quartz dominates over polycrystalline quartz. Most polycrystalline quartz grains comprise more than five (sutured and non-sutured) crystals. Feldspars present include plagioclase and potassium-feldspars. Alteration of feldspars into sericite was observed in thin section. Rock fragments consist of quartz-feldspar grains and polycrystalline quartz. Mica is present in small amounts in this sample and consists of biotite which tends to alter to chlorite. Most of the mica grains occur in the matrix. The sandstone sample is well cemented by calcite. Subrounded and irregular (occasionally zoned) zircon grains and tourmaline (green) grains are present and occur in trace amounts.

Sample B16

Sandstone sample B16 was sampled from borehole CKP8C-1 at depths between 321.10 m and 321.32 m (App. Fig. 11). The sandstone sample is moderately to well sorted and fine-grained (0.125 mm - 0.25 mm). It consists of subangular to subrounded detrital framework grains of quartz, feldspar and rock fragments. Quartz grains include both monocrystalline and polycrystalline grains. Polycrystalline quartz grains consist of two and greater than five quartz crystals. Feldspar grains include plagioclase, microcline and potassium-feldspar. Rock fragments comprise quartz-feldspar rock fragments. Biotite and muscovite are present within the sandstone. Some mica grains are bent and most of the mica minerals are aligned parallel to bedding. The sandstone exhibits clay-rich matrix. Accessory grains include zircons (subrounded and irregular shapes), tourmaline (green in colour and irregular in shape) and pyrite.

Sample B17

Sample B17 is from borehole CKP8C-1 and was sampled between depths of 278.19 m and 278.35 m (Fig. 4.4). The sandstone sample is moderately to well sorted and fine- to medium-grained (0.20 mm - 0.30 mm) in size. This sandstone consists of subangular to

subrounded detrital framework grains of quartz (monocrystalline and polycrystalline quartz), feldspar and rock fragments. Different types of polycrystalline quartz grains were identified in this thin section and are composed of more than two quartz crystals. Feldspar grains include plagioclase, microcline and other potassium-feldspars. Microcline is the most abundant feldspar. Rock fragments include argillaceous rock fragments, which in places have been replaced by calcite. Sample B17 is poorly-cemented by calcite and contains up to 1% mica minerals (muscovite and biotite). Accessory grains comprise trace amounts of zircon (irregular and subrounded), tourmaline, rutile, apatite (as rounded inclusions within quartz grains) and angular garnets.

Sample B18

Sample B18 was sampled from borehole CKP8C-1 at depths between 320.76 m and 320.83 m (App. Fig. 11). It is a moderately to well sorted fine-grained sandstone with a grain size range of 0.125 mm – 0.20 mm. The sandstone sample comprises subangular to subrounded detrital grains, with subangular grains most abundant. Detrital framework grains consist of quartz, feldspar, mica and rock fragments. Most of the polycrystalline quartz grains are composed of more than five sutured and non-sutured quartz crystals. Feldspars present are microcline, plagioclase and potassium feldspar. The sandstone is dominated by mica minerals including both muscovite and biotite. Some of the muscovite grains are bent and biotite grains alter to chlorite. Rock fragments occur in lesser amounts and include quartz-feldspar and polycrystalline quartz. Sample B18 is poorly cemented with calcite. Accessory minerals include subrounded zircon, tourmalines (green), garnet, apatite (in a form of inclusions within quartz grains) and pyrite.

Sample B19

Sample B19 was sampled from borehole CKP8C at depths between 320.83 m and 320.93 m (App. Fig. 10). It is a moderately to well sorted, fine-grained (0.125 mm - 0.20 mm) sandstone. The sandstone sample is dominated by angular to subangular detrital grains comprising framework grains of quartz, feldspar, mica and rock fragments. Quartz grains are dominantly monocrystalline quartz with lesser amounts of polycrystalline quartz. Most abundant polycrystalline quartz grains in this thin section are formed by more than three non-sutured quartz crystals. Feldspar grains include plagioclase, microcline and

other potassium-feldspars. Mica grains are present in the thin section and include both biotite and muscovite. Muscovite and biotite are aligned parallel to the bedding and are sometimes deformed. Rock fragments are present, but not dominant. They consist of grains of quartz-feldspar and polycrystalline quartz. The sandstone has a clay matrix and calcite cement. Accessory minerals include light pink garnet grains and zircons.

Sample BA

Sample BA was sampled from borehole CKP8C at depths between 277.35 m and 277.51 m (App. Fig. 10). The sandstone is moderately to well sorted and fine-grained (0.125 mm – 0.25 mm). It is composed of subangular to subrounded detrital grains, with the subangular grains dominanting. Framework grains comprise quartz, feldspar and rock fragments. Monocrystalline quartz dominates over polycrystalline quartz grains. Polycrystalline quartz grains consist of two (non-sutured) and more than five (sutured and non-sutured) crystals of quartz. Plagioclase, microcline and potassium-feldspars make the total feldspars in this sample. Rock fragments are quartz-feldspar and polycrystalline quartz. Mica grains are present and consist of biotite and muscovite. Mica grains are aligned parallel to the bedding orientation and some of the mica grains are deformed. The sandstone sample is well cemented by calcite minerals. Accessory grains include zircon (subrounded), garnets and pyrite.

Sample BB

Sample BB was sampled from borehole CKP8C at depths between 298.93 m and 299.00 m (App. Fig. 10). This sandstone sample is moderately sorted, medium- to coarse-grained (0.30 mm – 1 mm) and characterised by subangular to subrounded detrital grains. Framework grains making up this sandstone include abundant monocrystalline quartz, lesser amounts of polycrystalline quartz (three and more than five non-sutured quartz crystals), feldspar (plagioclase, microcline and other potassium-feldspars) and rock fragments (quartzo-feldspathic and argillaceous). Some of the argillaceous rock fragments have been replaced by calcite. The sandstone is partially cemented by calcite and the matrix consists of clay minerals. Mica is present and includes muscovite, chlorite and biotite. Deformed mica was observed. Accessory minerals consist of subrounded

zircons, rutile, apatite and pyrite. Subrounded apatite minerals are present as inclusions within quartz grains.

Sample BC

Sample BC was sampled from borehole CKP8C at depths between 326.00 m and 326.09 m (App. Fig. 10). It is well sorted, fine-grained (0.130 mm - 0.25 mm) and composed of subangular to subrounded detrital grains. Framework grains within the sandstone consist of quartz, feldspar, mica and rock fragments. Quartz grains occur as both monocrystalline and polycrystalline quartz, with monocrystalline quartz dominant. Polycrystalline quartz grain types are present and are characterised by three (non-sutured), and more than five (non-sutured and sutured) quartz crystals. Feldspar present includes plagioclase, microcline and other potassium-feldspars. Mica is present in the rock sample and consists of bent muscovite and biotite in places. Chlorite is present and is an alteration product of biotite. Most of the mica minerals are aligned parallel to bedding. Rock fragments include quartz-feldspar and argillaceous rock fragments, which in places are replaced by calcite. This sandstone sample is poorly cemented by calcite. Accessory framework grains include trace amounts of subrounded zircon, garnet and pyrite.

5. Facies association 8 sandstones (northern Gemsbok Sub-basin)

Facies association 8 in the northern part of the study area consists of sandstone sample numbered B1.

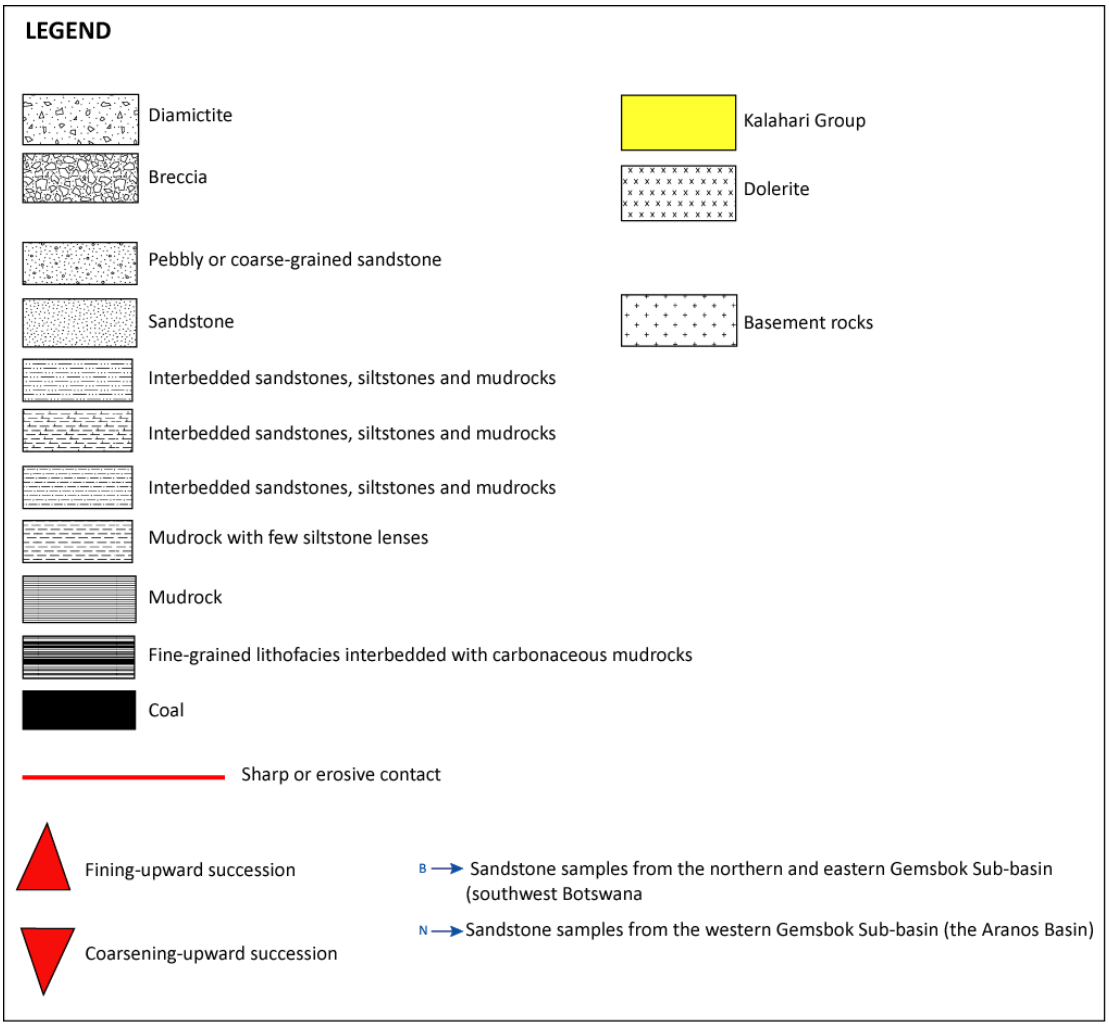
Descriptions of facies association 8 sandstone sample (northern Gemsbok Sub-basin):

Sample B1

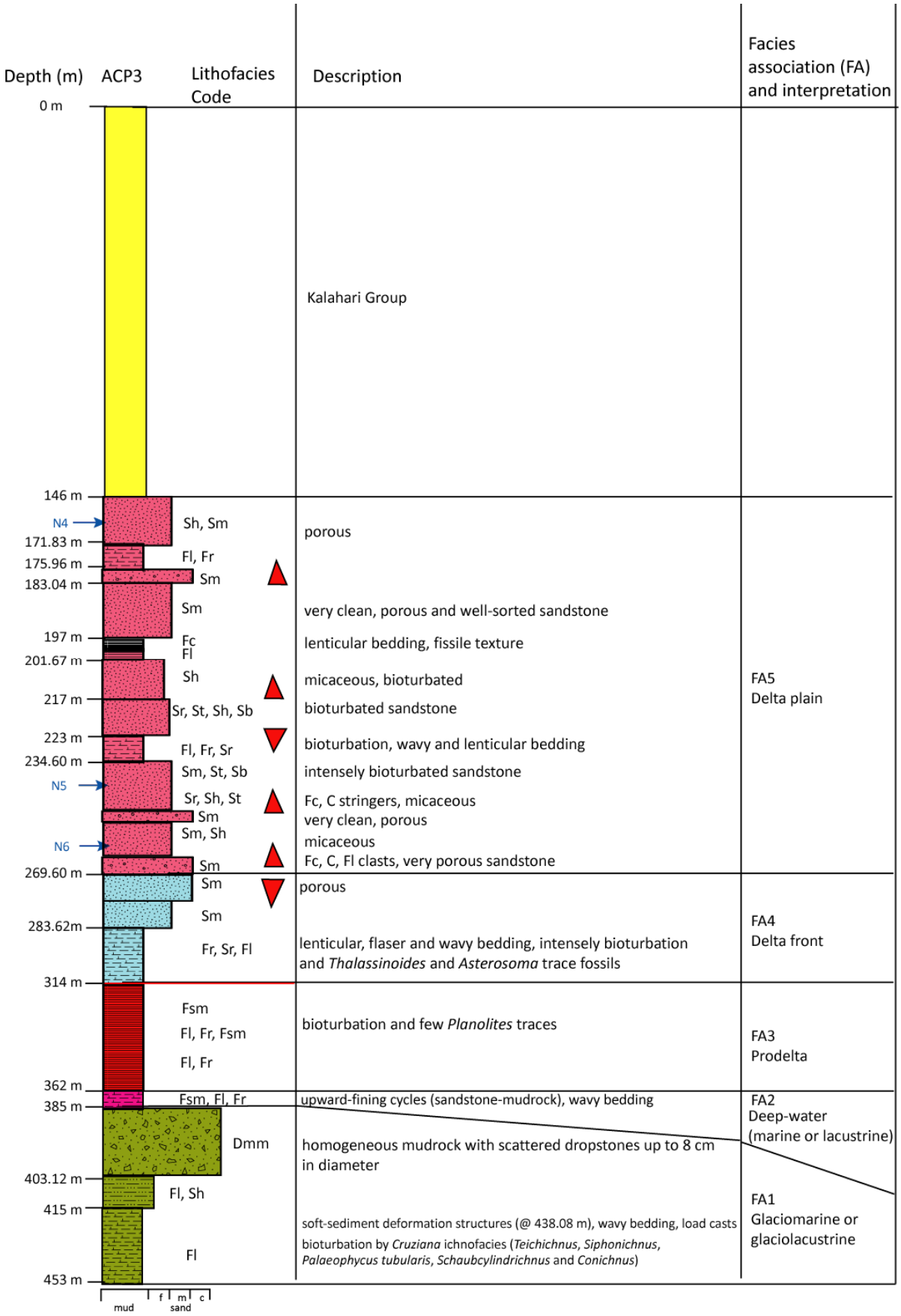
Sample B1 is from borehole W1 and was sampled at depths between 96.81 m and 96.90 m (Fig. 4.6). The sandstone sample is well sorted and fine-grained (0.125 mm - 0.25 mm). Detrital grains that make up this sample are subangular to subrounded. The sample is dominated by detrital grains of quartz followed by feldspar grains and lithic fragments. The quartz component of this sandstone comprises monocrystalline quartz and polycrystalline quartz, with the monocrystalline quartz content being greater.

Polycrystalline quartz is formed by more than five non-sutured quartz crystals. Subrounded quartz grains with inclusions of subrounded and elongate shape apatite were observed. The sandstone sample contains lesser amount of feldspar. Feldspar grains include microcline and plagioclase. The sample contains minor amounts of rock fragments (argillaceous and polycrystalline quartz). Carbonate cement and clay matrix are present in lesser amounts. No mica minerals were found in this thin section. Accessory minerals include zircons (zoned and subrounded), rutile (subrounded), tourmaline (green in colour, zoned and subrounded) and garnet (angular).

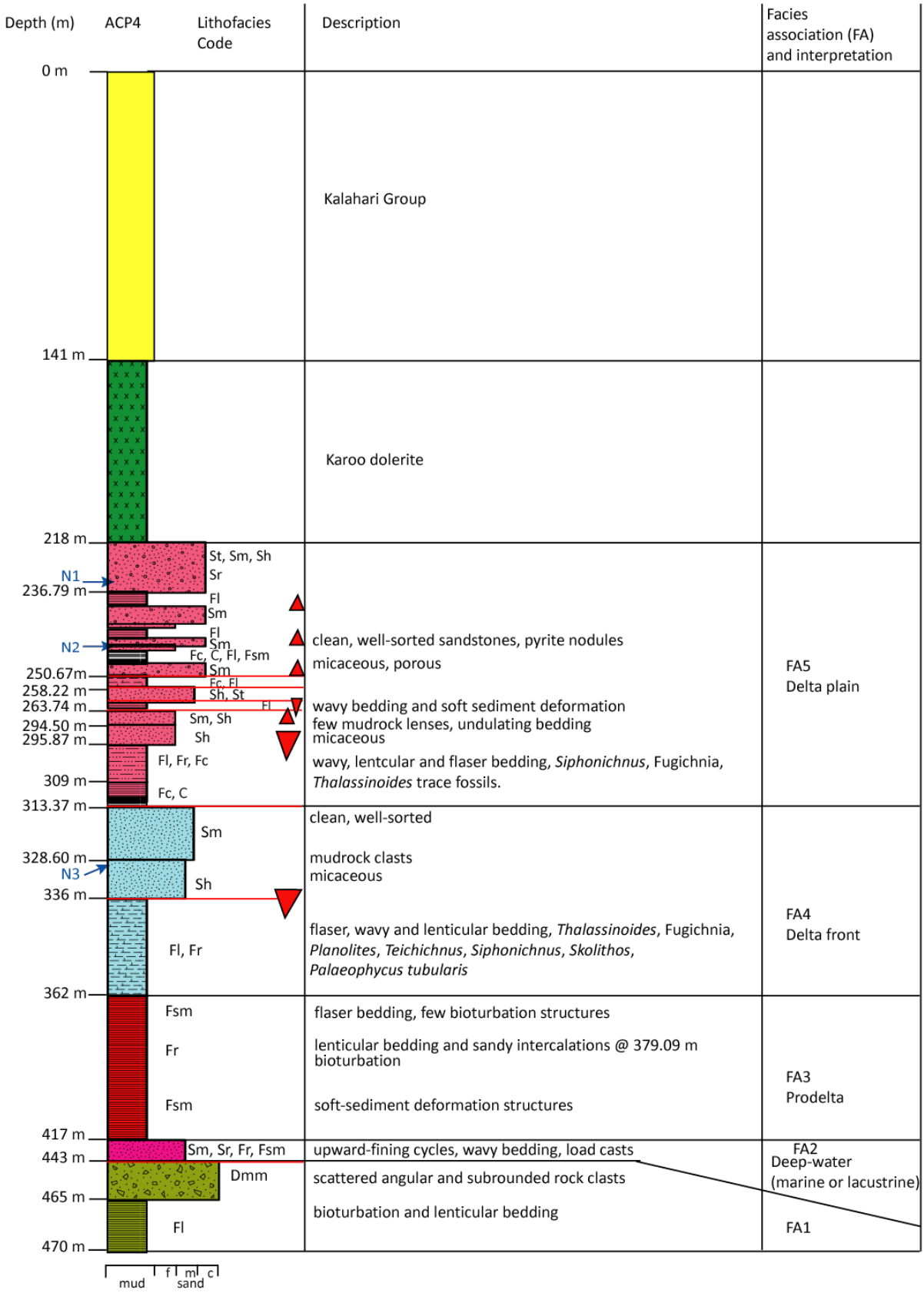
APPENDIX B


LEGEND
Diamictite
Breccia
Pebbly or coarse-grained sandstone
Sandstone
Interbedded sandstones, siltstones and mudrocks
Interbedded sandstones, siltstones and mudrocks
Interbedded sandstones, siltstones and mudrocks
Mudrock with few siltstone lenses
Mudrock
Fine-grained lithofacies interbedded with carbonaceous mudrocks
Coal
Sharp or erosive contact
Fining-upward succession
Coarsening-upward succession
Kalahari Group
Dolerite
Basement rocks
B → Sandstone samples from the northern and eastern Gemsbok Sub-basin (southwest Botswana
N → Sandstone samples from the western Gemsbok Sub-basin (the Aranos Basin)

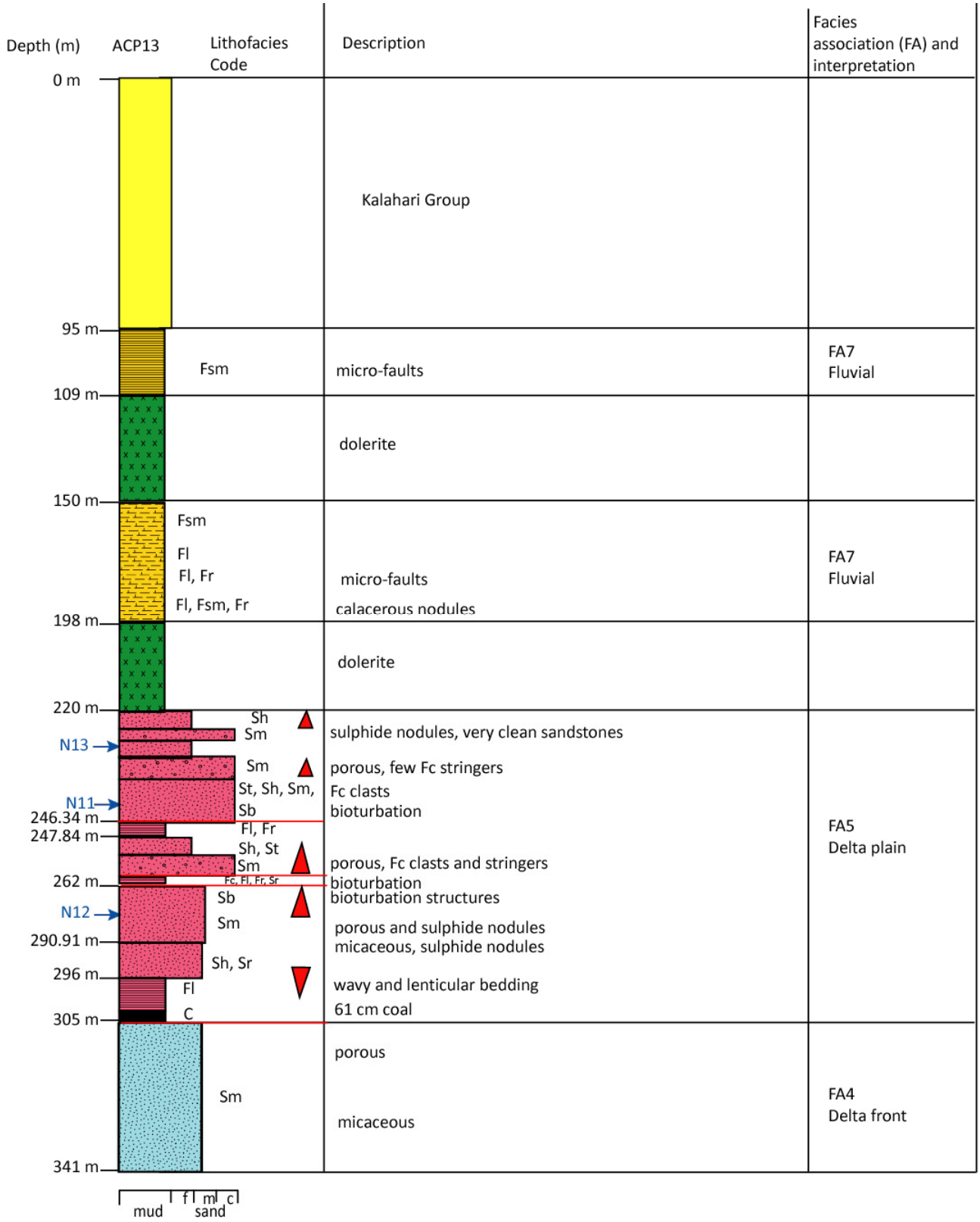
Appendix Figure. 1



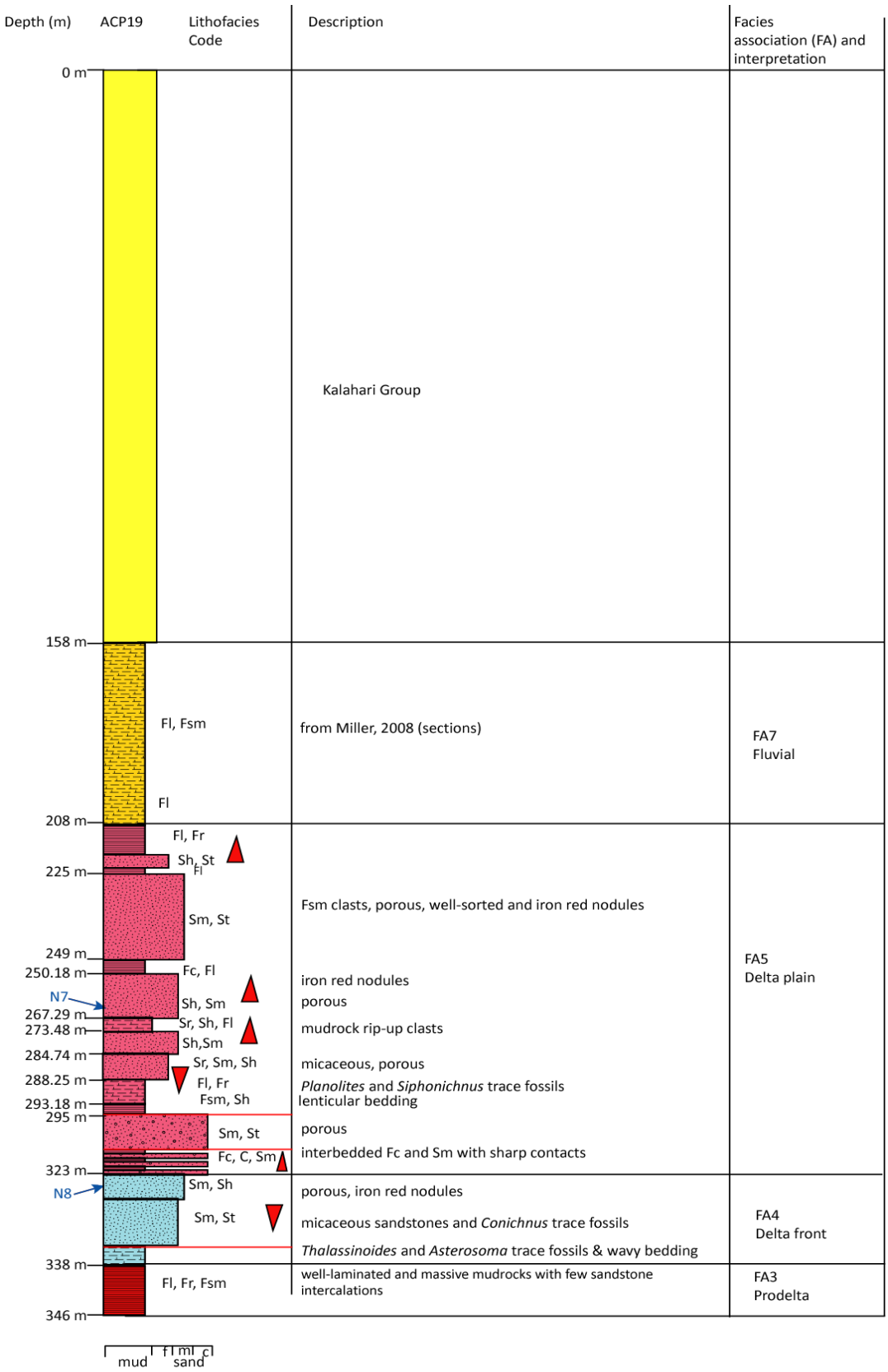
Appendix Figure. 2



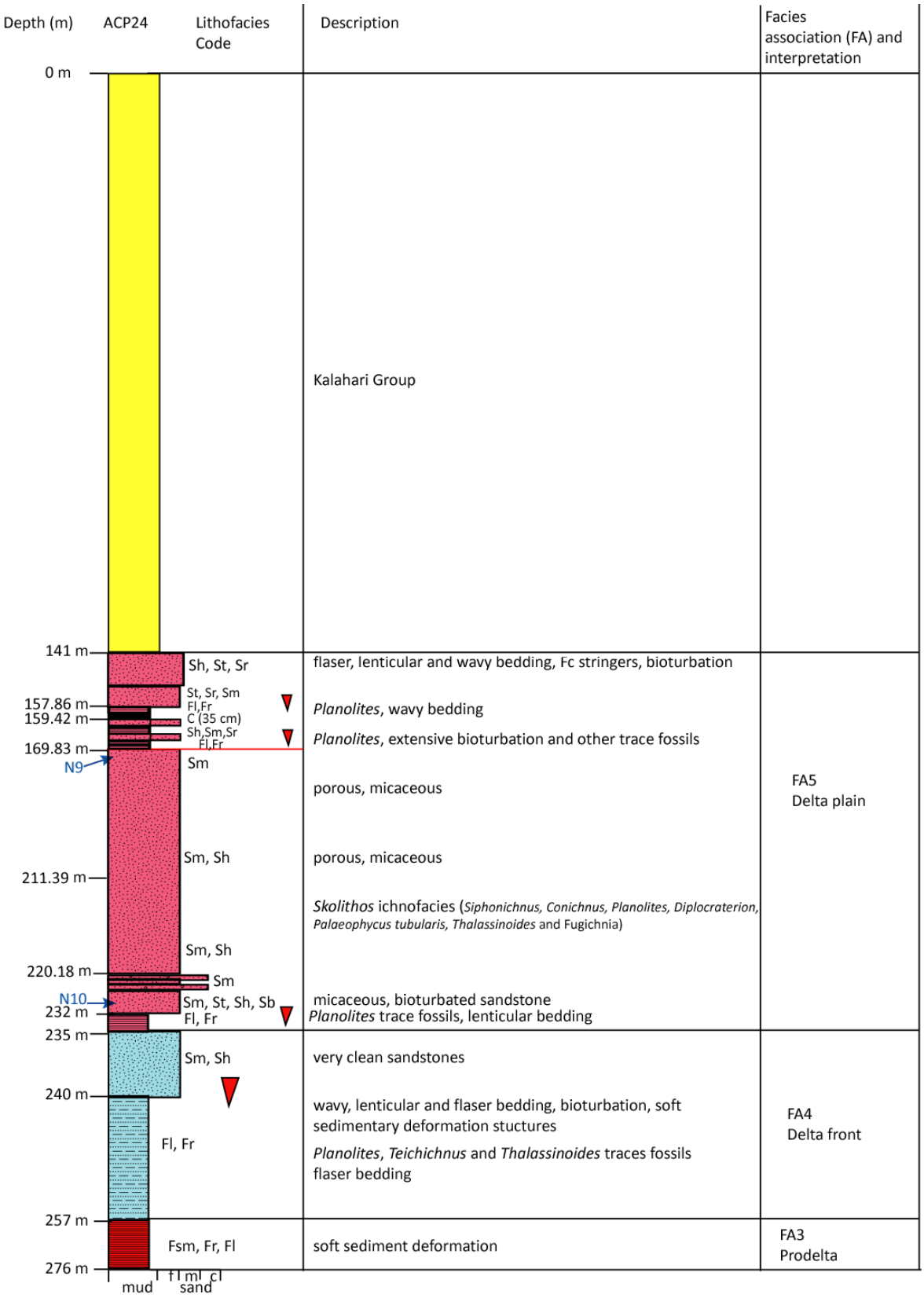
Appendix Figure. 3



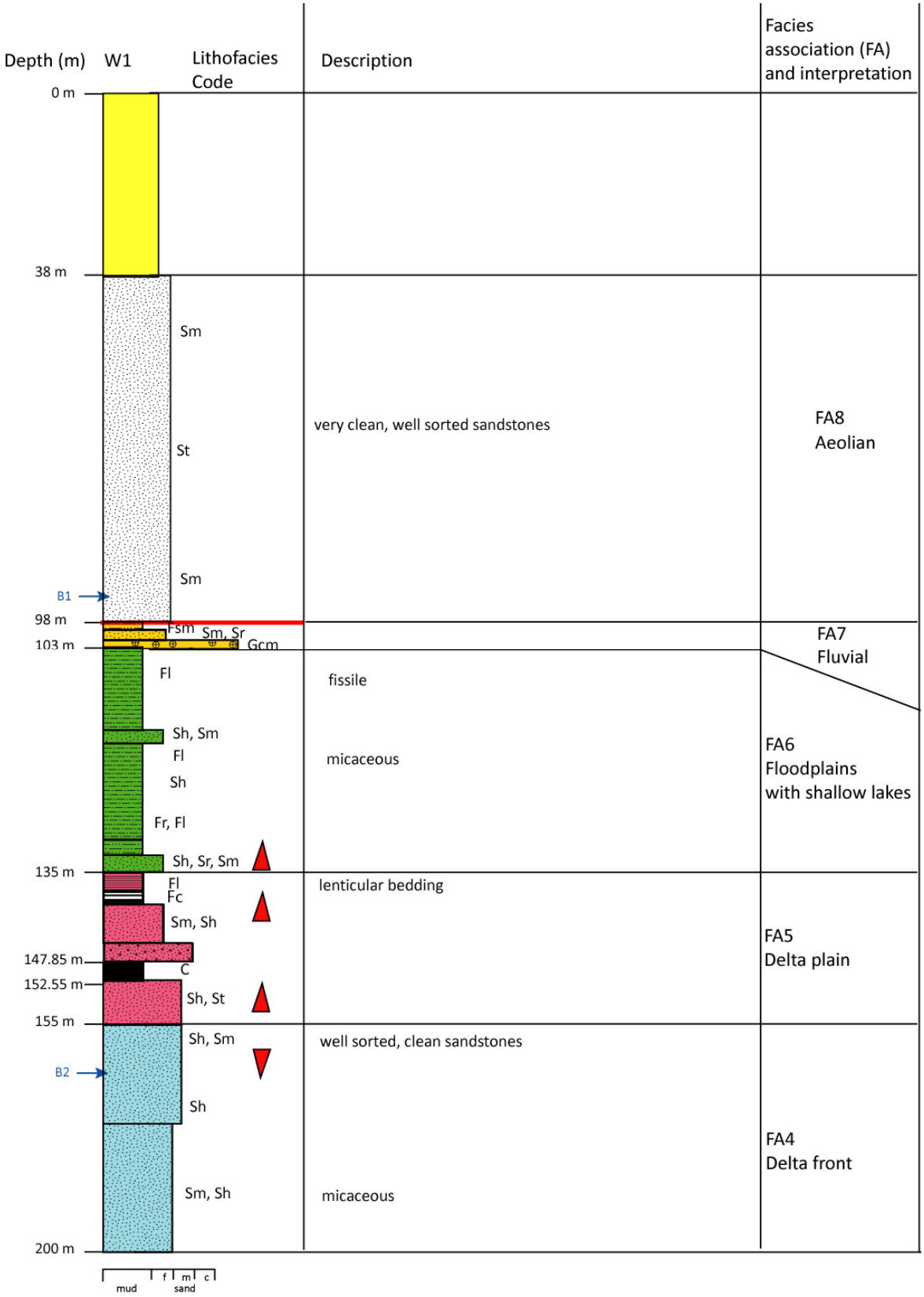
Appendix Figure. 4



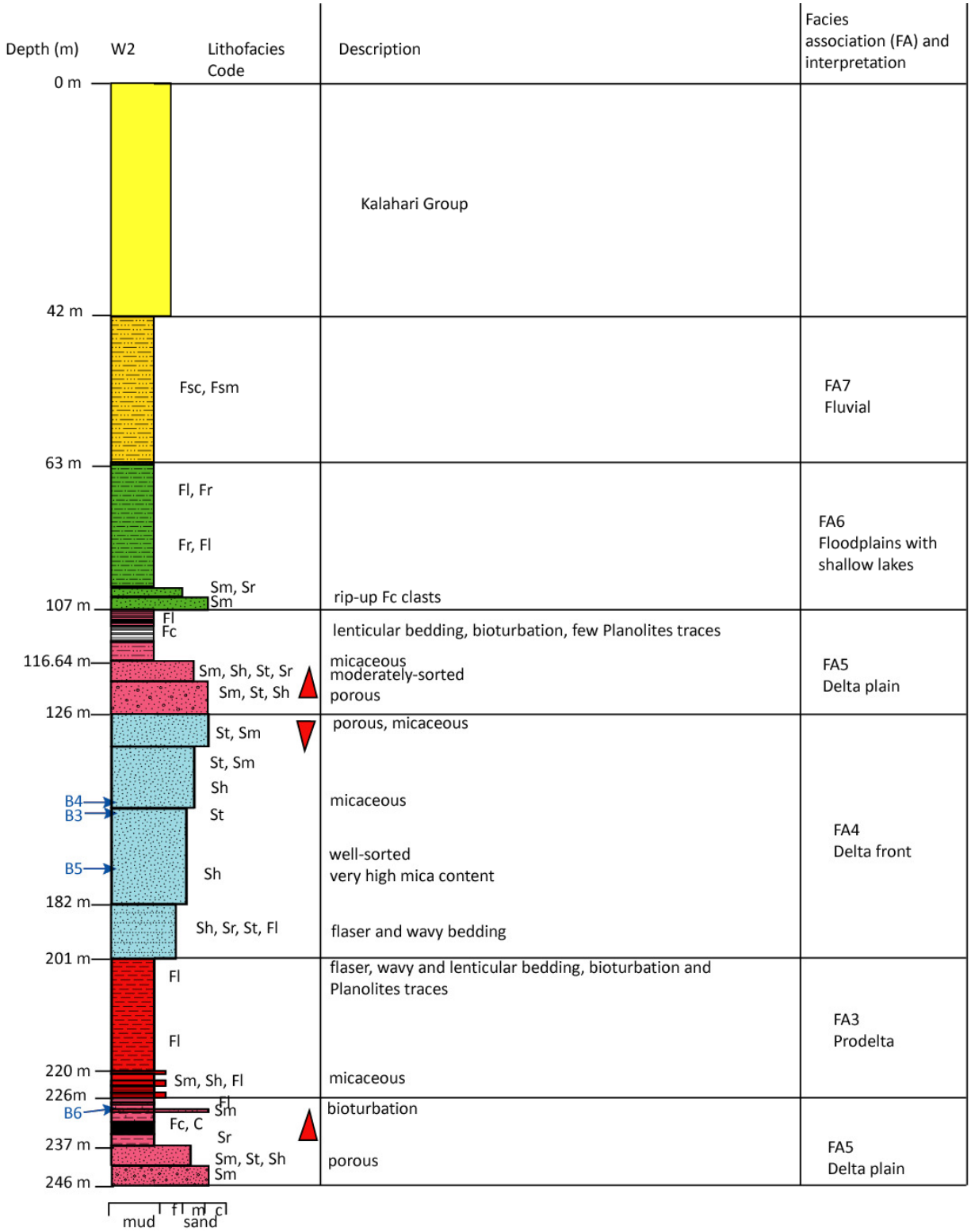
Appendix Figure. 5



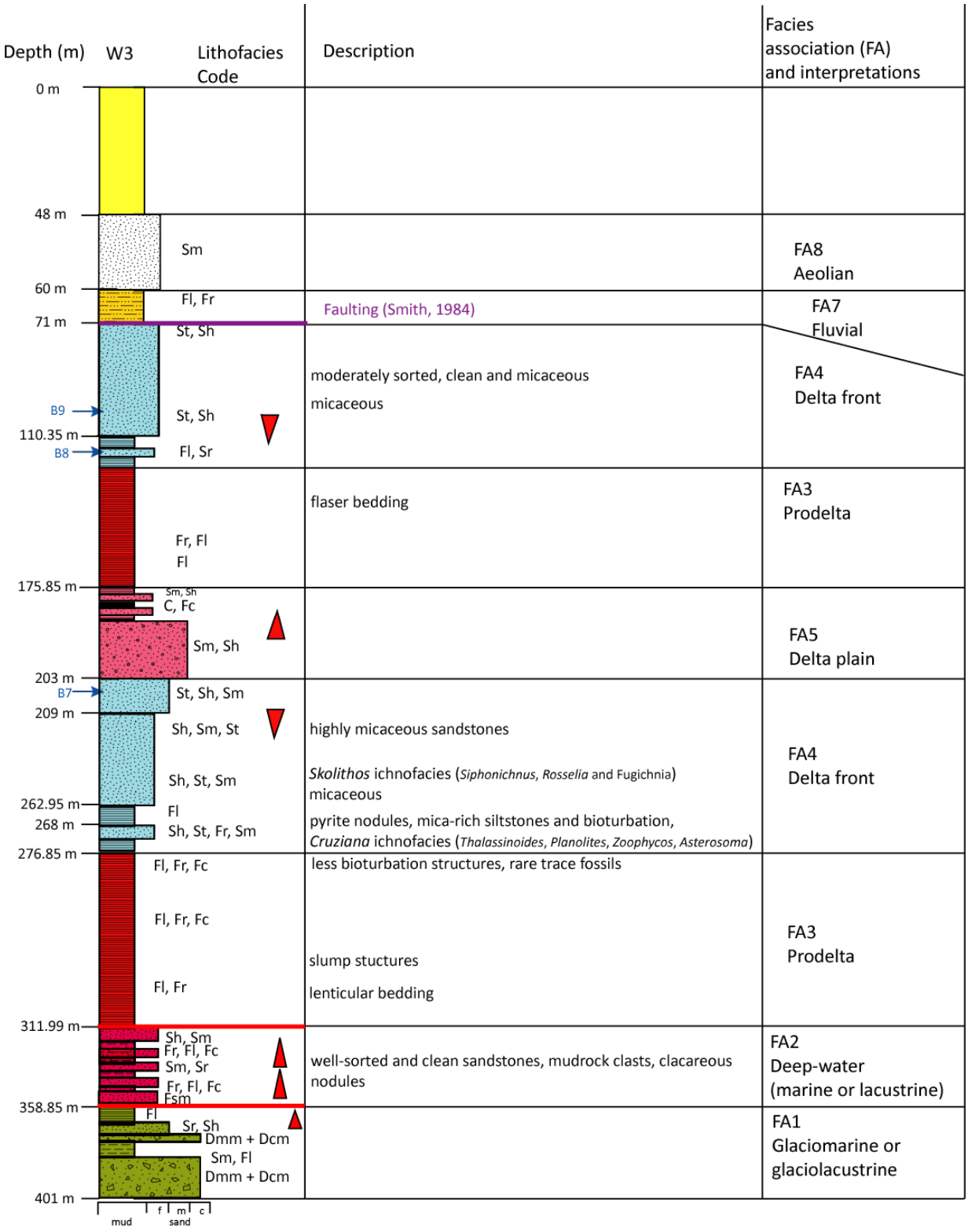
Appendix Figure. 6



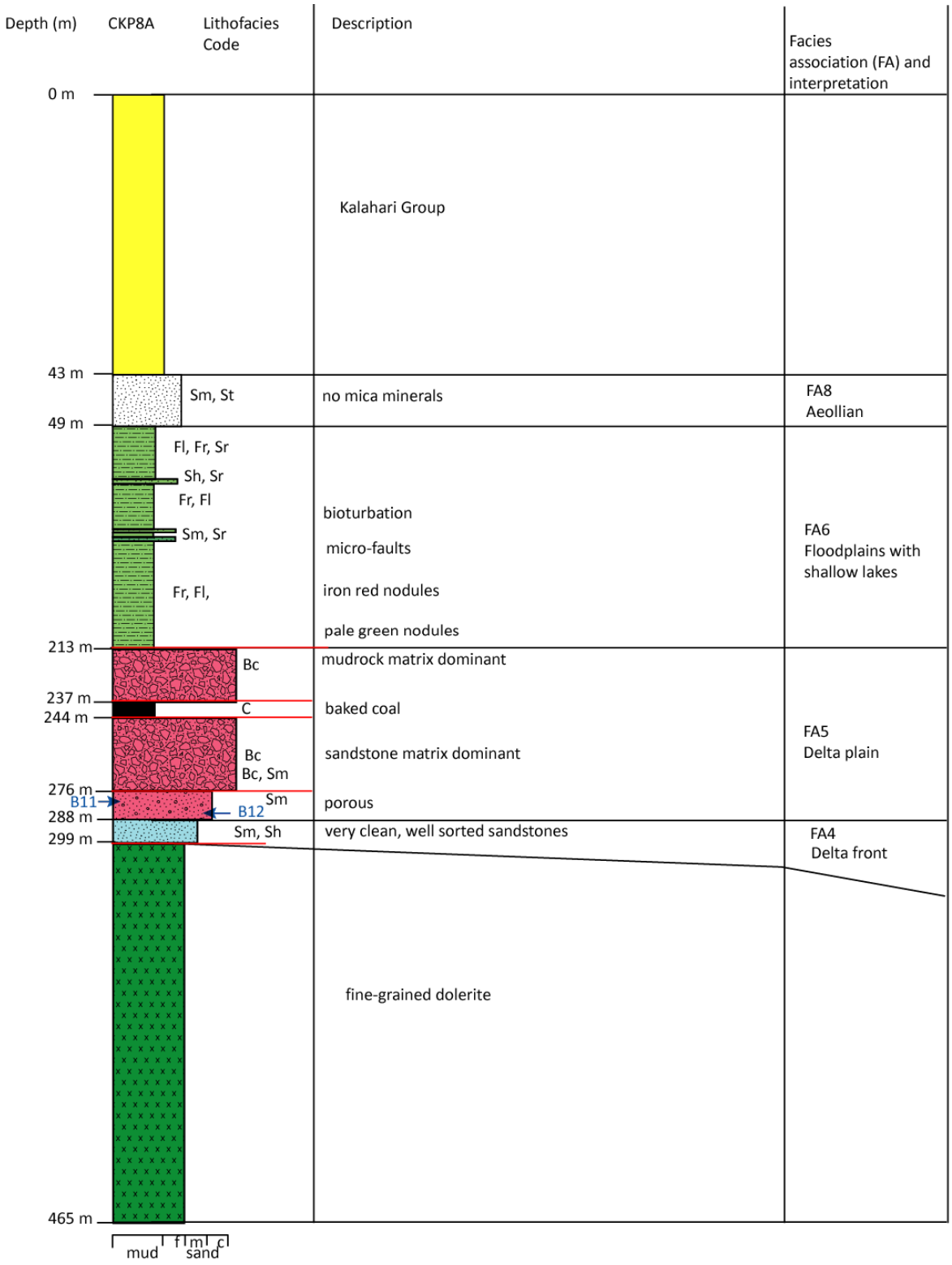
Appendix Figure. 7



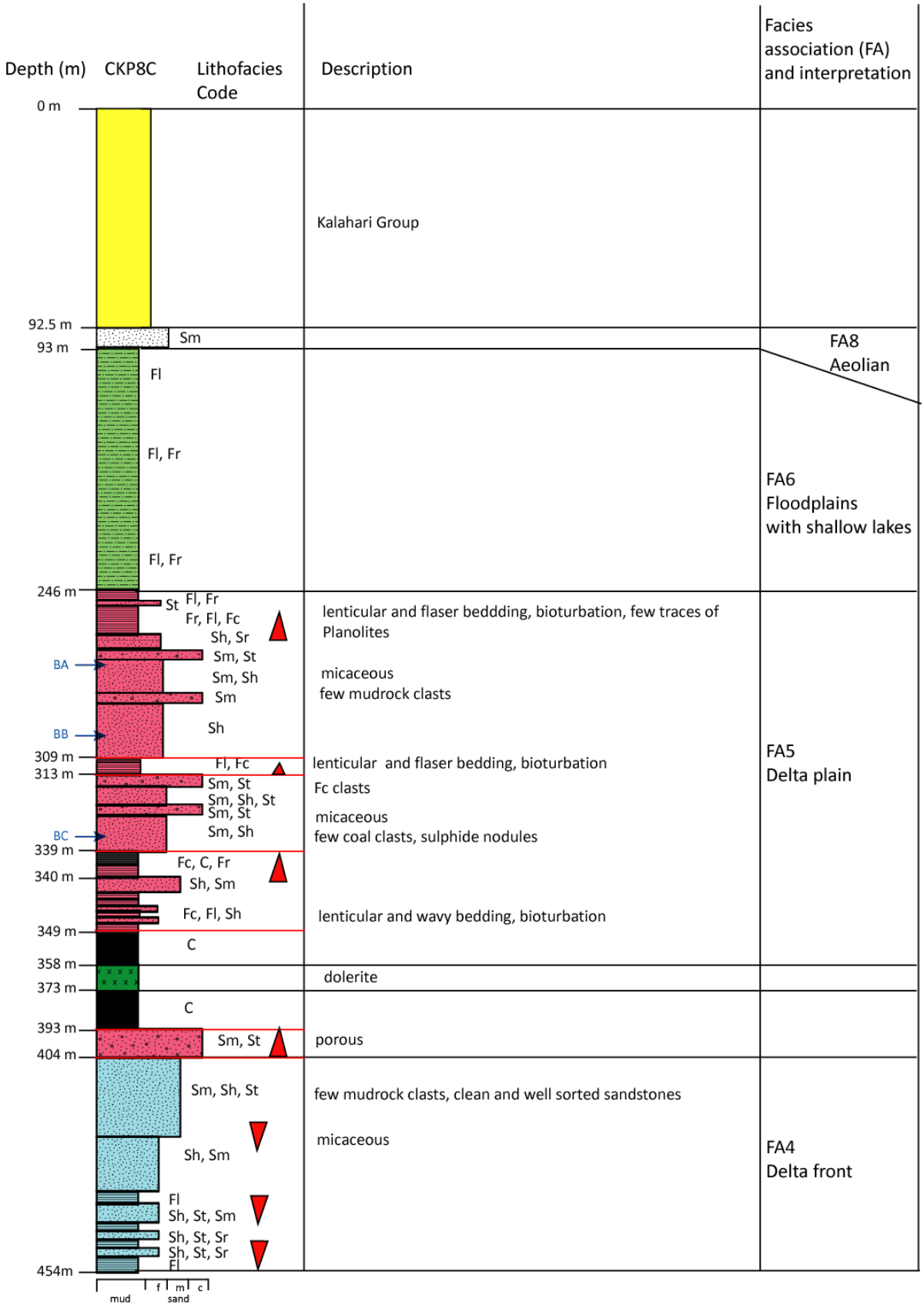
Appendix Figure. 8



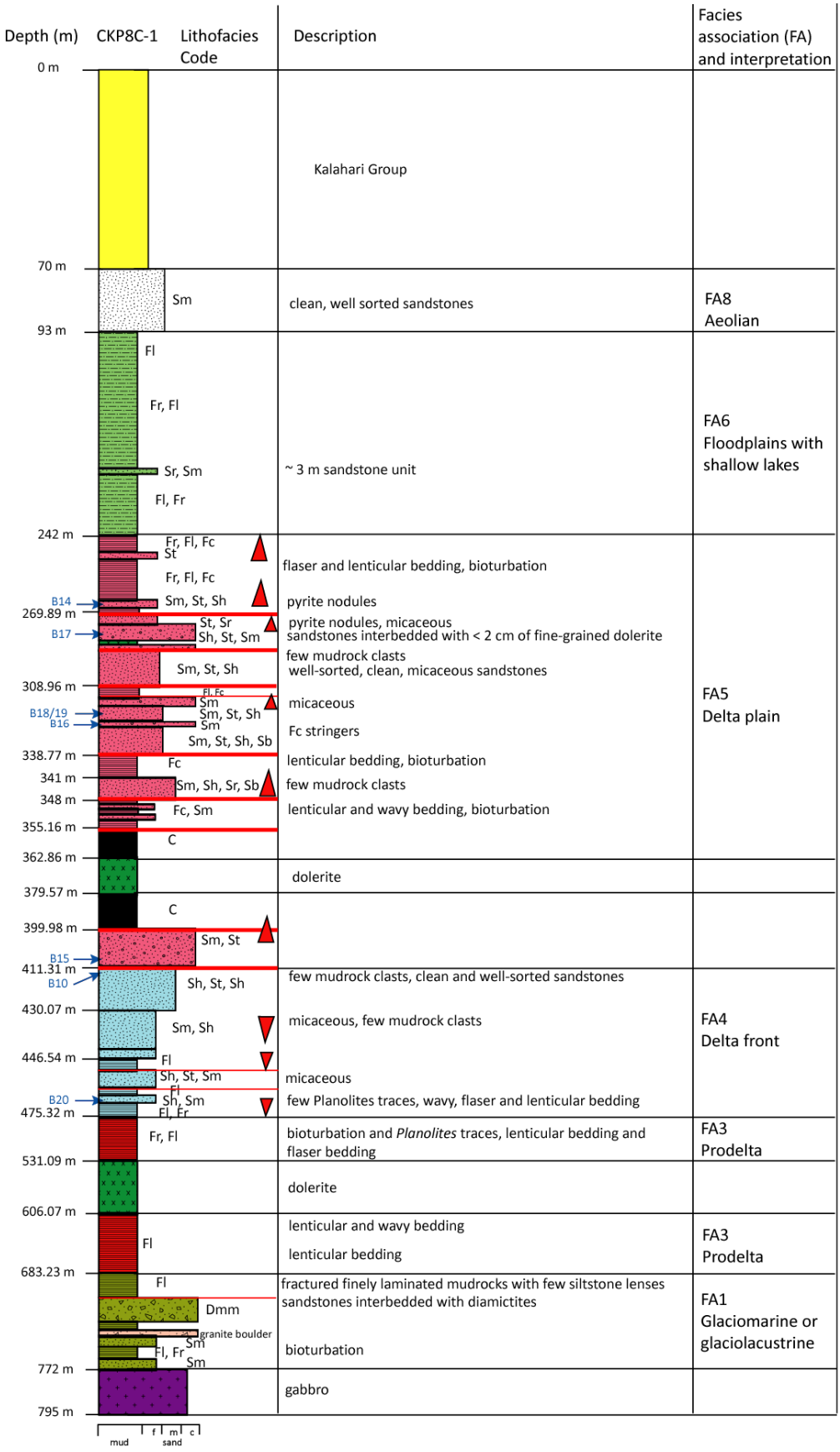
Appendix Figure. 9



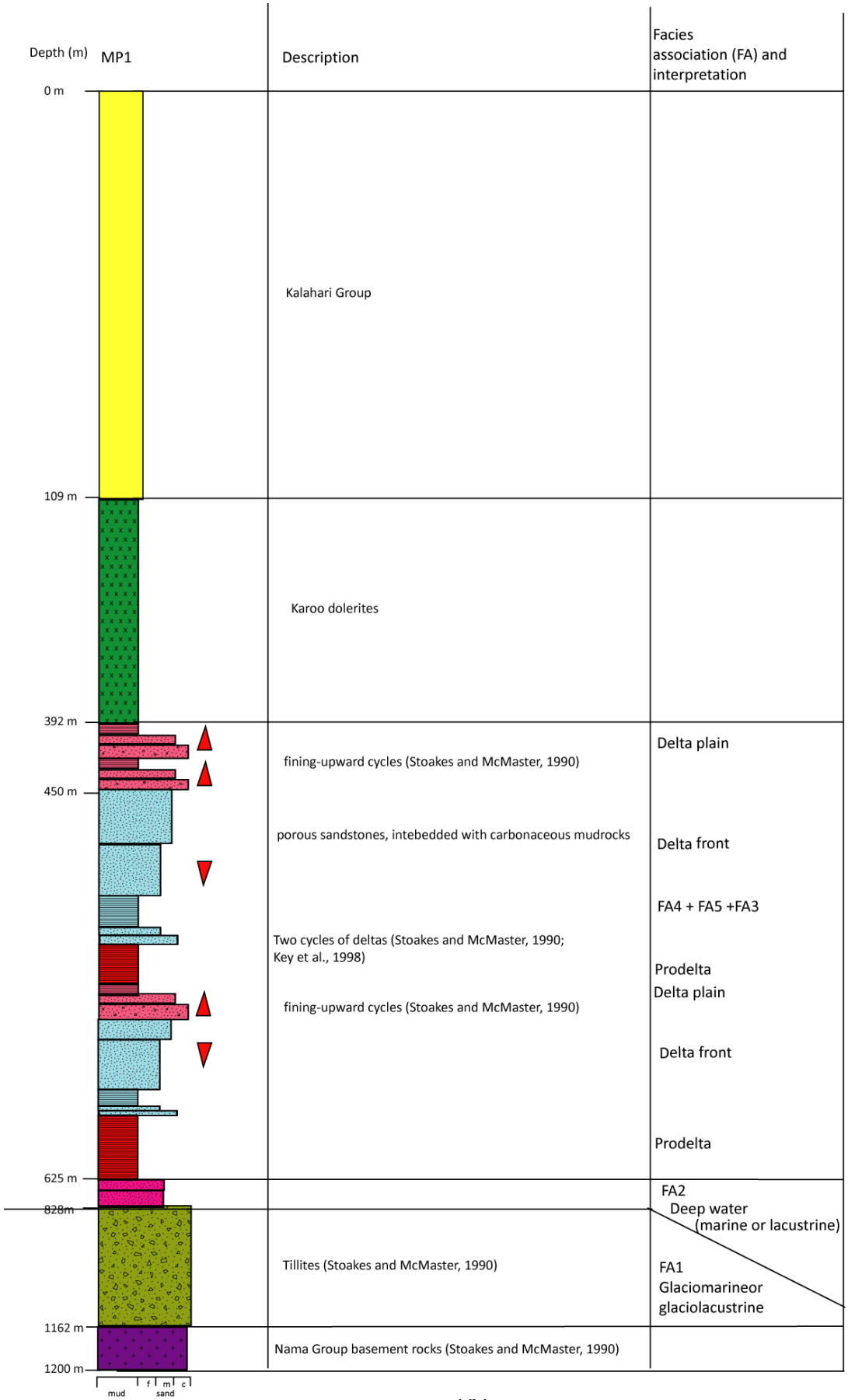
Appendix Figure. 10



Appendix Figure. 11



Appendix Figure. 12



Appendix Figure. 13

